

EARLY TRANSITION METAL CATALYSTS FOR THE
LIVING POLYMERIZATION OF OLEFINS AND ALKYNES

by

JENNIFER ADAMCHUK

B.A. (Honors) in Chemistry
Cornell University, 2001

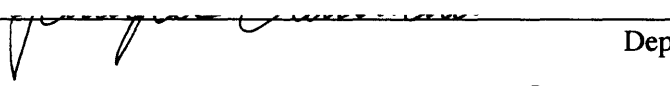
SUBMITTED TO THE DEPARTMENT OF CHEMISTRY IN PARTIAL
FULFILLMENT OF THE REQUIREMENTS FOR THE DEGREE OF

DOCTOR OF PHILOSOPHY IN CHEMISTRY
AT THE
MASSACHUSETTS INSTITUTE OF TECHNOLOGY

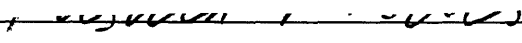
February 2006

© 2006 Massachusetts Institute of Technology. All rights reserved.

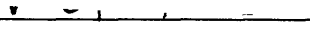
Signature of
Author

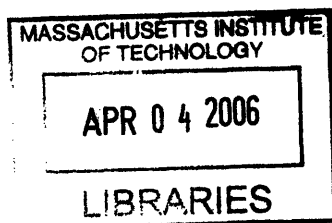

Department of Chemistry
November 29th, 2005

Certified
By


Richard R. Schrock
Thesis Supervisor

Accepted
By

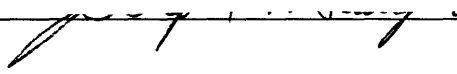

Robert W. Field
Chairman, Departmental Committee on Graduate Students



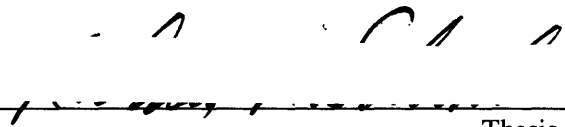
ARCHIVES

This doctoral thesis has been examined by a Committee of the Department of Chemistry as follows:

Professor Joseph P.
Sadighi


Chairman

Professor Richard R.
Schrock


Thesis Supervisor

Professor Christopher C.
Cummins



To my parents and Chris

Early Transition Metal Catalysts for the
Living Polymerization of Olefins and Alkynes

by

Jennifer Adamchuk

Submitted to the Department of Chemistry On November 29th, 2005 in Partial Fulfillment of the
Requirements for the Degree of Doctor of Philosophy in Chemistry

ABSTRACT

Zirconium and Hafnium Ziegler-Natta catalysts containing the $[(2,6\text{-Cl}_2\text{C}_6\text{H}_3\text{NCH}_2\text{CH}_2)_2\text{NMe}]^{2-}$ ($[\text{Ar}_{\text{Cl}}\text{N}_2\text{NMe}]^{2-}$) ligand were prepared and employed in the polymerization of 1-hexene. Hafnium Ziegler-Natta catalysts containing the $[(2,6\text{-X}_2\text{C}_6\text{H}_3\text{NHCH}_2)_2\text{C}(\text{CH}_3)(2\text{-C}_3\text{H}_4\text{N})]$ ($[\text{Ar}_{\text{X}_2}\text{NPy}]^{2-}$) ($\text{X} = \text{Cl}$ or F) ligand were also prepared for use in 1-hexene polymerization studies. Compounds of the type $[\text{Ligand}]\text{MR}_2$ ($\text{R} = \text{Me}$, *i*-Bu) were activated with $\{\text{Ph}_3\text{C}\}\{\text{B}(\text{C}_6\text{F}_5)_4\}$, $\text{B}(\text{C}_6\text{F}_5)_3$, or $\{\text{PhNMe}_2\text{H}\}\{\text{B}(\text{C}_6\text{F}_5)_4\}$ to yield monoalkyl cationic initiators paired with a weakly coordinating anion. Rates of consumption of 1-hexene were monitored, decomposition pathways studied, and living behavior assessed. Catalysts containing the $[\text{Ar}_{\text{Cl}}\text{N}_2\text{NMe}]^{2-}$ ligand were more stable than those containing the analogous $[\text{MesN}_2\text{NMe}]^{2-}$ ligand; however, living behavior was only observed for zirconium catalysts. Substitution of the mesityl amido substituents in $[\text{ArylNpy}]^{2-}$ hafnium complexes with aryl groups containing chlorines or fluorines (especially the latter) in the *ortho* positions was found to be detrimental to the development of living olefin polymerization catalysts of this general type. The catalytic activity steadily decreased in the order aryl = Mes > 2,6-Cl₂C₆H₃ > 2,6-F₂C₆H₃ and 1,2 and 2,1 β-hydride elimination increased in the order aryl = Mes < 2,6-Cl₂C₆H₃ < 2,6-F₂C₆H₃.

Quinuclidine adducts of $\text{Mo}(\text{NAr})(\text{CHCMe}_3)(\text{O-}t\text{-Bu})_2$ and $\text{Mo}(\text{NAr})(\text{CHFc})(\text{O-}t\text{-Bu})_2$ ($\text{Ar} = 2,6\text{-diisopropylphenyl}$) were prepared and used as catalysts for the cyclopolymerization of diethyl dipropargylmalonate (DEDPM). $\text{Mo}(\text{NAr})(\text{trans-CHCHCHMe})(\text{O-}t\text{-Bu})_2(\text{quin})$ and $\text{Mo}(\text{NAr})(\text{CH}[5])(\text{O-}t\text{-Bu})_2$, a species containing a five-membered ring alkylidene group analogous to the alkylidene that results from the cyclopolymerization of 1 equivalent of DEDPM by $\text{Mo}(\text{NAr})(\text{CHCR})(\text{O-}t\text{-Bu})_2$, were also synthesized for use in DEDPM polymerization studies. These catalysts cyclopolymerized DEDPM to produce polyenes with very low PDI values and $M_n(\text{found})/M_n(\text{calculated})$ ratios ≈ 1.1 . Ratios of the rate of propagation relative to initiation for these catalysts were less than 1, enabling the synthesis, isolation, and analysis of short oligomers. The initiation and polymerization processes were studied in detail using NMR spectroscopy.

Thesis Supervisor: Richard R. Schrock

Title: Frederick G. Keyes Professor of Chemistry

CHAPTER ABSTRACTS

Chapter 1

The triamine (2,6-Cl₂C₆H₃NHCH₂CH₂)₂NMe (H₂[Ar_{Cl}N₂NMe]) can be prepared through the Pd-catalyzed coupling between 1-bromo-2,6-dichlorobenzene and (H₂NCH₂CH₂)₂NH to give (2,6-Cl₂C₆H₃NHCH₂CH₂)₂NH, followed by methylation of the central nitrogen with MeI. Zirconium and hafnium complexes that were prepared include [Ar_{Cl}N₂NMe]M(NMe₂)₂ (M = Hf or Zr), [Ar_{Cl}N₂NMe]MCl₂, [Ar_{Cl}N₂NMe]MMe₂, [Ar_{Cl}N₂NMe]HfCl(*i*-Bu), [Ar_{Cl}N₂NMe]HfMe(*i*-Bu), and [Ar_{Cl}N₂NMe]Hf(*i*-Bu)₂. An X-ray crystal structure shows [Ar_{Cl}N₂NMe]Hf(*i*-Bu)₂ to be a square pyramid in which one of the isobutyl groups occupies the apical position. Activation of dimethyl species with {Ph₃C}{B(C₆F₅)₄}, B(C₆F₅)₃, or {PhNMe₂H}{B(C₆F₅)₄} yielded {[Ar_{Cl}N₂NMe]MMe}⁺ cations paired with {B(C₆F₅)₄}⁻ or {MeB(C₆F₅)₃}⁻ anions; these species are active for the polymerization of 1-hexene. Activation of [Ar_{Cl}N₂NMe]Hf(*i*-Bu)₂ with {Ph₃C}{B(C₆F₅)₄} or B(C₆F₅)₃ produced {[Ar_{Cl}N₂NMe]Hf(*i*-Bu)}{B(C₆F₅)₄} and {[Ar_{Cl}N₂NMe]Hf(*i*-Bu)}{HB(C₆F₅)₃}, which are also active for the polymerization of 1-hexene. Isobutene was found to insert slowly into the M-R bond of these initiators in a 1,2 manner, and was oligomerized at high concentrations of isobutene. Activation of [Ar_{Cl}N₂NMe]HfMe(*i*-Bu) with B(C₆F₅)₃ resulted in selective abstraction of a methyl group to generate 95% {[Ar_{Cl}N₂NMe]Hf(*i*-Bu)}{MeB(C₆F₅)₃}. The rate of consumption of 1-hexene followed a first-order dependence on 1-hexene (and hafnium or zirconium), with zirconium catalysts having higher activity than hafnium catalysts. Although poly(1-hexene) generated by the zirconium catalyst was characteristic of a living system, significant β-hydride elimination was observed in polymerizations by hafnium catalysts. The hafnium product of β-hydride elimination was observed to reinitiate the polymerization of 1-hexene.

Chapter 2

The pyridyldiamines (2,6-X₂C₆H₃NHCH₂)₂C(CH₃)(2-C₅H₄N) (H₂[Ar_{X₂}Npy]) (X = Cl or F) can be prepared in good yield through the Pd-catalyzed coupling between 2,6-dihalobromobenzene and (H₂NCH₂)₂C(CH₃)(2-C₅H₄N). Zirconium and hafnium complexes that contain these ligands were prepared through traditional routes; they include [Ar_{Cl₂}Npy]M(NMe₂)₂ (M = Zr or Hf), [Ar_{Cl₂}Npy]MCl₂, [Ar_{Cl₂}Npy]MMe₂, [Ar_{Cl₂}Npy]Hf(*i*-Bu)₂, [Ar_{F₂}Npy]Hf(*i*-Bu)₂, and [Ar_{F₂}Npy]HfMe₂. Attempts to prepare [Ar_{F₂}Npy]Hf(NMe₂)₂ in a reaction between Hf(NMe₂)₄ and free ligand led to compounds in which one or two dimethylamido groups had been exchanged with one or two *ortho*-fluorines on the 2,6-difluorophenyl rings. Compounds whose structures were determined in X-ray studies include [Ar_{F₂}Npy]Hf(*i*-Bu)₂ and [Ar_{(FNM₂)₂}Npy]Hf(F)Cl, a compound that contains 2-fluoro-6-dimethylaminophenyl rings. In the first compound one chloride is weakly bonded to the metal, in the second two fluorides are weakly bonded to the metal, and in the third two dimethylamino groups are strongly bonded to the metal. Activation of dimethyl species with {Ph₃C}{B(C₆F₅)₄} in bromobenzene led initially to the formation of dimeric monocations such as {[Ar_{X₂}Npy]₂M₂Me₃}{B(C₆F₅)₄}, which are inactive for polymerization of 1-hexene. The {[Ar_{X₂}Npy]₂M₂Me₃}{B(C₆F₅)₄} compounds react further with {Ph₃C}{B(C₆F₅)₄} to give {[Ar_{X₂}Npy]MMe}{B(C₆F₅)₄} species, which are active for polymerization of 1-hexene. Activation of [Ar_{X₂}Npy]Hf(*i*-Bu)₂ complexes with {Ph₃C}{B(C₆F₅)₄} in bromobenzene led to the formation of {[Ar_{X₂}Npy]Hf(*i*-Bu)}{B(C₆F₅)₄} species that are also active for the polymerization of 1-hexene. The rate of consumption of 1-hexene followed a first order dependence on 1-hexene (and hafnium), although the rates were

substantially slower compared to those for the known catalyst with mesityl substituents on the amido nitrogens, and slower when $X = F$ than when $X = Cl$. The ease of preparation of the cations also followed the order Aryl = Mesityl > 2,6-Cl₂C₆H₃ > 2,6-F₂C₆H₃. Finally, the quality of the polymerization, in terms of its living characteristics, deteriorated markedly when the aryl substituent was 2,6-F₂C₆H₃.

Chapter 3

Quinuclidine adducts of Mo(NAr)(CHCMe₃)(O-*t*-Bu)₂ and Mo(NAr)(CHFc)(O-*t*-Bu)₂ (Ar = 2,6-diisopropylphenyl) were prepared and used as catalysts for the cyclopolymerization of diethyl dipropargylmalonate (DEDPM). Reactions were performed starting at -30 °C in dichloromethane. The resulting polyenes contained ~95% five-membered rings and were characterized by polydispersities between 1.13 and 1.30 and M_n(found)/M_n(calculated) ratios between 1.4 and 1.9. In order to increase the rate of initiation relative to propagation, catalysts containing alkylidene groups more akin to the propagating alkylidene chain were prepared. Mo(NAr)(*trans*-CHCHCHMe)(O-*t*-Bu)₂(quin) was synthesized from Mo(NAr)(*trans*-CHCHCHMe)[OCMe(CF₃)₂]₂(quin) and LiO-*t*-Bu. An X-ray structure shows Mo(NAr)(*trans*-CHCHCHMe)(O-*t*-Bu)₂(quin) to be a trigonal bipyramidal species in which quinuclidine and the butenylidene group occupy axial positions, and the butenylidene group is oriented syn to the amido group. Mo(NAr)(CH[5])(O-*t*-Bu)₂ was synthesized by the metathesis reaction of Mo(NAr)(CHCMe₃)[OCMe(CF₃)₂]₂ with a five-membered ring triene substrate, followed by the addition of LiO-*t*-Bu. This species contains a five-membered ring alkylidene group analogous to the alkylidene that results from the cyclopolymerization of 1 equivalent of DEDPM by Mo(NAr)(CHCR)(O-*t*-Bu)₂. An X-ray structure shows Mo(NAr)(CH[5])(O-*t*-Bu)₂ to be a tetrahedral species in which the alkylidene group is oriented syn to the amido group. Rates of propagation relative to initiation (k_p/k_i) for Mo(NAr)(*trans*-CHCHCHMe)(O-*t*-Bu)₂(quin) and Mo(NAr)(CH[5])(O-*t*-Bu)₂(quin) were calculated to be less than 1 in both C₆D₆ and CD₂Cl₂. Mo(NAr)(*trans*-CHCHCHMe)(O-*t*-Bu)₂(quin) cyclopolymerizes DEDPM to produce polyenes with PDI values < 1.1 and M_n(found)/M_n(calculated) ratios ≈ 1.1. Resonances representing the insertion product alkylidene α-protons of the reaction of 0.2 to 30 equivalents of DEDPM with Mo(NAr)(*trans*-CHCHCHMe)(O-*t*-Bu)₂(quin) were partially identified in the ¹H NMR spectrum. Short, symmetric oligomers were synthesized and isolated in high yield employing Mo(NAr)(CH[5])(O-*t*-Bu)₂(quin) as a catalyst. Oligomers containing 2 to 10 monomers were purified by HPLC and analyzed spectroscopically.

TABLE OF CONTENTS

Title Page.....	1
Signature Page.....	2
Dedication.....	3
Abstract.....	4
Chapter Abstracts.....	5
Table of Contents.....	7
List of Abbreviations.....	10
List of Figures.....	12
List of Schemes.....	16
List of Tables.....	17
General Introduction for Chapters 1 and 2.....	19
Chapter 1. An Evaluation of Zirconium and Hafnium Complexes that Contain the Electron-Withdrawing Diamido-Donor Ligand, [(2,6-Cl₂C₆H₃NCH₂CH₂)₂NCH₃]²⁻, for the Polymerization of 1-Hexene.....	23
1.1 Introduction.....	24
1.2 Preparation of (2,6-Cl ₂ C ₆ H ₃ NHCH ₂ CH ₂) ₂ NMe (H ₂ [Ar _{Cl} N ₂ NMe]) and Complexes that Contain the [Ar _{Cl} N ₂ NMe] ²⁻ Ligand	24
1.3 Activation of Dialkyl Complexes.....	29
1.3.1 Activation of [Ar _{Cl} N ₂ NMe]MMe ₂ (M = Hf, Zr).....	29
1.3.2 Activation of [Ar _{Cl} N ₂ NMe]Hf(<i>i</i> -Bu) ₂	30
1.4 Polymerization of 1-Hexene.....	33
1.5 β-Hydride Elimination.....	38
1.6 Inhibition Studies.....	40
1.7 Conclusions.....	45
1.8 Experimental Section.....	45
1.9 Acknowledgements.....	53
Chapter 2: Zirconium and Hafnium Complexes that Contain the Electron-Withdrawing Diamido-Donor Ligands, [(2,6-X₂C₆H₃NCH₂)₂C(2-C₅H₄N)(CH₃)]²⁻ (X = Cl or F). An Evaluation of the Role of <i>ortho</i>-Halides in 1-Hexene Polymerization.....	54
2.1 Introduction.....	55
2.1.1 Preparation of [(2,6-Cl ₂ C ₆ H ₃ NCH ₂) ₂ C(CH ₃)(2-C ₅ H ₄ N)] ²⁻ ([Ar _{Cl₂} Npy] ²⁻) Complexes.....	56
2.2 Preparation of [(2,6-F ₂ C ₆ H ₃ NCH ₂) ₂ C(CH ₃)(2-C ₅ H ₄ N)] ²⁻ ([Ar _{F₂} Npy] ²⁻) Complexes.....	58
2.3 Activation of [Ar _{Cl₂} Npy]M(Me) ₂ Complexes.....	67
2.4 Activation of [Ar _{Cl₂} Npy]Hf(<i>i</i> -Bu) ₂	69
2.5 Activation of [Ar _{F₂} Npy]HfMe ₂ Complexes.....	71
2.6 Activation of [Ar _{F₂} Npy]Hf(<i>i</i> -Bu) ₂ Complexes.....	71

2.7	Polymerization of 1-Hexene by $[\text{Ar}_{\text{Cl}_2}\text{Npy}]^{2-}$ Cationic Alkyls.....	72
2.8	Polymerization of 1-Hexene by $[\text{Ar}_{\text{F}_2}\text{Npy}]^{2-}$ Cationic Alkyls.....	77
2.9	Conclusions.....	79
2.10	Experimental Section.....	80
2.11	Acknowledgements.....	87

Chapter 3. Synthesis of Poly(alkynes) Using Well-Defined Molybdenum Imido Alkylidene Catalysts.....	88	
3.1	Introduction.....	89
3.2	Catalyst Synthesis.....	96
3.2.1	The Neopentylidene, Neophylidene, and Ferrocenemethylidene Catalysts	96
3.2.2	The Di- <i>tert</i> -butoxide and Hexafluoro- <i>tert</i> -Butoxide Butenylidene Catalysts.....	96
3.2.3	The Diadamantoxide Butenylidene Catalyst.....	102
3.2.4	The Di- <i>tert</i> -butoxide Five-Membered Ring Alkylidene (CH[5]) Catalyst.....	103
3.2.5	The Di- <i>tert</i> -butoxide Six-Membered Ring Alkylidene Catalyst.....	108
3.3	DEDPM Polymerization.....	109
3.3.1	The Neopentylidene, Neophylidene, and Ferrocenylmethylidene Catalysts.....	111
3.3.2	The Di- <i>tert</i> -butoxide and Hexafluoro- <i>tert</i> -Butoxide Butenylidene Catalysts.....	114
3.3.3	The Diadamantoxide Butenylidene Catalyst.....	118
3.3.4	The Five-Membered Ring Alkylidene Catalyst.....	120
3.3.5	The Mo(NAr)(CHR')(O- <i>t</i> -Bu) ₂ (quin) Propagating Catalyst (R' = polymer chain).....	121
3.4	Initiation studies.....	121
3.4.1	The Neopentylidene, Neophylidene, and Ferrocenylmethylidene Initiators.....	122
3.4.2	The Di- <i>tert</i> -butoxide and Hexafluoro- <i>tert</i> -Butoxide Butenylidene Initiators.....	123
3.4.2.1	Calculation of k_p/k_i for Mo(NAr)(<i>trans</i> -CHCHCHMe)(O- <i>t</i> -Bu) ₂ (quin) and Mo(NAr)(<i>trans</i> -CHCHCHMe)[OCMe(CF ₃) ₂] ₂ (quin).....	127
3.4.2.2	Identification of Alkylidene H _α Resonances (General).....	132
3.4.2.3	Identification of Alkylidene H _α Resonances Corresponding to Products in Which a Five-Membered Ring in the Alkylidene Chain is Adjacent to the Metal Center.....	132
3.4.2.4	Identification of Alkylidene H _α Resonances Corresponding to Products in Which a Six-Membered Ring in the Alkylidene Chain is Adjacent to the Metal Center.....	135

3.4.3	The Diadamantoxide Butenylidene Initiator.....	138
3.4.4	The Di- <i>tert</i> -butoxide Five-Membered Ring Alkylidene Initiator.....	139
3.5	Synthesis and Isolation of Oligomers.....	139
3.5.1	Synthesis of Oligomers by Mo(NAr)(<i>trans</i> -CHCHCHMe)(O- <i>t</i> -Bu) ₂ (quin).....	139
3.5.2	Synthesis of Oligomers by Mo(NAr)(CH[5])(O- <i>t</i> -Bu) ₂ (quin).....	144
3.6	DEDPM Polymerization Employing Various Schrock-Group Catalysts.....	148
3.7	Conclusions.....	150
3.8	Experimental Section.....	150
3.9	Acknowledgements.....	158
Appendix 1.	Synthesis and Reactions of [MesNpy]Hf(R)₂ (R = Np Bn).....	159
A.1	Introduction.....	160
A.2	Complexes and reactions of hafnium complexes containing the [(MesNCH ₂) ₂ C(CH ₃)(2-C ₃ H ₄ N)] ²⁻ ([MesNpy] ²⁻) ligand.....	160
A.3	Experimental Section.....	162
Appendix 2.	Crystallographic Parameters and Tables.....	166
References		176
Curriculum Vitae		184
General Acknowledgements		185

LIST OF ABBREVIATIONS

Ad	Adamantyl
anal	Analysis
Ar	Aryl
arom	aromatic
Ar _{Cl} N ₂ NMe	(2,6-Cl ₂ C ₆ H ₃ NCH ₂ CH ₂)NMe
Ar _{Cl₂} Npy	(2,6-Cl ₂ C ₆ H ₃ NCH ₂) ₂ C(2-C ₅ H ₄ N)(CH ₃)
Ar _{F₂} Npy	(2,6-F ₂ C ₆ H ₃ NCH ₂) ₂ C(2-C ₅ H ₄ N)(CH ₃)
br	broad
BINAP	2,2'-bis(diphenylphosphino)-1,1'-binaphthyl
Bn	benzyl, -CH ₂ (C ₆ H ₅)
<i>i</i> -Bu	<i>iso</i> -butyl, -CH ₂ CH(CH ₃) ₂
<i>n</i> -Bu	<i>n</i> -butyl, -CH ₂ CH ₂ CH ₂ CH ₃
<i>t</i> -Bu	<i>t</i> -butyl, -C(CH ₃) ₃
calcd	calculated
coord	coordinated
Cp	(C ₅ H ₅) ⁻
d	doublet
dba	dibenzylideneacetone
DEDPM	diethyl dipropargylmalonate
dimethylaniline	N,N-dimethylaniline
equiv	equivalents(s)
<i>fac</i>	<i>facial</i>
GCOSY	Gradient Correlation Spectroscopy
EI	Electron Impact
Et	ethyl
Fc	ferrocenyl
FTMS	Fourier Transform Mass Spectroscopy
GPC	Gel Permeation Chromatography
h	hour(s)
HPLC	High Pressure Liquid Chromatography
HRMS	High Resolution Mass Spectroscopy
ICR	Ion Cyclotron Resonance
<i>J</i>	coupling constant in Hertz
<i>k_d</i>	decomposition rate for polymerization reactions
<i>k_i</i>	initiation rate constant for polymerization reactions
<i>k_{obs}</i>	observed rate constant for polymerization reactions
<i>k_p</i>	propagation rate constant for polymerization reactions
K	equilibrium constant
Li-HMDS	lithium bis(trimethylsilyl)amide
m	multiplet(s)
M _n	number averaged molecular weight
M _w	weight averaged molecular weight
MALDI	Matrix Assisted Laser-Desorption Ionization
Me	methyl

Mes	mesityl
MesN ₂ NMe	(MesNCH ₂ CH ₂)NMe
MesNpy	(MesNCH ₂) ₂ C(2-C ₅ H ₄ N)(CH ₃)
<i>mer</i>	<i>meridional</i>
M _n (f/c)	M _n (found)/M _n (calculated)
MS	mass spectroscopy
NMR	nuclear magnetic resonance
Np	Neopentyl, -CH ₂ C(CH ₃) ₃
PDI	Poly Dispersity Index
Ph	phenyl
ppm	parts per million
<i>i</i> -Pr	<i>iso</i> -propyl, -CHMe ₂
py	pyridine
q	quartet
quat	quaternary
quin	quinuclidine
ROMP	Ring Opening Metathesis Polymerization
R.T.	room temperature
s	singlet
sept	septet
t	triplet
T	temperature
THF	tetrahydrofuran
TMS	trimethylsilyl
TOF	Time of Flight
β _{1,2} Product	olefinic product of β-hydride elimination following a 1,2 insertion of 1-hexene into the catalyst metal-carbon bond
β _{2,1} Product	olefinic product of β-hydride elimination following a 2,1 insertion of 1-hexene into the catalyst metal-carbon bond
δ	chemical shift downfield from tetramethylsilane in ppm
CH[5]	five-membered ring alkylidene

LIST OF FIGURES

Chapter 1

Figure 1.1.	Complexes containing the $[(ArNCH_2CH_2)_2NMe]^2-$ ligand (Ar = Mes, 2,6-Cl ₂ C ₆ H ₃).....	24
Figure 1.2.	Thermal ellipsoid drawing of $[Ar_{Cl}N_2NMe]Hf(i-Bu)_2$ at the 30% probability level.....	27
Figure 1.3.	Consumption of the final 13% of 100 equivalents of 1-hexene at 0 °C by 0.006 M $\{[Ar_{Cl}N_2NMe]HfMe\}\{B(C_6F_5)_4\}$ (formed by the activation of $[Ar_{Cl}N_2NMe]HfMe_2$ with $\{Ph_3C\}\{B(C_6F_5)_4\}$).....	34
Figure 1.4.	Molecular weights of poly(1-hexene) obtained with 3 mM $\{[Ar_{Cl}N_2NMe]ZrMe\}\{B(C_6F_5)_4\}$ in chlorobenzene at 0 °C.....	36
Figure 1.5.	Growth of the hafnium complex and olefin upon decomposition of the propagating species after completion of the polymerization of 1-hexene by $\{[Ar_{Cl}N_2NMe]Hf(i-Bu)\}\{HB(C_6F_5)_3\}$ at 0 °C in C ₆ D ₅ Br.....	39
Figure 1.6.	Consumption of 100 equivalents 1-hexene by $\{[Ar_{Cl}N_2NMe]HfMe\}\{B(C_6F_5)_4\}$ (formed by the activation of $[Ar_{Cl}N_2NMe]HfMe_2$ with $\{Ph_3C\}\{B(C_6F_5)_4\}$) in the presence of 1 to 20 equivalents of (<i>i</i> -Pr) ₂ O (0 °C, C ₆ D ₅ Br).....	42
Figure 1.7.	Plot of $[Hf]_0/k_{obs}$ versus $[(i-Pr)_2O]$ for the addition of 1-hexene to $\{[Ar_{Cl}N_2NMe]HfMe\}\{B(C_6F_5)_4\}$ in the presence of 1 to 20 equivalents of (<i>i</i> -Pr) ₂ O (0 °C, C ₆ D ₅ Br).....	42

Chapter 2

Figure 2.1.	Two diamido-donor ligand frameworks studied recently in the Schrock lab.....	55
Figure 2.2.	Thermal ellipsoid drawing of $[Ar_{Cl_2}Npy]Hf(i-Bu)_2$ at the 30% probability level.....	57
Figure 2.3.	Thermal ellipsoid drawing of $[Ar_{(FNM_e)_2}Npy]Hf(F)Cl$ (6) at the 30% probability level.....	63
Figure 2.4.	Thermal ellipsoid drawing of $[Ar_{F_2}Npy]Hf(i-Bu)_2$ at the 30% probability level.....	66
Figure 2.5.	Decomposition of $\{[Ar_{Cl_2}Npy]Hf(i-Bu)\}\{B(C_6F_5)_4\}$ (formed by $\{Ph_3C\}\{B(C_6F_5)_4\}$ activation of $[Ar_{Cl_2}Npy]Hf(i-Bu)_2$) at 0 °C by following the disappearance of the isobutyl methyl resonances in the ¹ H NMR spectrum.....	71
Figure 2.6.	Polymerization of 100 equivalents of 1-hexene in C ₆ D ₅ Br by 0.012 M $\{[Ar_{Cl_2}Npy]Hf(i-Bu)\}\{B(C_6F_5)_4\}$	74
Figure 2.7.	Molecular weight measurements for poly(1-hexene) obtained with $\{[Ar_{Cl_2}Npy]Hf(i-Bu)\}\{B(C_6F_5)_4\}$ as the initiator at 0 °C in C ₆ D ₅ Br.....	76

Figure 2.8.	Plots of $\ln([1\text{-hexene}]/[\text{Ph}_2\text{CH}_2])$ versus time for the consumption of 1-hexene by $\{[\text{Ar}_{\text{F}_2}\text{Npy}]\text{Hf}(i\text{-Bu})\}\{\text{B}(\text{C}_6\text{F}_5)_4\}$: (a) $[\text{Hf}_{\text{cat}}] = 0.012 \text{ M}$, $0 \text{ }^\circ\text{C}$, 50 equivalents of 1-hexene, $k_p = 0.0070 \text{ M}^{-1}\text{s}^{-1}$; (b) $[\text{Hf}_{\text{cat}}] = 0.015 \text{ M}$, $0 \text{ }^\circ\text{C}$, 100 equivalents of 1-hexene, $k_p = 0.0073 \text{ M}^{-1}\text{s}^{-1}$; (c) $[\text{Hf}_{\text{cat}}] = 0.012 \text{ M}$, $10 \text{ }^\circ\text{C}$, 100 equivalents of 1-hexene, $k_p = 0.0155 \text{ M}^{-1}\text{s}^{-1}$; (d) $[\text{Hf}_{\text{cat}}] = 0.012 \text{ M}$, $20 \text{ }^\circ\text{C}$, 100 equivalents of 1-hexene, $k_p = 0.028 \text{ M}^{-1}\text{s}^{-1}$	78
Figure 2.9.	Molecular weight measurements for poly(1-hexene) obtained with $\{[\text{Ar}_{\text{F}_2}\text{Npy}]\text{Hf}(i\text{-Bu})\}\{\text{B}(\text{C}_6\text{F}_5)_4\}$ as the initiator at $0 \text{ }^\circ\text{C}$ in $\text{C}_6\text{D}_5\text{Br}$	79

Chapter 3

Figure 3.1.	Polyenes containing all five- and six-membered rings.....	94
Figure 3.2.	Thermal ellipsoid drawing of $\text{Mo}(\text{NAr})(\text{trans-CHCHCHMe})(\text{O-}t\text{-Bu})_2(\text{quin})$ at the 50% probability level.....	99
Figure 3.3.	The partial (2.8 to 14 ppm) ^1H NMR spectrum of $\text{Mo}(\text{NAr})(\text{trans-CHCHCHMe})(\text{O-}t\text{-Bu})_2(\text{quin})$ ($20 \text{ }^\circ\text{C}$, $\text{C}_6\text{D}_5\text{CD}_3$).....	101
Figure 3.4.	The alkylidene H_α resonances of the chiral, anti rotamer, the chiral, syn rotamer, and the achiral, syn rotamer of $\text{Mo}(\text{NAr})(\text{trans-CHCHCHMe})(\text{O-}t\text{-Bu})_2(\text{quin})$ at $-70 \text{ }^\circ\text{C}$ in $\text{C}_6\text{D}_5\text{CD}_3$	102
Figure 3.5.	The partial (2.8 to 13 ppm) ^1H NMR spectrum of $\text{Mo}(\text{NAr})(\text{CH}[5])(\text{O-}t\text{-Bu})_2$ ($22 \text{ }^\circ\text{C}$, CD_2Cl_2).....	106
Figure 3.6.	Thermal ellipsoid drawing of $\text{Mo}(\text{NAr})(\text{CH}[5])(\text{O-}t\text{-Bu})_2$ at the 50% probability level.....	107
Figure 3.7.	The partial (2.8 to 13.4 ppm) ^1H NMR spectrum of $\text{Mo}(\text{NAr})(\text{CH}[5])(\text{O-}t\text{-Bu})_2$ ($22 \text{ }^\circ\text{C}$, C_6D_6).....	108
Figure 3.8.	Poly(DEDPM) containing approximately 95% five-membered rings.....	112
Figure 3.9.	Number average molecular weight (M_n) of poly(DEDPM) (g/mol) Produced by $\text{Mo}(\text{NAr})(\text{CHR})(\text{O-}t\text{-Bu})_2(\text{quin})$ ($\text{R} = \text{CMe}_3$; Neopentylidene Catalyst, <i>trans</i> -CHCHMe; Butenylidene Catalyst) versus equivalents of monomer (See Table 3.4 for data).....	114
Figure 3.10.	Consumption of 40 equivalents of DEDPM by $\text{Mo}(\text{NAr})(\text{trans-CHCHCHMe})(\text{O-}t\text{-Bu})_2(\text{quin})$ in CD_2Cl_2 at $0 \text{ }^\circ\text{C}$ ($k_p = 0.24 \text{ M}^{-1}\text{s}^{-1}$).....	116
Figure 3.11.	Plot of $\ln(k/T)$ versus $1/T$ (K^{-1}) for $\text{Mo}(\text{NAr})(\text{trans-CHCHCHMe})(\text{O-}t\text{-Bu})_2(\text{quin})$: $\Delta\text{H}^\ddagger = 10 \text{ kcal/mol}$ and $\Delta\text{S}^\ddagger = -24 \text{ cal/mol}\cdot\text{K}$	117
Figure 3.12.	MALDI-TOF spectrum of ferrocene-capped polymer formed by the polymerization of 38 equivalents of DEDPM by $\text{Mo}(\text{NAr})(\text{trans-CHCHCHMe})(\text{O-}t\text{-Bu})_2(\text{quin})$ in CH_2Cl_2 at $22 \text{ }^\circ\text{C}$ ($\text{PDI} = 1.02$, M_n (f/c) = 1.1).....	118
Figure 3.13.	Consumption of 40 equivalents of DEDPM by $\text{Mo}(\text{NAr})(\text{trans-CHCHCHMe})(\text{OAd})_2(\text{quin})$ in CD_2Cl_2 at $0 \text{ }^\circ\text{C}$ ($k_p = 0.13 \text{ M}^{-1}\text{s}^{-1}$).....	119

- Figure 3.14. Plot of $\ln(k/T)$ versus $1/T$ (K^{-1}) for $\text{Mo}(\text{NAr})(\text{trans-CHCHCHMe})(\text{OAd})_2(\text{quin})$: $\Delta H^\ddagger = 10$ kcal/mol and $\Delta S^\ddagger = -26$ cal/mol•K.....120
- Figure 3.15. ^1H NMR spectrum (CD_2Cl_2 , 22 °C) of the alkylidene region for reaction of 1.10 equivalents of DEDPM with $\text{Mo}(\text{NAr})(\text{trans-CHCHCHMe})(\text{O-}t\text{-Bu})_2(\text{quin})$124
- Figure 3.16. ^1H NMR spectrum (CD_2Cl_2 , 22 °C) of the alkylidene region for the reaction of 1.10 equivalents of DEDPM with $\text{Mo}(\text{NAr})(\text{trans-CHCHCHMe})[\text{OCMe}(\text{CF}_3)_2]_2(\text{quin})$, followed by the addition of excess $\text{LiO-}t\text{-Bu}$ to the reaction.....126
- Figure 3.17. Chart A: the percentage of each alkylidene H_α peak, including that of the remaining starting material (12.14 ppm), that is present after the reactions of 0.2 to 10.0 equivalents of DEDPM with $\text{Mo}(\text{NAr})(\text{trans-CHCHCHMe})(\text{O-}t\text{-Bu})_2(\text{quin})$ in C_6D_6 at 22 °C. Chart B: the percentage of each insertion product alkylidene H_α peak compared to the total integration of all insertion product alkylidene H_α peaks generated under the same conditions as in Chart A.128
- Figure 3.18. Chart A: the percentage of each alkylidene H_α peak, including that of the remaining starting material (11.85 ppm), that is present after the reactions of 0.2 to 10.0 equivalents of DEDPM with $\text{Mo}(\text{NAr})(\text{trans-CHCHCHMe})(\text{O-}t\text{-Bu})_2(\text{quin})$ in CD_2Cl_2 at 22 °C. Chart B: the percentage of each insertion product alkylidene H_α peak compared to the total integration of all insertion product alkylidene H_α peaks generated under the same conditions as in Chart A.....129
- Figure 3.19. Chart A: the percentage of each alkylidene H_α peak, including that of the remaining starting material (11.85 ppm), that is present after the reactions of 0.2 to 10.0 equivalents of DEDPM with $\text{Mo}(\text{NAr})(\text{trans-CHCHCHMe})[\text{OCMe}(\text{CF}_3)_2]_2(\text{quin})$ in CD_2Cl_2 at 22 °C, followed by the addition of excess $\text{LiO-}t\text{-Bu}$. Chart B: the percentage of each insertion product alkylidene H_α peak compared to the total integration of all insertion product alkylidene H_α peaks generated under the same conditions as in Chart A.....130
- Figure 3.20. Two possible first insertion products formed during the cyclopolymerization of DEDPM by $\text{Mo}(\text{NAr})(\text{trans-CHCHCHMe})(\text{O-}t\text{-Bu})_2(\text{quin})$132
- Figure 3.21. The partial (5.4 to 6.6 ppm) ^1H NMR spectrum of the reaction of 0.2 equivalents of DEDPM with $\text{Mo}(\text{NAr})(\text{trans-CHCHCHMe})(\text{O-}t\text{-Bu})_2(\text{quin})$ at 22 °C in CD_2Cl_2133
- Figure 3.22. Two possible second insertion products (Mo-5-5 and Mo-5-6) in which a five-membered ring in the alkylidene chain is adjacent to the metal.....134
- Figure 3.23. The partial (5.4 to 6.6 ppm) ^1H NMR spectrum of the reaction of 0.2 equivalents of DEDPM with $\text{Mo}(\text{NAr})(\text{trans-CHCHCHMe})[\text{OCMe}(\text{CF}_3)_2]_2(\text{quin})$ at room temperature in CD_2Cl_2 , followed by the addition of excess $\text{LiO-}t\text{-Bu}$136
- Figure 3.24. Three possible insertion products (Mo-6-5, Mo-6-6, and Mo-6-5) in which a

	six-membered ring in the alkylidene chain is adjacent to the metal.....	136
Figure 3.25.	Dimeric product containing two five-membered rings formed by the reaction of Mo(NAr)(<i>trans</i> -CHCHCHMe)(O- <i>t</i> -Bu) ₂ (quin) with DEDPM and isolated via column chromatography.....	142
Figure 3.26.	CDCl ₃ ¹ H NMR of the dimeric product containing two five-membered rings formed by the reaction of Mo(NAr)(<i>trans</i> -CHCHCHMe)(O- <i>t</i> -Bu) ₂ (quin) with DEDPM.....	142
Figure 3.27.	CDCl ₃ ¹ H NMR of the trimeric products containing three five-membered rings formed by the reaction of Mo(NAr)(<i>trans</i> -CHCHCHMe)(O- <i>t</i> -Bu) ₂ (quin) with DEDPM.....	143
Figure 3.28.	Different possible five-membered ring trimeric isomers formed by reacting DEDPM with Mo(NAr)(<i>trans</i> -CHCHCHMe)(O- <i>t</i> -Bu) ₂ (quin) and quenching with benzaldehyde.....	143
Figure 3.29.	Symmetric trimeric and dimeric products produced by the reaction of DEDPM with Mo(NAr)(CH[5])(O- <i>t</i> -Bu) ₂ (quin) and isolated by column chromatography.....	144
Figure 3.30.	CDCl ₃ ¹ H NMR of the symmetric trimeric product containing three five-membered rings (See Figure 3.29) formed by the reaction of Mo(NAr)(CH[5])(O- <i>t</i> -Bu) ₂ (quin) with DEDPM.....	145
Figure 3.31.	CDCl ₃ ¹ H NMR of the symmetric tetramer containing four five-membered rings (See Figure 3.29) formed by the reaction of Mo(NAr)(CH[5])(O- <i>t</i> -Bu) ₂ (quin) with DEDPM.....	146
Figure 3.32.	HPLC separation of oligomers comprised of 4 to 6 five-membered rings.....	147
Figure 3.33.	300 K absorption spectra of oligomers comprised of 2 to 10 five-membered rings.....	148

Appendix 1

Figure A.1.	Possible configurations of the benzyl cation {MesNpy}Hf(Bn){B(C ₆ F ₅) ₄ } produced by the activation of [MesNpy]Hf(Bn) ₂ with {Ph ₃ C}{B(C ₆ F ₅) ₄ }.....	161
--------------------	---	-----

LIST OF SCHEMES

Introduction

Scheme I.1. The activation and initiation steps in a typical polymerization reaction.....21

Chapter 1

Scheme 1.1. Synthesis of $[\text{Ar}_{\text{Cl}_1}\text{N}_2\text{NMe}]\text{MCl}_2$ (M = Hf, Zr).....25

Scheme 1.2. Insertion of isobutene into $\{[\text{Ar}_{\text{Cl}_1}\text{N}_2\text{NMe}]\text{Hf}(i\text{-Bu})\}\{\text{B}(\text{C}_6\text{F}_5)_4\}$32

Chapter 2

Scheme 2.1. Synthesis of Synthesis of $[(2,6\text{-Cl}_2\text{C}_6\text{H}_3\text{NHCH}_2)_2\text{C}(\text{CH}_3)(2\text{-C}_5\text{H}_4\text{N})][\text{Ar}_{\text{Cl}_2}\text{Npy}]\text{H}_2$56

Scheme 2.2. Synthesis of $[\text{Ar}_{\text{Cl}_2}\text{Npy}]\text{MCl}_2$ (M = Zr, Hf).....56

Scheme 2.3. Reactions leading to products **1** through **7**.....60

Scheme 2.4. Formation of dimeric monocations, $\{[\text{Ar}_{\text{Cl}_2}\text{Npy}]_2\text{M}_2\text{Me}_3\}^+$68

Scheme 2.5. Activation of $[\text{Ar}_{\text{Cl}_2}\text{Npy}]\text{Hf}(i\text{-Bu})_2$ with $\{\text{Ph}_3\text{C}\}\{\text{B}(\text{C}_6\text{F}_5)_4\}$70

Chapter 3

Scheme 3.1. ADMET Polymerization and ROMP techniques used for the synthesis of conjugated polyenes.....90

Scheme 3.2. Alkyne polymerization employing transition metal catalysts.....91

Scheme 3.3. Cyclopolymerization of 1,6-heptadiynes.....92

Scheme 3.4. Reaction of $\text{Mo}(\text{NR}')(\text{CHR}'')(\text{OR})_2$ with 1,6-heptadiyne derivatives (for DEDPM, X = C(CO₂Et)₂).....93

Scheme 3.5. Synthesis of $\text{Mo}(\text{NAr})(\text{trans-CHCHCHMe})(\text{O-}t\text{-Bu})_2(\text{quin})$97

Scheme 3.6. Possible Rotamers of $\text{Mo}(\text{NAr})(\text{trans-CHCHCHMe})(\text{OR})_2$ and $\text{Mo}(\text{NAr})(\text{trans-CHCHCHMe})(\text{OR})_2(\text{quin})$98

Scheme 3.7. Synthesis of $\text{Mo}(\text{NAr})(\text{CH}[5])(\text{O-}t\text{-Bu})_2$104

Scheme 3.8. Synthesis of the five-membered ring triene substrate (**8c**).....105

Scheme 3.9. Synthesis of $\text{Mo}[1\text{-methylidene-3-methylen-5,5-bis(carboxyethyl)cyclohex-1-ene}][\text{NAr}](\text{O-}t\text{-Bu})_2$ (**9b**).....109

Appendix 1

Scheme A.1. Activation of $[\text{MesNpy}]\text{Hf}(\text{Bn})_2$ with $\text{B}(\text{C}_6\text{F}_5)_3$162

LIST OF TABLES

Chapter 1

Table 1.1.	Bond lengths [Å] and angles [°] for $[\text{Ar}_{\text{Cl}}\text{N}_2\text{NMe}]\text{Hf}(i\text{-Bu})_2$	27
Table 1.2.	Crystal data and structure refinement for $[\text{Ar}_{\text{Cl}}\text{N}_2\text{NMe}]\text{Hf}(i\text{-Bu})_2$	28
Table 1.3.	Poly(1-hexene) prepared using the $\{[\text{Ar}_{\text{Cl}}\text{N}_2\text{NMe}]\text{ZrMe}\}\{\text{B}(\text{C}_6\text{F}_5)_4\}$ initiator.....	34
Table 1.4.	Poly(1-hexene) prepared using the $\{[\text{Ar}_{\text{Cl}}\text{N}_2\text{NMe}]\text{Hf}(\text{R})\}^+$ initiator.....	35
Table 1.5.	Equivalents of β -hydride elimination versus initiator present after two successive polymerizations of 300 equivalents of 1-hexene by $\{[\text{Ar}_{\text{Cl}}\text{N}_2\text{NMe}]\text{Hf}(\text{R})\}\{\text{B}(\text{C}_6\text{F}_5)_4\}$	40
Table 1.6.	Polymer analysis results for the consumption of 1-hexene by $\{[\text{Ar}_{\text{Cl}}\text{N}_2\text{NMe}]\text{HfMe}\}\{\text{B}(\text{C}_6\text{F}_5)_4\}$ in the presence of $(i\text{-Pr})_2\text{O}$	43

Chapter 2

Table 2.1.	Bond lengths [Å] and angles [°] for $[\text{Ar}_{\text{Cl}_2}\text{Npy}]\text{Hf}(i\text{-Bu})_2$	58
Table 2.2.	Bond lengths [Å] and angles [°] for $[\text{Ar}_{(\text{FNMe}_2)_2}\text{Npy}]\text{Hf}(\text{F})\text{Cl}$	63
Table 2.3.	Crystal data and structure refinement for $[\text{Ar}_{(\text{FNMe}_2)_2}\text{Npy}]\text{Hf}(\text{F})\text{Cl}$ and $[\text{Ar}_{\text{F}_2}\text{Npy}]\text{Hf}(i\text{-Bu})_2$	64
Table 2.4.	Bond lengths [Å] and angles [°] for $[\text{Ar}_{\text{F}_2}\text{Npy}]\text{Hf}(i\text{-Bu})_2$	67
Table 2.5.	Kinetic data for polymerization of 1-hexene by $\{[\text{Ar}_{\text{Cl}_2}\text{Npy}]\text{Hf}(i\text{-Bu})\}\{\text{B}(\text{C}_6\text{F}_5)_4\}$ and $\{[\text{Ar}_{\text{F}_2}\text{Npy}]\text{Hf}(i\text{-Bu})\}\{\text{B}(\text{C}_6\text{F}_5)_4\}$. ^a Values reported by Dr. Klaus Ruhland.....	74
Table 2.6.	β -Hydride elimination associated with the polymerization of 1-hexene catalyzed by $\{[\text{Ar}_{\text{X}_2}\text{Npy}]\text{Hf}(i\text{-Bu})\}\{\text{B}(\text{C}_6\text{F}_5)_4\}$ in $\text{C}_6\text{D}_5\text{Br}$	75

Chapter 3

Table 3.1.	Selected bond lengths [Å] and angles [°] for $\text{Mo}(\text{NAr})(\text{trans-CHCHCHMe})(\text{O-}t\text{-Bu})_2(\text{quin})$	99
Table 3.2.	Selected bond lengths [Å] and angles [°] for $\text{Mo}(\text{NAr})(\text{CH}[5])(\text{O-}t\text{-Bu})_2(\text{quin})$	107
Table 3.3.	Reaction conditions for the synthesis of poly(DEDPM) and the percentages of five-membered rings produced during the cyclopolymerization.....	111
Table 3.4.	Molecular weights and polydispersities for polyenes formed by the cyclopolymerization of DEDPM by $\text{Mo}(\text{NAr})(\text{CHR})(\text{O-}t\text{-Bu})_2(\text{quin})$ ($\text{R} = \text{trans-CHCHMe}, \text{CMe}_3, [5]$) in CD_2Cl_2	113
Table 3.5.	Rates constants of polymerization (k_p) of 40 equivalents of DEDPM by $\text{Mo}(\text{NAr})(\text{trans-CHCHCHMe})(\text{O-}t\text{-Bu})_2(\text{quin})$ in CD_2Cl_2 from -10 to 10 °C...	116
Table 3.6.	Rates constants of polymerization (k_p) of 40 equivalents of DEDPM by $\text{Mo}(\text{NAr})(\text{trans-CHCHCHMe})(\text{OAd})_2(\text{quin})$	120

Table 3.7.	Molecular weight ratios ($M_n(f/c) = M_n(\text{found})/M_n(\text{calculated})$) and polydispersities for polyenes formed by the cyclopolymerization of DEDPM by $\text{Mo}(\text{NAr})(\text{CH}[5])(\text{O}-t\text{-Bu})_2(\text{quin})$ in dichloromethane, starting at $-30\text{ }^\circ\text{C}$...121
Table 3.8.	Rates of propagation versus rates of initiation for reactions of $\text{Mo}(\text{NAr})(\text{trans-CHCHCHMe})(\text{O}-t\text{-Bu})_2(\text{quin})$ with 1.06 to 2.53 equivalents of DEDPM at $22\text{ }^\circ\text{C}$ (for comparison, $k_p/k_i = 5.8$ for $\text{Mo}(\text{NAr})(\text{CHCMe}_3)(\text{O}-t\text{-Bu})_2(\text{quin})$).....124
Table 3.9.	Rates of propagation versus rates of initiation for reactions of $\text{Mo}(\text{NAr})(\text{trans-CHCHCHMe})[\text{OCMe}(\text{CF}_3)_2]_2(\text{quin})$ with 0.78 to 2.40 equivalents of DEDPM at $22\text{ }^\circ\text{C}$126
Table 3.10.	Rates of propagation versus rates of initiation for reactions of $\text{Mo}(\text{NAr})(\text{trans-CHCHCHMe})(\text{OAd})_2(\text{quin})$ with DEDPM at $22\text{ }^\circ\text{C}$138
Table 3.11.	Rates of propagation versus rates of initiation for reactions of $\text{Mo}(\text{NAr})(\text{CH}[5])(\text{O}-t\text{-Bu})_2(\text{quin})$ with 1.05 to 1.37 equivalents of DEDPM in CD_2Cl_2 at $22\text{ }^\circ\text{C}$139
Table 3.12.	$E(0-1)$ (λ_{max}) and $E(0-0)$ values for oligomers comprised of 2 to 10 five-membered rings.147
Table 3.13.	Polymerization of 30 equivalents of DEDPM by recently developed Schrock-group catalysts. ^a Catalysts synthesized by Amritanshu Sinha. ^b Catalysts prepared by Tatiana Pilyugina.....149

Appendix 2

Table A.1.	Atomic coordinates ($\times 10^4$) and equivalent isotropic displacement parameters ($\text{\AA}^2 \times 10^3$) for $[\text{Ar}_{\text{Cl}}\text{N}_2\text{NMe}]\text{Hf}(i\text{-Bu})_2$. $U(\text{eq})$ is defined as one third of the trace of the orthogonalized U^{ij} tensor.....167
Table A.2.	Atomic coordinates ($\times 10^4$) and equivalent isotropic displacement parameters ($\text{\AA}^2 \times 10^3$) for $[\text{Ar}_{(\text{FNMMe}_2)_2}\text{Npy}]\text{Hf}(\text{F})\text{Cl}$. $U(\text{eq})$ is defined as one third of the trace of the orthogonalized U^{ij} tensor.....168
Table A.3.	Atomic coordinates ($\times 10^4$) and equivalent isotropic displacement parameters ($\text{\AA}^2 \times 10^3$) for $[\text{Ar}_{\text{F}_2}\text{Npy}]\text{Hf}(i\text{-Bu})_2$. $U(\text{eq})$ is defined as one third of the trace of the orthogonalized U^{ij} tensor.....169
Table A.4.	Crystal data and structure refinement for $\text{Mo}(\text{NAr})(\text{trans-CHCHCHMe})(\text{O}-t\text{-Bu})_2(\text{quin})$170
Table A.5.	Atomic coordinates ($\times 10^4$) and equivalent isotropic displacement parameters ($\text{\AA}^2 \times 10^3$) for $\text{Mo}(\text{NAr})(\text{CHCHCHMe})(\text{O}-t\text{-Bu})_2(\text{quin})$. $U(\text{eq})$ is defined as one third of the trace of the orthogonalized U^{ij} tensor.....171
Table A.6.	Crystal data and structure refinement for $\text{Mo}(\text{NAr})(\text{CH}[5])(\text{O}-t\text{-Bu})_2$173
Table A.7.	Atomic coordinates ($\times 10^4$) and equivalent isotropic displacement Parameters ($\text{\AA}^2 \times 10^3$) for $\text{Mo}(\text{NAr})(\text{CH}[5])(\text{O}-t\text{-Bu})_2$. $U(\text{eq})$ is defined as one third of the trace of the orthogonalized U^{ij} tensor.....174

General Introduction for Chapters 1 and 2

An important goal of synthetic polymer chemistry is the design of catalysts that are capable of polymerizing α -olefins in a living manner. Since the physical and mechanical properties of polyolefins are dependent upon polymer composition and architecture, the ability to synthesize custom-designed polymers is highly desirable. The living nature of a polymerization is evaluated by several criteria,¹ and we are interested in synthesizing catalysts that polymerize α -olefins in a truly living manner.

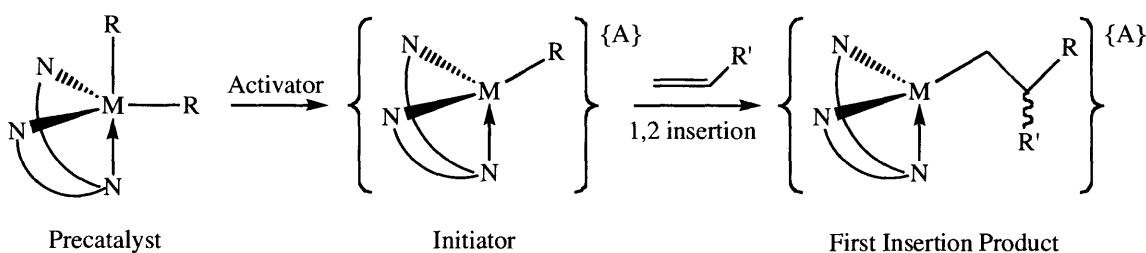
In a living polymerization, each catalyst forms a single polymer chain. The propagating species is stable throughout the reaction, and chain termination does not occur in the absence of monomer. Complete monomer conversion is observed, and chain growth continues upon further monomer addition. Polymer molecular weights match those calculated based on the number of equivalents of monomer added, and molecular weight distributions are very narrow, with the ratio of the weight average molecular weight to the number average molecular weight (M_w/M_n) approaching 1. All of these criteria must be met in order for a polymerization to proceed in a truly living manner.¹

Recent activity in the area of living Ziegler-Natta catalysis has centered on the development of well-behaved, non-metallocene systems.¹⁻⁵ Since McConville's discovery of titanium and zirconium olefin polymerization catalysts that contain simple aryl-substituted diamido ligands,⁶⁻⁹ a variety of non-metallocene group 4 catalysts have been reported,¹ including those developed by Sita,¹⁰⁻¹³ Kol,¹⁴⁻¹⁸ Coates,^{1,3,19,20} Jeon,²¹ Brookhart,^{22,23} Mashima,²⁴ and Fujita.²⁵⁻²⁹

Our attention has recently focused on zirconium and hafnium dialkyl complexes that contain diamido-donor ligands.³⁰⁻⁴⁵ For example, catalysts containing a diamido oxygen donor ligand with a phenolate backbone ($[(t\text{-BuN-}o\text{-C}_6\text{H}_4)_2\text{O}]^{2-}$)^{30,33,35,37,42} or a diamido pyridine donor ligand with an enforced facial geometry ($[(\text{MesitylNCH}_2)_2\text{C}(\text{CH}_3)(2\text{-C}_5\text{H}_4\text{N})]^{2-}$) were found to polymerize 1-hexene in a highly living manner.⁴⁶⁻⁴⁹ These tridentate ligands may adopt a pseudo-meridional (mer) or a pseudo-facial (fac) conformation about the metal center, depending on the geometry of the ligand backbone. Catalyst systems containing these ligands can be fine-tuned by

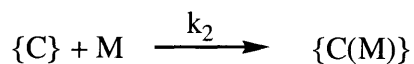
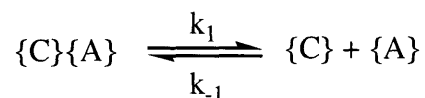
modifying substituents on the amido and donor groups.

In a typical polymerization reaction, the activator reacts with the dialkyl complex to generate a monoalkyl cation that is paired with a weakly coordinating anion (Scheme I.1). Typical activators include $\{\text{Ph}_3\text{C}\}\{\text{B}(\text{C}_6\text{F}_5)_4\}$, $\{\text{PhNMe}_2\text{H}\}\{\text{B}(\text{C}_6\text{F}_5)_4\}$, and $\text{B}(\text{C}_6\text{F}_5)_3$. The α -olefin can insert into the metal-carbon bond of the monoalkyl cation in a 1,2 or 2,1 manner. In these studies, 1-hexene is employed as a monomer because it is a liquid and is therefore easy to measure and work with. In polymerization reactions employing catalysts containing diamido-donor ligands, 1-hexene typically inserts into the metal-carbon bond in a 1,2 manner. After the first insertion product is generated, initiation is complete. The propagating species is generated when additional equivalents of olefin insert into the metal-carbon bond of the alkyl chain. In a truly living polymerization, it is important that the rate of initiation (k_i) is greater than or equal to the rate of propagation (k_p).



Scheme I.1. The activation and initiation steps in a typical polymerization reaction.

If the polymerization is living, a first-order dependence on metal concentration as well as on olefin concentration is observed. As shown below, the cation ($\{\text{C}\}$) must dissociate from the anion ($\{\text{A}\}$) before it may react with olefin (M) to produce the propagating species ($\{\text{C}(\text{M})\}$).⁵⁰



The following equation may be derived based on simple first-order kinetics: $\ln[M] = \ln[M_0] - k_{\text{obs}}(t)$, where $[M]$ = monomer concentration, $[M_0]$ = initial monomer concentration, t = time, and $k_{\text{obs}} = (k_1 k_2 [\{C_{\text{total}}\}] / (k_{-1} [\{A\}])$.⁵¹ The plot of the $\ln[M]$ versus time should be linear, and the observed rate constant (k_{obs}) is equal to the slope. The first-order rate constant of polymerization (k_p) is equal to k_{obs} divided by the catalyst concentration.

The goal of this research is to develop and evaluate new catalysts for the living polymerization of α -olefins. The effects of ligand modification on catalyst behavior and polymer characteristics are explored in detail. The majority of the work presented in Chapters 1 and 2 has already appeared in print.^{52,53}

Chapter 1

An Evaluation of Zirconium and Hafnium Complexes that Contain the Electron-Withdrawing Diamido-Donor Ligand, $[(2,6\text{-Cl}_2\text{C}_6\text{H}_3\text{NCH}_2\text{CH}_2)_2\text{NCH}_3]^2-$, for the Polymerization of 1-Hexene

Much of this work has already appeared in print.⁵³

1.1 Introduction

Cationic zirconium alkyl complexes that contain the $[(\text{MesitylNCH}_2\text{CH}_2)_2\text{NMe}]^{2-}$ ligand (Figure 1.1) undergo *ortho*-methyl C-H activation during polymerization, which leads to the formation of a catalytically inactive complex.^{30,34} Preliminary studies showed that ligand decomposition can be avoided through the use of 2,6- $\text{Cl}_2\text{C}_6\text{H}_3$ amido substituents instead of mesityl substituents.³⁴ The reaction of $[\text{Ar}_{\text{Cl}}\text{N}_2\text{NMe}]\text{ZrMe}_2$ with $\{\text{PhNMe}_2\text{H}\}\{\text{B}(\text{C}_6\text{F}_5)_4\}$ in bromobenzene at $-20\text{ }^\circ\text{C}$ produced methane and $\{[\text{Ar}_{\text{Cl}}\text{N}_2\text{NMe}]\text{ZrMe}(\text{PhNMe}_2)\}\{\text{B}(\text{C}_6\text{F}_5)_4\}$, which was highly active for the polymerization of 1-hexene. Although the polydispersities of the resulting polymers were less than 1.1, $M_n(\text{found})/M_n(\text{calculated})$ ratios were significantly greater than 1. This research examines in detail the behavior of zirconium and hafnium alkyl complexes that contain the $[(2,6\text{-Cl}_2\text{C}_6\text{H}_3\text{NCH}_2\text{CH}_2)_2\text{NMe}]^{2-}$ ligand in the polymerization of 1-hexene.

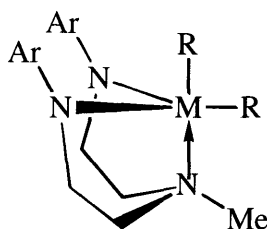


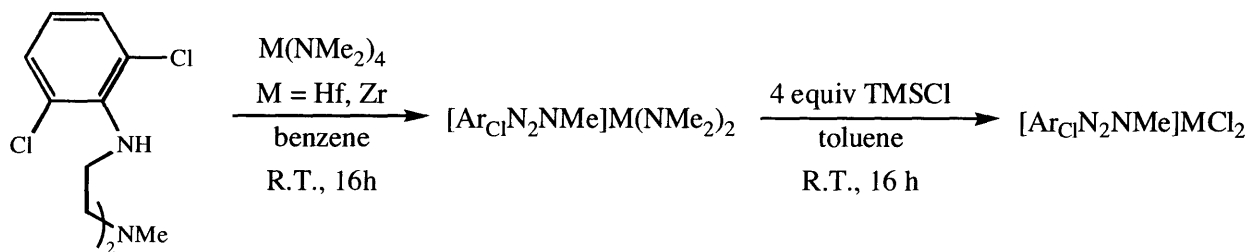
Figure 1.1. Complexes containing the $[(\text{ArNCH}_2\text{CH}_2)_2\text{NMe}]^{2-}$ ligand (Ar = Mes, 2,6- $\text{Cl}_2\text{C}_6\text{H}_3$).

1.2 Preparation of (2,6- $\text{Cl}_2\text{C}_6\text{H}_3\text{NHCH}_2\text{CH}_2$)₂NMe ($\text{H}_2[\text{Ar}_{\text{Cl}}\text{N}_2\text{NMe}]$) and Complexes that Contain the $[\text{Ar}_{\text{Cl}}\text{N}_2\text{NMe}]^{2-}$ Ligand

The palladium-catalyzed coupling reaction between 2-bromo-1,3-dichlorobenzene and $(\text{H}_2\text{NCH}_2\text{CH}_2)_2\text{NH}$ produces oily $\text{H}_2[(2,6\text{-Cl}_2\text{C}_6\text{H}_3\text{NCH}_2\text{CH}_2)_2\text{NH}]$ ($\text{H}_2[\text{Ar}_{\text{Cl}}\text{N}_2\text{NH}]$) in 75-85% yield.³⁴ Impurities are present that we suspect result primarily from competitive coupling at the 2 and 6 positions. Ligand purification via column chromatography and recrystallization at this stage produced pure $\text{H}_2[\text{Ar}_{\text{Cl}}\text{N}_2\text{NH}]$ in 56% yield. The central nitrogen in $\text{H}_2[\text{Ar}_{\text{Cl}}\text{N}_2\text{NH}]$ was

then methylated with MeI in the presence of K_2CO_3 in CH_3CN to give $H_2[Ar_{Cl}N_2NMe]$ in 63% yield.

$H_2[Ar_{Cl}N_2NMe]$ reacts smoothly with $M(NMe_2)_4$ ($M = Hf, Zr$) to give $[Ar_{Cl}N_2NMe]M(NMe_2)_2$ ^{34,54} in 80 to 90% yield (Scheme 1.1). The dimethylamido resonances in the proton NMR spectra of $[Ar_{Cl}N_2NMe]M(NMe_2)_2$ are found as two singlets. This complex is characterized by mirror symmetry, and the aryl groups rotate freely on the NMR timescale. The reaction of 3 to 5 equivalents of $TMSCl$ with $[Ar_{Cl}N_2NMe]M(NMe_2)_2$ affords $[Ar_{Cl}N_2NMe]MCl_2$ ^{34,54} a molecule whose NMR spectra are also consistent with mirror symmetry. Alkylation of the $[Ar_{Cl}N_2NMe]MCl_2$ species with $MeMgBr$ yields $[Ar_{Cl}N_2NMe]MMe_2$ complexes, which are white powders that are only sparingly soluble in toluene and bromobenzene. A single resonance for two methyl groups appears at 0.60 ppm in the room temperature 1H NMR spectrum of $[Ar_{Cl}N_2NMe]ZrMe_2$ ³⁴ in C_6D_6 , while two methyl resonances appear at 0.18 and 0.49 ppm in the spectrum of $[Ar_{Cl}N_2NMe]HfMe_2$ ⁵⁴. The two methyl resonances in the zirconium compound are accidentally coincident, appearing as two resonances in C_6D_5Br at 0.29 and 0.33 ppm in the 1H NMR spectrum and at 45.32 and 46.13 ppm in the ^{13}C NMR spectrum.



Scheme 1.1. Synthesis of $[Ar_{Cl}N_2NMe]MCl_2$ ($M = Hf, Zr$).

On the basis of 1H NOESY experiments,⁵⁴ the resonance for the MMe group closest to the ligand NMe group is found downfield of the resonance for the other MMe group in the proton NMR spectrum. The MMe group nearest the ligand NMe group will be called the Me_{syn} group, and that furthest from the ligand NMe group will be called the Me_{anti} group. Although the

resonance for the Me_{syn} group is found downfield of the resonance for the Me_{anti} group in the proton NMR spectrum, the resonance for the Me_{syn} group is found *upfield* of the resonance for the Me_{anti} group in the *carbon* NMR spectrum.

Treatment of [Ar_{Cl}N₂NMe]ZrCl₂ with 2 equivalents of isobutyl lithium appeared to yield [Ar_{Cl}N₂NMe]Zr(*i*-Bu)₂, although this compound decomposed at room temperature and therefore could not be isolated. However, addition of 2 equivalents of isobutyl lithium to [Ar_{Cl}N₂NMe]HfCl₂ produced [Ar_{Cl}N₂NMe]Hf(*i*-Bu)₂ in 73% yield. Recrystallization of [Ar_{Cl}N₂NMe]Hf(*i*-Bu)₂ from pentane at -30 °C yielded single crystals suitable for X-ray diffraction (Figure 1.2). Bond lengths and angles can be found in Table 1.1 and crystal parameters can be found in Table 1.2. The structure is approximately a square pyramid in which one of the isobutyl groups (C(5)) occupies the apical position. The C(1)-Hf-N(3) bond angle is 139.59°, which is 9.17° greater than the analogous bond angle in [Ar_{Cl}N₂NMe]ZrMe₂,³⁴ the C(5)-Hf-N(3) angle therefore is only 118.79°, while the C(1)-Hf-C(5) angle is 101.62°. The Hf-N(3) bond distance of 2.378(3) Å is somewhat long for a donor-M distance in compounds of this type. The Hf-N_{amido} and Hf-C_α bond distances are within the expected range. The CHMe₂ group of the syn isobutyl group is turned away from the NMe group toward the anti isobutyl group, pushing the CHMe₂ group of the anti isobutyl group away. The Hf-C_α-C_β angles are similar (123.8° and 126.6°). There is no significant interaction between the metal and one of the *ortho*-chlorines in the aryl group, which was found to be the case in a related complex, [(2,6-Cl₂C₆H₃NHCH₂)₂C(CH₃)(2-C₅H₄N)]Hf(*i*-Bu)₂.⁵²

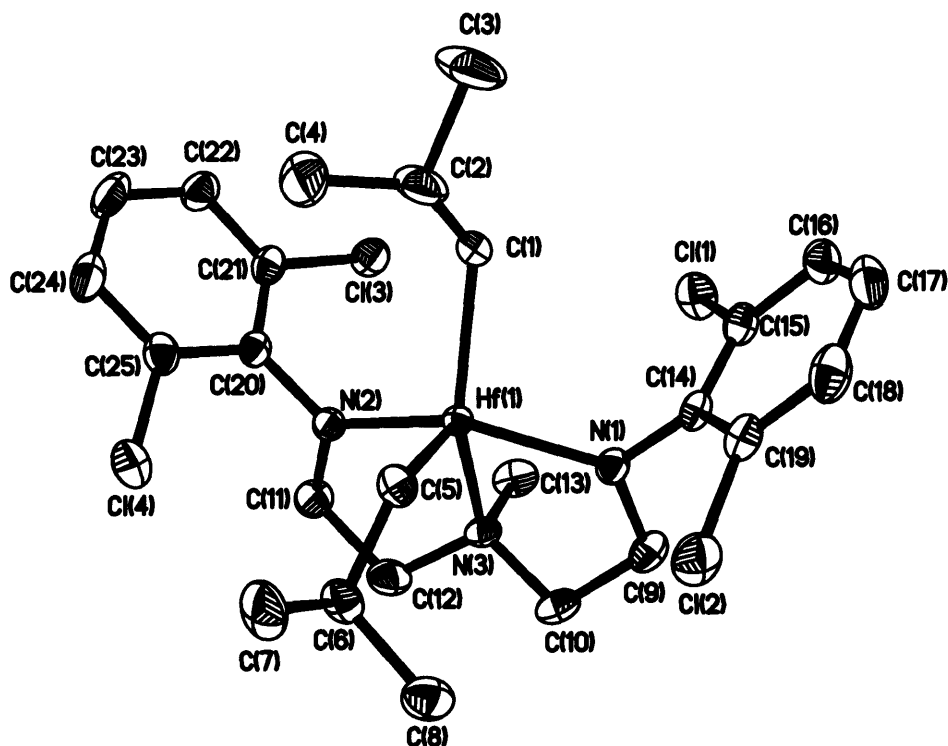


Figure 1.2. Thermal ellipsoid drawing of $[\text{Ar}_{\text{C1}}\text{N}_2\text{NMe}]\text{Hf}(i\text{-Bu})_2$ at the 30% probability level.

Table 1.1. Bond lengths [\AA] and angles [$^\circ$] for $[\text{Ar}_{\text{C1}}\text{N}_2\text{NMe}]\text{Hf}(i\text{-Bu})_2$.

Hf-N(1)	2.104(3)	N(3)-Hf-C(1)	139.59(12)
Hf-N(2)	2.105(3)	N(3)-Hf-C(5)	118.79(11)
Hf-N(3)	2.378(3)	C(1)-Hf-C(5)	101.62(14)
Hf-C(1)	2.220(4)	C(20)-N(2)-Hf	124.39(19)
Hf-C(5)	2.207(3)	C(11)-N(2)-Hf	123.7(2)
N(1)-Hf-N(2)	141.77(10)	C(14)-N(1)-Hf	123.1(2)
N(1)-Hf-C(1)	100.48(11)	C(9)-N(1)-Hf	124.4(2)
N(1)-Hf-C(5)	103.17(12)	C(6)-C(5)-Hf	126.6(2)
N(1)-Hf-N(3)	71.19(10)	C(12)-N(3)-Hf	106.2(2)
N(2)-Hf-C(1)	102.49(11)	C(10)-N(3)-Hf	107.0(2)
N(2)-Hf-C(5)	101.61(12)	C(13)-N(3)-Hf	111.5(2)
N(2)-Hf-N(3)	71.47(10)	C(2)-C(1)-Hf	123.8(3)

Table 1.2. Crystal data and structure refinement for $[\text{Ar}_{\text{Cl}}\text{N}_2\text{NMe}]\text{Hf}(i\text{-Bu})_2$.

Empirical formula	$\text{C}_{25}\text{H}_{35}\text{Cl}_4\text{HfN}_3$	
Formula weight	697.85	
Temperature	193(2) K	
Wavelength	0.71073 Å	
Crystal system	Monoclinic	
Space group	$P2_1/c$	
Unit cell dimensions	$a = 11.0327(7)$ Å	$\alpha = 90^\circ$
	$b = 13.0463(9)$ Å	$\beta = 94.8850(10)^\circ$
	$c = 19.8936(13)$ Å	$\gamma = 90^\circ$
Volume	$2853.0(3)$ Å ³	
Z	4	
Density (calculated)	1.625 mg/m ³	
Absorption coefficient	4.049 mm ⁻¹	
F(000)	1384	
Crystal size	$0.1 \times 0.1 \times 0.09$ mm ³	
Theta range for data collection	1.85 to 28.29°	
Index ranges	$-8 \leq h \leq 14$, $-16 \leq k \leq 17$, $-26 \leq l \leq 26$	
Reflections collected	17941	
Independent reflections	6725 [R(int) = 0.0565]	
Completeness to theta = 28.29°	94.7 %	
Refinement method	Full-matrix least-squares on F ²	
Data / restraints / parameters	6725 / 0 / 304	
Goodness-of-fit on F ²	0.810	
Final R indices [I > 2s(I)]	R1 = 0.0270, wR2 = 0.0733	
R indices (all data)	R1 = 0.0342, wR2 = 0.0779	
Extinction coefficient	0.00000(7)	
Largest diff. peak and hole	0.967 and -0.897 eÅ ⁻³	

Addition of 1 or more equivalents of *i*-BuMgCl to $[\text{Ar}_{\text{Cl}}\text{N}_2\text{NMe}]\text{HfCl}_2$ led to the formation of $[\text{Ar}_{\text{Cl}}\text{N}_2\text{NMe}]\text{Hf}(i\text{-Bu})\text{Cl}$.⁵⁴ Samples of $[\text{Ar}_{\text{Cl}}\text{N}_2\text{NMe}]\text{Hf}(i\text{-Bu})\text{Cl}$ were found to consist of two isomers, presumably those in which either the alkyl or the chloride is in the "syn" position nearest the NMe group. Recrystallization of mixtures of isomers of $[\text{Ar}_{\text{Cl}}\text{N}_2\text{NMe}]\text{Hf}(i\text{-Bu})\text{Cl}$ from ether resulted in a mixture that contained ~75% $[\text{Ar}_{\text{Cl}}\text{N}_2\text{NMe}]\text{Hf}(i\text{-Bu}_{\text{syn}})\text{Cl}_{\text{anti}}$, according to the chemical shift of the isobutyl methylene group.

The reaction of $[\text{Ar}_{\text{Cl}}\text{N}_2\text{NMe}]\text{Hf}(i\text{-Bu})\text{Cl}$ with 1 equivalent of MeMgCl afforded $[\text{Ar}_{\text{Cl}}\text{N}_2\text{NMe}]\text{Hf}(i\text{-Bu})\text{Me}$. Samples enriched in $[\text{Ar}_{\text{Cl}}\text{N}_2\text{NMe}]\text{Hf}(i\text{-Bu}_{\text{anti}})\text{Cl}_{\text{syn}}$ or $[\text{Ar}_{\text{Cl}}\text{N}_2\text{NMe}]\text{Hf}(i\text{-Bu}_{\text{syn}})\text{Cl}_{\text{anti}}$ form $[\text{Ar}_{\text{Cl}}\text{N}_2\text{NMe}]\text{Hf}(i\text{-Bu})\text{Me}$ mixtures that are enriched in the analogous isomer, according to ^1H NOESY experiments.⁵⁴ Mixtures of $[\text{Ar}_{\text{Cl}}\text{N}_2\text{NMe}]\text{Hf}(i\text{-Bu}_{\text{syn}})\text{Me}_{\text{anti}}$ and $[\text{Ar}_{\text{Cl}}\text{N}_2\text{NMe}]\text{Hf}(i\text{-Bu}_{\text{anti}})\text{Me}_{\text{syn}}$ then evolve to yield an equilibrium mixture of the two, with the isomer in which the methyl group is in the "syn" position predominating at higher temperatures. The anti/syn isomerization process for $[\text{Ar}_{\text{Cl}}\text{N}_2\text{NMe}]\text{Hf}(i\text{-Bu})\text{Me}$ between 30 °C and 90 °C was found to follow first-order kinetics. At temperatures higher than 70 °C, slow β -hydride elimination occurred, and isobutene gradually appeared in the ^1H NMR spectrum. During the isomerization of $[\text{Ar}_{\text{Cl}}\text{N}_2\text{NMe}]\text{Hf}(i\text{-Bu}_{\text{syn}})\text{Me}_{\text{anti}}$ to $[\text{Ar}_{\text{Cl}}\text{N}_2\text{NMe}]\text{Hf}(i\text{-Bu}_{\text{anti}})\text{Me}_{\text{syn}}$, which we call $\text{Me}_{\text{anti}} \rightarrow \text{Me}_{\text{syn}}$ isomerization, neither $[\text{Ar}_{\text{Cl}}\text{N}_2\text{NMe}]\text{Hf}(i\text{-Bu})_2$ nor $[\text{Ar}_{\text{Cl}}\text{N}_2\text{NMe}]\text{HfMe}_2$ is observed. The rate constants measured for the $\text{Me}_{\text{anti}} \rightarrow \text{Me}_{\text{syn}}$ process at different temperatures using a first-order approach to equilibrium are listed in the experimental section. The $\text{Me}_{\text{anti}} \rightarrow \text{Me}_{\text{syn}}$ conversion was found to take place with $\Delta H^\ddagger = 82.9$ kJ/mol and $\Delta S^\ddagger = -65.7$ J/mol·K and with $\Delta H = 2.2$ kJ/mol and $\Delta S = 8.3$ J/mol·K. It is unclear whether the ligand's central nitrogen donor remains bound to the metal or not during the $\text{Me}_{\text{anti}} \rightarrow \text{Me}_{\text{syn}}$ conversion process, and the ΔS^\ddagger value is not especially helpful in answering this question.

1.3 Activation of dialkyl complexes.

1.3.1 Activation of $[\text{Ar}_{\text{Cl}}\text{N}_2\text{NMe}]\text{MMe}_2$ (M = Hf, Zr)

Addition of 1 equivalent of $\{\text{Ph}_3\text{C}\}\{\text{B}(\text{C}_6\text{F}_5)_4\}$ to $[\text{Ar}_{\text{Cl}}\text{N}_2\text{NMe}]\text{MMe}_2$ (M = Hf, Zr) in $\text{C}_6\text{D}_5\text{Br}$ at -30 °C produced $\{[\text{Ar}_{\text{Cl}}\text{N}_2\text{NMe}]\text{MMe}\}\{\text{B}(\text{C}_6\text{F}_5)_4\}$ and Ph_3CCH_3 quantitatively, and was accompanied by an immediate color change of the solution from deep orange to yellow.^{54,55} Proton NMR spectra of the zirconium and hafnium cations at 0 °C are almost identical. The backbone methylene protons appear as four well-resolved multiplets between 2.6 ppm and 3.9 ppm and the NMe resonance appears at 2.3 ppm for both hafnium and zirconium complexes.

Free rotation of the aryl rings is evidenced by the presence of a sharp doublet representing 4 equivalent aryl *meta*-protons. Sharp M-Me resonances are found at 0.49 ppm for hafnium cations and 0.62 ppm for zirconium cations. While the zirconium and hafnium methyl cations are stable at 0 °C for at least 24 hours, both species slowly decompose at roughly similar rates at temperatures greater than 40 °C. Multiple decomposition products formed and could not be identified.

Abstraction of a methyl group from $[\text{Ar}_{\text{Cl}}\text{N}_2\text{NMe}]\text{MMe}_2$ (M = Hf, Zr) by $\text{B}(\text{C}_6\text{F}_5)_3$ in $\text{C}_6\text{D}_5\text{Br}$ at -30 °C yielded $\{[\text{Ar}_{\text{Cl}}\text{N}_2\text{NMe}]\text{MMe}\}\{\text{MeB}(\text{C}_6\text{F}_5)_3\}$. The reaction solution acquired a yellow color a few seconds after addition of $\text{B}(\text{C}_6\text{F}_5)_3$ as the cationic complex was formed. Proton NMR spectra of hafnium and zirconium methyl cations paired with the $\{\text{MeB}(\text{C}_6\text{F}_5)_3\}^-$ anion are essentially identical to those paired with the $\{\text{B}(\text{C}_6\text{F}_5)_4\}^-$ anion. These complexes are also stable at 0 °C for at least 24 hours and there is no significant difference in the stability of zirconium versus hafnium methyl cations.

As communicated previously,³⁴ protonation of a Zr-Me group in $[\text{Ar}_{\text{Cl}}\text{N}_2\text{NMe}]\text{ZrMe}_2$ with $\{\text{PhNMe}_2\text{H}\}\{\text{B}(\text{C}_6\text{F}_5)_4\}$ in bromobenzene at -20 °C produced methane and $\{[\text{Ar}_{\text{Cl}}\text{N}_2\text{NMe}]\text{ZrMe}(\text{PhNMe}_2)\}\{\text{B}(\text{C}_6\text{F}_5)_4\}$, which has mirror symmetry on the NMR timescale. The analogous activation of $[\text{Ar}_{\text{Cl}}\text{N}_2\text{NMe}]\text{HfMe}_2$ with $\{\text{PhNMe}_2\text{H}\}\{\text{B}(\text{C}_6\text{F}_5)_4\}$ yielded $\{[\text{Ar}_{\text{Cl}}\text{N}_2\text{NMe}]\text{HfMe}(\text{PhNMe}_2)\}\{\text{B}(\text{C}_6\text{F}_5)_4\}$, which also has mirror symmetry. As the temperature is lowered from room temperature to -10 °C, the Hf-Me resonance at 0.2 ppm broadens considerably compared to the Zr-Me resonance. We propose that this reversible process involves unsymmetrical interaction of bromobenzene with the metal center or hindered rotation of bound dimethylaniline about the M-N bond, or both. Free dimethylaniline is observed in the ^1H NMR spectra of both hafnium and zirconium cations at temperatures higher than 40 °C.

1.3.2 Activation of $[\text{Ar}_{\text{Cl}}\text{N}_2\text{NMe}]\text{Hf}(i\text{-Bu})_2$

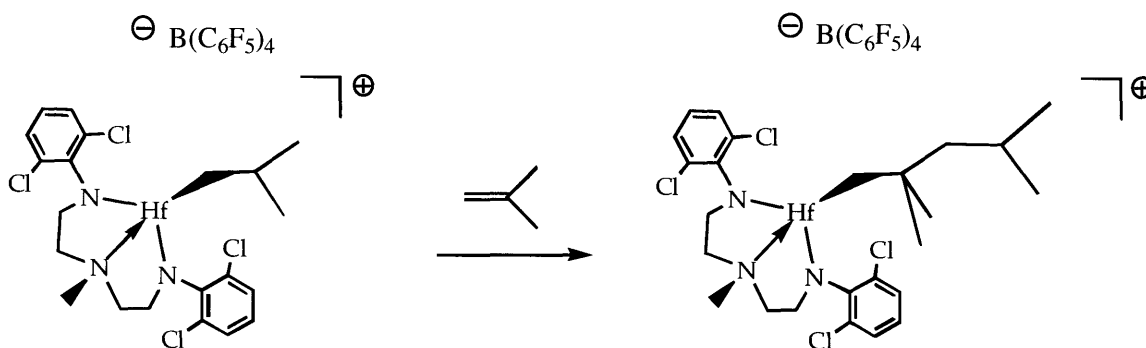
Addition of $\text{B}(\text{C}_6\text{F}_5)_3$ to $[\text{Ar}_{\text{Cl}}\text{N}_2\text{NMe}]\text{Hf}(i\text{-Bu})_2$ almost immediately yielded isobutene and pale yellow $\{[\text{Ar}_{\text{Cl}}\text{N}_2\text{NMe}]\text{Hf}(i\text{-Bu})\}\{\text{HB}(\text{C}_6\text{F}_5)_3\}$. In $\text{C}_6\text{D}_5\text{Br}$ at 0 °C, the isobutyl CH_3 and CH_2

resonances appear as broadened singlets at 0.91 and 0.96 ppm, respectively. On the basis of integration values, the methine resonance overlaps with the ligand NMe resonance at 2.58 ppm and cannot be distinguished from the NMe resonance as the temperature is varied from -30 to 40 °C. Resonances outside the range of 0 to 10 ppm are not observed. Broadening of the isobutyl resonances can be attributed to exchange processes that involve various ways for the anion or solvent to bind to the metal. In toluene, the expected splitting pattern for a freely rotating isobutyl group is observed (isobutyl CH_3 and CH_2 resonances are doublets found at 0.88 and 1.02 ppm, respectively). The methine resonance again appears to overlap with the NMe resonance as well as with a ligand ethylene resonance at 2.39 ppm.

Activation of $[\text{Ar}_{\text{Cl}}\text{N}_2\text{NMe}]\text{Hf}(i\text{-Bu})_2$ with $\{\text{Ph}_3\text{C}\}\{\text{B}(\text{C}_6\text{F}_5)_4\}$ in $\text{C}_6\text{D}_5\text{Br}$ at 0 °C yielded isobutene, $\{[\text{Ar}_{\text{Cl}}\text{N}_2\text{NMe}]\text{Hf}(i\text{-Bu})\}\{\text{B}(\text{C}_6\text{F}_5)_4\}$, and Ph_3CH , and was accompanied by an immediate color change of the solution from deep orange to yellow. The isobutyl CH_3 and CH_2 ^1H NMR resonances of the $\{[\text{Ar}_{\text{Cl}}\text{N}_2\text{NMe}]\text{Hf}(i\text{-Bu})\}^+$ ion also appear as broadened singlets at 0 °C, and the ^1H NMR spectrum is not markedly different from that of $\{[\text{Ar}_{\text{Cl}}\text{N}_2\text{NMe}]\text{Hf}(i\text{-Bu})\}\{\text{HB}(\text{C}_6\text{F}_5)_3\}$. Chemical shifts for the four ligand ethylene CH_2 resonances and the two ligand aryl proton resonances for these isobutyl cations are nearly identical to the corresponding shifts in the hafnium methyl cations.

The hafnium isobutyl cation, paired with either the $\{\text{HB}(\text{C}_6\text{F}_5)_3\}^-$ or $\{\text{B}(\text{C}_6\text{F}_5)_4\}^-$ anion, slowly reacts with isobutene produced during activation to afford what is proposed, on the basis of NMR data, to be the 1,2 insertion product of isobutene into the M-R bond of the isobutyl cation (Scheme 1.2). A downfield shift of the NMe resonance from 2.58 to 2.60 ppm is observed for the cation with the longer alkyl chain. The insertion product began to decompose after several hours at 0 °C; complete insertion required 1.5 weeks at -30 °C. Therefore, it was not possible to generate a pure sample of the insertion product. Addition of 1-hexene to a solution that contained the insertion product at 0 °C resulted in consumption of the insertion product and polymerization behavior that was not significantly different from that of the isobutyl cation.

Under 1 atm. of isobutene gas at 0 °C, $\{[\text{Ar}_{\text{Cl}}\text{N}_2\text{NMe}]\text{Hf}(i\text{-Bu})\}\{\text{HB}(\text{C}_6\text{F}_5)_3\}$ (formed by the activation of $[\text{Ar}_{\text{Cl}}\text{N}_2\text{NMe}]\text{Hf}(i\text{-Bu})_2$ with $\text{B}(\text{C}_6\text{F}_5)_3$) oligomerized isobutene.



Scheme 1.2. Insertion of isobutene into $\{[\text{Ar}_{\text{Cl}}\text{N}_2\text{NMe}]\text{Hf}(i\text{-Bu})\}\{\text{B}(\text{C}_6\text{F}_5)_4\}$.

Protonation of $[\text{Ar}_{\text{Cl}}\text{N}_2\text{NMe}]\text{Hf}(i\text{-Bu})_2$ with 1 equivalent of $\{\text{PhNMe}_2\text{H}\}\{\text{B}(\text{C}_6\text{F}_5)_4\}$ in bromobenzene produced isobutane, $\{[\text{Ar}_{\text{Cl}}\text{N}_2\text{NMe}]\text{Hf}(i\text{-Bu})\}\{\text{B}(\text{C}_6\text{F}_5)_4\}$, and free dimethylaniline. $\{[\text{Ar}_{\text{Cl}}\text{N}_2\text{NMe}]\text{Hf}(i\text{-Bu})\}\{\text{B}(\text{C}_6\text{F}_5)_4\}$ slowly reacted with dimethylaniline to form isobutene and an asymmetric complex that was not active for polymerization of 1-hexene. The asymmetric decomposition product was also observed upon addition of dimethylaniline to $\{[\text{Ar}_{\text{Cl}}\text{N}_2\text{NMe}]\text{Hf}(i\text{-Bu})\}\{\text{HB}(\text{C}_6\text{F}_5)_3\}$ (formed by activation of $[\text{Ar}_{\text{Cl}}\text{N}_2\text{NMe}]\text{Hf}(i\text{-Bu})_2$ with $\text{B}(\text{C}_6\text{F}_5)_3$). Complete conversion of the isobutyl cation to the asymmetric decomposition product was not observed, even when 10 equivalents of dimethylaniline were added and the solution stored at -30 °C for several weeks. According to ^1H NMR studies, added diethyl ether coordinates to the isobutyl cation, but not to the asymmetric decomposition product. Unfortunately, this asymmetric decomposition product could not be identified using 1D and 2D (gcosy) NMR techniques. A related cation, $\{[(\text{MesNCH}_2)_2\text{C}(\text{CH}_3)(2\text{-C}_5\text{H}_4\text{N})]\text{Hf}(i\text{-Bu})\}^+$ reacted with dimethylaniline to produce isobutane and a species with mirror symmetry that was proposed to contain an *ortho*-dimethylaminophenyl group.⁴⁶ The asymmetric decomposition product cannot be the same type as the one that contains the *ortho*-dimethylaminophenyl group, but it might result from a related CH activation process.

It would be possible to study the polymerization behavior of the hafnium isobutyl complex in the absence of isobutene if a methyl group could be selectively abstracted from $[\text{Ar}_{\text{Cl}}\text{N}_2\text{NMe}]\text{Hf}(i\text{-Bu})\text{Me}$. The reaction between mixtures of $[\text{Ar}_{\text{Cl}}\text{N}_2\text{NMe}]\text{Hf}(i\text{-Bu})\text{Me}$ isomers and $\{\text{Ph}_3\text{C}\}\{\text{B}(\text{C}_6\text{F}_5)_4\}$ in $\text{C}_6\text{D}_5\text{Br}$ at $0\text{ }^\circ\text{C}$ yielded 72% $\{[\text{Ar}_{\text{Cl}}\text{N}_2\text{NMe}]\text{Hf}(i\text{-Bu})\}\{\text{B}(\text{C}_6\text{F}_5)_4\}$ and 28% $\{[\text{Ar}_{\text{Cl}}\text{N}_2\text{NMe}]\text{Hf}(\text{Me})\}\{\text{B}(\text{C}_6\text{F}_5)_4\}$. Activation of $[\text{Ar}_{\text{Cl}}\text{N}_2\text{NMe}]\text{Hf}(i\text{-Bu})\text{Me}$ isomers with $\text{B}(\text{C}_6\text{F}_5)_3$ led to the nearly selective abstraction of a methyl group and the formation of about 95% $\{[\text{Ar}_{\text{Cl}}\text{N}_2\text{NMe}]\text{Hf}(i\text{-Bu})\}\{\text{MeB}(\text{C}_6\text{F}_5)_3\}$. Protonolysis by $\{\text{PhNMe}_2\text{H}\}\{\text{B}(\text{C}_6\text{F}_5)_4\}$ resulted in the exclusive formation of $\{[\text{Ar}_{\text{Cl}}\text{N}_2\text{NMe}]\text{Hf}(i\text{-Bu})\}\{\text{B}(\text{C}_6\text{F}_5)_4\}$, which subsequently reacted with dimethylaniline as described above. The outcome of activation of the mixed dialkyl species does not appear to depend on which isomer of the mixed alkyl complex predominates in the mixture. On the basis of these results, 100% selective removal of a methyl group in the isobutyl/methyl species does not appear to be possible under the conditions we have employed so far.

1.4 Polymerization of 1-Hexene

Consumption of up to 500 equivalents of 1-hexene by the $\{[\text{Ar}_{\text{Cl}}\text{N}_2\text{NMe}]\text{MMe}\}^+$ ($\text{M} = \text{Hf}, \text{Zr}$) initiator, formed by activation of $[\text{Ar}_{\text{Cl}}\text{N}_2\text{NMe}]\text{MMe}_2$ with either $\{\text{Ph}_3\text{C}\}\{\text{B}(\text{C}_6\text{F}_5)_4\}$ or $\text{B}(\text{C}_6\text{F}_5)_3$, is rapid and nearly complete within minutes at $0\text{ }^\circ\text{C}$ and therefore difficult to follow using ordinary NMR techniques. At zirconium catalyst concentrations up to 6 mM, plots of $\ln[1\text{-hexene}]$ versus time for the final 4 to 8% of the polymerization were linear, with k_p values ranging between 0.63 and 0.85 $\text{M}^{-1}\text{s}^{-1}$ (Table 1.3). These values agree with the value of 0.80 $\text{M}^{-1}\text{s}^{-1}$ estimated for polymerization of 1-hexene by $\{[\text{Ar}_{\text{Cl}}\text{N}_2\text{NMe}]\text{ZrMe}\}\{\text{B}(\text{C}_6\text{F}_5)_4\}$ in the absence of dimethylaniline base.³⁴ The consumption of the final 13% of 1-hexene at $0\text{ }^\circ\text{C}$ by $\{[\text{Ar}_{\text{Cl}}\text{N}_2\text{NMe}]\text{HfMe}\}\{\text{B}(\text{C}_6\text{F}_5)_4\}$ (Figure 1.3) was characterized by lower k_p values between 0.15 and 0.25 $\text{M}^{-1}\text{s}^{-1}$ (Table 1.4). In all reactions, $\{[\text{Ar}_{\text{Cl}}\text{N}_2\text{NMe}]\text{MMe}\}\{\text{B}(\text{C}_6\text{F}_5)_4\}$ ($\text{M} = \text{Hf}, \text{Zr}$) was completely consumed in the presence of 100 or more equivalents of 1-hexene.

Table 1.3. Poly(1-hexene) prepared using the $\{[Ar_{Cl}N_2NMe]ZrMe\}\{B(C_6F_5)_4\}$ initiator.

T (°C)	Solvent	[Zr] (M)	Equiv. 1-Hexene	M_n (f/c) ^a	PDI	$\beta_{1,2}\text{-H}^b$	k_p (M ⁻¹ s ⁻¹)
0	C ₆ H ₅ Cl	0.003	100	1.12	1.07		
0	C ₆ H ₅ Cl	0.003	200	0.97	1.10		
0	C ₆ H ₅ Cl	0.003	300	0.95	1.10		
0	C ₆ H ₅ Cl	0.003	400	0.97	1.08		
0	C ₆ H ₅ Cl	0.003	500	0.96	1.08		
0	C ₆ D ₅ Br	0.003	300			0.1	0.63
0	C ₆ D ₅ Br	0.006	100			0.1	0.85
-30	C ₆ D ₅ Br	0.006	200	1.1	1.08		

^a $M_n(\text{found})/M_n(\text{calculated})$. ^b $\beta_{1,2}\text{-H} = \beta\text{-hydride elimination following a 1,2 insertion versus initiator}$.

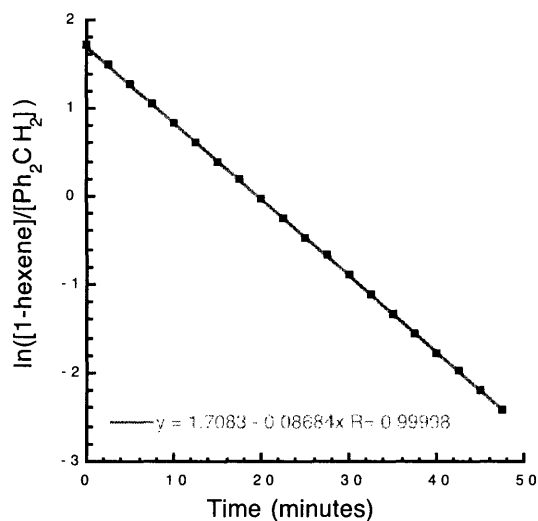


Figure 1.3. Consumption of the final 13% of 100 equivalents of 1-hexene at 0 °C by 0.006 M $\{[Ar_{Cl}N_2NMe]HfMe\}\{B(C_6F_5)_4\}$ (formed by the activation of $[Ar_{Cl}N_2NMe]HfMe_2$ with $\{Ph_3C\}\{B(C_6F_5)_4\}$).

Table 1.4. Poly(1-hexene) prepared using the $\{[\text{Ar}_{\text{Cl}}\text{N}_2\text{NMe}]\text{Hf}(\text{R})\}^+$ initiator.

R	T (°C)	[Hf] (M)	Anion	Equiv. 1-hexene	PDI	M_n (f/c) ^a	$\beta_{1,2}\text{-H}^b$	k_p (M ⁻¹ s ⁻¹)
Me	-30	0.006	$\{\text{B}(\text{C}_6\text{F}_5)_4\}$	200	1.04	1.1		
Me	0	0.006	$\{\text{B}(\text{C}_6\text{F}_5)_4\}$	100	1.1	0.8	0.6	0.24
Me	0	0.012	$\{\text{B}(\text{C}_6\text{F}_5)_4\}$	100	1.3	0.7	0.9	0.25
Me	0	0.012	$\{\text{B}(\text{C}_6\text{F}_5)_4\}$	269	1.3	0.8		
Me	0	0.003	$\{\text{B}(\text{C}_6\text{F}_5)_4\}$	400	1.4	0.7	0.6	0.15
Me	0	0.006	$\{\text{B}(\text{C}_6\text{F}_5)_4\}$	400	1.4	0.4	1.5	0.17
Me	0	0.006	$\{\text{MeB}(\text{C}_6\text{F}_5)_3\}^-$	200	1.2	0.9	0.4	0.19
<i>i</i> -Bu	-30	0.006	$\{\text{B}(\text{C}_6\text{F}_5)_4\}^-$	200	1.2	0.88		
<i>i</i> -Bu	0	0.003	$\{\text{B}(\text{C}_6\text{F}_5)_4\}^-$	500	1.3	0.55		
<i>i</i> -Bu	0	0.003	$\{\text{B}(\text{C}_6\text{F}_5)_4\}^-$	300	1.3	0.59	1.4	0.13
<i>i</i> -Bu	0	0.013	$\{\text{HB}(\text{C}_6\text{F}_5)_3\}^-$	50			1.0	0.25
<i>i</i> -Bu	0	0.012	$\{\text{B}(\text{C}_6\text{F}_5)_4\}^-$	100	1.2	0.51	1.9	

^a $M_n(\text{found})/M_n(\text{calculated})$. ^b $\beta_{1,2}\text{-H} = \beta\text{-hydride elimination following a 1,2 insertion versus initiator}$.

Polymerization of 100 to 500 equivalents of 1-hexene by 3 mM $\{[\text{Ar}_{\text{Cl}}\text{N}_2\text{NMe}]\text{ZrMe}\}\{\text{B}(\text{C}_6\text{F}_5)_4\}$ in chlorobenzene at 0 °C yielded poly(1-hexene) with M_n values close to those calculated for a perfectly living system (Figure 1.4, Table 1.3) and with PDI values ranging from 1.07 to 1.10. While the product of $\beta\text{-hydride elimination following a 2,1 insertion of 1-hexene ("}\beta_{2,1}\text{ product"}$) was not observed, a broad vinylidene resonance corresponding to the olefinic product of $\beta\text{-hydride elimination following a 1,2 insertion ("}\beta_{1,2}\text{ product"}$) grew in at 4.86 ppm^{50,56} in the ¹H NMR spectrum as 1-hexene was consumed. The final amount of the $\beta_{1,2}$ product was approximately 10% of the initiator present.

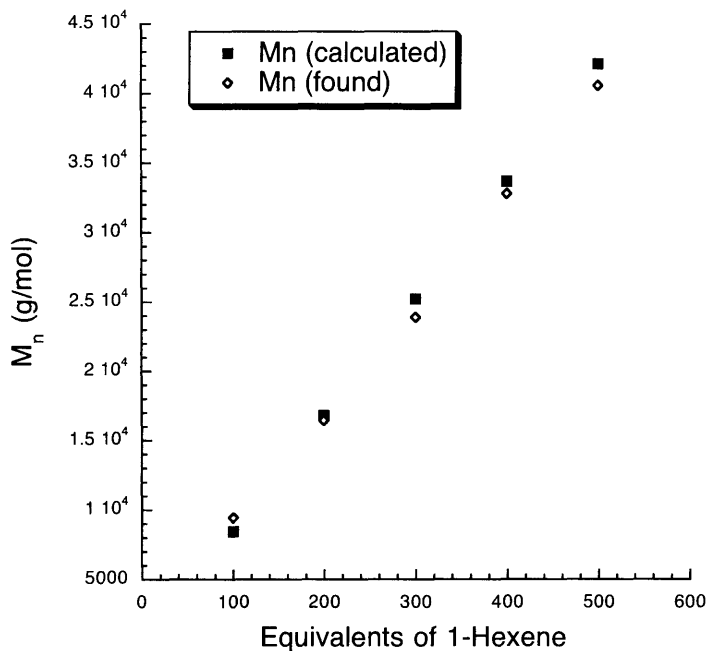


Figure 1.4. Molecular weights of poly(1-hexene) obtained with 3 mM $\{[\text{Ar}_{\text{Cl}}\text{N}_2\text{NMe}]\text{ZrMe}\}\{\text{B}(\text{C}_6\text{F}_5)_4\}$ in chlorobenzene at 0 °C.

When $\{[\text{Ar}_{\text{Cl}}\text{N}_2\text{NMe}]\text{HfMe}\}\{\text{B}(\text{C}_6\text{F}_5)_4\}$ or $\{[\text{Ar}_{\text{Cl}}\text{N}_2\text{NMe}]\text{HfMe}\}\{\text{MeB}(\text{C}_6\text{F}_5)_3\}$ was employed as an initiator at 0 °C, the resulting poly(1-hexene) had PDI values that ranged from 1.1 to 1.4 (Table 1.4). These systems are susceptible to a significant amount of β -hydride elimination and slower rates of initiation relative to propagation. Olefinic resonances between 5.3 and 5.5 ppm ascribed to a $\beta_{2,1}$ product^{46,56} were observed in amounts up to 1.5 equivalents of the initiator present. Since the resonances due to the $\beta_{2,1}$ products were not observed to grow after all of the 1-hexene had been consumed, it appears that a 2,1 β -hydride elimination product forms only when 1-hexene is present in higher concentrations. An olefinic resonance for the $\beta_{1,2}$ product grew in at 4.86 ppm in the ¹H NMR spectrum as 1-hexene was consumed (to between 0.6 and 1.5 equivalents versus initiator) and continued to grow to approximately 1 equivalent versus initiator after all 1-hexene had been consumed (integrations are not highly accurate under

these conditions, and the $\beta_{1,2}$ product, like isobutene, may be polymerized itself in the presence of $\{\text{Ph}_3\text{C}\}\{\text{B}(\text{C}_6\text{F}_5)_4\}$ under these conditions).

GPC analysis revealed a multimodal trace, with $M_n(\text{found})/M_n(\text{calculated})$ ratios for the primary peaks (~80% of the polymer product) ranging from 0.4 to 0.9 for the polymerization of 100 to 400 equivalents of 1-hexene at 0 °C (Table 1.4). While premature termination reactions were limited at -30 °C, small low molecular weight peaks with $M_n(\text{found})/M_n(\text{calculated})$ ratios of about 0.2 were observed for polymerizations at 0 °C. Lower than expected experimental M_n values, as well as pseudo first-order kinetics for consumption of 1-hexene, suggest that the hafnium product of β -hydride elimination is active for polymerization.

Polymer analysis of reactions employing the $\{[\text{Ar}_{\text{Cl}}\text{N}_2\text{NMe}]\text{HfMe}\}^+$ initiator at -30 °C also showed small high molecular weight peaks with $M_n(\text{found})/M_n(\text{calculated})$ ratios between 4 and 6, resulting from a faster rate of propagation than initiation. In order to eliminate initiation problems observed when the hafnium methyl cations were employed, $[\text{Ar}_{\text{Cl}}\text{N}_2\text{NMe}]\text{Hf}(i\text{-Bu})_2$ was employed as a precatalyst, since the greater steric bulk of the isobutyl group is sterically more akin to the alkyl group in the growing polymer chain. If 1-hexene is added immediately after $[\text{Ar}_{\text{Cl}}\text{N}_2\text{NMe}]\text{Hf}(i\text{-Bu})_2$ and the activator are mixed, the insertion of 1-hexene will be greatly preferred over the relatively slow insertion of isobutene.

The rate constant for polymerization by $\{[\text{Ar}_{\text{Cl}}\text{N}_2\text{NMe}]\text{Hf}(i\text{-Bu})\}\{\text{B}(\text{C}_6\text{F}_5)_4\}$ was not significantly different than rate constant for polymerization by $\{[\text{Ar}_{\text{Cl}}\text{N}_2\text{NMe}]\text{HfMe}\}\{\text{B}(\text{C}_6\text{F}_5)_4\}$. Polydispersities of the resulting poly(1-hexene) ranged from 1.1 to 1.3 and experimental M_n values were approximately half of those calculated for a perfectly living system (Table 1.4). GPC analysis of the polymer formed at -30 °C revealed a single sharp peak with a large sloping low-molecular weight tail (refractive index detector). No high molecular weight peak was observed. The overall PDI was 1.16 and the $M_n(\text{found})/M_n(\text{calculated})$ ratio was 0.88. The polymerization of 1-hexene at 0 °C and -30 °C by $\{[\text{Ar}_{\text{Cl}}\text{N}_2\text{NMe}]\text{Hf}(i\text{-Bu})\}\{\text{MeB}(\text{C}_6\text{F}_5)_3\}$, formed by the activation of $[\text{Ar}_{\text{Cl}}\text{N}_2\text{NMe}]\text{Hf}(i\text{-Bu})\text{Me}$ with $\text{B}(\text{C}_6\text{F}_5)_3$, proceeded at a rate essentially identical to that of polymerization by the isobutyl cation in the presence of isobutene

to produce poly(1-hexene) having similar PDI values and $M_n(\text{found})/M_n(\text{calculated})$ ratios.

1.5 β -Hydride Elimination

During the polymerization of 1-hexene by hafnium methyl or isobutyl cations, the initiator was completely consumed, and the active propagating species was generated. The propagating species is characterized by a new set of broadened ligand resonances in the ^1H NMR spectrum. After consumption of 1-hexene was complete, these broadened resonances were gradually replaced by sharp ligand resonances characteristic of a single cationic species that did not contain a polymeric alkyl chain. There appears to be a direct relationship between the growth of this hafnium product and the olefinic $\beta_{1,2}$ product resonance at 4.86 ppm. Upon complete consumption of 1-hexene by $\{[\text{Ar}_{\text{Cl}}\text{N}_2\text{NMe}]\text{Hf}(i\text{-Bu})\}\{\text{HB}(\text{C}_6\text{F}_5)_3\}$ at 0 °C, the growth of the olefinic resonance at 4.86 ppm and a ligand ethylene CH_2 resonance at 3.9 ppm were each measured in comparison to an internal standard. The concentrations of these species in relation to the concentration of the initiator (calculated from the integration of $[\text{Ph}_2\text{CH}_2]$) were plotted as a function of time (Figure 1.5). Any isobutene remaining in solution did not appear to be involved in the process, and the use of the $\text{B}(\text{C}_6\text{F}_5)_3$ activator ensured that the olefinic β -hydride elimination product would not be polymerized by trace amounts of $\{\text{Ph}_3\text{C}\}^+$.

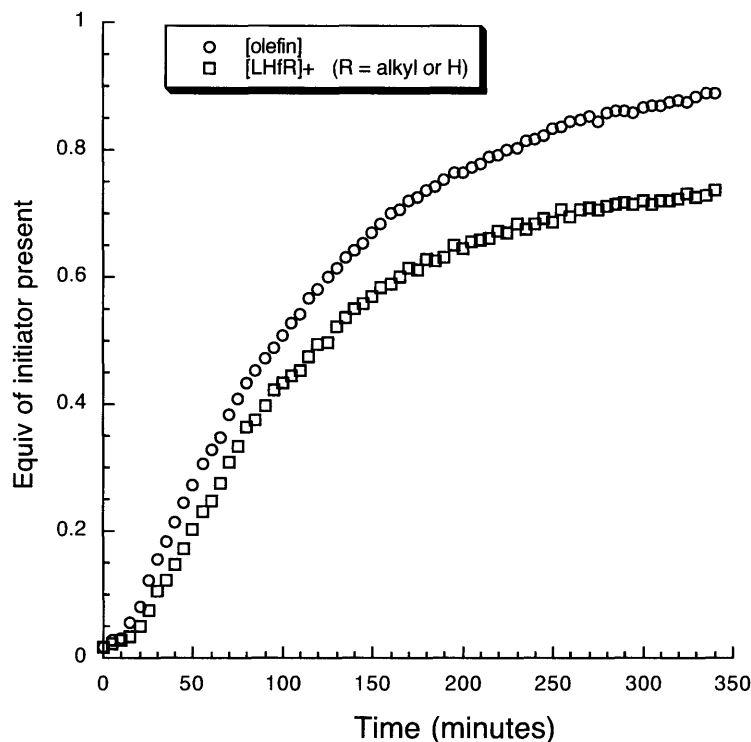


Figure 1.5. Growth of the hafnium complex and olefin upon decomposition of the propagating species after completion of the polymerization of 1-hexene by $\{[\text{Ar}_{\text{Cl}}\text{N}_2\text{NMe}]\text{Hf}(i\text{-Bu})\}\{\text{HB}(\text{C}_6\text{F}_5)_3\}$ at 0 °C in $\text{C}_6\text{D}_5\text{Br}$.

In order to determine whether the hafnium product of β -hydride elimination was still active for polymerization, 1-hexene was added in two batches consecutively. 1-Hexene (300 equivalents) was polymerized by $\{[\text{Ar}_{\text{Cl}}\text{N}_2\text{NMe}]\text{Hf}(i\text{-Bu})\}\{\text{B}(\text{C}_6\text{F}_5)_4\}$ at 0 °C with a k_p of $0.13 \text{ M}^{-1}\text{s}^{-1}$ to produce polymer with an $M_n(\text{found})/M_n(\text{calculated})$ ratio of 0.6. After 10 hours, a ^1H NMR spectrum showed that the propagating species had decomposed by β -hydride elimination, and another 300 equivalents of 1-hexene were added to the solution at 0 °C. The resonances for the propagating chain reappeared in the ^1H NMR spectrum, and 1-hexene was polymerized with an identical k_p of $0.13 \text{ M}^{-1}\text{s}^{-1}$. The overall $M_n(\text{found})/M_n(\text{calculated})$ ratio was found to be 0.3. Six hours after the second batch of 1-hexene was consumed, the resonances for

the hafnium product of β -hydride elimination reemerged. Another 1.0 equivalent of olefin product was produced during this post-polymerization period to give a total of 4.7 equivalents of 1,2 β -hydride elimination and 3.0 equivalents of 2,1 β -hydride elimination (Table 1.5). The low molecular weight of the polymer and the observed pseudo first-order kinetics, despite extensive β -hydride elimination, suggest that the hafnium product of β -hydride elimination is indeed active for the polymerization of 1-hexene. Unfortunately, we have not been able to identify this compound.

Table 1.5. Equivalents of β -hydride elimination versus initiator present after two successive polymerizations of 300 equivalents of 1-hexene by $\{[\text{Ar}_{\text{Cl}}\text{N}_2\text{NMe}]\text{Hf}(\text{R})\}\{\text{B}(\text{C}_6\text{F}_5)_4\}$.

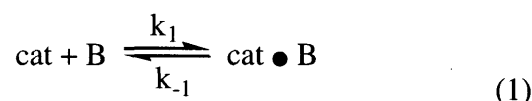
	$\beta_{2,1}$ -H Product	$\beta_{1,2}$ -H Product	$\beta_{1,2}$ -H Product (16 Hours)
First 300 Equiv.	1.0 equiv.	1.4 equiv.	2.3 equiv.
Second 300 Equiv.	3.0 equiv.	3.7 equiv.	4.7 equiv.

1.6 Inhibition Studies

Although $\{[\text{Ar}_{\text{Cl}}\text{N}_2\text{NMe}]\text{MR}\}^+$ cations polymerize 1-hexene at a rate that is too fast to be accurately monitored using NMR techniques, various bases can be added to slow the polymerization reaction. For example, addition of free dimethylaniline (4 to 16 equivalents) to $\{[\text{Ar}_{\text{Cl}}\text{N}_2\text{NMe}]\text{Zr}^*\text{Me}(\text{PhNMe}_2)\}\{\text{B}(\text{C}_6\text{F}_5)_4\}$ prior to the addition of 1-hexene resulted in increasingly slower rates of consumption of 1-hexene, consistent with competitive inhibition of 1-hexene polymerization by dimethylaniline.³⁴ A k_p value of $0.80 \text{ M}^{-1}\text{s}^{-1}$ was extrapolated from these data. Unfortunately, an increasing disparity between the experimental molecular weights and those calculated for a perfect living polymerization was observed with increasing amounts of dimethylaniline. Accordingly, increasing amounts of unconsumed initiator were also observed in solution. These problems were also observed when dimethylaniline was employed as an inhibitor for $\{[\text{Ar}_{\text{Cl}}\text{N}_2\text{NMe}]\text{HfMe}(\text{PhNMe}_2)\}\{\text{B}(\text{C}_6\text{F}_5)_4\}$. A k_p value of $0.05 \text{ M}^{-1}\text{s}^{-1}$ and a base binding constant (K) of 94 M^{-1} were extrapolated.

Since $(i\text{-Pr})_2\text{O}$ was found to be the most well-behaved inhibitor of $\{[\text{MesNpy}]\text{MR}\}\{\text{B}(\text{C}_6\text{F}_5)_4\}$ catalysts,⁴⁶ initiation studies of $\{[\text{Ar}_{\text{Cl}}\text{N}_2\text{NMe}]\text{MMe}\}\{\text{B}(\text{C}_6\text{F}_5)_4\}$ ($\text{M} = \text{Hf}, \text{Zr}$) catalysts were performed using $(i\text{-Pr})_2\text{O}$. The addition of 1.0 equivalent of $(i\text{-Pr})_2\text{O}$ to $\{[\text{Ar}_{\text{Cl}}\text{N}_2\text{NMe}]\text{HfMe}\}\{\text{B}(\text{C}_6\text{F}_5)_4\}$ at 0 °C yields $\{[\text{Ar}_{\text{Cl}}\text{N}_2\text{NMe}]\text{HfMe}[(i\text{-Pr})_2\text{O}]\}\{\text{B}(\text{C}_6\text{F}_5)_4\}$, a complex in which $(i\text{-Pr})_2\text{O}$ is coordinating to the metal. This complex is stable at 0 °C for at least 5 hours in the absence of 1-hexene. In the ^1H NMR spectrum, the Hf-Me peak is shifted from 0.49 ppm to 0.68 ppm in the species containing $(i\text{-Pr})_2\text{O}$. When more than 1 equivalent of $(i\text{-Pr})_2\text{O}$ is added, only 1 equivalent binds to the metal, and free $(i\text{-Pr})_2\text{O}$ is observed in solution (1.15 ppm: 12H, d, CH_3 and 3.48 ppm: 2H, p, CH).

In order for an accurate k_p value to be extrapolated, the equilibrium of base coordination to the initiator must be rapid and reversible (Equation 1). Equation 2 can then be derived to relate the observed rate constant to equivalents of base.^{46,50}



$$\frac{[\text{cat}]_0}{k_{\text{obs}}} = \frac{K}{k_p} [\text{B}] + \frac{1}{k_p} \quad (2)$$

Plots of $\ln([\text{1-hexene}]/[\text{Ph}_2\text{CH}_2])$ versus time (minutes) for the addition of 100 equivalents of 1-hexene to $\{[\text{Ar}_{\text{Cl}}\text{N}_2\text{NMe}]\text{HfMe}\}\{\text{B}(\text{C}_6\text{F}_5)_4\}$ in the presence of 1 to 20 equivalents of $(i\text{-Pr})_2\text{O}$ (0 °C, $\text{C}_6\text{D}_5\text{Br}$) are linear for the first 4 hours of polymerization (Figure 1.6). A plot of $[\text{Hf}]_0/k_{\text{obs}}$ versus $[(i\text{-Pr})_2\text{O}]$ (Figure 1.7) gives a value for k_p of $0.13 \text{ M}^{-1}\text{s}^{-1}$ and for K of 104 M^{-1} (Dr. Klaus Ruhland reported $k_p = 0.11 \text{ M}^{-1}\text{s}^{-1}$ and $K = 113 \text{ M}^{-1}$). This k_p value is roughly comparable to the k_p value of $0.20 \text{ M}^{-1}\text{s}^{-1}$ obtained for the final 13% of the uninhibited polymerization of 100 equivalents of 1-hexene by $\{[\text{Ar}_{\text{Cl}}\text{N}_2\text{NMe}]\text{HfMe}\}\{\text{B}(\text{C}_6\text{F}_5)_4\}$ at 0 °C. Unfortunately, experimental molecular weights were on the order of 20 to 30 times the calculated molecular weights for polymerizations by $\{[\text{Ar}_{\text{Cl}}\text{N}_2\text{NMe}]\text{HfMe}\}\{\text{B}(\text{C}_6\text{F}_5)_4\}$ catalysts at 0 °C in the presence of $(i\text{-Pr})_2\text{O}$ (Table 1.6).

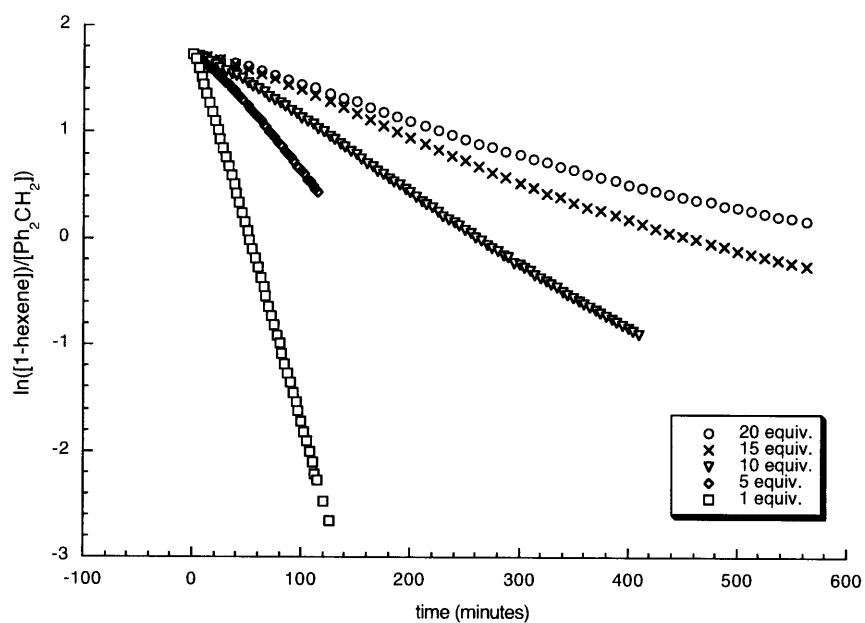


Figure 1.6. Consumption of 100 equivalents 1-hexene by $\{[\text{Ar}_{\text{Cl}}\text{N}_2\text{NMe}]\text{HfMe}\}\{\text{B}(\text{C}_6\text{F}_5)_4\}$ (formed by the activation of $[\text{Ar}_{\text{Cl}}\text{N}_2\text{NMe}]\text{HfMe}_2$ with $\{\text{Ph}_3\text{C}\}\{\text{B}(\text{C}_6\text{F}_5)_4\}$) in the presence of 1 to 20 equivalents of $(i\text{-Pr})_2\text{O}$ ($0\text{ }^\circ\text{C}$, $\text{C}_6\text{D}_5\text{Br}$).

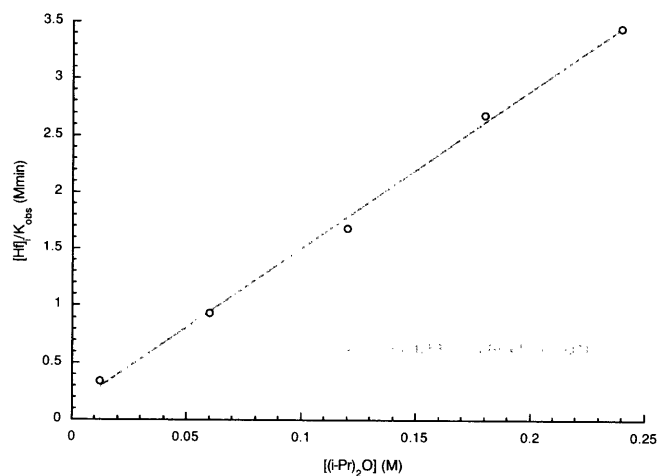


Figure 1.7. Plot of $[\text{Hf}]_0/k_{\text{obs}}$ versus $[(i\text{-Pr})_2\text{O}]$ for the addition of 1-hexene to $\{[\text{Ar}_{\text{Cl}}\text{N}_2\text{NMe}]\text{HfMe}\}\{\text{B}(\text{C}_6\text{F}_5)_4\}$ in the presence of 1 to 20 equivalents of $(i\text{-Pr})_2\text{O}$ ($0\text{ }^\circ\text{C}$, $\text{C}_6\text{D}_5\text{Br}$).

Table 1.6. Polymer analysis results for the consumption of 1-hexene at 0 °C by $\{[\text{Ar}_{\text{Cl}}\text{N}_2\text{NMe}]\text{MMe}\}\{\text{B}(\text{C}_6\text{F}_5)_4\}$ (formed by the activation of $[\text{Ar}_{\text{Cl}}\text{N}_2\text{NMe}]\text{MMe}_2$ with $\{\text{Ph}_3\text{C}\}\{\text{B}(\text{C}_6\text{F}_5)_4\}$) in the presence of $(i\text{-Pr})_2\text{O}$.

Equiv. $(i\text{-Pr})_2\text{O}$	Catalyst	[Catalyst] (M)	Equiv 1-Hexene	PDI	$^a\text{M}_n$ (f/c)
1	M = Hf	0.012	100	1.3	7.0
5	M = Hf	0.012	100	1.3	25.5
5	M = Zr	0.009	100	1.1	3.0
10	M = Hf	0.012	100	1.2	24.6
15	M = Hf	0.012	100	1.2	28.5
20	M = Hf	0.012	100	1.3	31.1

$^a\text{M}_n(\text{found})/\text{M}_n(\text{calculated})$.

$^a\beta_{2,1}\text{-H} = \beta\text{-hydride elimination following a 2,1 insertion versus initiator.}$

When 1-hexene was added to $\{[\text{Ar}_{\text{Cl}}\text{N}_2\text{NMe}]\text{HfMe}[(i\text{-Pr})_2\text{O}]\}\{\text{B}(\text{C}_6\text{F}_5)_4\}$, a significant decrease in the intensity of initiator peaks was not observed in the ^1H NMR spectra of the polymerization reaction, and no propagating species was observed. The addition of 0.67 equivalents of $(i\text{-Pr})_2\text{O}$ to $\{[\text{Ar}_{\text{Cl}}\text{N}_2\text{NMe}]\text{HfMe}\}\{\text{B}(\text{C}_6\text{F}_5)_4\}$ resulted in a 1:2 mixture of $\{[\text{Ar}_{\text{Cl}}\text{N}_2\text{NMe}]\text{HfMe}\}\{\text{B}(\text{C}_6\text{F}_5)_4\}$ and $\{[\text{Ar}_{\text{Cl}}\text{N}_2\text{NMe}]\text{HfMe}[(i\text{-Pr})_2\text{O}]\}\{\text{B}(\text{C}_6\text{F}_5)_4\}$, a ratio which remained constant up to at least 30 °C. When 100 equivalents of 1-hexene were added to this mixture at 0 °C, the $\{[\text{Ar}_{\text{Cl}}\text{N}_2\text{NMe}]\text{HfMe}\}\{\text{B}(\text{C}_6\text{F}_5)_4\}$ fraction was found to insert monomer, yielding the propagating species, while the $\{[\text{Ar}_{\text{Cl}}\text{N}_2\text{NMe}]\text{HfMe}[(i\text{-Pr})_2\text{O}]\}\{\text{B}(\text{C}_6\text{F}_5)_4\}$ fraction was not consumed. During the course of these polymerization reactions, significant decomposition of $\{[\text{Ar}_{\text{Cl}}\text{N}_2\text{NMe}]\text{HfMe}[(i\text{-Pr})_2\text{O}]\}\{\text{B}(\text{C}_6\text{F}_5)_4\}$ was not observed to occur. Higher than expected polymer molecular weights resulted from very low percentages of the initial catalyst participating in the polymerizations. The observed first-order kinetics suggest that complete initiation is repressed more than propagation due to stronger binding of $(i\text{-Pr})_2\text{O}$ to the methyl initiator than to the metal complex that contains the growing polymer chain.

Excess (*i*-Pr)₂O did not suppress initiation in polymerizations employing zirconium catalysts as much as in those employing hafnium catalysts. 100 Equivalents of 1-hexene were polymerized by {[Ar_{Cl}N₂NMe]ZrMe}{B(C₆F₅)₄} in the presence of 5 equivalents of (*i*-Pr)₂O with a k_p of 0.19 M⁻¹s⁻¹ to produce polymer with an M_n(found)/M_n(calculated) ratio of 3.2. In this case, 38% of the zirconium initiator was consumed during the polymerization.

A good inhibitor would bind weakly enough that k_i remains on the order or k_p. Up to 163 equivalents of (TMS)₂O did not slow the rate of polymerization by {[Ar_{Cl}N₂NMe]MMe}{B(C₆F₅)₄} (M = Zr, Hf) catalysts and did not affect polymer molecular weight. Isopropoxytrimethylsilyl ether, on the other hand, binds weakly to {[Ar_{Cl}N₂NMe]ZrMe}{B(C₆F₅)₄}, forming an {[Ar_{Cl}N₂NMe]ZrMe[(*i*-Pr)OTMS]}{B(C₆F₅)₄} adduct with new CH₂ and N-CH₃ resonances and broadened peaks corresponding to the CH₃ groups of the *i*-Pr and TMS moieties in the proton NMR spectrum. In the presence of 5 equivalents of isopropoxytrimethylsilyl ether, {[Ar_{Cl}N₂NMe]ZrMe[(*i*-Pr)OTMS]}{B(C₆F₅)₄} polymerized 100 equivalents of 1-hexene at 0 °C with k_p = 0.46 M⁻¹s⁻¹ to give a polymer with an M_n(found)/M_n(calculated) ratio of 1.7 and a polydispersity of 1.13. Although most of the initiator was consumed, the rate of initiation was still inhibited more than the rate of propagation. Therefore, inhibition studies of hafnium and zirconium methyl cations are not highly accurate.

Inhibition studies employing {[Ar_{Cl}N₂NMe]Hf(*i*-Bu)}{B(C₆F₅)₄} should be more accurate because the greater steric bulk of an isobutyl group than a methyl group prevents the base from binding strongly to the metal center in the initiator. One equivalent of (*i*-Pr)₂O binds weakly to the hafnium center in {[Ar_{Cl}N₂NMe]Hf(*i*-Bu)}{B(C₆F₅)₄}, and peak broadening in the alkyl region of the ¹H NMR spectrum is observed. When 5 equivalents of (*i*-Pr)₂O were added to the initiator, 100 equivalents of 1-hexene were polymerized with a k_p of 0.077 M⁻¹s⁻¹ to produce poly(1-hexene) with an M_n(found)/M_n(calculated) ratio of 0.64 and a PDI of 1.13. All of the initiator was consumed during the reaction. Unfortunately, zirconium diisobutyl complexes are not stable, and therefore cannot be used in inhibition studies for direct comparison with hafnium catalysts.

1.7 Conclusions

Replacement of the mesityl substituents in $[(\text{MesitylNCH}_2\text{CH}_2)_2\text{NMe}]^{2-}$ with 2,6- $\text{Cl}_2\text{C}_6\text{H}_3$ groups prevented competitive decomposition of the propagating species through CH activation. However, living behavior was only observed for zirconium catalysts in the polymerization of 1-hexene. In contrast to the zirconium catalysts, hafnium catalysts that contain the $[(2,6\text{-Cl}_2\text{C}_6\text{H}_3\text{NCH}_2\text{CH}_2)_2\text{NMe}]^{2-}$ ligand are prone to significant 1,2 and 2,1 β -hydride elimination. The hafnium product of β -hydride elimination appears to initiate the polymerization of 1-hexene at a rate equal to that of the methyl or isobutyl initiator. The hafnium catalyst $\{[(2,6\text{-Cl}_2\text{C}_6\text{H}_3\text{NCH}_2\text{CH}_2)_2\text{NMe}]\text{HfR}\}\{\text{B}(\text{C}_6\text{F}_5)_4\}$, for which $k_p \approx 0.20 \text{ M}^{-1}\text{s}^{-1}$ at 0°C , is also slower than the analogous zirconium catalyst, for which $k_p \approx 0.80 \text{ M}^{-1}\text{s}^{-1}$.

1.8 Experimental Section

General Details. All reactions were performed under an atmosphere of dinitrogen in a Vacuum Atmospheres drybox or using Schlenk techniques, and catalyst activation was performed in a drybox free of ether, THF, and other coordinating solvents. Non-deuterated solvents were sparged with nitrogen for 45 minutes, followed by passage through a 1 gallon column of activated alumina.⁵⁷ Bromobenzene, chlorobenzene, and deuterated solvents were stirred over CaH_2 for 48 hours, vacuum-transferred, and stored over 4 \AA molecular sieves. $\text{Hf}(\text{NMe}_2)_4$ and $\text{Zr}(\text{NMe}_2)_4$ were synthesized according to reported methods.⁵⁸ Unlabeled Grignard reagents were purchased from Aldrich and titrated prior to use with isopropanol using 1,10-phenanthroline as an indicator. All other commercial reagents were used without further purification. NMR data were recorded using Varian Inova-500, Varian Unity-300, or Varian Mercury-300 spectrometers. Chemical shifts are reported in parts per million (ppm) downfield of TMS. The residual protons or ^{13}C atoms of the deuterated solvents were used as internal references. Elemental analysis (C, H, N, Cl) was done by Kolbe Mikroanalytisches Laboratorium, Mülheim an der Ruhr, Germany. GPC analyses were conducted using a system equipped with two Waters 7.8 X 300 nm columns (Ultrastyrigel 10^4 \AA and Styragel HR5E) in

series and a Wyatt Technology mini Dawn light scattering detector coupled with a Knauer differential refractometer. A Knauer 64 HPLC pump was used to supply HPLC grade THF at a flow rate of 1.0 mL/min. The auxiliary constant of the apparatus (5.9×10^{-4}) was calibrated using a polystyrene standard ($M_n = 2.2 \times 10^5$), and M_n and M_w values for poly(1-hexene) were obtained using $dn/dc = 0.076$ mL/gr (Wyatt Technology). Data analysis was carried out using Astrette 1.2 software (Wyatt Technology).

(2,6-C₆H₃Cl₂NHCH₂CH₂)₂NH (H₂[Ar_{Cl}N₂NH]).³⁴ BINAP (0.664 g, 1.07 mmol) was taken up in toluene (100 mL), and the resulting suspension was heated until the BINAP dissolved. Pd(dba)₃ (0.488 g, 0.533 mmol) was added and the grey solution was heated until the reaction acquired an orange tint. The solution was filtered through packed celite, combined with HN(CH₂CH₂NH₂)₂ (3.668 g, 35.6 mmol), 2-bromo-1,3-dichlorobenzene (16.06 g, 71.11 mmol) and NaOt-Bu (10.59 g, 110.2 mmol) in toluene (250 mL), transferred to a sealed Schlenk flask, and heated at 95 °C for 17 hours under N₂. The hot reaction mixture was filtered through alumina, and toluene was removed in vacuo. The product was extracted in Et₂O (120 mL) against H₂O (2 x 80 mL) and saturated NaCl solution (80 mL) and combined with Et₂O (2 x 40 mL) containing product recovered through back-extraction with H₂O portions. The Et₂O portions were concentrated in vacuo to yield an impure brown oil that was dissolved in toluene and filtered through a silica gel plug column. Toluene (750 mL) was passed through 200 mL of silica gel to wash out impurities and the product was flushed out with Et₂O. After the solvent was removed, the resulting orange powder was recrystallized from Et₂O (50 mL) at 0 °C to afford transparent crystals; yield 7.759 g (56%). ¹H NMR (C₆D₆) δ 0.48 (br s, 1H, NH), 2.36 and 3.23 (m, 4H each, ligand CH₂), 4.76 (br t, 2H, aryl NH), 6.24 (t, 2H, *p*-H), 6.96 (d, 4H, *m*-H). FAB-MS: positive ion (M+H)⁺, measured (calcd.) 392.0242 ± 0.0012 (392.0255).

(2,6-C₆H₃Cl₂NHCH₂CH₂)₂NMe (H₂[Ar_{Cl}N₂NMe]).³⁴ K₂CO₃ (3.23 g, 23.4 mmol) was added to a solution of H₂[Ar_{Cl}N₂NH] (2.52g, 6.41 mmol) in 125 mL of anhydrous CH₃CN. The reaction mixture was sparged with N₂ for 15 minutes and MeI (0.459 mL, 6.73 mmol) was added dropwise *via* syringe with vigorous stirring. The reaction mixture was stirred for 24 hours and a

white suspension was filtered off. All volatile components were removed, and the residue was worked up with a mixture of ether and water. The organic layer was separated, washed several times with water, and dried over MgSO_4 . Removal of solvent in vacuo gave a pale-yellow powder; yield 1.66 g (63%). $^1\text{H NMR}$ (CDCl_3) δ 2.31 (s, 3H, NCH_3), 2.66 and 3.45 (m, 4H each, ligand CH_2), 4.76 (br s, 2H, aryl NH), 6.76 (t, 2H, *p*-H), 7.23 (d, 4H, *m*-H). FAB-MS: positive ion ($\text{M}+\text{H}$) $^+$, measured (calcd.): 406.0421 ± 0.0012 (406.0411).

$[\text{Ar}_{\text{Cl}}\text{N}_2\text{NMe}]\text{Zr}(\text{NMe}_2)_2$ 34 $\text{Zr}(\text{NMe}_2)_4$ (1.091 g, 4.078 mmol) was added to a solution of $\text{H}_2[\text{Ar}_{\text{Cl}}\text{N}_2\text{NMe}]$ (1.660 g, 4.077 mmol) in benzene (10 mL). The reaction mixture was stirred for 16 hours at room temperature. As the reaction mixture was concentrated in vacuo, a white solid precipitated. The product was collected via filtration and washed with pentane to give a white powder; yield 1.979 g (83%). $^1\text{H NMR}$ ($\text{C}_6\text{D}_5\text{CD}_3$) δ 2.31 (s, 3, NCH_3), 3.31 and 2.55 (s, 6H each, NMe_2), 3.05, 3.25, 3.92 (m, 8H, ligand CH_2), 6.42 (t, 2H, *p*-H), 7.12 (d, 4H, *m*-H). Anal. Calcd. for $\text{ZrCl}_4\text{N}_5\text{C}_{21}\text{H}_{29}$: C, 43.15; H, 5.00; N, 11.98; Cl, 24.26. Found: C, 43.02; H, 5.11; N, 11.85; Cl, 24.11.

$[\text{Ar}_{\text{Cl}}\text{N}_2\text{NMe}]\text{Hf}(\text{NMe}_2)_2$ 54 $\text{Hf}(\text{NMe}_2)_4$ (0.952 g, 2.68 mmol) was added to a solution of $\text{H}_2[\text{Ar}_{\text{Cl}}\text{N}_2\text{NMe}]$ (1.092 g, 2.683 mmol) in benzene (10 mL). The reaction mixture was stirred for 16 hours at room temperature. All volatile components were removed in vacuo, and the remaining solid was washed with pentane to give a yellow powder; yield 1.526 g (85%). $^1\text{H NMR}$ (C_6D_6) δ 2.23 (s, 3H, NCH_3), 2.34, 2.93, 3.27, and 3.93 (m, 2H each, ligand CH_2), 2.63 and 3.33 (s, 6H each, NMe_2), 6.39 (t, 2H, *p*-H), 7.21 (d, 4H, *m*-H). Anal. Calcd. for $\text{C}_{21}\text{H}_{29}\text{N}_3\text{Cl}_4\text{Hf}$: C, 37.55; H, 4.35; N, 10.42; Cl, 21.11. Found: C, 37.64; H, 4.28; N, 10.36; Cl, 21.16. Anal. Calcd. for $\text{C}_{21}\text{H}_{29}\text{N}_3\text{Cl}_4\text{Hf}$: C, 37.55; H, 4.35; N, 10.42; Cl, 21.11. Found: C, 37.64; H, 4.28; N, 10.36; Cl, 21.16.

$[\text{Ar}_{\text{Cl}}\text{N}_2\text{NMe}]\text{ZrCl}_2$ 34 TMSCl (1.289 g, 11.86 mmol) was added to a solution of $[\text{Ar}_{\text{Cl}}\text{N}_2\text{NMe}]\text{Zr}(\text{NMe}_2)_2$ (1.979 g, 3.39 mmol) in toluene (25 mL) that had been cooled to -30 °C. After stirring at room temperature for 16 hours, the reaction mixture was concentrated in vacuo to 3 mL and 15 mL of pentane was added. A precipitate formed and was collected and washed

with Et₂O and pentane to give a white powder; yield 1.375 g (72%). ¹H NMR (C₆D₆) δ 2.36 (s, 3H, NCH₃), 2.33, 2.81, 3.01, and 3.74 (m, 2H each, ligand CH₂), 6.32 (t, 2H, *p*-H), 6.95 (d, 4H, *m*-H).

[Ar_{Cl}N₂NMe]HfCl₂.⁵⁴ TMSCl (2.070 g, 15.40 mmol) was added to a solution of [Ar_{Cl}N₂NMe]Hf(NMe₂)₂ (1.673 g, 3.081 mmol) in toluene (15 mL) that had been cooled to -30 °C. After stirring at room temperature for 16 hours, the reaction mixture was concentrated in vacuo to 7 mL, and 5 mL of pentane was added. A precipitate formed and was collected and washed with Et₂O and pentane to give a white powder; yield 1.956 g (97%). ¹H NMR (C₆D₆) δ 2.33 (s, 3H, NCH₃), 2.28, 2.76, 3.13, and 3.92 (m, 2H each, ligand CH₂), 6.32 (t, 2H, *p*-H), 7.02 (d, 4H, *m*-H). ¹³C NMR (C₆D₅Br) δ 45.60 (1C, NCH₃), 52.14 and 56.51 (2C each, ligand CH₂), 152.89, 129.41, 129.62, and 147.55 (12C, Ph C).

[Ar_{Cl}N₂NMe]ZrMe₂.³⁴ A solution of MeMgBr in Et₂O (0.676 mL of a 3.45 M solution, 2.33 mmol) was added *via* syringe to a suspension of [Ar_{Cl}N₂NMe]ZrCl₂ (0.630 g, 1.11 mmol) in 20 mL of Et₂O that had been cooled to -30 °C. After 1 hour at room temperature, 1.0 mL of dioxane was added, which initiated the precipitation of a fine white powder. After an additional 5 minutes, all volatile components were removed in vacuo. The product was extracted into 25 mL of toluene. The solution was filtered through a pad of celite and concentrated to dryness in vacuo to give a white solid; yield 0.355 g (61%). ¹H NMR (C₆D₆) δ 0.60 (s, 6H, ZrCH₃), 2.19 (s, 3H, NCH₃), 2.03, 2.76, 3.21, and 3.70 (m, 2H each, ligand CH₂), 6.42 (t, 2H, *p*-H), 7.12 (d, 4H, *m*-H). ¹H NMR (C₆D₅Br) δ 0.29 (s, 3H, ZrCH₃), 0.33 (s, 3H, ZrCH₃), 2.41 (s, 3H, NCH₃), 2.44, 2.99, 3.23, and 3.75 (m, 2H each, ligand CH₂), 6.65 (t, 2H, *p*-H), 7.17 (d, 4H, *m*-H). ¹³C NMR (C₆D₅Br) δ 36.74 (1C, NCH₃), 45.32 and 46.13 (1C each, ZrCH₃), 53.81 and 59.83 (2C each, ligand CH₂), 125.41, 128.42, 135.71, and 146.47 (12C, Ph C). Anal. Calcd. for C₁₉H₂₃N₃Cl₄Zr: C, 43.60; H, 4.43; N, 8.03; Cl, 26.75. Found: C, 43.48; H, 4.48; N, 7.94; Cl, 26.66.

[Ar_{Cl}N₂NMe]HfMe₂.⁵⁴ A solution of MeMgBr in Et₂O (0.593 mL of a 3.45 M solution, 2.05 mmol) was added *via* syringe to a suspension of [Ar_{Cl}N₂NMe]HfCl₂ (0.638 g, 0.975 mmol) in 25 mL of Et₂O that had been cooled to -30 °C. After 1 hour at room temperature, 0.2 mL of

dioxane was added, which completed the precipitation of a fine white powder. The reaction was worked up using an analogous method to that of $[\text{Ar}_{\text{Cl}}\text{N}_2\text{NMe}]\text{ZrMe}_2$, yielding a white solid; yield 0.465 g (77%). $^1\text{H NMR}$ (C_6D_6) δ 0.18 and 0.49 (s, 3H, HfCH₃), 2.11 (s, 3H, NCH₃), 2.04, 3.69, 3.51 and 3.52 (m, 2H each, ligand CH₂), 6.40 (t, 2H, *p*-H), 7.12 (d, 4H, *m*-H); $^1\text{H NMR}$ ($\text{C}_6\text{D}_5\text{Br}$) δ -0.13 and 0.25 (s, 3H, HfCH₃), 2.41 (s, 3H, NCH₃), 2.42, 2.97, 3.56 and 3.60 (m, 2H each, ligand CH₂), 6.65 (t, 2H, *p*-H), 7.17 (d, 4H, *m*-H). $^{13}\text{C NMR}$ ($\text{C}_6\text{D}_5\text{Br}$) δ 39.41 (1C, NCH₃), 53.43 and 58.28 (2C each, ligand CH₂), 55.71 and 56.50 (1C each, HfCH₃), 125.31, 128.40, 135.42, and 147.17 (12C, Ph C). Anal. Calcd. for $\text{C}_{19}\text{H}_{23}\text{N}_3\text{Cl}_4\text{Hf}$: C, 37.18; H, 3.78; N, 6.85; Cl, 23.11. Found: C, 37.26; H, 3.71; N, 6.74; Cl, 23.19.

$[\text{Ar}_{\text{Cl}}\text{N}_2\text{NMe}]\text{Hf}(i\text{-Bu})_2$. $[\text{Ar}_{\text{Cl}}\text{N}_2\text{NMe}]\text{HfCl}_2$ (0.208 g, 0.318 mmol) was suspended in 7 mL of toluene, cooled to $-30\text{ }^\circ\text{C}$, and combined with a solution of *iso*-butyllithium (0.041 g, 0.64 mmol) which had also been cooled to $-30\text{ }^\circ\text{C}$. The reaction mixture was stirred at room temperature for 1 hour before all volatiles were removed in vacuo. The product was extracted into 10 mL of toluene. This solution was filtered through a pad of celite and concentrated in vacuo to give a yellow powder; yield 0.162 g (73%). $^1\text{H NMR}$ ($\text{C}_6\text{D}_5\text{Br}$) δ 0.24 (d, 2H, *i*-Bu CH₂), 0.58 (d, 6H, *i*-Bu CH₃), 0.74 (d, 2H, *i*-Bu CH₂), 1.04 (d, 6H, *i*-Bu CH₃), 1.65 (p, 1H, *i*-Bu CH), 2.42 (p, 1H, *i*-Bu CH), 2.46 (s, 3H, NCH₃), 2.44, 2.95, 3.43, and 3.62 (m, 2H each, ligand CH₂), 6.66 (t, 2H, *p*-CH), 7.20 (d, 4H, *m*-CH). $^{13}\text{C NMR}$ ($\text{C}_6\text{D}_5\text{Br}$) δ 28.87 (2C, *i*-Bu CH₃), 29.28 (1C, *i*-Bu CH), 29.44 (2C, *i*-Bu CH₃), 29.74 (1C, *i*-Bu CH), 42.75 (1C, NCH₃), 53.18 and 59.45 (2C each, ligand CH₂), 90.00 and 91.24 (1C each, *i*-Bu CH₂), 125.20, 128.47, 135.26, and 148.16 (12C, Ph C). Anal. Calcd. for $\text{C}_{25}\text{H}_{35}\text{N}_3\text{Cl}_4\text{Hf}$: C, 43.03; H, 5.06; N, 6.02; Cl, 20.32. Found: C, 42.87; H, 5.12; N, 6.09; Cl, 20.43.

$[\text{Ar}_{\text{Cl}}\text{N}_2\text{NMe}]\text{HfCl}(i\text{-Bu})$.⁵⁴ $[\text{Ar}_{\text{Cl}}\text{N}_2\text{NMe}]\text{HfCl}_2$ (0.520 g, 0.793 mmol) was suspended in 25 mL of diethyl ether and cooled to $-30\text{ }^\circ\text{C}$. A diethyl ether solution (0.350 mL, 0.915 mmol) of 2.61 M (*i*-Bu)MgCl was cooled to $-30\text{ }^\circ\text{C}$ and added to the reaction, which was stirred at room temperature for 1 hour. Dioxane (80 mg) was added, and the reaction filtered through celite. The filtrate was concentrated in vacuo, and the resulting pale yellow solid was washed

with 10 mL of pentane and dried in vacuo; yield: 0.487 g (91%). Two isomers are observed in solution. $^1\text{H NMR}$ (C_6D_6) δ 0.59 (d, 2H, $i\text{-Bu}_{\text{anti}}$ CH_2), 0.82 (d, 2H, $i\text{-Bu}_{\text{syn}}$ CH_2), 1.17 (d, 6H, $i\text{-Bu}_{\text{anti}}$ CH_3), 1.26 (d, 6H, $i\text{-Bu}_{\text{syn}}$ CH_3), 2.24 (s, 3H, NCH_3), 2.24 (s, 3H, NCH_3), 2.16, 2.71, 3.27, and 3.53 (m, 2H each, ligand CH_2 for $i\text{-Bu}_{\text{syn}}$ isomer), 2.16, 2.71, 3.17, and 3.81 (m, 2H each, ligand CH_2 for $i\text{-Bu}_{\text{anti}}$ isomer), 6.38 (t, 2H, $p\text{-CH}$), 6.38 (t, 2H, $p\text{-CH}$), 7.08 (d, 4H, $m\text{-CH}$), 7.09 (d, 4H, $m\text{-CH}$). Anal. Calcd. for $\text{C}_{21}\text{H}_{26}\text{N}_3\text{Cl}_3\text{Hf}$: C, 37.30; H, 3.88; N, 6.21; Cl, 26.21. Found: C, 37.23; H, 3.95; N, 6.12; Cl, 26.30.

$[\text{Ar}_{\text{Cl}}\text{N}_2\text{NMe}]\text{HfMe}(i\text{-Bu})$.⁵⁴ $[\text{Ar}_{\text{Cl}}\text{N}_2\text{NMe}]\text{HfCl}(i\text{-Bu})$ 0.319 g, 0.471 mmol) was suspended in 10 mL of diethyl ether and cooled to $-30\text{ }^\circ\text{C}$. A diethyl ether solution (0.350 mL, 0.520 mmol) of 3.66 M MeMgCl was cooled to $-30\text{ }^\circ\text{C}$ and added to the reaction, which was stirred at room temperature for 1 hour. The reaction mixture was filtered through celite, concentrated in vacuo, and redissolved in 4 mL of pentane. The solution was filtered and stored at $-30\text{ }^\circ\text{C}$ for 16 hours. Pale yellow crystals formed, and were collected via vacuum filtration; yield 0.206 g (67%). Two isomers are observed in solution. $^1\text{H NMR}$ ($\text{C}_6\text{D}_5\text{Br}$) δ -0.13 (s, 3H, Me_{anti}), 0.17 (d, 2H, $i\text{-Bu}_{\text{anti}}$ CH_2), 0.38 (s, 3H, Me_{syn}), 0.52 (d, 2H, $i\text{-Bu}_{\text{syn}}$ CH_2), 0.76 (d, 6H, $i\text{-Bu}_{\text{anti}}$ CH_3), 0.95 (d, 6H, $i\text{-Bu}_{\text{syn}}$ CH_3), 1.52 (m, 1H, $i\text{-Bu}_{\text{anti}}$ CH), 2.23 (m, 1H, $i\text{-Bu}_{\text{syn}}$ CH), 2.41 (s, 3H, NCH_3), 2.45 (s, 3H, NCH_3), 2.48, 3.00, 3.57, and 3.61 (m, 2H each, ligand CH_2 for $i\text{-Bu}_{\text{syn}}$ isomer), 2.48, 3.00, 3.45, and 3.70 (m, 2H each, ligand CH_2 for $i\text{-Bu}_{\text{anti}}$ isomer), 6.64 (t, 2H, $p\text{-CH}$), 6.65 (t, 2H, $p\text{-CH}$), 7.12 (d, 4H, $m\text{-CH}$), 7.14 (d, 4H, $m\text{-CH}$). $^{13}\text{C NMR}$ ($\text{C}_6\text{D}_5\text{Br}$) δ 28.48 (1C, $i\text{-Bu}_{\text{syn}}$ CH), 28.85, (2C, $i\text{-Bu}_{\text{anti}}$ CH_3), 28.88 (1C, $i\text{-Bu}_{\text{anti}}$ CH), 29.16 (2C, $i\text{-Bu}_{\text{syn}}$ CH_3), 41.33 (1C, NCH_3 for $i\text{-Bu}_{\text{syn}}$ isomer), 41.91 (1C, NCH_3 for $i\text{-Bu}_{\text{anti}}$ isomer), 53.06 and 57.29 (2C each, ligand CH_2 for $i\text{-Bu}_{\text{syn}}$ isomer), 53.26 and 56.92 (2C each, ligand CH_2 for $i\text{-Bu}_{\text{anti}}$ isomer), 56.01 (1C, CH_3_{syn}), 58.19 (1C, $\text{CH}_3_{\text{anti}}$), 86.99 (1C, $i\text{-Bu}_{\text{syn}}$ CH_2), 89.60 (1C, $i\text{-Bu}_{\text{anti}}$ CH_2), 125.18, 128.36, 135.21, and 147.73 (12C, Ph C for $i\text{-Bu}_{\text{anti}}$ isomer), 125.22, 128.36, 135.42, and 147.57 (12C, Ph C for $i\text{-Bu}_{\text{syn}}$ isomer). $^{13}\text{C NMR}$ ($\text{C}_6\text{D}_5\text{CD}_3$) δ 56.38 (1C, $^{13}\text{Me}_{\text{syn}}$), 59.19 (1C, $^{13}\text{Me}_{\text{anti}}$). Anal. Calcd. for $\text{C}_{22}\text{H}_{29}\text{N}_3\text{Cl}_4\text{Hf}$: C, 40.29; H, 4.46; N, 6.41; Cl, 21.62. Found: C, 40.21; H, 4.38; N, 6.50; Cl, 21.54.

The $\text{Me}_{\text{anti}} \rightarrow \text{Me}_{\text{syn}}$ isomerization process in $[\text{Ar}_{\text{Cl}}\text{N}_2\text{NMe}]\text{Hf}(i\text{-Bu})\text{Me}$ was studied by observing the disappearance of the Me_{anti} ^1H NMR resonance and the growth of the Me_{syn} resonance in relation to a known Ph_3CH standard. Thermodynamic parameters were calculated by employing Van't Hoff and Eyring plots. The data are the following: $T = 50\text{ }^\circ\text{C}$, $K = 1.10$, $k_1 = 0.00059\text{ s}^{-1}$; $60\text{ }^\circ\text{C}$, 1.13 , 0.0014 s^{-1} ; $65\text{ }^\circ\text{C}$, 1.15 , 0.0027 s^{-1} ; $70\text{ }^\circ\text{C}$, 1.16 , 0.0043 s^{-1} ; $75\text{ }^\circ\text{C}$, 1.18 , 0.0070 s^{-1} ; $80\text{ }^\circ\text{C}$, 1.20 , 0.099 s^{-1} .

General Procedure for Activation of $[\text{Ar}_{\text{Cl}}\text{N}_2\text{NMe}]\text{MR}_2$ ($M = \text{Hf, Zr}$). Solutions of $[\text{Ar}_{\text{Cl}}\text{N}_2\text{NMe}]\text{MR}_2$ (0.003 to 0.012 mmol; 1 equivalent) and $\{\text{Ph}_3\text{C}\}\{\text{B}(\text{C}_6\text{F}_5)_4\}$ (0.003 to 0.012 mmol; 1 equivalent), $\text{B}(\text{C}_6\text{F}_5)_3$ (0.003 to 0.012 mmol; 1 equivalent), or $\{\text{HNMe}_2\text{Ph}\}\{\text{B}(\text{C}_6\text{F}_5)_4\}$ (0.003 to 0.012 mmol; 1 equivalent) and the internal standard Ph_2CH_2 (0.048 mmol) in $\text{C}_6\text{D}_5\text{Br}$ ($X, Y = (1.0 - X - H)$ mL, respectively; $H =$ volume of 1-hexene to be added later in polymerization reactions only) were cooled to $-30\text{ }^\circ\text{C}$ and mixed. Activation was almost immediate for the $\{\text{Ph}_3\text{C}\}\{\text{B}(\text{C}_6\text{F}_5)_4\}$, $\text{B}(\text{C}_6\text{F}_5)_3$ and $\{\text{PhNMe}_2\text{H}\}\{\text{B}(\text{C}_6\text{F}_5)_4\}$ activators and accompanied by a change in color of the solution from deep orange to yellow when $\{\text{Ph}_3\text{C}\}\{\text{B}(\text{C}_6\text{F}_5)_4\}$ was the activator. The reaction mixture was transferred to an NMR tube which was frozen in liquid nitrogen, and the solution was thawed to $0\text{ }^\circ\text{C}$ at time = 0.

General Procedure for Polymerization Reactions. $[\text{Ar}_{\text{Cl}}\text{N}_2\text{NMe}]\text{MR}_2$ ($M = \text{Hf, Zr}$) was activated as described previously, and 1-hexene (50 to 500 equivalents) was immediately added to the vigorously stirred, cooled ($-30\text{ }^\circ\text{C}$) solution. The reaction mixture was transferred to an NMR tube, frozen in liquid nitrogen, and then thawed in the NMR probe at $0\text{ }^\circ\text{C}$. Upon complete consumption of 1-hexene, the reactions were quenched with methanol. After solvent removal, the polymer was dissolved in pentane and the solution filtered through silica gel. The solvent was removed in vacuo to give poly(1-hexene) in 100% yield.

$\{[\text{Ar}_{\text{Cl}}\text{N}_2\text{NMe}]\text{ZrMe}\}\{\text{B}(\text{C}_6\text{F}_5)_4\}$.⁵⁵ ^1H NMR ($0\text{ }^\circ\text{C}$, $\text{C}_6\text{D}_5\text{Br}$) δ 0.62 (s, 3H, HfCH_3), 2.34 (s, 3H, NCH_3), 2.65, 2.91, 3.76, and 3.83 (m, 2H each, ligand CH_2), 6.50 (t, 2H, $p\text{-H}$), 6.96 (d, 4H, $m\text{-H}$).

$\{[\text{Ar}_{\text{Cl}}\text{N}_2\text{NMe}]\text{HfMe}\}\{\text{B}(\text{C}_6\text{F}_5)_4\}$.⁵⁴ ^1H NMR (0 °C, $\text{C}_6\text{D}_5\text{Br}$) δ 0.49 (s, 3H, HfCH_3), 2.36 (s, 3H, NCH_3), 2.62, 2.95, 3.80 and 3.90 (m, 2H each, ligand CH_2), 6.57 (t, 2H, *p*-H), 6.96 (d, 4H, *m*-H).

$\{[\text{Ar}_{\text{Cl}}\text{N}_2\text{NMe}]\text{HfMe}\}\{\text{MeB}(\text{C}_6\text{F}_5)_3\}$. ^1H NMR (20 °C, $\text{C}_6\text{D}_5\text{Br}$) δ 0.80 (s, 3H, HfCH_3), 1.12 ($\text{MeB}(\text{C}_6\text{F}_5)_3$) 2.41 (s, 3H, NCH_3), 2.86, 2.23, 3.62 and 3.90 (m, 2H each, ligand CH_2), 6.62 (t, 2H, *p*-H), 7.18 (d, 4H, *m*-H).

$\{[\text{Ar}_{\text{Cl}}\text{N}_2\text{NMe}]\text{HfMe}(\text{NMe}_2\text{Ph})\}\{\text{B}(\text{C}_6\text{F}_5)_4\}$. ^1H NMR (0 °C, $\text{C}_6\text{D}_5\text{Br}$) δ 0.18 (v br s, 3H, HfCH_3), 2.39 (s, 3H, NCH_3), 2.45 (m, 2H, ligand CH_2), 2.58 (s, 6H, NMe_2Ph), 2.95, and 3.46 (br s, 2H each, ligand CH_2), 3.30 (v. br s, 2H, ligand CH_2), 6.72 (t, 2H, *p*-H), 7.19 (d, 4H, *m*-H), 6.0-7.2 ppm (5H, NMe_2Ph aryl Hs).

$\{[\text{Ar}_{\text{Cl}}\text{N}_2\text{NMe}]\text{Hf}(i\text{-Bu})\}\{\text{B}(\text{C}_6\text{F}_5)_4\}$. ^1H NMR (0 °C, $\text{C}_6\text{D}_5\text{Br}$) δ 0.92 (br s, 6H, *i*-Bu CH_3), 0.95 (br s, 2H, *i*-Bu CH_2), 2.55 (s, 3H, NCH_3), 2.55 (br s, 1H, *i*-Bu CH), 2.62, 3.07, 3.76, and 3.86 (m, 2H each, ligand CH_2), 6.53 to 7.20 (aryl Hs).

$\{[\text{Ar}_{\text{Cl}}\text{N}_2\text{NMe}]\text{Hf}(i\text{-Bu})\}\{\text{HB}(\text{C}_6\text{F}_5)_3\}$. ^1H NMR (0 °C, $\text{C}_6\text{D}_5\text{Br}$) δ 0.91 (br s, 6H, *i*-Bu CH_3), 0.96 (br s, 2H, *i*-Bu CH_2), 2.58 (s, 3H, NCH_3), 2.58 (br s, 1H, *i*-Bu CH), 2.66 and 3.10 and 3.71 and 3.81 (m, 2H each, ligand CH_2), 6.55 (t, 2H, *p*-H), 6.95 (d, 4H, *m*-H); ^1H NMR (0 °C, $\text{C}_6\text{D}_5\text{CD}_3$) δ 0.88 (d, 6H, *i*-Bu CH_3), 1.02 (d, 2H, *i*-Bu CH_2), 2.39 (s, 3H, NCH_3), 2.39 (p, 1H, *i*-Bu CH), 2.88, 2.92, 3.49, and 3.54 (m, 2H each, m, ligand CH_2), 6.35 (t, 2H, *p*-H), 6.82 (d, 4H, *m*-H).

$\{[\text{Ar}_{\text{Cl}}\text{N}_2\text{NMe}]\text{Hf}(\text{C}_8\text{H}_{17})\}\{\text{HB}(\text{C}_6\text{F}_5)_3\}$ (Isobutyl 1,2 insertion product). ^1H NMR (0 °C, $\text{C}_6\text{D}_5\text{Br}$) δ 0.57 (d, 6H, CH_3), 0.81 (s, 6H, CH_3) 0.91 (d, 2H, CH_2), 1.16 (s, 2H, CH_2), 1.26 (p, 1H, CH), 2.60 (s, 3H, NCH_3), 2.71, 3.11, 3.72, and 4.03 (m, 2H each, ligand CH_2), 6.56 (t, 2H, *p*-H), 6.96 (d, 4H, *m*-H).

Asymmetric product of the reaction of $\{[\text{Ar}_{\text{Cl}}\text{N}_2\text{NMe}]\text{Hf}(i\text{-Bu})\}\{\text{B}(\text{C}_6\text{F}_5)_4\}$ with dimethylaniline and $\{\text{HNMe}_2\text{Ph}\}\{\text{B}(\text{C}_6\text{F}_5)_4\}$ activation of $\{[\text{Ar}_{\text{Cl}}\text{N}_2\text{NMe}]\text{Hf}(i\text{-Bu})_2\}$. ^1H NMR (20 °C) δ 1.48 (s, 3H), 2.46 (s, 3H), 2.58 (s, 3H), 2.18, 2.31, 2.60, 3.20, 3.26, 3.34, 3.68, 4.32,

4.51 (m, 1H each), 2.90 and 3.20 (dd, 2H), 3.16 (d, 1H), 5.85 (t, 1H), 6.59 (d, 2H), 6.62 and 6.72 (t, 1H each, *m*-H), 6.78-6.86 (m, 2H), 7.05 (d, 2H), 7.08-7.20 (m).

$\{[\text{Ar}_{\text{Cl}}\text{N}_2\text{NMe}]\text{ZrMe}\}[(i\text{-Pr})\text{OTMS}]\{\text{B}(\text{C}_6\text{F}_5)_4\}$. $^1\text{H-NMR}$ (0°C , $\text{C}_6\text{D}_5\text{Br}$) δ 0.78 (br s, 9H, Si-CH₃), 0.55 (s, 3H, HfCH₃), 1.07 (br s, 6H, *i*-Pr CH₃), 2.56 (s, 3H, NCH₃), 2.61 and 2.88 and 3.24 and 3.56 (m, 2H each, ligand CH₂), 3.89 (p, 1H, *i*-Pr CH), 6.7 to 7.2 (aryl Hs). Free (*i*-Pr)OTMS: 0.95 (s, 9H, SiCH₃), 1.09 (d, 6H, *i*-Pr CH₃), 3.87 (p, 1H, *i*-Pr CH).

$\{[\text{Ar}_{\text{Cl}}\text{N}_2\text{NMe}]\text{HfMe}\}[(i\text{-Pr})_2\text{O}]\{\text{B}(\text{C}_6\text{F}_5)_4\}$.⁵⁴ $^1\text{H-NMR}$ (0°C , $\text{C}_6\text{D}_5\text{Br}$) δ 0.56 (d, 12H, (*i*-Pr)₂O CH₃), 0.68 (s, 3H, HfCH₃), 2.42 (s, 3H, NCH₃), 2.55, 3.66, (m, 2H, m, ligand CH₂), 3.07 (m, 4H, ligand CH₂), 3.58 (m, 2H, (*i*-Pr)₂O CH), 6.7 to 7.2 (aryl Hs). Free (*i*-Pr)₂O: 1.15, d, 12H, (*i*-Pr)₂O CH₃), 3.48 (m, 2H, (*i*-Pr)₂O CH).

1.9 Acknowledgements

I'd like to thank Dr. Klaus Ruhland for his collaboration in developing this research. I am also grateful to Pia Lopez for performing the X-ray crystallography studies and to Dr. William M. Davis for general help with X-ray crystallography. Funding from the Department of Energy (DE-FG02-86ER13564) is sincerely appreciated.

Chapter 2

Zirconium and Hafnium Complexes that Contain the Electron-Withdrawing Diamido-Donor Ligands, $[(2,6\text{-X}_2\text{C}_6\text{H}_3\text{NCH}_2)_2\text{C}(2\text{-C}_5\text{H}_4\text{N})(\text{CH}_3)]^2$ (X = Cl or F). An Evaluation of the Role of *ortho*-Halides in 1-Hexene Polymerization

Much of this work has already appeared in print.⁵²

2.1 Introduction

Hafnium and zirconium catalysts containing $[(\text{ArNCH}_2)_2\text{C}(\text{CH}_3)(2\text{-C}_5\text{H}_4\text{N})]^{2-}$ ($[\text{ArNpy}]^{2-}$) (Figure 2.1; **B**, Ar = Mes),⁴⁷⁻⁴⁹ which is an arylated version of the trimethylsilyl-substituted ligand developed by Gade,⁵⁹ are stable toward CH activation during the living polymerization of up to 600 equivalents of 1-hexene at 0 °C in bromobenzene or chlorobenzene.^{48,49} In contrast, cationic zirconium complexes formed from complexes of type **A** (Ar = Mes)^{34,35} are deactivated via aryl *ortho*-methyl CH activation. Since we found that 2,6-Cl₂C₆H₃ substituents were viable alternatives to mesityl amido groups in catalysts derived from complexes of type **A**,^{34,57} we became interested in the possibility of preparing catalysts of type **B** that contain 2,6-X₂C₆H₃ groups (X = Cl or F). We hoped to compare the catalytic activity of complexes that contain 2,6-X₂C₆H₃ aryl groups on the amido nitrogens with those that contain 2,4,6-Me₃C₆H₂ (mesityl) groups on the amido nitrogens.

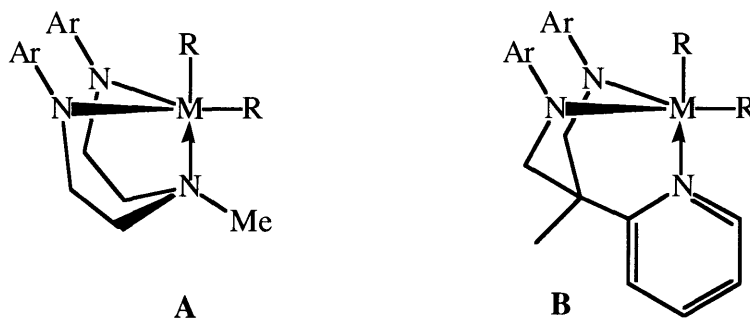
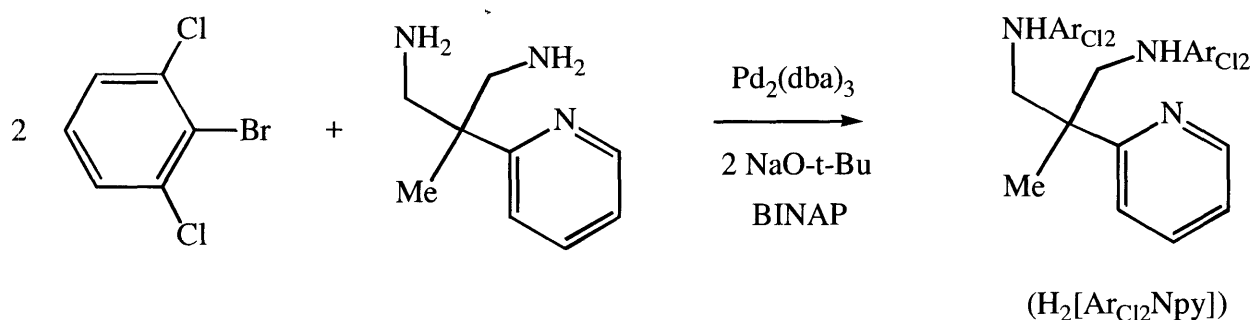


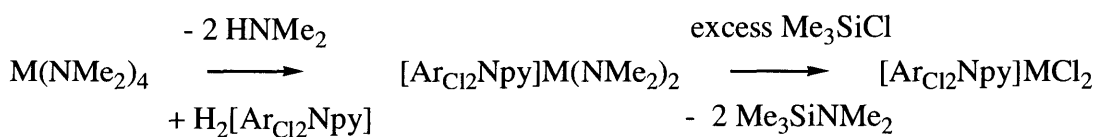
Figure 2.1. Two diamido-donor ligand frameworks studied recently in the Schrock lab.

2.1.1 Preparation of $[(2,6\text{-Cl}_2\text{C}_6\text{H}_3\text{NCH}_2)_2\text{C}(\text{CH}_3)(2\text{-C}_5\text{H}_4\text{N})]^{2-}$ ($[\text{Ar}_{\text{Cl}_2}\text{Npy}]^{2-}$) Complexes⁵⁴

The palladium-catalyzed coupling reaction^{60,61} between 2,6-dichlorobromobenzene and $(\text{H}_2\text{NCH}_2)_2\text{C}(\text{CH}_3)(2\text{-C}_5\text{H}_4\text{N})$ produces $\text{H}_2[\text{Ar}_{\text{Cl}_2}\text{Npy}]$ in about 65% yield (Scheme 2.1). Impurities arising from what is believed to be competitive coupling at the 2 and 6 positions of 2,6-dichlorobromobenzene (5%) cannot be eliminated, however, and impure $\text{H}_2[\text{Ar}_{\text{Cl}_2}\text{Npy}]$ must be employed to prepare zirconium and hafnium complexes. As shown in Scheme 2.2, $[\text{Ar}_{\text{Cl}_2}\text{Npy}]\text{MCl}_2$ is synthesized via an analogous method to that employed to prepare zirconium and hafnium complexes bearing $[\text{MesNpy}]^{2-}$ ligands.⁴⁷⁻⁴⁹ Alkylation of the $[\text{Ar}_{\text{Cl}_2}\text{Npy}]\text{MCl}_2$ complexes with Grignard reagents proceeds smoothly to yield $[\text{Ar}_{\text{Cl}_2}\text{Npy}]\text{MR}_2$ complexes, where $\text{M} = \text{Zr}$ and $\text{R} = \text{Me}$, or $\text{M} = \text{Hf}$ and $\text{R} = \text{Me}$ or *i*-Bu. $[\text{Ar}_{\text{Cl}_2}\text{Npy}]\text{Zr}(\textit{i}\text{-Bu})_2$ is unstable at room temperature and therefore could not be isolated. Impurities formed as a consequence of competitive coupling in the ligand synthesis are removed by recrystallization of either the $[\text{Ar}_{\text{Cl}_2}\text{Npy}]\text{M}(\text{NMe}_2)_2$ or $[\text{Ar}_{\text{Cl}_2}\text{Npy}]\text{MR}_2$ complexes.



Scheme 2.1. Synthesis of $[(2,6\text{-Cl}_2\text{C}_6\text{H}_3\text{NHCH}_2)_2\text{C}(\text{CH}_3)(2\text{-C}_5\text{H}_4\text{N})]$ ($[\text{Ar}_{\text{Cl}_2}\text{Npy}]\text{H}_2$).



Scheme 2.2. Synthesis of $[\text{Ar}_{\text{Cl}_2}\text{Npy}]\text{MCl}_2$ ($\text{M} = \text{Zr}, \text{Hf}$).

Table 2.1. Bond lengths [\AA] and angles [$^\circ$] for $[\text{Ar}_{\text{Cl}_2}\text{Npy}]\text{Hf}(i\text{-Bu})_2$.

Hf-N(1)	2.416(9)	N(2)-Hf-C(5)	97.4(4)
Hf-N(2)	2.112(9)	N(2)-Hf-Cl(1)	70.2(3)
Hf-N(3)	2.048(8)	N(3)-Hf-C(1)	106.6(4)
Hf-C(1)	2.261(11)	N(3)-Hf-C(5)	104.2(4)
Hf-C(5)	2.222(12)	N(3)-Hf-Cl(1)	161.8(3)
Hf-Cl(1)	2.760(3)	C(1)-Hf-Cl(1)	79.1(3)
N(1)-Hf-N(2)	75.2(3)	C(1)-Hf-C(5)	96.8(5)
N(1)-Hf-N(3)	83.2(4)	C(5)-Hf-Cl(1)	92.0(3)
N(1)-Hf-C(1)	86.7(4)	C(24)-N(2)-Hf	131.0(7)
N(1)-Hf-C(5)	170.4(4)	C(18)-N(3)-Hf	128.9(7)
N(1)-Hf-Cl(1)	79.8(2)	C(6)-C(5)-Hf	125.7(9)
N(2)-Hf-N(3)	99.1(3)	C(2)-C(1)-Hf	116.4(9)
N(2)-Hf-C(1)	146.5(4)		

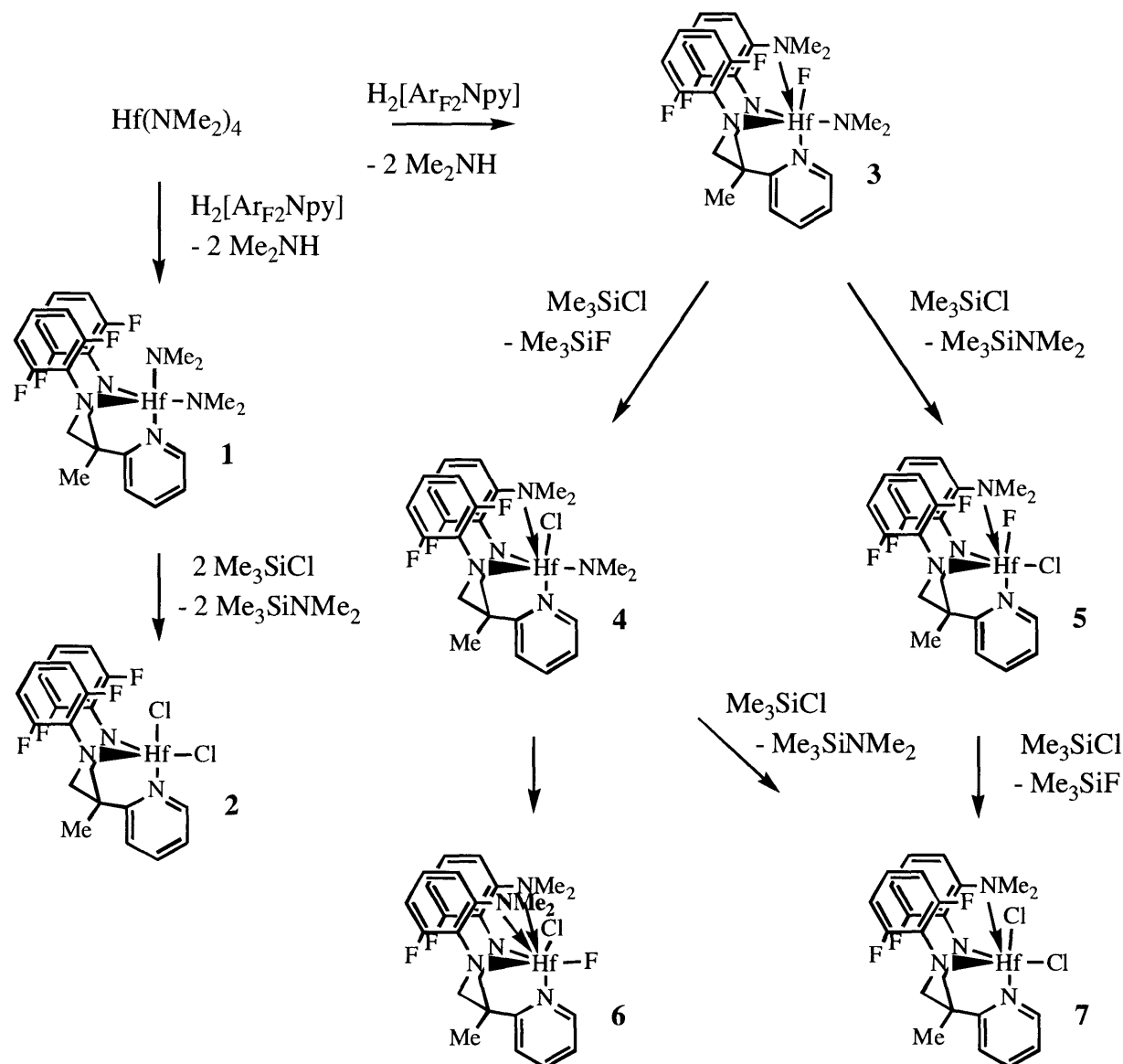
Room temperature NMR spectra of $[\text{Ar}_{\text{Cl}_2}\text{Npy}]\text{Hf}(i\text{-Bu})_2$ feature separate resonances for axial and equatorial alkyl groups, and mirror symmetry consistent with a TBP structure rather than an octahedral structure. Therefore the Hf-Cl interaction does not persist in solution at room temperature. ^1H -NOESY experiments exhibited a cross peak between the equatorial bound alkyl methylene and the pyridyl *ortho*-Proton (*o*-H), showing that the methylene resonance for the equatorial alkyl group is found at lower field than the methylene resonance for the axial alkyl group. In the zirconium dimethyl species, the ^1H NMR methyl resonances appear as two broadened singlets, characteristic of exchange of axial and equatorial methyl groups on the NMR timescale. Upon mixing $[\text{Ar}_{\text{Cl}_2}\text{Npy}]\text{Hf}^{13}\text{Me}_2$ and $[\text{Ar}_{\text{Cl}_2}\text{Npy}]\text{ZrMe}_2$ in benzene at 22 $^\circ\text{C}$, the methyl groups scrambled between the two metals within seconds. Therefore we believe that the broad methyl resonances can be ascribed to rapid intermolecular exchange.⁴⁷ In contrast, the *i*-Bu resonances are sharp because intermolecular exchange is relatively slow on the NMR timescale.

2.2 Preparation of $[(2,6\text{-F}_2\text{C}_6\text{H}_3\text{NCH}_2)_2\text{C}(\text{CH}_3)(2\text{-C}_5\text{H}_4\text{N})]^{2-}$ ($[\text{Ar}_{\text{F}_2}\text{Npy}]^{2-}$) Complexes

The coupling reaction between 1-bromo-2,6-difluorobenzene and $(\text{H}_2\text{NCH}_2)_2\text{C}(\text{CH}_3)(2\text{-C}_5\text{H}_4\text{N})$ proceeded at a much slower rate than the coupling reaction to give $\text{H}_2[\text{Ar}_{\text{Cl}_2}\text{Npy}]$, affording $\text{H}_2[\text{Ar}_{\text{F}_2}\text{Npy}]$ in only 37% yield. In contrast to the 24 hour reaction time required to

prepare $\text{H}_2[\text{Ar}_{\text{Cl}2}\text{Npy}]$, temperatures up to 120 °C for 4 to 5 days still failed to convert all of the monoarylated intermediate to the desired $\text{H}_2[\text{Ar}_{\text{F}2}\text{Npy}]$. Ultimately $\text{H}_2[\text{Ar}_{\text{F}2}\text{Npy}]$ was obtained free from impurities by column chromatography, in contrast to $\text{H}_2[\text{Ar}_{\text{Cl}2}\text{Npy}]$, which could not be separated from impurities in this manner.

$\text{H}_2[\text{Ar}_{\text{F}2}\text{Npy}]$ reacted readily with $\text{Hf}(\text{NMe}_2)_4$; however, the primary product was $[\text{Ar}_{\text{F}2:\text{FNMe}_2}\text{Npy}]\text{HfF}(\text{NMe}_2)$ (**3**), with $[\text{Ar}_{\text{F}2}\text{Npy}]\text{Hf}(\text{NMe}_2)_2$ (**1**) formed only in trace quantities (< 5%) (Scheme 2.3). In **3**, one of the four *ortho*-fluorines has been replaced by a dimethylamido group, and the fluoride transferred to the metal. The ^1H NMR and ^{19}F NMR spectra at 22 °C are indicative of an asymmetric complex with the aryl NMe_2 moiety coordinating strongly to the metal and the 2,6-difluoro aryl ring rotating freely. Two separate singlets, each representing three hydrogens, are observed for the donor NMe_2 group, while a singlet representing six hydrogens is observed for the covalently bound NMe_2 ligand. This type of exchange of a dimethylamido group for an aryl *ortho*-fluorine has been documented in a related molybdenum system,⁶³ and more recently in a related titanium system.⁶⁴



Scheme 2.3. Reactions leading to products 1 through 7.

The ^{19}F NMR spectrum of **3** consists of three resonances representing a total of four fluorine atoms. Two resonances at -128.6 and -122.0 ppm show fine structure as a consequence of coupling with aryl hydrogens ($J_{\text{FH}} = 6$ Hz). The resonance at -122.0 ppm (representing two fluorines) is further split into a doublet by the fluoride covalently bound to the metal ($J_{\text{FF}} = 32.9$ Hz). Conversely, the Hf-F resonance appears as a triplet ($J_{\text{FF}} = 32.9$ Hz) at 28.5 ppm, which is in the expected range for a metal bound fluoride.⁶⁵⁻⁶⁹ Observation of only one doublet for the two

fluorine atoms in the 2,6-F₂C₆H₃ ring confirms that the 2,6-F₂C₆H₃ ring rotates freely on the NMR timescale.

The presence of [Ar_{F₂}Npy]Hf(NMe₂)₂ (**1**) as a product of the reaction between Hf(NMe₂)₄ and H₂[Ar_{F₂}Npy] was overlooked initially. Compound **1** can be identified by a pyridyl *o*-H resonance at 8.42 ppm (the *o*-H resonance in free ligand is found at 8.35 ppm.). [Ar_{F₂}Npy]Hf(NMe₂)₂ is more soluble in both ether and pentane than **3**, and therefore is easily removed upon recrystallization of the crude product from ether and easily identified in the residue obtained from the mother liquor. The ¹⁹F NMR spectrum of **1** gives rise to one singlet at -125.1 ppm with fine structure (J_{FH} = 6.8 Hz) characteristic of aryl *ortho*-fluorines in a mirror symmetric species with two 2,6-F₂C₆H₃ rings that rotate freely on the NMR timescale at 22 °C. Subsequent reaction of the crude product with TMSCl led to formation of small amounts of [Ar_{F₂}Npy]HfCl₂ (**2**). NMR spectra of **2** are also consistent with the presence of a plane of symmetry on the NMR timescale and freely rotating aryl rings.

The reaction of pure **3** with excess TMSCl afforded [Ar_{F₂,FNMe₂}Npy]HfCl₂ (**7**) in good yield. Both the Hf-F and Hf-NMe₂ groups were replaced by chlorides upon reaction with excess TMSCl. Addition of one equivalent of TMSCl to **3** yielded [Ar_{F₂,FNMe₂}Npy]HfCl(NMe₂) (**4**), according to NMR experiments. This result suggests that **4** is a more likely intermediate than [Ar_{F₂,FNMe₂}Npy]Hf(F)Cl (**5**), and the fluoride bound to hafnium is replaced more readily than the dimethylamido group. The ¹⁹F spectrum of **7** contains a resonance for two fluorines at -120.9 ppm and a resonance for one fluoride at -129.7 ppm. A resonance characteristic of a fluoride on the metal is not observed downfield. Compound **7** is relatively insoluble in toluene and therefore could be isolated cleanly by filtration. In a typical reaction, several products remained in solution in addition to **7**. One was [Ar_{F₂}Npy]HfCl₂ (**2**), the presence of which confirmed that [Ar_{F₂}Npy]Hf(NMe₂)₂ was present in the sample of crude **3**. Another compound that was identified in the toluene solution was [Ar_{(FNMe₂)₂}Npy]Hf(F)Cl (**6**), a species with mirror symmetry in which a second *ortho*-fluorine has been exchanged with an amido group to give a compound

in which two aryl NMe₂ groups are coordinating to hafnium. Compound **6** could be derived directly from **4** as a result of dimethylamido/fluorine exchange.

Recrystallization of a sample of **7** from ether led to a product that was initially assumed to be a purer sample of **7**. Three successive recrystallizations were required to obtain X-ray quality yellow-orange, single crystals. In fact, the recrystallization process had succeeded in concentrating and purifying the least soluble component of the crude reaction, which turned out to be **6** (Scheme 2.1). The ¹⁹F NMR spectrum of **6** contains a resonance at -127.5 ppm for two equivalent aryl *ortho*-fluorines ($J_{\text{FH}} = 6.3$ Hz) and a resonance at 45.8 ppm for a single fluoride on the metal ($J_{\text{FH}} = 6.3$ Hz).

The X-ray structure of [Ar_{(F_{NMe₂)₂}Npy]Hf(F)Cl (**6**) is shown in Figure 2.3 (See also Tables 2.2 and 2.3). In this seven-coordinate species, the aryl NMe₂ donors are coordinated to the metal at a distance of 2.459(11) Å, while the pyridine donor is bound at a distance of 2.355(14) Å. The Hf-N_{donor} bond length (2.459(11) Å) is significantly longer than the covalent Hf-N bond lengths (2.136(10) Å). Also notable is the Hf-N(2)-C(8) bond angle of 119.6(7)°, which is smaller than in [Ar_{Cl₂}Npy]Hf(*i*-Bu)₂ as a consequence of strong coordination of the *o*-NMe₂ group. In a closely related molybdenum difluoride complex in which the substituent on the amido nitrogens is *ortho*-dimethylamidotetrafluorophenyl (Ar' in [(Ar'NCH₂CH₂)₂NMe]MoF₂),⁶³ the NMe₂ donors are coordinated to the metal at distances of 2.482(5) Å and 2.440(5) Å, the amine donor is bound at a distance of 2.330(5) Å, and the covalent Mo-N bond lengths are 2.008(5) Å and 2.013(5) Å. The M-F bond lengths in the two compounds are 1.989(9) Å (Hf) and 1.968(3) Å (Mo).}

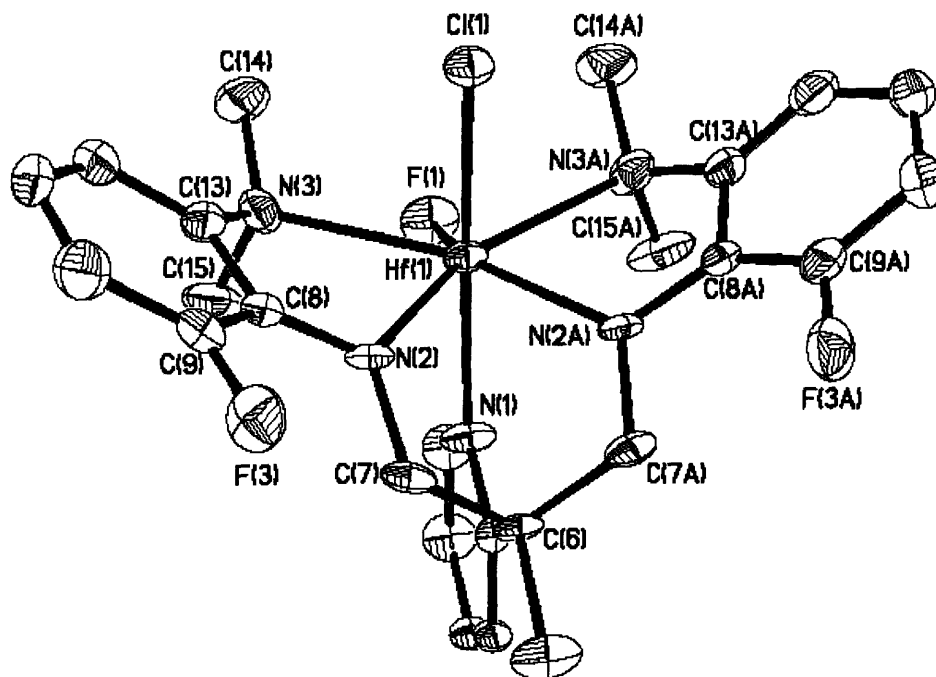


Figure 2.3. Thermal ellipsoid drawing of $[\text{Ar}_{(\text{FNMe}_2)_2}\text{Npy}]\text{Hf}(\text{F})\text{Cl}$ (**6**) at the 30% probability level.

Table 2.2. Bond lengths [\AA] and angles [$^\circ$] for $[\text{Ar}_{(\text{FNMe}_2)_2}\text{Npy}]\text{Hf}(\text{F})\text{Cl}$.

Hf-F(1)	1.989(9)	Hf-N(2)	2.136(10)
Hf-Cl(1)	2.440(4)	Hf-N(3)	2.459(11)
Hf-N(1)	2.355(14)	Hf-N(2)-C(8)	119.6(7)
F(1)-Hf-Cl(1)	108.0(4)	Cl(1)-Hf-N(3)	81.5(3)
F(1)-Hf-N(1)	79.8(5)	N(1)-Hf-N(2)	79.9(3)
F(1)-Hf-N(2)	132.1(3)	N(1)-Hf-N(3)	101.2(3)
F(1)-Hf-N(3)	72.8(3)	N(2)-Hf-N(3)	154.0(4)
Cl(1)-Hf-N(1)	172.2(4)	N(2)-Hf-N(2A)	85.5(5)
Cl(1)-Hf-N(2)	94.4(3)		

Table 2.3. Crystal data and structure refinement for
 $[\text{Ar}_{(\text{FNMMe}_2)_2}\text{Npy}]\text{Hf}(\text{F})\text{Cl}$, and $[\text{Ar}_{\text{F}_2}\text{Npy}]\text{Hf}(i\text{-Bu})_2$.

	$[\text{Ar}_{(\text{FNMMe}_2)_2}\text{Npy}]\text{Hf}(\text{F})\text{Cl}$	$[\text{Ar}_{\text{F}_2}\text{Npy}]\text{Hf}(i\text{-Bu})_2$
Empirical formula	$\text{C}_{25}\text{H}_{29}\text{ClF}_3\text{HfN}_5$	$\text{C}_{29}\text{H}_{35}\text{F}_4\text{HfN}_3$
Formula weight	670.47	680.09
Temperature (K)	293(2)	273(2)
Crystal system, space group	Monoclinic, P2(1)	Monoclinic, C2/c
Unit cell dimensions	$a = 8.4334(14) \text{ \AA}$ $b = 17.106(3) \text{ \AA}$ $c = 9.2935(16) \text{ \AA}$ $\alpha = 90^\circ$ $\beta = 111.336(3)^\circ$ $\gamma = 90^\circ$	$a = 15.2329(9) \text{ \AA}$ $b = 12.1484(7) \text{ \AA}$ $c = 29.4719(17) \text{ \AA}$ $\alpha = 90^\circ$ $\beta = 96.2770(10)^\circ$ $\gamma = 90^\circ$
Volume (\AA^3)	1248.8(4)	5421.2(5)
Z, Calculated density (Mg/m^3)	2, 1.783	8, 1.667
Absorption coefficient (mm^{-1})	4.330	3.899
F(000)	660	2704
Theta range for data collection	2.35 to 20.98°	2.48 to 28.31°
Limiting indices	$-8 \leq h \leq 8$, $-14 \leq k \leq 17$, $-9 \leq l \leq 9$	$-18 \leq h \leq 18$, $-16 \leq k \leq 7$, $-39 \leq l \leq 37$
Reflections collected / unique	4017	14787
Independent reflections	1398 [R(int) = 0.0536]	6180 [R(int) = 0.0735]
Completeness to theta max	99.8 %	91.8 %
Data / restraints / parameters	1398 / 0 / 178	6180 / 0 / 340
Goodness-of-fit on F ²	1.263	1.020
Final R indices [I > 2σ(I)]	R1 = 0.0540 wR2 = 0.1152	R1 = 0.0367 wR2 = 0.0898
R indices (all data)	R1 = 0.0574 wR2 = 0.1166	R1 = 0.0498 wR2 = 0.0945
Largest diff. peak and hole ($\text{e}\text{\AA}^{-3}$)	1.533 and -2.586	2.496 and -1.215

^a In each case the wavelength was 0.71073 Å and the refinement method was full-matrix least-squares on F². No absorption correction was applied.

The reaction between **7** and 2.1 equivalents of *i*-BuMgCl produced $[\text{Ar}_{\text{F}_2;\text{FNMe}_2}\text{Npy}]\text{HfCl}(\textit{i}\text{-Bu})$. As expected, no metal bound fluoride could be found in the ^{19}F NMR spectrum. Further substitution of the chloride to give $[\text{Ar}_{\text{F}_2;\text{FNMe}_2}\text{Npy}]\text{Hf}(\textit{i}\text{-Bu})_2$ did not occur, most likely because $[\text{Ar}_{\text{F}_2;\text{FNMe}_2}\text{Npy}]\text{HfCl}(\textit{i}\text{-Bu})$ is much more crowded than **7**, and the metal is not as electrophilic. However, **7** reacted with 2 equivalents of MeMgBr in 1 hour at room temperature to give $[\text{Ar}_{\text{F}_2;\text{FNMe}_2}\text{Npy}]\text{HfMe}_2$, according to NMR spectra. Activation of $[\text{Ar}_{\text{F}_2;\text{FNMe}_2}\text{Npy}]\text{HfMe}_2$ with $\{\text{Ph}_3\text{C}\}\{\text{B}(\text{C}_6\text{F}_5)_4\}$ yielded a monomethyl cationic species that did not react readily with 1-hexene under the conditions employed in related experiments described later.

Because $\text{Hf}(\text{NMe}_2)_4$ could not be employed in the synthesis of $[\text{Ar}_{\text{F}_2}\text{Npy}]\text{HfR}_2$ complexes, the synthesis of $[\text{Ar}_{\text{F}_2}\text{Npy}]\text{Hf}(\textit{i}\text{-Bu})_2$ was attempted "directly" from HfCl_4 by forming a complex between HfCl_4 and the ligand prior to the addition of 4.1 equivalents of *i*-BuMgCl. After several experiments in ether and toluene, dichloromethane was found to be the most suitable solvent for forming the initial adduct. In order for the reaction to succeed, complete dissolution of HfCl_4 in the presence of ligand is essential. After 36 hours, the solvent was removed in vacuo to afford the adduct between $\text{H}_2[\text{Ar}_{\text{F}_2}\text{Npy}]$ and HfCl_4 as a yellow powder. Isobutylmagnesium chloride (4.1 equivalents) was then added to a suspension of this adduct in ether that had been cooled to $-30\text{ }^\circ\text{C}$. After filtering the mixture through Celite, the ether soluble portion was concentrated in vacuo and the product recrystallized from a mixture of ether and pentane (1:4) to give $[\text{Ar}_{\text{F}_2}\text{Npy}]\text{Hf}(\textit{i}\text{-Bu})_2$ in 52% yield. When equivalent amounts of $\text{H}_2[\text{Ar}_{\text{F}_2}\text{Npy}]$ and HfCl_4 were used, free ligand (< 5%) was present as an impurity and could not be removed easily. When a slight excess of HfCl_4 was employed, however, clean $[\text{Ar}_{\text{F}_2}\text{Npy}]\text{Hf}(\textit{i}\text{-Bu})_2$ was obtained without successive recrystallization. Although this is not a high yield route to $[\text{Ar}_{\text{F}_2}\text{Npy}]\text{Hf}(\textit{i}\text{-Bu})_2$, it is the only one available thus far.

The X-ray structure of $[\text{Ar}_{\text{F}_2}\text{Npy}]\text{Hf}(\textit{i}\text{-Bu})_2$ is shown in Figure 2.4 (See also Table 2.3 for crystal and structure refinement data and Table 2.4 for selected bond lengths and angles). Two

ortho-fluorines in the 2,6-difluorophenyl rings interact weakly with the metal at distances of 2.443(3) Å and 2.674(3) Å to form a sterically congested seven-coordinate complex. The pyridine donor is bound at a distance of 2.442(4) Å and the covalent Hf-N bond lengths are 2.103(3) Å and 2.117(4) Å, which are similar to those found in the analogous compound that contains 2,6-dichlorophenyl substituents. The Hf-N(2)-C(24) and Hf-N(3)-C(18) angles are smaller than those in $[\text{Ar}_{\text{Cl}_2}\text{Npy}]\text{Hf}(i\text{-Bu})_2$ (124.8° and 125.2°, respectively, compared to 131.0° and 128.9°, respectively), but larger than those in **6** (119.6°). We propose that two aryl *ortho*-fluorines are interacting with the metal in this complex (versus only one chlorine in $[\text{Ar}_{\text{Cl}_2}\text{Npy}]\text{Hf}(i\text{-Bu})_2$) as a consequence of the more electron-poor nature of the metal and the smaller size of a fluorine versus a chlorine atom.

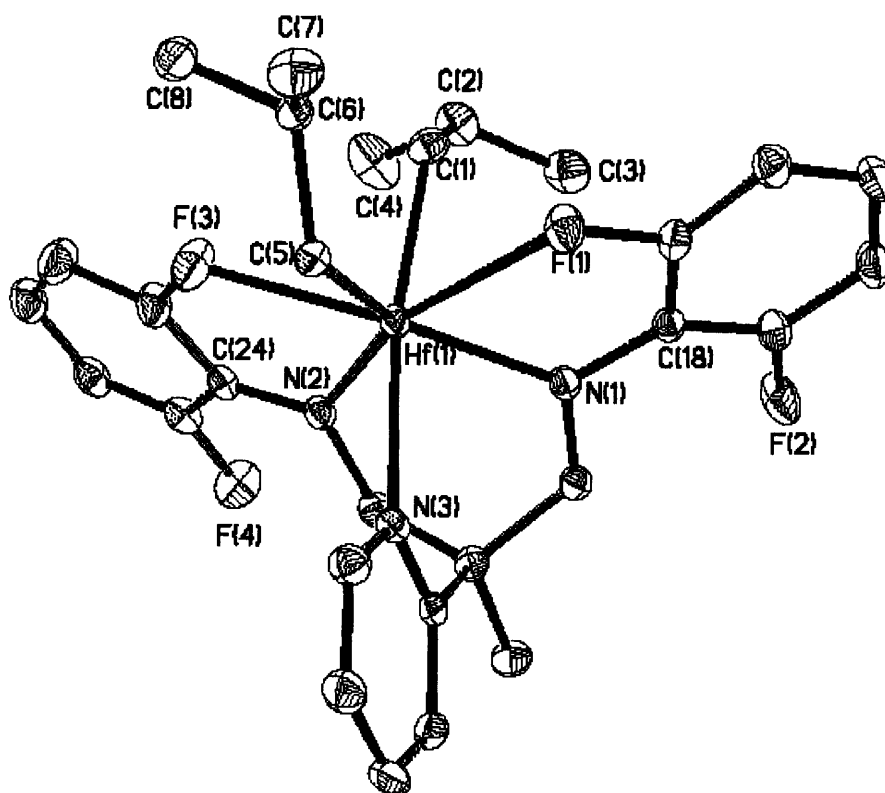


Figure 2.4. Thermal ellipsoid drawing of $[\text{Ar}_{\text{F}_2}\text{Npy}]\text{Hf}(i\text{-Bu})_2$ at the 30% probability level.

Table 2.4. Bond lengths [Å] and angles [°] for [Ar_{F2}Npy]Hf(*i*-Bu)₂.

Hf-N(2)	2.103(3)	N(1)-Hf-F(3)	162.34(13)
Hf-N(1)	2.117(4)	N(1)-Hf-N(2)	96.38(14)
Hf-C(1)	2.261(5)	F(1)-Hf-C(5)	67.16(13)
Hf-C(5)	2.277(4)	F(1)-Hf-C(1)	78.37(15)
Hf-N(3)	2.442(4)	F(1)-Hf-F(3)	130.41(9)
Hf-F(3)	2.443(3)	F(1)-Hf-N(2)	161.59(12)
Hf-F(1)	2.674(3)	C(5)-Hf-C(1)	99.06(16)
N(3)-Hf-N(1)	76.36(13)	C(5)-Hf-F(3)	71.33(14)
N(3)-Hf-F(1)	96.09(11)	C(5)-Hf-N(2)	129.16(15)
N(3)-Hf-C(5)	85.48(14)	C(1)-Hf-N(2)	104.23(16)
N(3)-Hf-C(1)	170.66(15)	C(1)-Hf-F(3)	82.65(16)
N(3)-Hf-F(3)	106.59(12)	N(2)-Hf-F(3)	67.76(13)
N(3)-Hf-N(2)	78.67(13)	C(18)-N(1)-Hf	125.2(3)
N(1)-Hf-F(1)	65.22(11)	C(24)-N(2)-Hf	124.8(3)
N(1)-Hf-C(5)	126.28(15)	C(2)-C(1)-Hf	129.3(4)
		C(6)-C(5)-Hf	120.4(3)

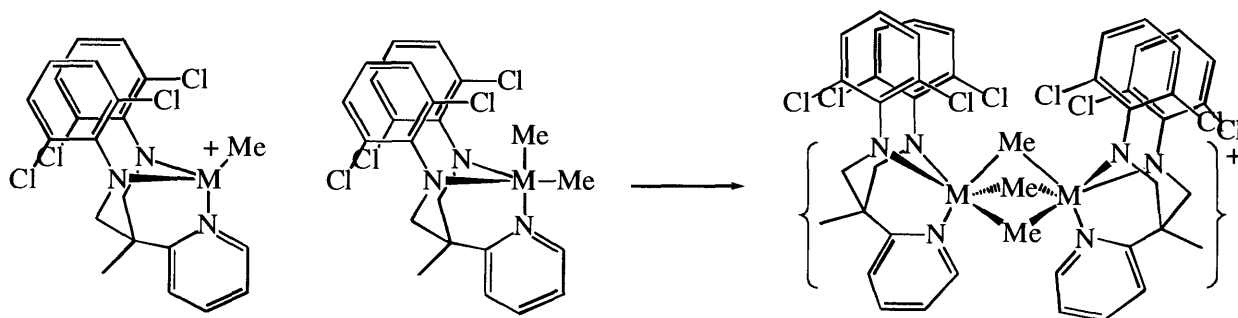
The synthesis of [Ar_{F2}Npy]HfMe₂ was also successful through the direct route. The initial yield was much higher (89%); however, the reaction was not as clean as in the case of [Ar_{F2}Npy]Hf(*i*-Bu)₂, with an unidentifiable impurity being formed (~10%). This impurity could be removed through recrystallization, leading to pure [Ar_{F2}Npy]HfMe₂ in a yield of 43%.

Attempts to prepare [Ar_{Cl2}Npy]Hf(*i*-Bu)₂ in a similar direct manner failed. Only trace amounts of [Ar_{Cl2}Npy]Hf(*i*-Bu)₂ were observed. The synthesis of [Ar_{Cl2}Npy]HfMe₂ in this manner was more promising, although clean [Ar_{Cl2}Npy]HfMe₂ could be obtained in only 10% yield.

2.3 Activation of [Ar_{Cl2}Npy]M(Me)₂ Complexes

The addition of {Ph₃C}{B(C₆F₅)₄} to the [Ar_{Cl2}Npy]MMe₂ complexes (M = Zr or Hf) results in formation of dimeric monocations, {[Ar_{Cl2}Npy]₂M₂Me₃}⁺; {[Ar_{Cl2}Npy]MMe}⁺ is formed and captured rapidly by [Ar_{Cl2}Npy]HfMe₂, as shown in Scheme 2.3.⁵⁴ Therefore only 0.5 equivalents of {Ph₃C}{B(C₆F₅)₄} are consumed. Proton and carbon NMR spectra of this

hafnium species show a broad resonance for the methyl group at around 1.3 ppm in the proton NMR spectrum and around 42.9 ppm in the carbon NMR spectrum. In the zirconium species, these resonances are found at 1.13 and 44.64 ppm ($^1J_{\text{CH}} = 109.5$ Hz), respectively, and are not as broad as in the hafnium case. Variable temperature ^{13}C NMR studies of the hafnium species showed that the broad methyl resonance splits into two at 52.2 (3 protons) and 38.0 (6 protons) at -60 °C, consistent with two types of methyl groups being present in the dimer.⁵⁴ These observations are similar to those made for $\{[\text{ArNpy}]_2\text{Zr}_2\text{Me}_3\}^+$ (Ar = Mes or 2,4,6-*i*-Pr₃C₆H₂) species.⁴⁶ A dimeric monocation of this general type, but with the $[(\text{MesNCH}_2\text{CH}_2)_2\text{NMe}]^{2-}$ ligand, was shown in an X-ray study to contain one bridging methyl group.³³ In the analogous $\{[\text{MesNpy}]_2\text{M}_2\text{Me}_3\}^+$ species, it was proposed that three bridging methyl groups are present in the ratio of 2:1 by virtue of the mirror plane of symmetry. The same is proposed to be the case in $\{[\text{Ar}_{\text{Cl}_2}\text{Npy}]_2\text{M}_2\text{Me}_3\}^+$, as shown in Scheme 2.4. The mechanism by which the three methyl groups average intramolecularly is not known. We cannot discount the possibility that the pyridyl donor dissociates from the metal at one or both metal centers, thereby leading to a five-coordinate metal center that can rearrange by a pseudorotation or turnstile mechanism.



Scheme 2.4. Formation of dimeric monocations, $\{[\text{Ar}_{\text{Cl}_2}\text{Npy}]_2\text{M}_2\text{Me}_3\}^+$.

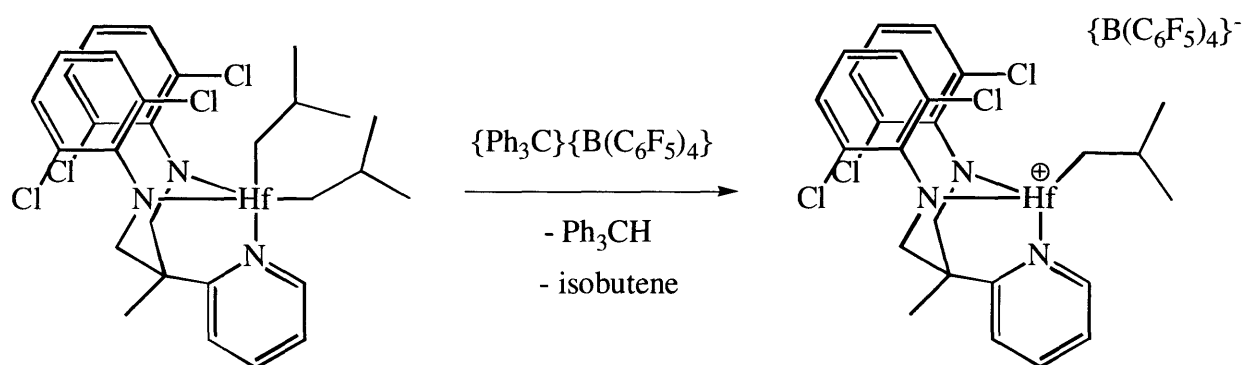
The $\{[\text{Ar}_{\text{Cl}_2}\text{Npy}]_2\text{M}_2\text{Me}_3\}^+$ cations are slowly converted into monomeric monocations in the presence of $\{\text{Ph}_3\text{C}\}\{\text{B}(\text{C}_6\text{F}_5)_4\}$. In the zirconium system the conversion requires a few minutes at 20 °C at the concentrations employed (12 - 17 mM), while more than 2 hours are required in the hafnium system under similar conditions.⁵⁴ We have proposed that the dimeric

monocation dissociates to a small extent to give the monomethyl cation, $\{[\text{Ar}_{\text{Cl}_2}\text{Npy}]\text{MMe}\}^+$ and the dimethyl species, $[\text{Ar}_{\text{Cl}_2}\text{Npy}]\text{MMe}_2$. $\{\text{Ph}_3\text{C}\}\{\text{B}(\text{C}_6\text{F}_5)_4\}$ then reacts with the dimethyl species in competition with recombination of $[\text{Ar}_{\text{Cl}_2}\text{Npy}]\text{MMe}_2$ with $\{[\text{Ar}_{\text{Cl}_2}\text{Npy}]\text{MMe}\}^+$; we do not believe that $\{\text{Ph}_3\text{C}\}\{\text{B}(\text{C}_6\text{F}_5)_4\}$ reacts with the dimeric monocation itself. In contrast, in the mesityl system, $\{[\text{MesNpy}]_2\text{Zr}_2\text{Me}_3\}^+$ dissociates into $\{[\text{MesNpy}]\text{ZrMe}\}^+$ and $[\text{MesNpy}]\text{ZrMe}_2$ significantly more slowly, and therefore pure $\{[\text{MesNpy}]\text{ZrMe}\}\{\text{B}(\text{C}_6\text{F}_5)_4\}$ species could not be prepared.⁴⁶ We propose that the *ortho*-chlorines assist in breaking up the $\{[\text{Ar}_{\text{Cl}_2}\text{Npy}]_2\text{M}_2\text{Me}_3\}^+$ cation by coordinating weakly to the metal, and perhaps also by stabilizing $\{[\text{Ar}_{\text{Cl}_2}\text{Npy}]\text{MMe}\}^+$, thereby making $[\text{Ar}_{\text{Cl}_2}\text{Npy}]\text{MMe}_2$ available in a high enough concentration to react with $\{\text{Ph}_3\text{C}\}\{\text{B}(\text{C}_6\text{F}_5)_4\}$ at a practical rate. The methyl resonances in the $\{[\text{Ar}_{\text{Cl}_2}\text{Npy}]\text{MMe}\}^+$ species are found in the proton NMR spectra at 0.88 ppm for M = Zr and 0.63 ppm for M = Hf in $\text{C}_6\text{D}_5\text{Br}$ at room temperature, while the carbon resonances in the ^{13}C labeled compounds are found at 60.32 ppm ($J_{\text{CH}} = 115$ Hz) for the hafnium complex. It is clear on the basis of proton NMR spectra that these cations are not formed quantitatively and/or that they decompose slowly at 22 °C in bromobenzene over a period of hours. The decomposition products have not been identified.

2.4 Activation of $[\text{Ar}_{\text{Cl}_2}\text{Npy}]\text{Hf}(i\text{-Bu})_2$

Addition of 1 equivalent of $\{\text{Ph}_3\text{C}\}\{\text{B}(\text{C}_6\text{F}_5)_4\}$ to $[\text{Ar}_{\text{Cl}_2}\text{Npy}]\text{Hf}(i\text{-Bu})_2$ in bromobenzene yields $\{[\text{Ar}_{\text{Cl}_2}\text{Npy}]\text{Hf}(i\text{-Bu})\}\{\text{B}(\text{C}_6\text{F}_5)_4\}$, triphenylmethane, and isobutene quantitatively in seconds (Scheme 2.5). The decomposition of $\{[\text{Ar}_{\text{Cl}_2}\text{Npy}]\text{Hf}(i\text{-Bu})\}\{\text{B}(\text{C}_6\text{F}_5)_4\}$ at 0 °C has been monitored by observing the disappearance of the isobutyl methyl resonance (0.77 ppm) in the proton NMR spectrum compared to the Ph_3CH standard as a function of time for varying concentrations of catalyst (Figure 2.5). In the 0.008 M sample (and in many other similar runs) the catalyst initially displayed first-order decomposition with a $k_{\text{decomp}} \approx 0.0005 \text{ min}^{-1}$. The rate of decomposition then accelerated to a rate approximately 6 times faster than that for $\{[\text{MesNpy}]\text{Hf}(i\text{-Bu})\}\{\text{B}(\text{C}_6\text{F}_5)_4\}$ ($k_{\text{decomp}} \approx 0.003 \text{ min}^{-1}$ for Ar = Ar_{Cl_2} , $k_{\text{decomp}} \approx 0.00055 \text{ min}^{-1}$ for

Ar = Mes,⁴⁶) before decreasing again after 2 hours to a value roughly comparable to the initial value. We have not been able to determine the origin of this strange behavior, although it appears to be linked in some way to the polymerization of any isobutene that is present and possibly also to the presence of traces of $\{\text{Ph}_3\text{C}\}\{\text{B}(\text{C}_6\text{F}_5)_4\}$. Isobutene is polymerized in the presence of $\{\text{Ph}_3\text{C}\}^+$, not by the cationic hafnium complex itself, as found in the parent system that contains the mesityl-substituted ligand.⁴⁶ Purification of the reactants through recrystallization did not alter the results. Similar observations have been made for the decomposition of $\{[\text{MesNpy}]\text{Hf}(i\text{-Bu})\}\{\text{B}(\text{C}_6\text{F}_5)_4\}$ at 22 °C, although the decomposition followed first-order kinetics at 0 °C.⁴⁶



Scheme 2.5. Activation of $[\text{Ar}_{\text{Cl}_2}\text{Npy}]\text{Hf}(i\text{-Bu})_2$ with $\{\text{Ph}_3\text{C}\}\{\text{B}(\text{C}_6\text{F}_5)_4\}$.

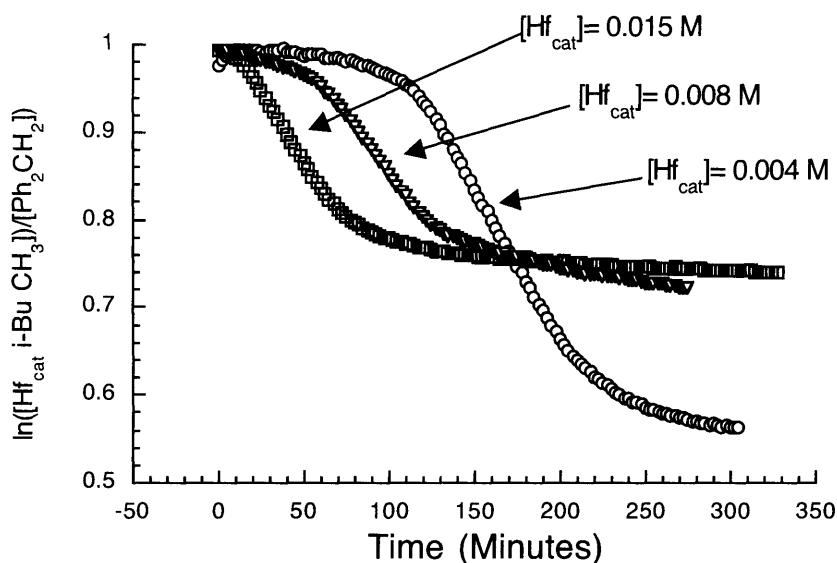


Figure 2.5. Decomposition of $\{[\text{Ar}_{\text{Cl}_2}\text{Npy}]\text{Hf}(i\text{-Bu})\}\{\text{B}(\text{C}_6\text{F}_5)_4\}$ (formed by $\{\text{Ph}_3\text{C}\}\{\text{B}(\text{C}_6\text{F}_5)_4\}$ activation of $[\text{Ar}_{\text{Cl}_2}\text{Npy}]\text{Hf}(i\text{-Bu})_2$) at 0 °C by following the disappearance of the isobutyl methyl resonances in the ^1H NMR spectrum.

2.5 Activation of $[\text{Ar}_{\text{F}_2}\text{Npy}]\text{HfMe}_2$ Complexes

$[\text{Ar}_{\text{F}_2}\text{Npy}]\text{HfMe}_2$ may be activated with $\{\text{Ph}_3\text{C}\}\{\text{B}(\text{C}_6\text{F}_5)_4\}$ to yield $\{[\text{Ar}_{\text{F}_2}\text{Npy}]\text{HfMe}\}\{\text{B}(\text{C}_6\text{F}_5)_4\}$ (~70% pure) and Ph_3CCH_3 . The dissociation of the $\{[\text{Ar}_{\text{X}_2}\text{Npy}]_2\text{Hf}_2\text{Me}_3\}^+$ dimer required only 15 minutes at room temperature when $\text{X} = \text{F}$ compared to 2.5 hours when $\text{X} = \text{Cl}$. This lends further evidence that the halides assist in breaking up the dimer by coordinating to hafnium, with $\text{X} = \text{F}$ being more efficient than $\text{X} = \text{Cl}$. Dissociation of the dimer may also be faster because $[\text{Ar}_{\text{F}_2}\text{Npy}]\text{HfMe}_2$ is a weaker base than $[\text{Ar}_{\text{Cl}_2}\text{Npy}]\text{HfMe}_2$.

2.6 Activation of $[\text{Ar}_{\text{F}_2}\text{Npy}]\text{Hf}(i\text{-Bu})_2$ Complexes

Activation of $[\text{Ar}_{\text{F}_2}\text{Npy}]\text{Hf}(i\text{-Bu})_2$ with $\{\text{Ph}_3\text{C}\}\{\text{B}(\text{C}_6\text{F}_5)_4\}$ at 0 °C in $\text{C}_6\text{D}_5\text{Br}$ did not produce $\{[\text{Ar}_{\text{F}_2}\text{Npy}]\text{Hf}(i\text{-Bu})\}\{\text{B}(\text{C}_6\text{F}_5)_4\}$ as cleanly as $\{[\text{Ar}_{\text{Cl}_2}\text{Npy}]\text{Hf}(i\text{-Bu})\}\{\text{B}(\text{C}_6\text{F}_5)_4\}$ was

produced. Several very small resonances for impurities were observed, none of them amounting to more than 8% of the initial dialkyl; however, in combination they comprised nearly 20% of the monocationic initiator. Decomposition of $\{[\text{Ar}_{\text{F}_2}\text{Npy}]\text{Hf}(i\text{-Bu})\}\{\text{B}(\text{C}_6\text{F}_5)_4\}$ is also more rapid than the decomposition of $\{[\text{Ar}_{\text{Cl}_2}\text{Npy}]\text{Hf}(i\text{-Bu})\}\{\text{B}(\text{C}_6\text{F}_5)_4\}$, a trend that was most apparent at room temperature. After 20 minutes at room temperature, nearly 65% of the initial $\{[\text{Ar}_{\text{F}_2}\text{Npy}]\text{Hf}(i\text{-Bu})\}\{\text{B}(\text{C}_6\text{F}_5)_4\}$ decomposed, whereas only ~20% of the initial $\{[\text{Ar}_{\text{Cl}_2}\text{Npy}]\text{Hf}(i\text{-Bu})\}\{\text{B}(\text{C}_6\text{F}_5)_4\}$ decomposed. At 0 °C, approximately 38% of $\{[\text{Ar}_{\text{F}_2}\text{Npy}]\text{Hf}(i\text{-Bu})\}\{\text{B}(\text{C}_6\text{F}_5)_4\}$ decomposed in 270 minutes, which is about 1.5 times more than $\{[\text{Ar}_{\text{Cl}_2}\text{Npy}]\text{Hf}(i\text{-Bu})\}\{\text{B}(\text{C}_6\text{F}_5)_4\}$ decomposed in the same time. For comparison, after 270 minutes at 0 °C, only ~5% of the $\{[\text{MesNpy}]\text{Hf}(i\text{-Bu})\}\{\text{B}(\text{C}_6\text{F}_5)_4\}$ initiator had decomposed. It is clear that the stabilities of the $\{[\text{ArNpy}]\text{Hf}(i\text{-Bu})\}\{\text{B}(\text{C}_6\text{F}_5)_4\}$ species follow the order $\text{Ar} = \text{Mes} > \text{Ar}_{\text{Cl}_2} > \text{Ar}_{\text{F}_2}$, even though the decompositions are not smooth and the rates are not reproducible.

2.7 Polymerization of 1-Hexene by $[\text{Ar}_{\text{Cl}_2}\text{Npy}]^2\text{-Cationic Alkyls}$

It is possible to prepare $\{[\text{Ar}_{\text{Cl}_2}\text{Npy}]\text{HfMe}\}\{\text{B}(\text{C}_6\text{F}_5)_4\}$ for use as an initiator in 1-hexene polymerization, although 2.5 hours are required at room temperature, and some impurities are generated in the process. A plot of $\ln([1\text{-hexene}]/[\text{standard}])$ versus time at 0 °C is curved before becoming linear after 10 minutes, a trend that suggests a slower initiation than propagation. The slower initiation rate may be ascribed to either tighter binding of the anion to the methyl cation than to the propagating cation formed upon 1,2-insertion and/or to a stronger interaction of an aryl *ortho*-chlorine with the metal in the methyl cation than in the propagating cation. At 0 °C, the observed rate constant for propagation was found to be 0.024 min^{-1} at a catalyst concentration of 15 mM, with $k_p = 0.027 \text{ M}^{-1} \text{ s}^{-1}$. A second run produced a value of $k_p = 0.031 \text{ M}^{-1} \text{ s}^{-1}$. If the initiator is prepared at 30 °C, only 45 minutes is required in order to produce a maximum yield. A k_p value of $0.034 \text{ M}^{-1} \text{ s}^{-1}$ was measured when the initiator was prepared in this manner. These values for k_p are ~60% of those obtained with the analogous isobutyl

initiator (see below), suggesting that ~40% of the metal that is present is not available to polymerize 1-hexene. Although $\{[\text{Ar}_{\text{Cl}_2}\text{Npy}]_2\text{Hf}_2\text{Me}_3\}\{\text{B}(\text{C}_6\text{F}_5)_4\}$ loses $[\text{Ar}_{\text{Cl}_2}\text{Npy}]\text{HfMe}_2$ slowly and $\{[\text{Ar}_{\text{Cl}_2}\text{Npy}]_2\text{Hf}_2\text{Me}_3\}\{\text{B}(\text{C}_6\text{F}_5)_4\}$ is eventually converted into $\{[\text{Ar}_{\text{Cl}_2}\text{Npy}]\text{HfMe}\}\{\text{B}(\text{C}_6\text{F}_5)_4\}$, $\{[\text{Ar}_{\text{Cl}_2}\text{Npy}]\text{HfMe}\}\{\text{B}(\text{C}_6\text{F}_5)_4\}$ begins to decompose slowly to unknown products before $\{[\text{Ar}_{\text{Cl}_2}\text{Npy}]_2\text{Hf}_2\text{Me}_3\}\{\text{B}(\text{C}_6\text{F}_5)_4\}$ is completely consumed.

As described previously, addition of 1.0 equivalent of $\{\text{Ph}_3\text{C}\}\{\text{B}(\text{C}_6\text{F}_5)_4\}$ to $[\text{Ar}_{\text{Cl}_2}\text{Npy}]\text{Hf}(i\text{-Bu})_2$ at $-40\text{ }^\circ\text{C}$, followed by warming to $0\text{ }^\circ\text{C}$, affords $\{[\text{Ar}_{\text{Cl}_2}\text{Npy}]\text{Hf}(i\text{-Bu})\}\{\text{B}(\text{C}_6\text{F}_5)_4\}$, triphenylmethane, and isobutene. Consumption of 1-hexene by this initiator was first-order in both [1-hexene] and [hafnium] at $0\text{ }^\circ\text{C}$. The polymerization of 1-hexene was followed until consumption of 1-hexene was essentially complete ($> 98\%$) and k_p values were obtained from plots of $\ln([1\text{-hexene}]/[\text{standard}])$ versus time. At $0\text{ }^\circ\text{C}$ (Table 2.5), the average k_p value was $0.049\text{ M}^{-1}\text{s}^{-1}$, demonstrating that the $\{[\text{Ar}_{\text{Cl}_2}\text{Npy}]\text{Hf}(\text{CH}_2\text{R})\}\{\text{B}(\text{C}_6\text{F}_5)_4\}$ catalyst system polymerizes 1-hexene at half the rate of the $\{[\text{MesNpy}]\text{Hf}(\text{CH}_2\text{R})\}\{\text{B}(\text{C}_6\text{F}_5)_4\}$ system, for which k_p was found to be $0.10\text{ M}^{-1}\text{s}^{-1}$ at $0\text{ }^\circ\text{C}$.⁴⁶ Plots of $\ln[1\text{-hexene}]$ versus time at $10\text{ }^\circ\text{C}$ and $20\text{ }^\circ\text{C}$ were also linear (Figure 2.6). An Eyring plot of the rate constants between 0 and $20\text{ }^\circ\text{C}$ gave $\Delta H^\ddagger = 7.23\text{ kcal/mol}$ and $\Delta S^\ddagger = -37.9\text{ cal/mol}\cdot\text{K}$ (at $[\text{Hf}] = 1\text{ M}$). This should be compared with polymerization of 1-hexene by $\{[\text{MesNpy}]\text{Hf}(i\text{-Bu})\}\{\text{B}(\text{C}_6\text{F}_5)_4\}$ in $\text{C}_6\text{D}_5\text{Br}$, where $\Delta H^\ddagger = 10.82\text{ kcal}$ and $\Delta S^\ddagger = -23.0\text{ cal/mol}\cdot\text{K}$ (at $[\text{Hf}] = 1\text{ M}$).

Table 2.5. Kinetic data for polymerization of 1-hexene by $\{[Ar_{x_2}Npy]Hf(i-Bu)\}B(C_6F_5)_4$.
^aValues reported by Dr. Klaus Ruhland.

X	Temp (°C)	[Hf] (M)	Equiv. 1-hexene	k_p ($M^{-1} s^{-1}$)
Cl	20	0.012	100	0.12, 0.15
Cl	10	0.012	100	0.080
Cl	10	0.012	100	0.088
Cl	0	0.015	50	0.032 ^a
Cl	0	0.012	100	0.049, 0.050, 0.052
Cl	0	0.012	300	0.047, 0.056, 0.039
Cl	0	0.012	400	0.055
Cl	-5	0.015	50	0.023 ^a
Cl	-10	0.015	50	0.018 ^a
F	20	0.012	100	0.028
F	10	0.012	100	0.016
F	0	0.012	50	0.0007
F	0	0.012	100	0.0007

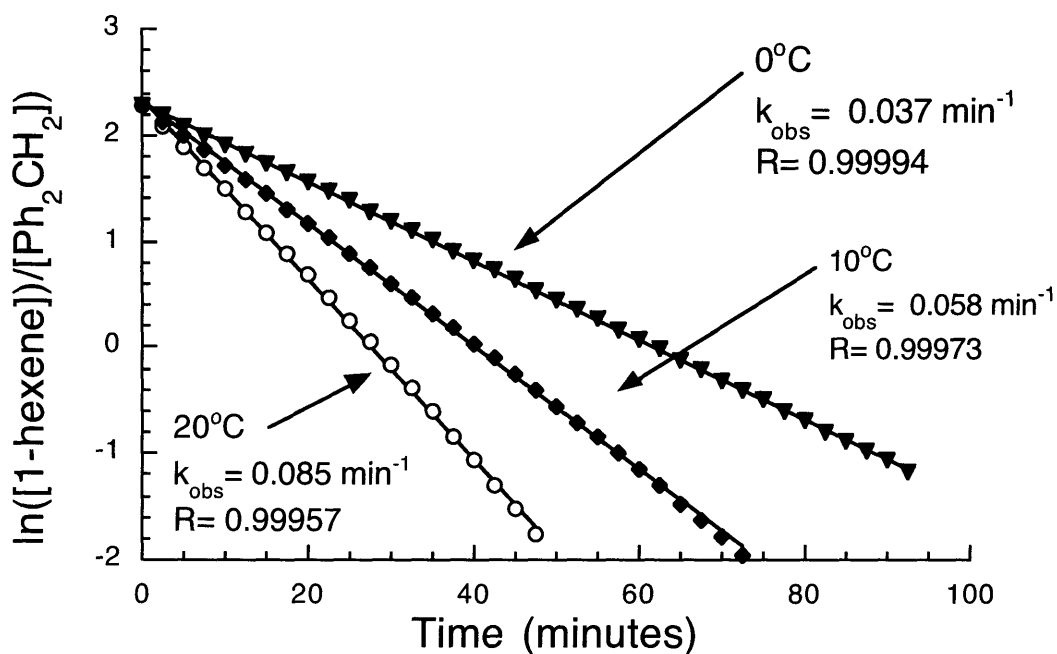


Figure 2.6. Polymerization of 100 equivalents of 1-hexene in C_6D_5Br by $0.012 M \{[Ar_{Cl_2}Npy]Hf(i-Bu)\}B(C_6F_5)_4$.

Despite the linearity of the plots of $\ln([1\text{-hexene}]/[\text{standard}])$ versus time over more than 5 half lives, significant β -hydride elimination was observed to occur by ^1H NMR. A broad vinylidene resonance corresponding to the olefinic product of 1,2 β -hydride elimination ($\beta_{1,2}$ product) grew in at 4.86 ppm^{46,56} in the $\text{C}_6\text{D}_5\text{Br}$ ^1H NMR spectrum as 1-hexene was consumed at 0 °C (to approximately 15% of $[\text{Hf}_{\text{cat}}]_i$ after ~98% consumption of 1-hexene) and continued to grow after the polymerization was complete (to about 70% $[\text{Hf}_{\text{cat}}]_i$ after 48 hours). The ratio of the $\beta_{1,2}$ product to the initial hafnium concentration was obtained by comparing the integration of the olefinic product peak to a known Ph_2CH_2 standard concentration (Table 2.6). Under the conditions of 1-hexene polymerization employed here, the half-life for the consumption of 1-hexene is ~40 minutes (for $[\text{Hf}] = 0.012 \text{ M}$), so consumption is complete in ~200 minutes. During this time, 10 to 20% of chain termination by β -hydride elimination from a 1,2 insertion product has taken place.

Table 2.6. β -Hydride elimination associated with the polymerization of 1-hexene catalyzed by $\{[\text{Ar}_{\text{x}_2}\text{Npy}]\text{Hf}(i\text{-Bu})\}\{\text{B}(\text{C}_6\text{F}_5)_4\}$ in $\text{C}_6\text{D}_5\text{Br}$.

X	T (°C)	Equiv. 1-hexene	% Complete	$\beta\text{-H}_{1,2}$	$\beta\text{-H}_{2,1}$	$\beta\text{-H}_{1,2}$ (48 hours)
Cl	0	100	100	0.1-0.2	~ 0.05	0.7
Cl	10	100	100	0.5-0.8	~ 0.05	0.8
Cl	20	100	100	1.0-1.1	~ 0.05	1.1
Cl	0	300	100	0.1-0.2	0.1-0.3	1.0
F	0	50	93	0.2	0.2	0.6
F	0	50	77	0.2	0.2	0.8
F	0	100	77	0.4	0.2	0.9
F	10	100	77	0.6	0.4	-
F	10	100	98	1.3	0.6	-
F	20	100	77	1.4	1.5	1.9

When 300 equivalents of 1-hexene were polymerized at 0 °C, vinylene resonances corresponding to the olefinic product of β -hydride elimination after a 2,1 insertion ($\beta_{2,1}$ product) grew in between 5.36 and 5.40 ppm^{46,56} and integrated to about 0.1 to 0.2 equivalents of $[\text{Hf}_{\text{cat}}]_i$. In runs where 100 equivalents of 1-hexene were employed at 0 °C, however, only 0.05

equivalents of the $\beta_{2,1}$ product were observed. The resonance due to the $\beta_{2,1}$ product was not observed to grow after all of the 1-hexene had been consumed.

Based on olefinic peak integration alone we cannot say in this case whether the metal containing product of β -hydride elimination (assumed to be a hydride) reacts with 1-hexene to generate a new polymer chain, or whether the hafnium product of β -hydride elimination is inactive even in the presence of 1-hexene. However, the linearity of the plots of $\ln([1\text{-hexene}]/[\text{standard}])$ versus time over more than 5 half-lives suggests that the hafnium hydride product of 1,2 or 2,1 β -hydride elimination may still be active for polymerization in the presence of a high enough concentration of 1-hexene. A plot of the expected molecular weight versus equivalents of 1-hexene added for a series of experiments run at 0 °C in bromobenzene with the $\{[\text{Ar}_{\text{C12}}\text{Npy}]\text{Hf}(i\text{-Bu})\}\{\text{B}(\text{C}_6\text{F}_5)_4\}$ initiator yielded linear plots, with molecular weight values being ~90% of the expected molecular weight values for a perfect living system (Figure 2.7). Polydispersities (M_w/M_n) also were quite low, ranging from 1.01 to 1.05. We believe that these data accurately show that a small amount of 1,2 β -hydride elimination takes place during the polymerization reaction, and that the product of this decomposition reacts with more 1-hexene to form polymer. However, the amount of 1,2 β -hydride elimination apparently is not great enough to affect the polydispersity values to any significant degree.

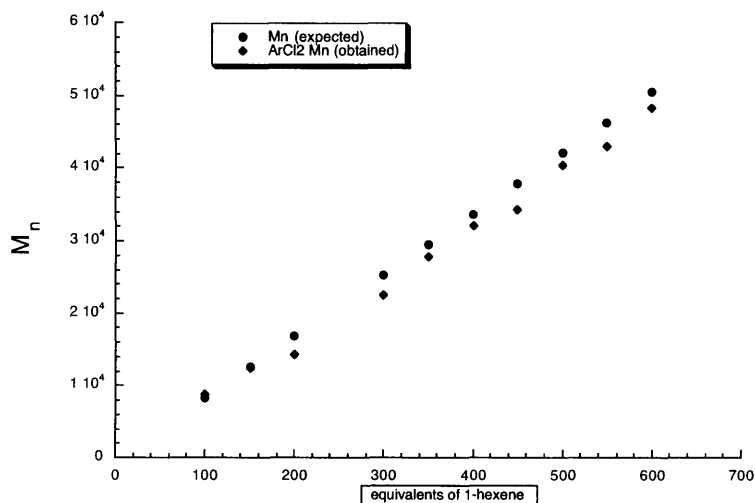


Figure 2.7. Molecular weight measurements for poly(1-hexene) obtained with $\{[\text{Ar}_{\text{C12}}\text{Npy}]\text{Hf}(i\text{-Bu})\}\{\text{B}(\text{C}_6\text{F}_5)_4\}$ as the initiator at 0 °C in $\text{C}_6\text{D}_5\text{Br}$.

2.8 Polymerization of 1-Hexene by $[\text{Ar}_{\text{F}_2}\text{Npy}]^2\text{ Cationic Alkyls}$

Although the reaction of $[\text{Ar}_{\text{F}_2}\text{Npy}]\text{HfMe}_2$ with $\{\text{Ph}_3\text{C}\}\{\text{B}(\text{C}_6\text{F}_5)_4\}$ to give $\{[\text{Ar}_{\text{F}_2}\text{Npy}]\text{HfMe}\}\{\text{B}(\text{C}_6\text{F}_5)_4\}$ at 0 °C was the most rapid as a consequence of the greater ease of dissociation of intermediate $\{[\text{Ar}_{\text{F}_2}\text{Npy}]_2\text{Hf}_2\text{Me}_3\}\{\text{B}(\text{C}_6\text{F}_5)_4\}$ into $\{[\text{Ar}_{\text{F}_2}\text{Npy}]\text{HfMe}\}\{\text{B}(\text{C}_6\text{F}_5)_4\}$ and $[\text{Ar}_{\text{F}_2}\text{Npy}]\text{HfMe}_2$, $\{[\text{Ar}_{\text{F}_2}\text{Npy}]\text{HfMe}\}\{\text{B}(\text{C}_6\text{F}_5)_4\}$ was not formed quantitatively before $\{[\text{Ar}_{\text{F}_2}\text{Npy}]_2\text{Hf}_2\text{Me}_3\}\{\text{B}(\text{C}_6\text{F}_5)_4\}$ was consumed due to concomitant decomposition of $\{[\text{Ar}_{\text{F}_2}\text{Npy}]\text{HfMe}\}\{\text{B}(\text{C}_6\text{F}_5)_4\}$ and formation of side products during the activation process. At 0 °C, k_p was found to be $0.002(1) \text{ M}^{-1}\text{s}^{-1}$ for $\{[\text{Ar}_{\text{F}_2}\text{Npy}]\text{HfMe}\}\{\text{B}(\text{C}_6\text{F}_5)_4\}$ prepared in this manner. This value was lower than that for $\{[\text{Ar}_{\text{F}_2}\text{Npy}]\text{Hf}(i\text{-Bu})\}\{\text{B}(\text{C}_6\text{F}_5)_4\}$ (see below) as a consequence of formation of inactive side products during polymerization and a slower initiation relative to propagation. Approximately 50% of the $\{[\text{Ar}_{\text{F}_2}\text{Npy}]\text{HfMe}\}\{\text{B}(\text{C}_6\text{F}_5)_4\}$ initiator remained in solution after the consumption of 50 equivalents of 1-hexene.

Polymerization of 1-hexene by $\{[\text{Ar}_{\text{F}_2}\text{Npy}]\text{Hf}(i\text{-Bu})\}\{\text{B}(\text{C}_6\text{F}_5)_4\}$ led to plots of $\ln([1\text{-hexene}]/[\text{standard}])$ versus time that were linear throughout the reaction for temperatures ranging from 0 to 20 °C (Figure 2.8). For polymerizations of 50 and 100 equivalents of 1-hexene at 0 °C, k_p was found to be $0.007 \text{ M}^{-1}\text{s}^{-1}$. This should be compared with $k_p = 0.10 \text{ M}^{-1}\text{s}^{-1}$ for $\{[\text{MesNpy}]\text{Hf}(i\text{-Bu})\}\{\text{B}(\text{C}_6\text{F}_5)_4\}$ ⁴⁶ and $0.049 \text{ M}^{-1}\text{s}^{-1}$ for $\{[\text{Ar}_{\text{Cl}_2}\text{Npy}]\text{Hf}(i\text{-Bu})\}\{\text{B}(\text{C}_6\text{F}_5)_4\}$. Both 1,2 and 2,1 β -hydride elimination also were more prominent in the $\{[\text{Ar}_{\text{F}_2}\text{Npy}]\text{Hf}(\text{CH}_2\text{R})\}\{\text{B}(\text{C}_6\text{F}_5)_4\}$ catalyst system than in the $\{[\text{Ar}_{\text{Cl}_2}\text{Npy}]\text{Hf}(\text{CH}_2\text{R})\}\{\text{B}(\text{C}_6\text{F}_5)_4\}$ catalyst system. The vinylidene resonance corresponding to the $\beta_{1,2}$ product was again found at 4.86 ppm and the vinylene resonances corresponding to the $\beta_{2,1}$ products were found between 5.36 and 5.40 ppm and also at 5.48 ppm. For the polymerization of 50 equivalents of 1-hexene at 0 °C, the $\beta_{1,2}$ product peak (representing 2 protons) integrated to 0.2 equivalents of $[\text{Hf}_{\text{cat}}]_1$ after approximately 77% consumption of 1-hexene was observed (the polymerization was stopped after 77% polymerization due to time restraints). At 20 °C, the $\beta_{1,2}$ product peak (representing 2

protons) integrated to 1.4 equivalents of the $[\text{Hf}_{\text{cat}}]_i$ after 77% of the 1-hexene was consumed, and grew to 1.9 equivalents after a period of 48 hours. 2,1 β -hydride elimination was also more prominent in this system, with the $\beta_{2,1}$ product peaks growing to a total of 1.5 equivalents at 20 °C.

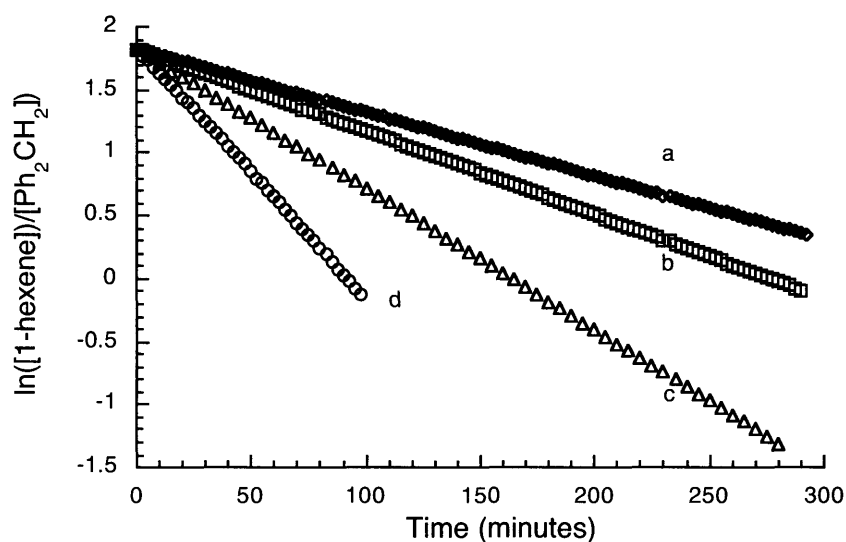


Figure 2.8. Plots of $\ln([1\text{-hexene}]/[\text{Ph}_2\text{CH}_2])$ versus time for the consumption of 1-hexene by $\{[\text{Ar}_{\text{F}_2}\text{Npy}]\text{Hf}(i\text{-Bu})\}\{\text{B}(\text{C}_6\text{F}_5)_4\}$: (a) $[\text{Hf}_{\text{cat}}] = 0.012 \text{ M}$, 0 °C, 50 equivalents of 1-hexene, $k_p = 0.0070 \text{ M}^{-1}\text{s}^{-1}$; (b) $[\text{Hf}_{\text{cat}}] = 0.015 \text{ M}$, 0 °C, 100 equivalents of 1-hexene, $k_p = 0.0073 \text{ M}^{-1}\text{s}^{-1}$; (c) $[\text{Hf}_{\text{cat}}] = 0.012 \text{ M}$, 10 °C, 100 equivalents of 1-hexene, $k_p = 0.0155 \text{ M}^{-1}\text{s}^{-1}$; (d) $[\text{Hf}_{\text{cat}}] = 0.012 \text{ M}$, 20 °C, 100 equivalents of 1-hexene, $k_p = 0.028 \text{ M}^{-1}\text{s}^{-1}$.

Virtually all of the propagating catalyst decomposed after a period of 48 hours at 0 °C to give one or more unidentifiable metal complexes. If the metal containing product of β -hydride elimination (assumed to be a hydride) decomposes before it can react with 1-hexene, then the amount of β -hydride elimination product from 1,2 insertion cannot be greater than the amount of initiator initially present, unless the hydride is able to react with 1-hexene to start a new polymer chain. Since the total equivalents of β -hydride elimination product was significantly greater than the amount of catalyst present initially at 20 °C, it seems probable that new polymer chains can be generated at this temperature when 1-hexene is present. Molecular weights for

polymerization reactions at 0 °C were much lower than expected (~50% of theory) (Figure 2.9), suggesting that the decomposition product may indeed react with 1-hexene to reform poly(1-hexene), thus leading to the observed first-order kinetics. The polydispersities varied between 1.1 and 1.4, consistent with less than perfect characteristics for a living polymerization reaction.

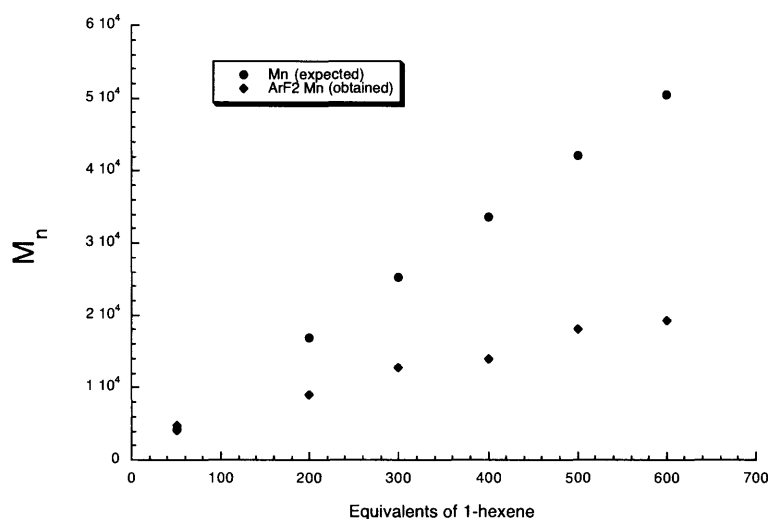


Figure 2.9. Molecular weight measurements for poly(1-hexene) obtained with $\{[Ar_{F_2}Npy]Hf(i-Bu)\}\{B(C_6F_5)_4\}$ as the initiator at 0 °C in C_6D_5Br .

2.9 Conclusions

The main goal of this work was to determine the behavior of $\{[2,6-X_2C_6H_3Npy]Hf(i-Bu)\}\{B(C_6F_5)_4\}$ ($X = Cl$ or F) initiators in 1-hexene polymerization and to compare their behavior with the system in which 2,4,6-Me₃C₆H₂ (mesityl) groups are present on the amido nitrogens. Ultimately, substitution of the mesityl amido substituents in $[ArylNpy]^{2-}$ complexes with aryl groups containing chlorines or fluorines (especially the latter) in the *ortho* positions is detrimental to the development of living olefin polymerization catalysts of this general type.. The catalytic activity steadily decreases in the order aryl = Mesityl > 2,6-Cl₂C₆H₃ > 2,6-F₂C₆H₃ and 1,2 and 2,1 β-hydride elimination increases in the order aryl = Mesityl < 2,6-Cl₂C₆H₃ < 2,6-F₂C₆H₃. Several different explanations for these effects are plausible.

The electron-withdrawing effect of the halides may increase the strength of anion binding to the cationic metal center. The resulting stronger interaction between cation and anion would hinder olefin binding to the metal and insertion into the metal-carbon bond, thereby decreasing the rate of polymerization. The increased electrophilicity of the metal center could also promote β -hydride elimination.

Another explanation is that an aryl *ortho*-fluorine or chlorine moiety coordinates to the cationic metal center, competing with olefin binding and inhibiting polymerization. Metal-halide binding is not strong enough to observe readily by NMR methods, in contrast to binding of an *ortho*-NMe₂ group, but it may be detected in terms of a decrease in polymerization rate. There is considerable evidence that *ortho*-fluorines in aryl rings can coordinate to early transition metals such as zirconium^{66,70} or tantalum.⁷¹ The interaction of the halide with the metal may also serve to accelerate the rate of β -hydride elimination.

It is also possible that hydrogen bonding occurs between the *ortho*-chlorine, or especially the *ortho*-fluorine, and α or β protons in the alkyl group in cationic monoalkyl species. There is some evidence that interactions between fluorines and α ⁷² or β protons^{25,73} can significantly alter olefin polymerization pathways. Hydrogen bonding interactions between *ortho*-halogens and alkyl α or β protons in cationic monoalkyl species may promote more rapid 1,2 β -hydride elimination. These results would be in contrast to recent evidence, which suggests that such a hydrogen bonding interaction between a fluorine and an alkyl β proton *stabilizes* a titanium system against 1,2 β -hydride elimination processes, enabling living polymerization to occur at room temperature.²⁵

2.10 Experimental Section

General Details. All reactions were conducted under an atmosphere of dinitrogen in a Vacuum Atmospheres drybox or using standard Schlenk techniques, and catalyst activation was performed in an inert atmosphere (dinitrogen) box free of ether, THF, or other coordinating solvents. Non-deuterated solvents were sparged with nitrogen for 45 minutes, followed by

passage through a 1 gallon column of activated alumina as described in the literature.⁵⁷ Bromobenzene and deuterated solvents were stirred over CaH₂ for 48 hours, vacuum-transferred, and stored over 4 Å molecular sieves. Commercial reagents were used without further purification. The parent pyridyl diamine (NH₂CH₂)₂C(CH₃)(2-C₅H₄N)),^{74,75} Hf(NMe₂)₄, and Zr(NMe₂)₄⁵⁸ were synthesized according to reported methods. All hafnium complexes containing the [(2,6-Cl₂C₆H₃NCH₂)₂C(CH₃)(2-C₅H₄N)]²⁻ ([Ar_{Cl₂}Npy]²⁻) ligand were synthesized according to reported procedures.⁵² Ordinary Grignard reagents were bought from Aldrich and titrated prior to use with isopropanol using 1,10-phenanthroline as an indicator. NMR data were recorded using Varian Inova-500, Varian Unity-300, or Varian Mercury-300 spectrometers. Chemical shifts are reported in parts per million (ppm) downfield of TMS, and coupling constants are reported in Hertz. The residual protons or ¹³C atoms of the deuterated solvents were used as internal references. ¹⁹F NMR chemical shifts were referenced to the external standard C₆F₆. Elemental analyses (C, H, N, Cl) were done by Kolbe Mikroanalytisches Laboratorium, Mülheim an der Ruhr, Germany.

GPC analyses were conducted using a system equipped with two Waters 7.8 X 300 nm columns (Ultrastayragel 10⁴ Å and Styragel HR5E) in series and a Wyatt Technology mini Dawn light scattering detector coupled with a Knauer differential refractometer. A Knauer 64 HPLC pump was used to supply HPLC grade THF at a flow rate of 1.0 mL/min. The auxiliary constant of the apparatus (5.9 × 10⁻⁴) was calibrated using a polystyrene standard (M_n = 2.2 × 10⁵) and M_n and M_w values for poly(1-hexene) were obtained using dn/dc = 0.076 mL/gr (Wyatt Technology). Data analysis was carried out using Astrette 1.2 software (Wyatt Technology).

[(2,6-F₂C₆H₃NHCH₂)₂C(CH₃)(2-C₅H₄N)] (H₂[Ar_{F₂}Npy]). BINAP (0.113 g, 0.181 mmol) was added to 25 mL of toluene, and the resulting suspension was heated until the BINAP dissolved. Pd(dba)₃ (0.083 g, 0.091 mmol) was added, and the solution was heated until the reaction mixture turned orange. The solution was filtered through Celite and combined with the parent diamine (1.00 g, 6.05 mmol), 1-bromo-2,6-difluorobenzene (2.34 g, 12.1 mmol), and NaO-*t*-Bu (1.34 g, 0.0139 mmol) in 40 mL of toluene. The reaction mixture was heated at 95 °C

for 5 days under N₂ in a sealed Schlenk flask. The hot reaction mixture was filtered and toluene was removed in vacuo. The product was extracted into 300 mL of ether, and the ether solution was washed with water (400 mL total) and saturated NaCl solution (200 mL). The combined water extracts were then washed with ether (200 mL total). The volume of the combined ether extracts was reduced to 6 mL, and pentane (10 mL) was added. A brown precipitate was filtered off through a bed of packed Celite. The filtrate was collected, and the solvent was removed in vacuo to yield a brown oil, which was purified via column chromatography (silica gel, ethyl acetate solvent) to give a red-brown oil; yield 1.20 g (37%). ¹H NMR (CDCl₃) δ 1.43 (3H, s, CH₃), 3.79 (4H, m, CHH), 4.60 (2H, s, NH), 6.63 (2H, m, arom. *p*-H), 6.77 (4H, m, arom. *m*-H), 7.16 (1H, dd, py H), 7.42 (1H, d, py H), 7.67 (1H, t, py H), 8.62 (1H, d, py H). ¹H NMR (C₆D₆) δ 1.42 (3H, s, CH₃), 3.78 (4H, m, CHH), 4.98 (2H, s, NH), 6.22, 6.98, 6.55 (9H total, 3 py H, 6 arom. H), 8.35 (1H, d, py *o*-H). ¹⁹F NMR (C₆D₆) δ -130.0 (4F, s, arom. *o*-F). HRMS (ESI) Calcd. for C₂₁H₁₉N₃F₄ [M+Na] 412.1407. Found [M+Na] 412.1402.

[Ar_{F2;FNMe2}Npy]Hf(F)(NMe₂) (3). H₂[Ar_{F2}Npy] (0.852 g, 2.19 mmol) and Hf(NMe₂)₄ (0.739 g, 2.08 mmol) were dissolved in a mixture of pentane (30 mL) and benzene (5 mL). After 20 hours, the solvent was removed in vacuo to yield a brown powder that was recrystallized from ether at -30 °C to yield yellow crystals; yield 1.189 g (87%). ¹H NMR (C₆D₆) δ 1.15 (3H, s, CH₃), 2.07 (3H, s, ArNCH₃), 2.82 (3H, s, ArNCH₃), 2.94 (6H, s, HfNCH₃), 3.20 (1H, d, CHH), 3.55 (1H, dd, CHH), 4.58 (1H, d, CHH), 4.91 (1H, dd, CHH), 6.2-7.0 (9H, complex, 3 py H, 6 arom. H), 9.19 (1H, d, py *o*-H). ¹⁹F NMR (C₆D₆) δ -128.6 (1F, s, arom. uncoord. *o*-F, J_{FH} = 5.9), -122.0 (2F, d, J_{FF} = 32.9, arom. *o*-F, J_{FH} = 6.5), 28.5 (1F, t, J_{FF} = 32.9, Hf-F). Anal. Calcd. for C₂₅H₂₉N₃F₄Hf: C, 45.91; H, 4.47; N, 10.71. Found C, 46.08; H, 4.41; N, 10.64.

[Ar_{F2}Npy]Hf(NMe₂)₂ (1). This compound was a byproduct of the synthesis of **3**, identified in solution only; yield < 5%. ¹H NMR (C₆D₆) δ 1.18 (3H, s, CH₃), 2.89 (6H, s, N(CH₃)₂), 3.07 (6H, s, N(CH₃)₂), 3.39 (2H, d, CHH), 4.35 (2H, d, CHH; J_{HH} = 10.6), 6.1-7.0 (6H, arom. protons), 8.42 (1H, d, py *o*-H). ¹⁹F NMR (C₆D₆) δ -125.1 (4F, s, arom. *o*-F, J_{FH} = 6.84).

[Ar_{F₂;FNMe₂}Npy]Hf(Cl)(NMe₂) (4). [Ar_{F₂;FNMe₂}Npy]Hf(F)NMe₂ (**3**, 0.300 g, 0.465 mmol) and TMSCl (0.050 g, 0.465 mmol) were dissolved in toluene (7 mL), and the solution was stirred for 30 hours. The reaction mixture was filtered through Celite, and the solvent removed in vacuo from the filtrate to afford a yellow powder. The product was recrystallized from ether in order to remove unreacted [Ar_{F₂;FNMe₂}Npy]Hf(F)(NMe₂); yield = 0.126 g (41%). ¹H NMR (C₆D₆) δ 1.07 (3H, s, CH₃), 2.05 (3H, s, ArNCH₃), 2.85 (3H, s, ArNCH₃), 2.91 (6H, s, HfNCH₃), 3.43 (1H, d, CHH), 3.57 (1H, dd, CHH), 3.70 (1H, d, CHH), 4.95 (1H, dd, CHH), 6.2-7.0 (9H, multiplets, 3 py H, 6 arom. H), 9.19 (1H, d, py *o*-H). ¹⁹F NMR (C₆D₆) δ -127.9 (1F, s, arom. uncoord. *o*-F, *J*_{FH} = 5.9), -119.3 (2F, d, *J*_{FF} = 32.9, arom. *o*-F, *J*_{FH} = 6.5).

[Ar_{F₂;FNMe₂}Npy]HfCl₂ (7). [Ar_{F₂;FNMe₂}Npy]Hf(F)NMe₂ (**3**, 0.771 g, 1.18 mmol) and TMSCl (0.767 g, 7.07 mmol) were dissolved in toluene (25 mL), and the solution was stirred for 30 hours. The yellow precipitate was filtered off and washed with ether (10 mL) and pentane (10 mL); yield 0.634 g (83%). ¹H NMR (C₆D₆) δ 0.93 (3H, s, CH₃), 2.32 (3H, s, ArNCH₃), 3.03 (1H, d, CHH), 3.07, (3H, s, ArNCH₃), 3.63 (1H, dd, CHH), 4.05 (1H, d, CHH), 4.55 (1H, dd, CHH), 6.3-6.9 (9H, ms, 3 py H, 6 arom. H), 9.44 (1H, d, py *o*-H). ¹⁹F NMR (C₆D₆) δ -129.7 (1F, s, arom. uncoord. *o*-F, *J*_{FH} = 6.3), -120.9 (2F, s, arom. *o*-F, *J*_{FH} = 6.3). Anal. Calcd. for C₂₃H₂₃N₄F₃HfCl₂: C, 41.74; H, 3.5; N, 8.47; Cl, 10.71. Found C, 41.50; H, 3.43; N, 8.43; Cl, 10.71.

[Ar_{F₂;FNMe₂}Npy]HfCl(*i*-Bu). A suspension of [Ar_{F₂;FNMe₂}Npy]HfCl₂ (0.600 g, 0.907 mmol) in ether (25 mL) was cooled to -30 °C, and *i*-BuMgCl (0.228 g, 1.952 mmol, 2.7 M in ether) was added. The mixture was stirred at room temperature for 24 hours and filtered through Celite. The solvent was removed in vacuo from the filtrate, and the resulting residue was triturated thoroughly with pentane to give a yellow powder; yield 0.203 g (33%). ¹H NMR (C₆D₆) δ 0.72 (1H dd, CHHCH(CH₃)₂), 0.90 (3H, d, CH₂CH(CH₃)₂), 0.94 (3H, s, CH₃), 1.06 (3H, dd, CHHCH(CH₃)₂), 1.17 (3H, d, CH₂CH(CH₃)₂), 2.02 (3H, s, ArNCH₃), 2.24 (1H, sept, CH₂CH(CH₃)₂), 3.02 (3H, s, ArNCH₃), 3.05 (1H, d, CHH), 3.45 (1H, dd, CHH), 4.12 (1H, d, CHH), 4.93 (1H, dd, CHH), 6.3-7.0 (9H, ms, 3 py H, 6 arom. H), 9.29 (1H, d, py *o*-H). ¹⁹F NMR

(C₆D₆) δ -127.3 (1F, s, arom. uncoord. *o*-F, $J_{\text{FH}} = 6.12$), -119.2 (2F, s, arom. *o*-F, $J_{\text{FH}} = 6.10$). Anal. Calcd. for C₂₇H₃₂N₄F₃Cl₁Hf: C, 47.48; H, 4.65; N, 8.12; Cl, 5.25. Found C, 47.45; H, 4.72; N, 8.2; Cl, 5.19.

[Ar_{F₂;FNMe₂}Npy]HfMe₂. A suspension of [Ar_{F₂;FNMe₂}Npy]HfCl₂ (0.100 g, 0.151 mmol) in ether (5 mL) was cooled to -30 °C, and MeMgBr (0.038 g, 0.317 mmol, 3.45 M in ether) was added. The mixture was stirred at room temperature for 1 hour, and the mixture was filtered through a bed of Celite. The solvent was removed in vacuo from the filtrate, and the resulting residue was triturated thoroughly with pentane to yield a pale yellow powder; yield 0.043 g (46%): ¹H NMR (C₆D₆) δ 0.28 (3H, m, HfCH₃), 0.57 (3H, m, HfCH₃), 1.04 (3H, s, CH₃), 2.14 (3H, s, ArNCH₃), 2.75 (3H, s, ArNCH₃), 3.27 (1H, d, CHH), 3.59 (1H, dd, CHH), 4.17 (1H, d, CHH), 4.77 (1H, dd, CHH), 6.2-7.0 (9H, ms, 3 py H, 6 arom. H), 8.66 (1H, d, py *o*-H).

[Ar_{(FNMe₂)₂}Npy]Hf(F)Cl (6). This compound was a byproduct of the synthesis of [Ar_{F₂;FNMe₂}Npy]HfCl₂ ($\leq 5\%$). It was identified only by its NMR spectrum. ¹H NMR (C₆D₆) δ 1.10 (3H, s, CH₃), 2.22 (3H, s, ArNCH₃), 3.10, (3H, s, ArNCH₃), 3.39 (2H, dd, CHH), 4.90 (2H, dd, CHH), 6.2-7.0 (9H, complex, 3 py H, 6 arom. H), 9.11 (1H, d, py *o*-H). ¹⁹F NMR (C₆D₆) δ -127.5 (2F, s, arom. uncoord. *o*-F, $J_{\text{FH}} = 6.28$), 45.8 (1F, s, Hf-F, $J_{\text{FH}} = 6.26$).

[Ar_{F₂}Npy]HfCl₂. This compound was the byproduct of the direct method reaction. ¹H NMR (C₆D₆) δ 0.84 (3H, s, CH₃), 3.26 (2H, d, CHH), 4.39 (2H, d, CHH), 6.18 (2H, m, ArF₂ *p*-H), 6.36 (1H, t, py H), 6.52 (4H, m, ArF₂ *m*-H), 6.61 (1H, d, py H), 6.80 (1H, t, py H), 9.52 (1H, d, py *o*-H). ¹⁹F NMR (C₆D₆): δ -118.7 (4F, s, arom. *o*-F, $J_{\text{FH}} = 6.03$).

[Ar_{F₂}Npy]Hf(*i*-Bu)₂. HfCl₄ (0.428 g, 1.34 mmol) and H₂[Ar_{F₂}Npy] (0.496g, 1.27 mmol) were dissolved in dichloromethane (150 mL), and the reaction mixture was stirred at room temperature for 36 hours. Dichloromethane was removed in vacuo to afford a yellow powder, which was suspended in ether (100 mL). The mixture was cooled to -30 °C, *i*-BuMgCl (0.631 g, 5.40 mmol) was added, and the reaction mixture was stirred at room temperature for 1 hour. A white precipitate was filtered off through Celite, and the solution was concentrated in vacuo to afford an orange residue, which was washed with pentane (25 mL). The resulting yellow powder

was recrystallized in a 1:4 mixture of ether and pentane; yield 0.488 g (52%). $^1\text{H NMR}$ (C_6D_6) δ 0.09 (2H, m, $\text{CH}_2\text{CH}(\text{CH}_3)_2$), 0.96 (3H, s, CH_3), 1.05 (6H, d, $\text{CH}_2\text{CH}(\text{CH}_3)_2$), 1.12 (2H, m, $\text{CH}_2\text{CH}(\text{CH}_3)_2$), 1.48 (6H, d, $\text{CH}_2\text{CH}(\text{CH}_3)_2$), 2.31 (1H, p, $\text{CH}_2\text{CH}(\text{CH}_3)_2$), 2.93 (1H, p, $\text{CH}_2\text{CH}(\text{CH}_3)_2$), 3.56 (2H, d, ligand CHH), 4.47 (2H, d, ligand CHH), 6.12 (2H, m, ArF_2 *p*-H), 6.37 (1H, t, py H), 6.68 (4H, m, ArF_2 *m*-H), 6.69 (1H, d, py H), 6.83 (1H, t, py H), 8.69 (1H, d, py *o*-H). $^{19}\text{F NMR}$ (C_6D_6) δ -117.4 (4F, s, arom. *o*-F). Anal. Calcd. for $\text{C}_{29}\text{H}_{35}\text{N}_3\text{F}_4\text{Hf}$: C, 51.22; H, 5.19; N, 6.18. Found C, 51.31; H, 5.14; N, 6.06.

$[\text{Ar}_{\text{F}_2}\text{Npy}]\text{HfMe}_2$. HfCl_4 (0.229 g, 0.715 mmol) and $\text{H}_2[\text{Ar}_{\text{F}_2}\text{Npy}]$ (0.265g, 0.681 mmol) were dissolved in dichloromethane (150 mL), and the reaction mixture was stirred at room temperature for 36 hours. Dichloromethane was removed in vacuo to give a yellow powder, which was suspended in ether (150 mL). The mixture was cooled to $-30\text{ }^\circ\text{C}$, MeMgBr (0.337 g, 2.83 mmol) was added, and the reaction mixture was stirred at room temperature for 1 hour. A white precipitate was filtered off through Celite, and the resulting solution was concentrated in vacuo and to afford a brown residue. This residue was triturated with pentane (20 mL) to afford a brown powder. The resulting brown powder was dissolved in pentane. The solution was filtered and cooled to $-30\text{ }^\circ\text{C}$ to afford yellow crystals; yield 0.172 g (43%). $^1\text{H NMR}$ ($\text{C}_6\text{D}_6\text{Br}$) δ 0.08 (3H, m, HfCH_3), 0.68 (3H, m, HfCH_3), 1.23 (3H, s, CH_3), 3.55 (2H, d, CHH), 4.38 (2H, d, CHH), 6.26 (2H, m, arom. *p*-H), 6.76 (4H, m, arom. *m*-H), 6.80 (1H, t, py H), 7.09 (1H, d, py H), 7.36 (1H, t, py H), 8.67 (1H, d, py *o*-H). $^{19}\text{F NMR}$ ($\text{C}_6\text{D}_6\text{Br}$): δ -114.6(4F, s, arom. *o*-F). Anal. Calcd. for $\text{C}_{23}\text{H}_{23}\text{N}_3\text{F}_4\text{Hf}$: C, 46.36; H, 3.89; N, 7.05. Found C, 46.42; H, 3.95; N, 6.88.

General procedure for kinetic studies of 1-hexene polymerization. Suspensions of $\{\text{Ph}_3\text{C}\}\{\text{B}(\text{C}_6\text{F}_5)_4\}$ (0.0036g to 0.0139g; 0.004 to 0.015 mmol) and an equimolar amount of $[\text{Ar}_{\text{X}_2}\text{Npy}]\text{HfR}_2$, in equal volumes of $\text{C}_6\text{D}_5\text{Br}$ (total solution volume, including 1-hexene = 1 mL), were cooled to $-40\text{ }^\circ\text{C}$ and mixed along with the internal standard Ph_2CH_2 (\sim 0.005 g, 0.030 mmol, R = *i*-Bu) or hexamethylbenzene (\sim 0.005g, 0.031 mmol, R = Me). The dimethyl complexes were stirred at room temperature for 10 minutes when M = Zr and for 3 hours when M = Hf, or at $30\text{ }^\circ\text{C}$ for 45 minutes when M = Hf. Activation of the diisobutyl complexes

occurred immediately for both $M = \text{Zr}$ and $M = \text{Hf}$ and was marked by a change in color from an orange to a yellow solution. The activated complex was transferred to a J-Young NMR tube and cooled to $-40\text{ }^{\circ}\text{C}$. To this solution, the appropriate volume of 1-hexene was added. The NMR tube was shaken immediately, brought out of the glove box, and frozen in liquid nitrogen. The frozen sample was brought to the NMR machine that had been precooled to a defined temperature. Disappearance of the olefinic signals of the 1-hexene was measured against the internal standard.

General procedure for the preparative polymerization of 1-hexene at $0\text{ }^{\circ}\text{C}$.

Suspensions of $\{\text{Ph}_3\text{C}\}\{\text{B}(\text{C}_6\text{F}_5)_4\}$ (0.0221g; 0.024 mmol) and an equimolar amount of $[\text{Ar}_{\text{Cl}_2}\text{Hf}(i\text{-Bu})_2]$ in equal volumes of bromobenzene (total solution volume, including 1-hexene = 3 mL) were cooled to $-40\text{ }^{\circ}\text{C}$ and mixed. The activated complex was again cooled to $-40\text{ }^{\circ}\text{C}$ and transferred to a reaction bomb to which 1-hexene was added. The reaction bomb was sealed with a teflon screw cap, shaken, removed from the glove box, and cooled in an ice bath for the length of the polymerization. Methanol was added to the reaction after 6 hours when $\{[\text{Ar}_{\text{Cl}_2}\text{Npy}]\text{Hf}(i\text{-Bu})\}\{\text{B}(\text{C}_6\text{F}_5)_4\}$ was employed as a catalyst and after 9 hours when $\{[\text{Ar}_{\text{F}_2}\text{Npy}]\text{Hf}(i\text{-Bu})\}\{\text{B}(\text{C}_6\text{F}_5)_4\}$ was employed as a catalyst. After the solution was stirred at room temperature for 1 minute, all volatiles were removed, and the polymer was extracted into pentane. The pentane solution was filtered through silica gel and Celite and concentrated in vacuo to afford a clear, viscous oil that was used for further NMR and GPC studies.

Activation of $[\text{Ar}_{\text{x}_2}\text{Npy}]\text{HfR}_2$ with $\{\text{Ph}_3\text{C}\}\{\text{B}(\text{C}_6\text{F}_5)_4\}$.

(i) To give $\{[\text{Ar}_{\text{Cl}_2}\text{Npy}]\text{Hf}(i\text{-Bu})\}\{\text{B}(\text{C}_6\text{F}_5)_4\}$, Ph_3CH , and isobutene. ^1H NMR ($\text{C}_6\text{D}_5\text{Br}$) δ 0.77 (6H, d, $\text{CH}_2\text{CH}(\text{CH}_3)_2$), 1.03 (2H, d, $\text{CH}_2\text{CH}(\text{CH}_3)_2$), 1.26 (3H, s, CH_3), 1.62 (6H, s, isobutene), 2.09 (1H, p, CH_2CHMe_2), 3.64 (2H, d, CHH), 4.13 (2H, d, CHH), 4.70 (2H, s, isobutene), 5.45 (1H, s, Ph_3CH) 6.61-7.59 (aromatics), 8.29 (1H, d, py *o*-H).

(ii) To give $\{[\text{Ar}_{\text{Cl}_2}\text{Npy}]\text{ZrMe}\}\{\text{B}(\text{C}_6\text{F}_5)_4\}$ and Ph_3CCH_3 : ^1H NMR ($\text{C}_6\text{D}_5\text{Br}$) δ 0.88 (3H, s, Zr- CH_3), 1.30 (3H, s, CH_3), 2.09 (3H, s, Ph_3CCH_3), 3.06 (2H, d, CHH), 4.54 (2H, d, CHH), 6.69 (2H, arom. *p*-H), 7.25 (1H, d, *m*-py H), 7.63 (1H, t, *p*-py H), 8.25 (1H, d, py *o*-H).

(iii) To give $\{[\text{Ar}_{\text{Cl}_2}\text{Npy}]\text{HfMe}\}\{\text{B}(\text{C}_6\text{F}_5)_4\}$ and Ph_3CCH_3 . ^1H NMR ($\text{C}_6\text{D}_5\text{Br}$) δ 0.63 (3H, s, Hf- CH_3), 1.33 (3H, s, CH_3), 2.09 (3H, s, Ph_3CCH_3), 3.45 (2H, d, *CHH*), 4.45 (2H, d, *CHH*), 6.64 (2H, t, arom. *p*-H), 7.27 (1H, d, py *m*-H), 7.64 (1H, t, py *p*-H), 8.25 (1H, d, py *o*-H). ^{13}C NMR δ 60.32 (s, Hf- CH_3).

(iv) To give $\{[\text{Ar}_{\text{F}_2}\text{Npy}]\text{Hf}(i\text{-Bu})\}\{\text{B}(\text{C}_6\text{F}_5)_4\}$, Ph_3CH , and isobutene. ^1H NMR ($\text{C}_6\text{D}_5\text{Br}$) δ 0.97 (6H, d, $\text{CH}_2\text{CH}(\text{CH}_3)_2$), 1.09 (2H, q, $\text{CH}_2\text{CH}(\text{CH}_3)_2$), 1.22 (3H, s, CH_3), 1.62 (6H, s, isobutene), 2.31 (1H, p, CH_2CHMe_2), 3.67 (2H, d, ligand *CHH*), 4.02 (2H, d, ligand *CHH*), 4.70 (2H, s, isobutene), 5.45 (1H, s, Ph_3CH), 6.48-7.66 (aromatics), 8.35 (1H, d, py-*o*-H). ^{19}F NMR (C_6D_6): δ -117.2 (4F, s, arom. *o*-F).

(v) To give $\{[\text{Ar}_{\text{F}_2}\text{Npy}]\text{HfMe}\}\{\text{B}(\text{C}_6\text{F}_5)_4\}$ and Ph_3CCH_3 . ^1H NMR ($\text{C}_6\text{D}_6\text{Br}$) δ 0.44 (3H, s, Hf- CH_3), 1.23 (3H, s, ligand CH_3), 2.09 (3H, s, Ph_3CCH_3), 3.78 (2H, d, *CHH*), 3.94 (2H, d, *CHH*), 6.40-7.80 (aromatics), 8.26 (1H, d, *o*-py H). ^{19}F NMR (C_6D_6) δ -116.1 (4F, s, arom. *o*-F).

(vi) To give $\{[\text{Ar}_{\text{F}_2;\text{FNM}_2}\text{Npy}]\text{HfMe}\}\{\text{B}(\text{C}_6\text{F}_5)_4\}$ and Ph_3CCH_3 . ^1H NMR ($\text{C}_6\text{D}_6\text{Br}$) δ 0.38 (3H, s, Hf- CH_3), 1.25 (3H, s, CH_3), 2.09 (3H, s, Ph_3CCH_3), 2.13 (3H, s, ArNCH_3), 2.78 (3H, s, ArNCH_3), 3.35 (1H, d, *CHH*), 3.39 (1H, dd, *CHH*), 3.97 (1H, d, *CHH*), 4.23 (1H, dd, *CHH*), 6.3-7.6 (aromatics), 8.20 (1H, d, py-*o*-H).

2.11 Acknowledgements

I'd like to thank Dr. Klaus Ruhland for laying the foundation for polymerization studies employing $\{[\text{Ar}_{\text{Cl}_2}\text{Npy}]\text{HfR}\}\{\text{B}(\text{C}_6\text{F}_5)_4\}$ ($\text{M} = \text{Hf}, \text{Zr}, \text{R} = \text{Me}; \text{M} = \text{Hf}, i\text{-Bu}$) catalysts. I also grateful to Pia Lopez for performing the X-ray crystallography studies and to Dr. William M. Davis for general help with X-ray crystallography. Funding from Department of Energy (DE-FG02-86ER13564) is sincerely appreciated.

Chapter 3

Synthesis of Poly(alkynes) Using Well-Defined Molybdenum Imido Alkylidene Catalysts

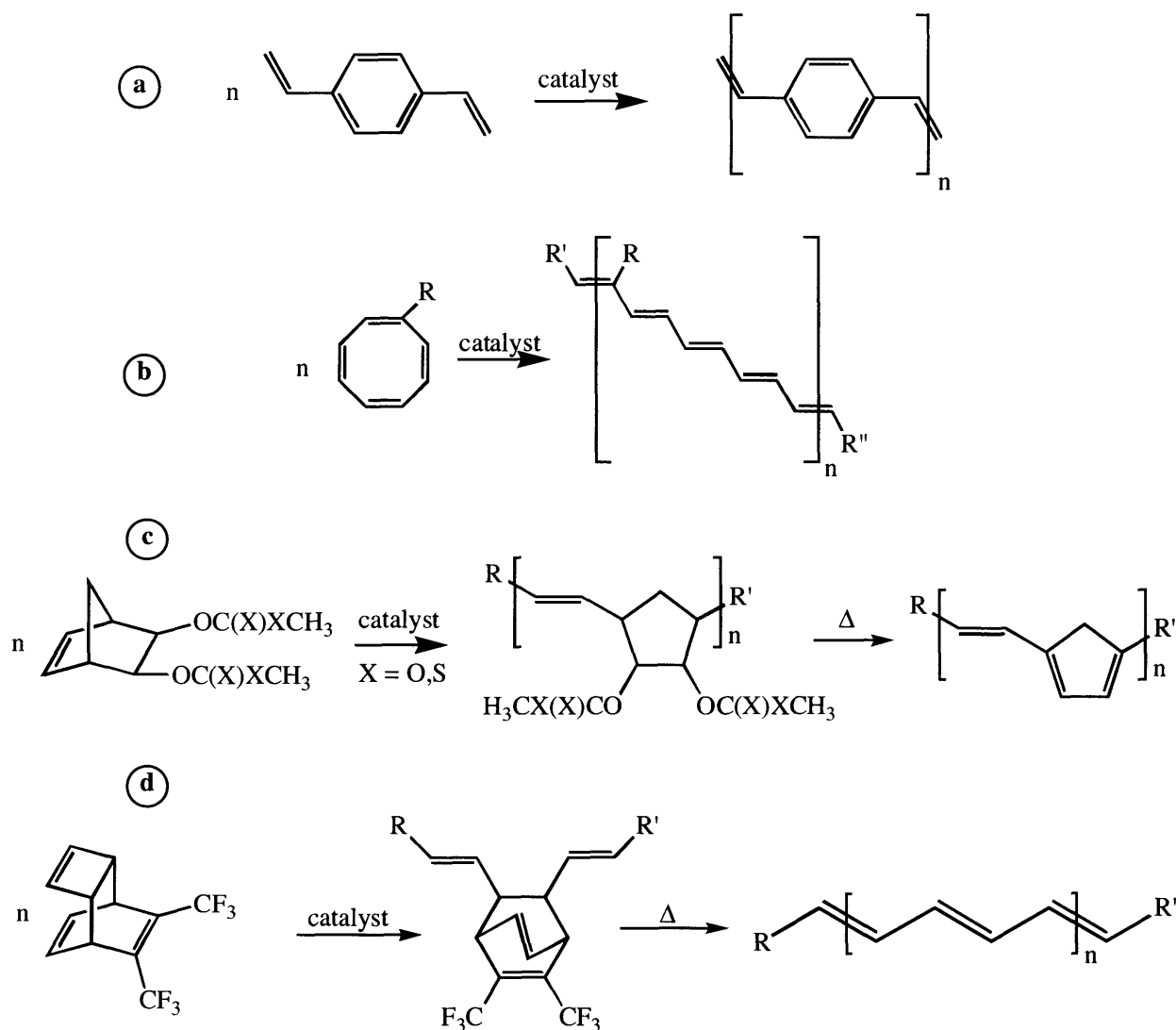
3.1 Introduction

Conjugated, organic oligomers and polymers possess a variety of interesting optical and electronic properties.⁷⁶⁻⁸³ Potential applications include organic semiconductors, optoelectronics, and photonics. Polyacetylene, the simplest π -conjugated organic polymer, is highly conductive when doped, particularly when oriented, and possesses a high third-order susceptibility ($\chi^{(3)}$).⁸²⁻⁸⁵ However, polyacetylene is unstable toward oxygen and insoluble in common organic solvents, making it difficult to process and study. Alternatively, many substituted polyenes are soluble and relatively air-stable. Substituted polyenes retain many of the same properties as unsubstituted polyacetylene and can be synthesized through a variety of processes.

This research focuses on the development of well-defined metathesis catalysts for the living synthesis of substituted polyenes. In order for a metathesis-based polymerization reaction to be living, the same requirements discussed previously for a living Ziegler-Natta polymerization must be met.⁸⁶⁻⁸⁸ A polymer produced in a living manner is characterized by a low polydispersity and has a molecular weight that is based on the amount of monomer added. For the polymerization to be truly living, both the PDI value and the $M_n(\text{found})/M_n(\text{calculated})$ ratio should approach 1.

Two common methods of preparing polyenes that employ well-defined molybdenum, tungsten, and ruthenium based carbenes as catalysts are Acyclic Diene Metathesis (ADMET) Polymerization and Ring Opening Metathesis Polymerization (ROMP). ADMET polymerization can be used to prepare poly(*p*-phenylenevinylene)s from divinylbenzene derivatives (Scheme 3.1a).⁸⁹⁻⁹⁴ $\text{Mo}(\text{NAr})(\text{CHR})(\text{OR}')_2$ initiators can be employed in ROMP for several types of monomers. Substituted and unsubstituted cyclooctatetraenes or paracyclophanes can be polymerized using ROMP,^{92,95-99} although the resulting polyenes tend to aggregate and cross-link (Scheme 3.1b). ROMP of norbornene-bis(*S*-methyl dicarbonate) and norbene-bis(*S*-methyl carbonate), followed by thermal decomposition, also produces polyenes (Scheme 3.1c).^{100,101} Finally, polyacetylene may be synthesized via ROMP of 7,8-(bistrifluoromethyl)tricyclo[4,2,2,0]deca-3,7,9-trienes (Scheme 3.1d).¹⁰²⁻¹⁰⁴ A soluble precursor

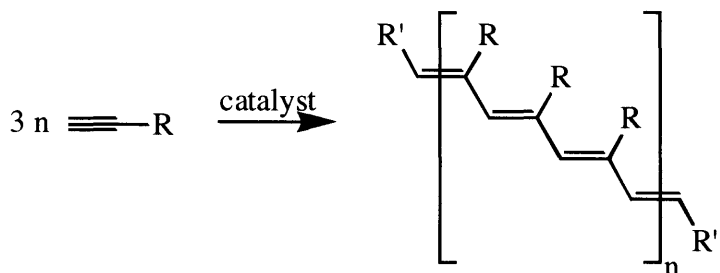
polyacetylene is generated that decomposes thermally to produce polyacetylene with well-defined chain-ends and a narrow molecular weight distribution (Scheme 3.1d).



Scheme 3.1. ADMET Polymerization and ROMP techniques used for the synthesis of conjugated polyenes.

Catalysts based on mixtures of binary and ternary transition metals (molybdenum, tungsten, tantalum, niobium, and rhodium) and alkylating cocatalysts polymerize a variety of mono- and di-substituted alkynes.¹⁰⁵⁻¹⁴⁴ Ziegler-Natta titanium, scandium, iron, nickel, and

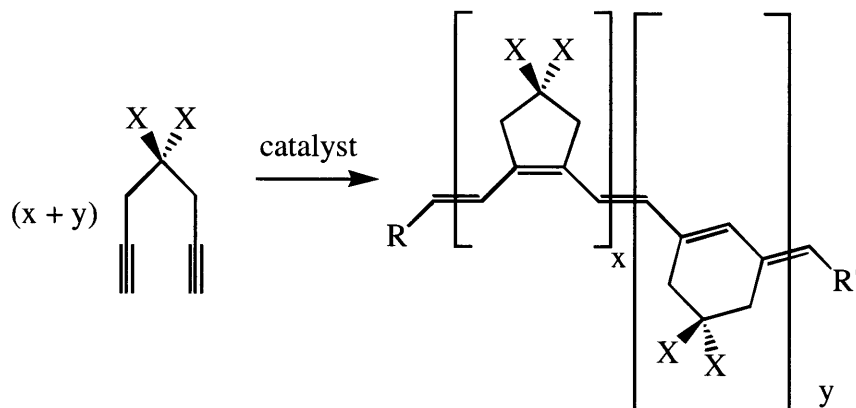
palladium catalysts have also been successfully employed in these types of reactions.¹⁴⁵⁻¹⁴⁹ While these polymerizations may proceed in a living manner, little is known about initiation processes in these ill-defined catalytic systems. Substituted polyacetylenes can also be synthesized in a living manner by well-defined molybdenum and tantalum alkylidene complexes using 2-butyne,¹⁵⁰ *tert*-butylacetylene,¹⁵¹⁻¹⁵³ ethynyl-substituted metallocenes,¹⁵⁴⁻¹⁶¹ or *ortho*-substituted phenylacetylenes^{153,162,163} as monomers (Scheme 3.2). For example, Mo(NAd)(CHCMe₂Ph)[OCH(CF₃)₂]₂(2,4-lutidine) polymerizes *ortho*-trimethylsilylphenylacetylene exclusively by α -addition.^{162,163} Unfortunately, 1,3 interactions of the substituents of polyenes prepared from 1- and 2-alkynes decrease the effective chain length of conjugation in these polyacetylenes.



Scheme 3.2. Alkyne polymerization employing transition metal catalysts.

One of the most promising methods for the living synthesis of polyenes is the cyclopolymerization of 1,6-heptadiyne derivatives containing substituents at the 4-position (Scheme 3.3). Polyenes with cyclic recurring units based on either five- or six-membered rings along the backbone can be synthesized using Ziegler-Natta,^{98,164,165} palladium,^{166,167} ruthenium,^{159,168-174} and binary or ternary molybdenum or tungsten^{157,167,174-208} based catalysts. Catalyst systems based on MoCl₅-*n*-Bu₄Sn-EtOH-quinuclidine and MoOCl₄-*n*-Bu₄Sn-EtOH-quinuclidine were recently shown to cyclopolymerize 1,6-heptadiynes to give highly regular polyenes consisting exclusively of 1,2-(cyclopent-1-enylene)-vinylene units.¹⁹⁷ Modified

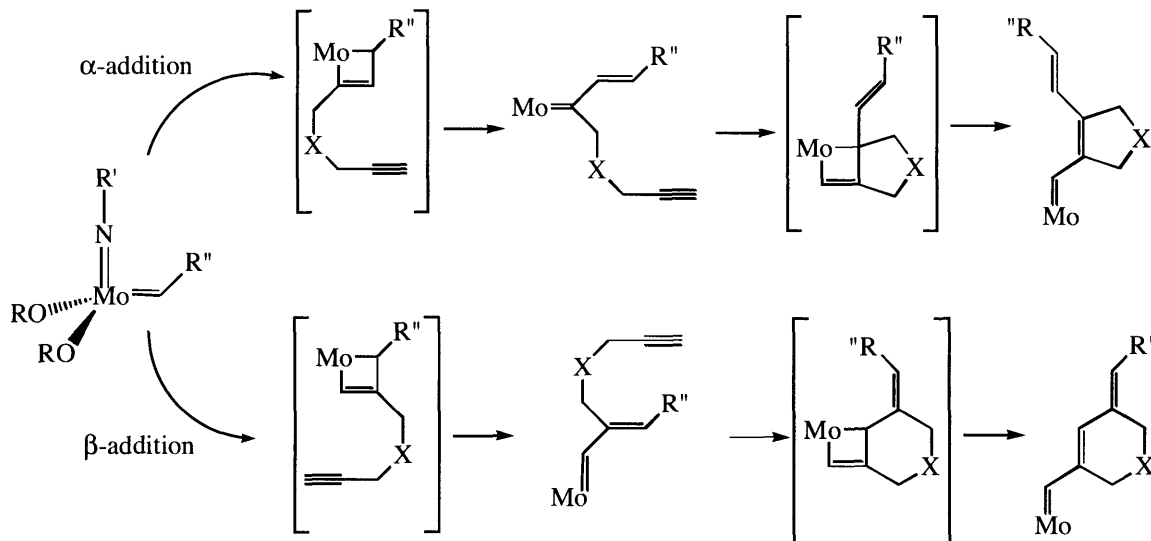
Grubbs-Hoveyda catalysts with enhanced polarization across the ruthenium-carbon double bond are capable of producing poly(1,6-heptadiyne)s consisting of up to 100% five-membered rings.^{169,174} Reactions employing these ruthenium based catalysts proceed in a living manner and are tolerant of both water as a reaction medium and polar functional groups.



Scheme 3.3. Cyclopolymerization of 1,6-heptadiynes.

Well-defined molybdenum imido alkylidene initiators also cyclopolymerize 1,6-heptadiynes in a living manner^{95,157,159,172,174,199,200,209-216} and are capable of producing polyenes solely consisting of five- or six-membered rings. As shown in Scheme 3.4, these initiators react with 1,6-heptadiynes by either an α -addition to produce a five-membered ring or a β -addition to produce a six-membered ring (Scheme 3.4).²¹⁴ Previous work^{213,214} demonstrated that $\text{Mo}(\text{NAr})(\text{CHCMe}_2\text{Ph})[\text{OCMe}(\text{CF}_3)_2]_2$ ($\text{Ar} = 2,6\text{-diisopropylphenyl}$) polymerizes diethyl dipropargylmalonate (DEDPM), a commonly used, substituted 1,6-heptadiyne, in a living manner to yield polymers with unimodal GPC traces in THF, PDI values ≤ 1.25 , and $M_n(\text{found})/M_n(\text{calculated})$ ratios between 1 and 2. The resulting poly(DEDPM) was comprised of a mixture of five- and six-membered rings and was characterized by a λ_{max} of 550 nm. In order to encourage regioselective addition of the first triple bond to the alkylidene to give only a β -substituted metallacyclobutene, bulky carboxylate ligands were introduced.^{212,215} Polymerization of DEDPM by $\text{Mo}(\text{NAr})(\text{CHCMe}_3)(\text{O}_2\text{CCPh}_3)_2$ catalysts led to the formation of

> 99% six-membered rings. The resulting poly[1,3-(cyclohex-1-enylene)-methylidene] was characterized by a λ_{\max} of 511 nm.



Scheme 3.4. Reaction of $\text{Mo}(\text{NR}')(\text{CHR}'')(\text{OR})_2$ with 1,6-heptadiyne derivatives (for DEDPM, $\text{X} = \text{C}(\text{CO}_2\text{Et})_2$).

The coplanarity of the double bonds in the polyene backbone, described by the effective conjugation length (N_{eff}), is a prerequisite for most applications. When N_{eff} is high, overlap of the p_z -orbitals of the double bonds produces a narrow bandgap material which shows low energy charge-transfer (CT) bands and bathochromic shifts in absorption with increasing N_{eff} values.²¹⁷ The λ_{\max} values in these systems arise from $\pi-\pi^*$ electronic transitions along the polyene backbone. Where N is the number of conjugated double bonds in the polyene and A and B are constants, the transition energies can be expressed as $E(0-0) = A + B/N$.²¹⁷ Polyenes containing all five-membered rings give rise to the greatest N_{eff} ^{209,210} and therefore show the most potential as polyacetylene substitutes. The higher observed conjugation most likely results from the alignment of adjacent rings on opposite sides of the polyene backbone, leading to a more planar configuration of the double bonds (Figure 3.1). This planar arrangement is not possible in polymer containing all six-membered rings, and the polyene chain is likely to twist in order to

relieve steric congestion. Hence, a route to preparing polymer containing all five-membered rings is very desirable.

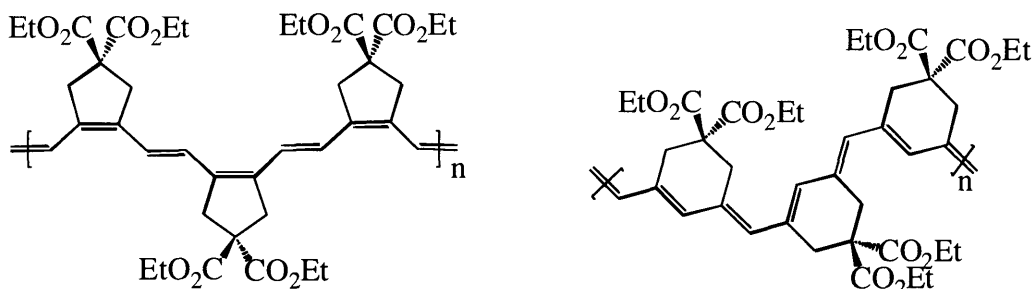


Figure 3.1. Polyenes containing all five- and six-membered rings.

While the incorporation of small fluorinated alkoxides ($\text{OR} = \text{OCH}(\text{CF}_3)_2$) into $\text{Mo}(\text{NAr})(\text{CHCMe}_2\text{Ph})(\text{OR})_2$ ($\text{Ar} = 2,6\text{-diisopropylphenyl}$) only resulted in a 10% increase in α -selectivity, the incorporation of *iso*-butoxide and *tert*-butoxide groups ($\text{OR} = \text{OCHMe}_2, \text{OCMe}_3$) lead to very high α -selectivity.^{209,210} The preferential synthesis of five-membered rings was attributed to a faster rate of interconversion²¹⁸⁻²²¹ between *syn* and *anti* rotamers of catalysts containing non-fluorinated alkoxides.²⁰⁹ Addition of quinuclidine to make “adducts” with $\text{Mo}(\text{NAr})(\text{CHCMe}_2\text{Ph})(\text{OR})_2$ ($\text{Ar} = 2,6\text{-diisopropylphenyl}$; $\text{R} = i\text{-Pr}, t\text{-Bu}$) led to the formation of > 95% five-membered rings.^{209,210} The alternating *cis/trans* 1,2-(cyclopent-1-enylene)vinylenes produced by $\text{Mo}(\text{NAr})(\text{CHCMe}_2\text{Ph})(\text{O}-t\text{-Bu})_2(\text{quin})$ were characterized by $M_n(\text{found})/M_n(\text{calculated})$ ratios between 1.5 and 2, according to light scattering ($\lambda = 690 \text{ nm}$), PDI values between 1.15 and 1.26 according to GPC, and a λ_{max} of 591 nm.^{209,210} Higher than expected polydispersities and $M_n(\text{found})/M_n(\text{calculated})$ ratios were primarily attributed to faster rates of propagation relative to initiation.

A better understanding of the structural, optical, and electronic properties of long polyenes ($N > 100$) can be gained by studying the structural, optical, and electronic properties of

short polyenes ($N < 15$). The absorbance spectra of longer polyenes show systematic broadening with increasing N due to conformational disorder in the polyene chain.^{217,222,223} Many different permutations of conjugated chains containing a given number of monomers are possible, and broadened absorbance spectra result from the superposition of the absorption spectra of these shorter polyene segments.^{217,222} Therefore, the analysis of short polyenes ($N < 15$) can be used to establish a smooth theoretical connection between the optical properties of short and long polyenes.

HPLC purification techniques were used to separate short polyenes consisting of 3 to 15 monomers that were generated during the cyclopolymerization of 30 equivalents of DEDPM by $\text{Mo}(\text{NAr})(\text{CHCMe}_2\text{Ph})[\text{OCMe}(\text{CF}_3)_2]_2$ ($\text{Ar} = 2,6\text{-diisopropylphenyl}$).²¹⁷ Long polyenes were also produced, and the shorter, more soluble polyenes were extracted from the mixture with pentane. The soluble polyenes were purified by HPLC, and oligomers consisting of a single chain length were isolated and analyzed spectroscopically.²¹⁷ Unfortunately, polyenes produced in this manner contained a mixture of both five- and six-membered rings, and structural variations along the polyene backbone were observed to occur in polyenes of a single chain length.

One solution would be to employ $\text{Mo}(\text{NAr})(\text{CHCMe}_2\text{Ph})(\text{O-}t\text{-Bu})_2(\text{quin})$ in producing conjugated oligomers solely consisting of five-membered rings. However, the faster rate of initiation relative to propagation associated with the $\text{Mo}(\text{NAr})(\text{CHCMe}_2\text{Ph})(\text{O-}t\text{-Bu})_2(\text{quin})$ initiator prohibits the efficient synthesis of short oligomers. Longer than expected oligomers are produced, and portions of initiator remain unconsumed during reactions with small amounts of monomer. In order to use metathesis polymerization as an efficient synthetic tool for producing short oligomers in high yield, the rate of propagation should be less than or equal to the rate of initiation.

An important objective of this research is to find a way to increase the rate of initiation relative to propagation for these well-defined molybdenum imido alkylidene catalysts. By studying the behavior of these catalysts and the process of initiation, we hope to gain a better understanding of the cyclopolymerization process. This information can then be used to develop

better catalysts that allow for complete catalytic control. By fine-tuning the electronic and steric effects around the molybdenum center, we hope to create new catalysts that cyclopolymerize DEDPM to produce highly regular polyenes containing > 95% five-membered rings and cis/trans regularity in a truly living manner. This work is important because it enables the custom-designed synthesis of conjugated polymers and oligomers.

3.2 Catalyst Synthesis

3.2.1 The Neopentylidene, Neophylidene, and Ferrocenemethylidene Catalysts

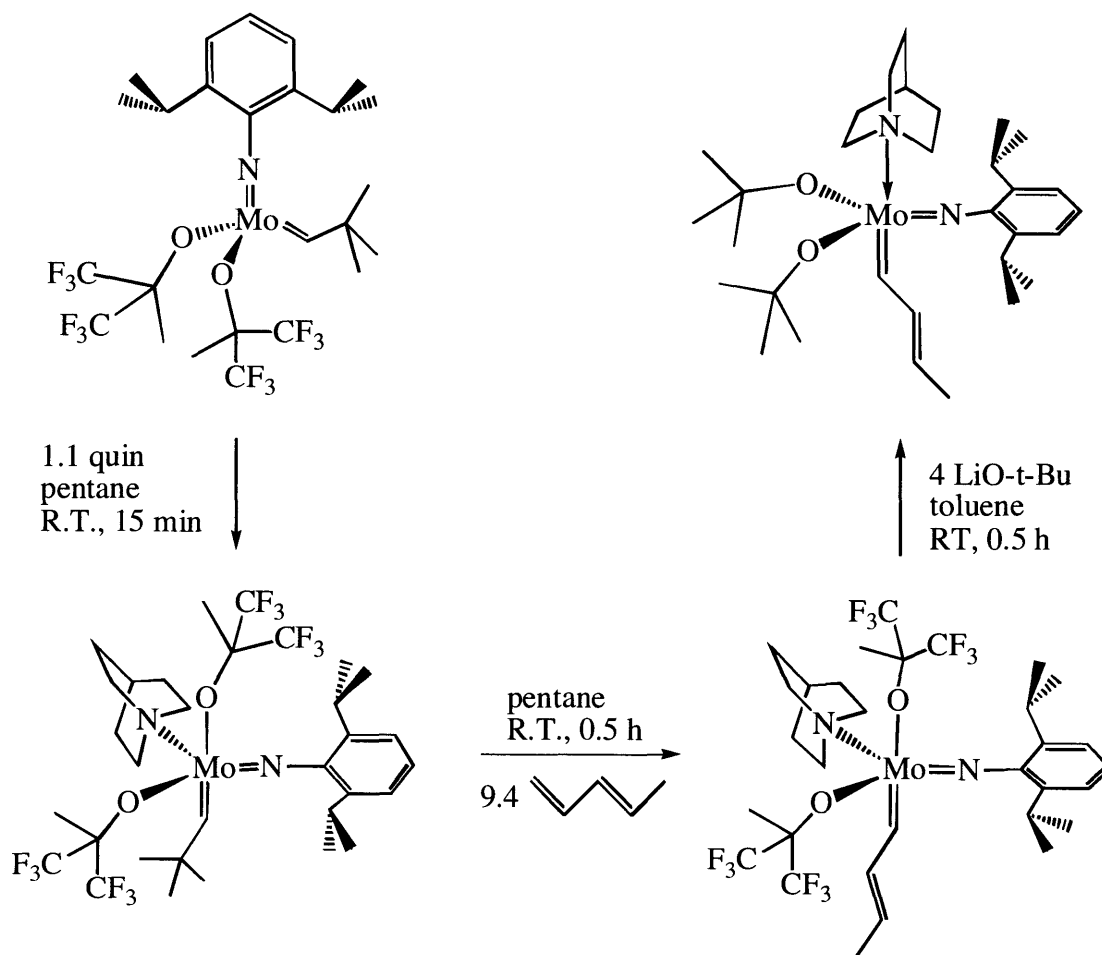
Improving catalytic performance requires establishing a basis for comparison, and to this end, $\text{Mo}(\text{NAr})(\text{CHCMe}_2\text{Ph})[\text{OCMe}(\text{CF}_3)_2]_2$, $\text{Mo}(\text{NAr})(\text{CHCMe}_3)[\text{OCMe}(\text{CF}_3)_2]_2$, $\text{Mo}(\text{NAr})(\text{CHCMe}_2\text{Ph})(\text{O}-t\text{-Bu})_2$, and $\text{Mo}(\text{NAr})(\text{CHCMe}_3)(\text{O}-t\text{-Bu})_2$ (Ar = 2,6-diisopropylphenyl) were synthesized according to reported procedures.^{224,225} In order to improve the potential crystalline quality of oligomers and to synthesize polymers capped with two redox active end groups, $\text{Mo}(\text{NAr})(\text{CHFc})(\text{O}-t\text{-Bu})_2$ ²²⁶ was also synthesized.

3.2.2 The Di-*tert*-butoxide and Hexafluoro-*tert*-Butoxide Butenylidene Catalysts

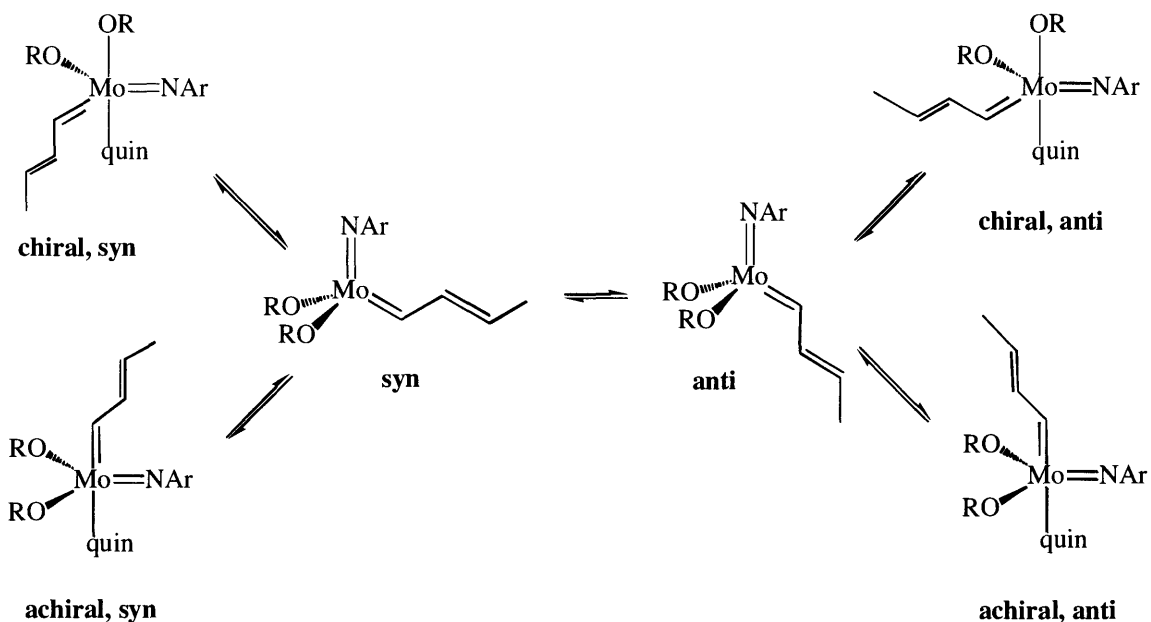
In order to increase the rate of initiation, an alkylidene more akin to the propagating species was incorporated into the $\text{Mo}(\text{NAr})(\text{CHR})(\text{O}-t\text{-Bu})_2(\text{quin})$ (Ar = 2,6-diisopropylphenyl) framework. The di-*tert*-butoxide butenylidene complex was synthesized first because $\text{Mo}(\text{NAr})(\text{trans-CHCHCHMe})[\text{OCMe}(\text{CF}_3)_2]_2(\text{quin})$ (Ar = 2,6-diisopropylphenyl) can be synthesized in high yield employing commercially available 1,3-pentadiene.²²⁷ Unfortunately, base-free $\text{Mo}(\text{NAr})(\text{trans-CHCHCHMe})(\text{O}-t\text{-Bu})_2$ could not be isolated and is likely to be thermally unstable.

$\text{Mo}(\text{NAr})(\text{trans-CHCHCHMe})[\text{OCMe}(\text{CF}_3)_2]_2(\text{quin})$ (Ar = 2,6-diisopropylphenyl) was synthesized according to a reported procedure²²⁷ by reacting $\text{Mo}(\text{NAr})(\text{CHCMe}_3)[\text{OCMe}(\text{CF}_3)_2]_2$ with 9.4 equivalents of 1,3-pentadiene in the presence of excess quinuclidine (Scheme 3.5). In

this case, quinuclidine is required for catalyst stabilization and crystallization. Three rotamers are observed in solution (CD_2Cl_2): the chiral, anti rotamer ($H_\alpha = 13.04$ ppm), the chiral, syn rotamer ($H_\alpha = 12.90$ ppm), and the achiral, syn rotamer ($H_\alpha = 12.55$ ppm) (Scheme 3.6). “Anti” refers to a rotamer in which the alkylidene substituent points away from the imido nitrogen atom, and “syn” refers to a rotamer in which the alkylidene substituent points toward the imido nitrogen atom. The initial ratio of rotamers varies with reaction conditions. While the two syn rotamers interconvert rapidly, the two syn rotamers interconvert more slowly with the anti rotamer.²²⁷ The chiral, anti rotamer was selectively isolated by recrystallization and used for initiation experiments discussed later. The use of secondary batches of crystals containing mixtures of the chiral and achiral, syn rotamers led to similar results.



Scheme 3.5. Synthesis of $\text{Mo}(\text{NAr})(\text{trans-CHCHCHMe})(\text{O-}t\text{-Bu})_2(\text{quin})$.



Scheme 3.6. Possible Rotamers of $\text{Mo}(\text{NAr})(\text{trans-CHCHCHMe})(\text{OR})_2$ and $\text{Mo}(\text{NAr})(\text{trans-CHCHCHMe})(\text{OR})_2(\text{quin})$.²²⁷

The synthesis of $\text{Mo}(\text{NAr})(\text{trans-CHCHCHMe})(\text{O-}t\text{-Bu})_2(\text{quin})$ was achieved by the addition of 4 equivalents of $\text{LiO-}t\text{-Bu}$ to $\text{Mo}(\text{NAr})(\text{trans-CHCHCHMe})[\text{OCMe}(\text{CF}_3)_2]_2(\text{quin})$ (Scheme 3.5). An excess of 2 equivalents of $\text{LiO-}t\text{-Bu}$ is not required; however, it is essential that $\text{Mo}(\text{NAr})(\text{trans-CHCHCHMe})[\text{OCMe}(\text{CF}_3)_2]_2(\text{quin})$ react completely. While excess $\text{LiO-}t\text{-Bu}$ in the product mixture may affect polymer molecular weights due to error associated with the calculated molecular weights, any remaining $\text{Mo}(\text{NAr})(\text{trans-CHCHCHMe})[\text{OCMe}(\text{CF}_3)_2]_2(\text{quin})$ will inherently alter the nature of the polymerization in terms of both rate and five- versus six-membered ring polymer content.

$\text{Mo}(\text{NAr})(\text{trans-CHCHCHMe})(\text{O-}t\text{-Bu})_2(\text{quin})$ was isolated as large dark purple crystals in 81% yield after successive recrystallizations. Single crystals containing the achiral, syn rotamer were obtained by recrystallization of the bulk material from pentane. The X-ray structure features a trigonal bipyramid in which quinuclidine is coordinated *trans* to the

butenyldiene group (Figure 3.2, Table 3.1). The Mo(1)-N(2)-C(21) bond angle is 172.47° and the Mo(1)-C(1)-C(2) bond angle is $128.99(2)^\circ$. Quinuclidine is bound with a Mo(1)-N(1) bond distance of $2.4955(2) \text{ \AA}$ and the Mo(1)-N(2) and Mo(1)-C bond distances are within the expected ranges.

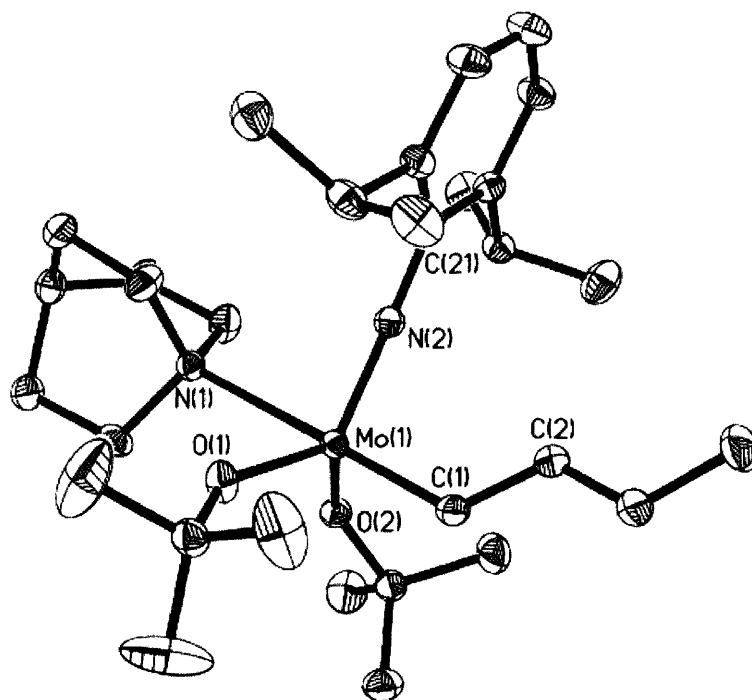


Figure 3.2. Thermal ellipsoid drawing of Mo(NAr)(*trans*-CHCHCHMe)(O-*t*-Bu)₂(quin) at the 50% probability level.

Table 3.1. Selected bond lengths [\AA] and angles [$^\circ$] for Mo(NAr)(*trans*-CHCHCHMe)(O-*t*-Bu)₂(quin).

Bond Lengths [\AA]			
Mo(1)-N(2)	1.7440(2)	Mo(1)-O(1)	1.9139(2)
Mo(1)-C(1)	1.952(2)	Mo(1)-O(2)	1.9233(1)
Mo(1)-N(1)	2.4955(2)		
Bond Angles [$^\circ$]			
N(2)-Mo(1)-C(1)	93.08(8)	N(2)-Mo(1)-O(1)	120.97(8)
N(2)-Mo(1)-N(1)	87.12(7)	N(2)-Mo(1)-O(2)	116.88(8)
O(1)-Mo(1)-C(1)	100.04(8)	O(1)-Mo(1)-O(2)	115.97(6)
O(2)-Mo(1)-C(1)	102.01(8)	N(1)-Mo(1)-C(1)	178.70(8)
O(1)-Mo(1)-N(1)	78.76(6)	Mo(1)-N(2)-C(21)	172.47(2)
O(2)-Mo(1)-N(1)	79.04(6)	Mo(1)-C(1)-C(2)	128.99(2)

$\text{Mo}(\text{NAr})(\text{trans-CHCHCHMe})(\text{O-}t\text{-Bu})_2(\text{quin})$ is stable when stored as a solid at $-30\text{ }^\circ\text{C}$ for several months, in contrast to the related dimer, $(\text{CH})_6[\text{Mo}(\text{NAr})(\text{O-}t\text{-Bu})_2(\text{quin})]_2$, which decomposes within several days at $-40\text{ }^\circ\text{C}$.²²⁸ However, $\text{Mo}(\text{NAr})(\text{trans-CHCHCHMe})(\text{O-}t\text{-Bu})_2(\text{quin})$ is unstable in CDCl_3 , and showed 20% decomposition in CD_2Cl_2 after 3 hours. After 14 hours in C_6D_6 at room temperature, the integral value of each alkylidene resonance decreased to 37% of the original value compared to a standard.

The proton resonances for bound and free quinuclidine overlap in the $20\text{ }^\circ\text{C}$ $\text{C}_6\text{D}_5\text{CD}_3$ ^1H NMR spectrum of $\text{Mo}(\text{NAr})(\text{trans-CHCHCHMe})(\text{O-}t\text{-Bu})_2(\text{quin})$ (Figure 3.3). Line broadening of these resonances suggests that bound and free quinuclidine are exchanging rapidly on the NMR timescale. The weak quinuclidine coordination is not surprising due to the greater electron donating ability of *tert*-butoxide groups versus hexafluoro-*tert*-butoxide groups. A broad doublet alkylidene H_α resonance for the achiral, syn rotamer is observed at 12.11 ppm with a J_{CH} coupling constant of 121.5 Hz ($J_{\text{HH}} = 11\text{ Hz}$). In solution, the mirror plane of the syn rotamer is evidenced by a single broadened septet at 4.15 ppm in the $\text{C}_6\text{D}_5\text{CD}_3$ ^1H NMR spectrum corresponding to two equivalent isopropyl methine protons, a doublet at 1.34 ppm corresponding to 12 equivalent isopropyl methyl protons, and a large singlet at 1.38 ppm corresponding to 18 equivalent *tert*-butyl methyl protons.

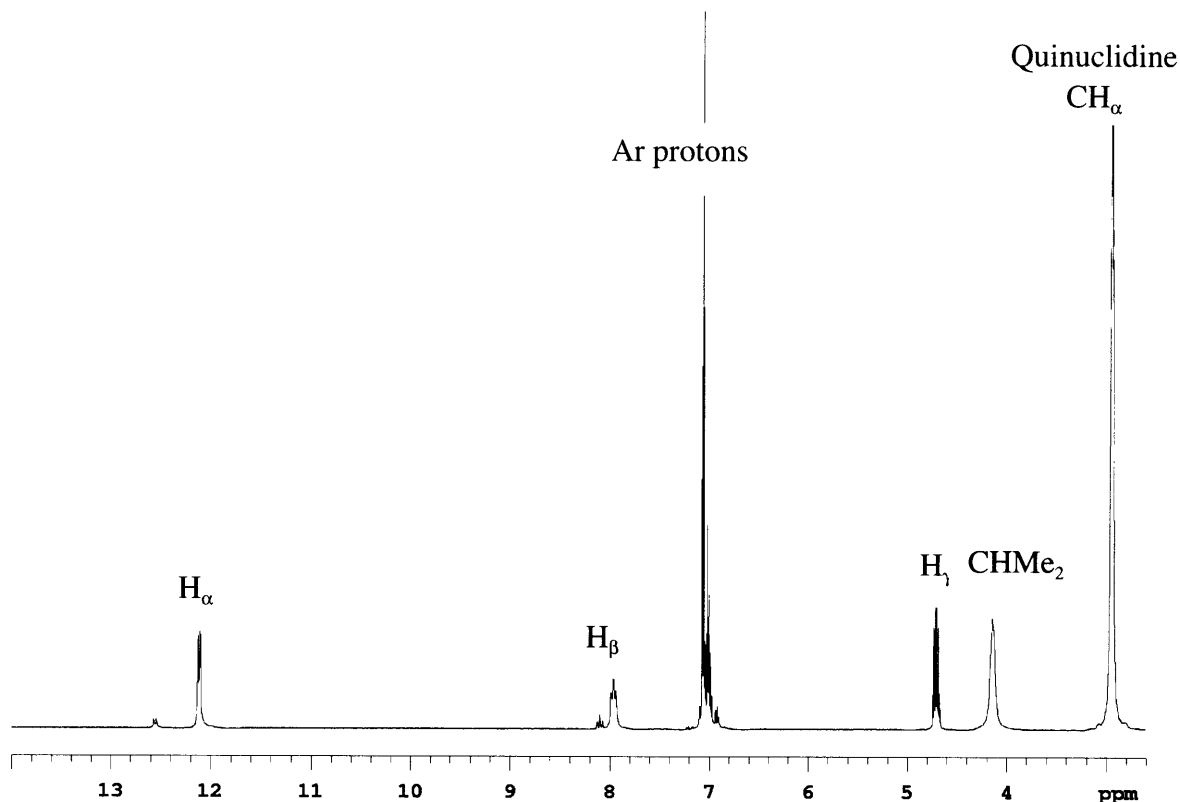


Figure 3.3. The partial (2.8 to 14 ppm) ^1H NMR spectrum of $\text{Mo}(\text{NAr})(\text{trans-CHCHCHMe})(\text{O-}t\text{-Bu})_2(\text{quin})$ (20 °C, $\text{C}_6\text{D}_5\text{CD}_3$).

Based on a VT NMR study, the chiral, anti rotamer ($H_\alpha = 12.70$ ppm, $J_{\text{CH}} = 141.7$ Hz, $J_{\text{HH}} = 13$ Hz in $\text{C}_6\text{D}_5\text{CD}_3$) is most likely the other product present in solution at 22 °C. The rotamers interconvert rapidly in solution, and an equilibrium mixture of 91% achiral, syn and 9% chiral, anti rotamers is quickly established. The anti versus syn assignment is based on the J_{CH} coupling constants, the equivalence or inequivalence of key protons, and previous evidence that the alkylidene H_α resonance of the anti species is found downfield of the alkylidene H_α resonance of the syn species.²²⁷ Addition of 10 equivalents of quinuclidine to $\text{Mo}(\text{NAr})(\text{trans-CHCHCHMe})(\text{O-}t\text{-Bu})_2(\text{quin})$ in C_6D_6 did not significantly affect the ratio of rotamers present in solution.

At -70 °C, 3 rotamers are present: the achiral, syn rotamer (72%; $H_\alpha = 12.22$ ppm, $J_{\text{HH}} = 11$ Hz), the chiral, syn rotamer (18%; $H_\alpha = 12.56$ ppm, $J_{\text{HH}} = 11$ Hz), and the chiral, anti rotamer

(10%; $H_{\alpha} = 12.81$ ppm, $J_{HH} = 13$ Hz) (Figure 3.4). The isopropyl methine proton resonances of the two minor products are observed as pairs of septets representing one proton each and are found at 3.71 and 4.60 ppm for the chiral, syn rotamer, and at 3.80 and 4.71 ppm for the chiral, anti rotamer. The isopropyl methyl proton resonances and the *tert*-butyl methyl proton resonances are difficult to distinguish due to overlap; however, a mirror plane of symmetry is clearly absent in these species, and quinuclidine is expected to be bound to the metal at low temperature. Upon warming to room temperature, the 91% syn rotamer and 9% chiral, anti rotamer equilibrium is restored. An alkylidene H_{α} resonance at 12.49 ppm appears as the temperature is raised above 60 °C; however, significant catalyst decomposition precludes the identification of this species.

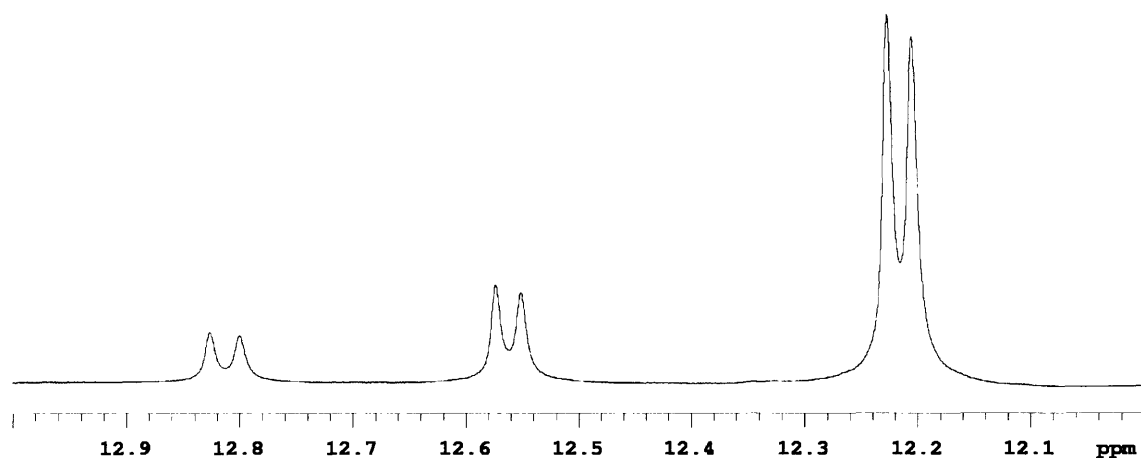


Figure 3.4. The alkydene H_{α} resonances of the chiral, anti rotamer, the chiral, syn rotamer, and the achiral, syn rotamer of $\text{Mo}(\text{NAr})(\text{trans-CHCHCHMe})(\text{O-}t\text{-Bu})_2(\text{quin})$ at -70 °C in $\text{C}_6\text{D}_5\text{CD}_3$.

3.2.3 The Diadamantoxide Butenylidene Catalyst

$\text{Mo}(\text{NAr})(\text{trans-CHCHCHMe})(\text{OAd})_2(\text{quin})$ (Ar = 2,6 diisopropylphenyl, Ad = adamantyl) was synthesized by a method analogous to that used for the synthesis of $\text{Mo}(\text{NAr})(\text{trans-CHCHCHMe})(\text{O-}t\text{-Bu})_2(\text{quin})$. The equilibrium solution (22 °C, $\text{C}_6\text{D}_5\text{CD}_3$) is comprised of approximately 90% of the achiral, syn rotamer ($H_{\alpha} = 12.19$ ppm, $J_{CH} = 128.2$ Hz,

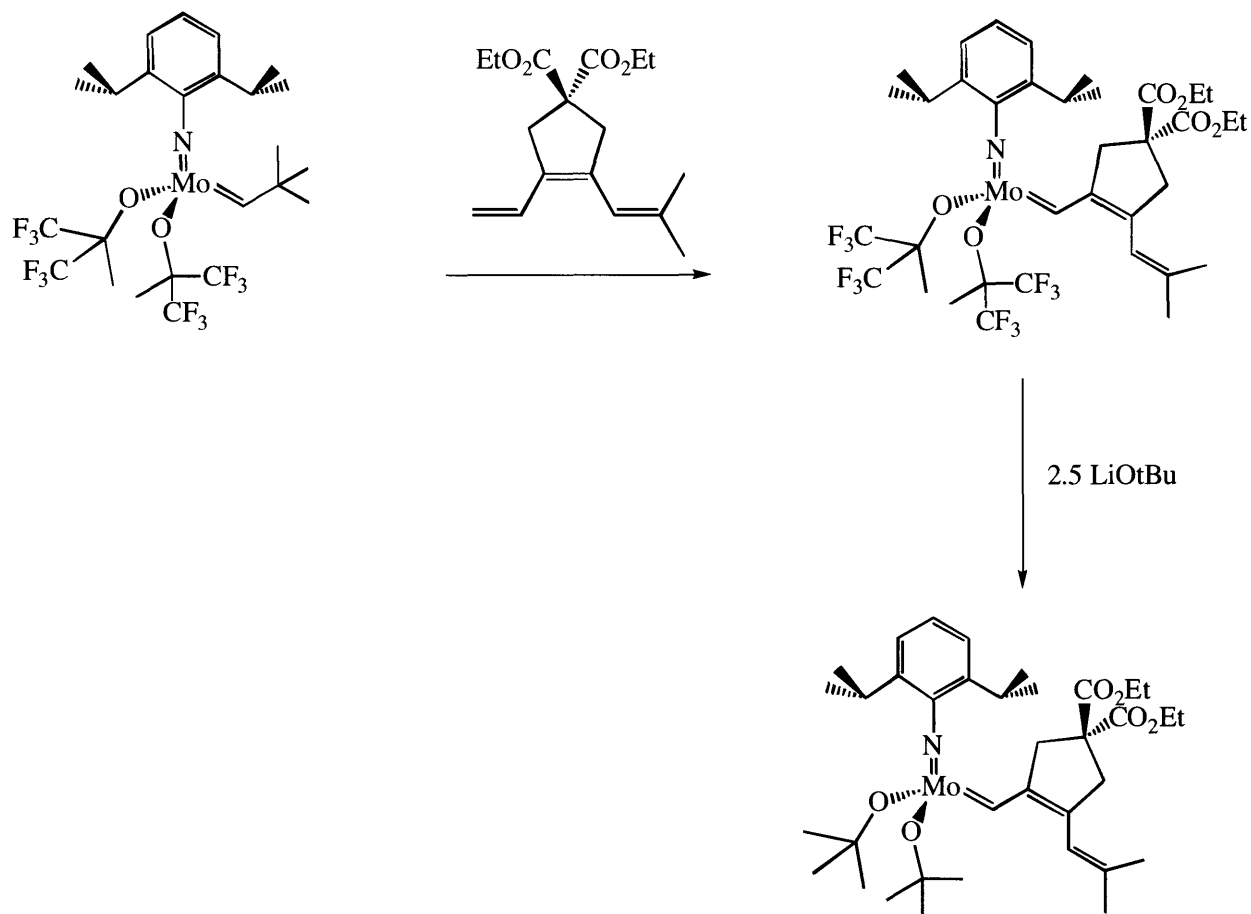
$J_{\text{HH}} = 10$ Hz) and 10% of the chiral, anti species ($H_{\alpha} = 12.49$ ppm, $J_{\text{HH}} = 12$ Hz). At -70 °C, three rotamers are present in solution: the achiral, syn rotamer (78%; $H_{\alpha} = 12.33$ ppm), the chiral, syn rotamer (11%; $H_{\alpha} = 12.65$ ppm), and the chiral, anti rotamer (11%; $H_{\alpha} = 12.85$ ppm). The only notable difference in the ^1H NMR spectrum of $\text{Mo}(\text{NAr})(\text{trans-CHCHCHMe})(\text{OAd})_2(\text{quin})$ from that of $\text{Mo}(\text{NAr})(\text{trans-CHCHCHMe})(\text{O-}t\text{-Bu})_2(\text{quin})$ is the substantial broadening of the quinuclidine proton resonances. A splitting pattern is absent in the quinuclidine H_{α} resonance near 3 ppm, and this broadened resonance narrows below 10 °C and above 70 °C, at which point the complex decomposes rapidly.

3.2.4 The Di-*tert*-butoxide Five-Membered Ring Alkylidene (CH[5]) Catalyst

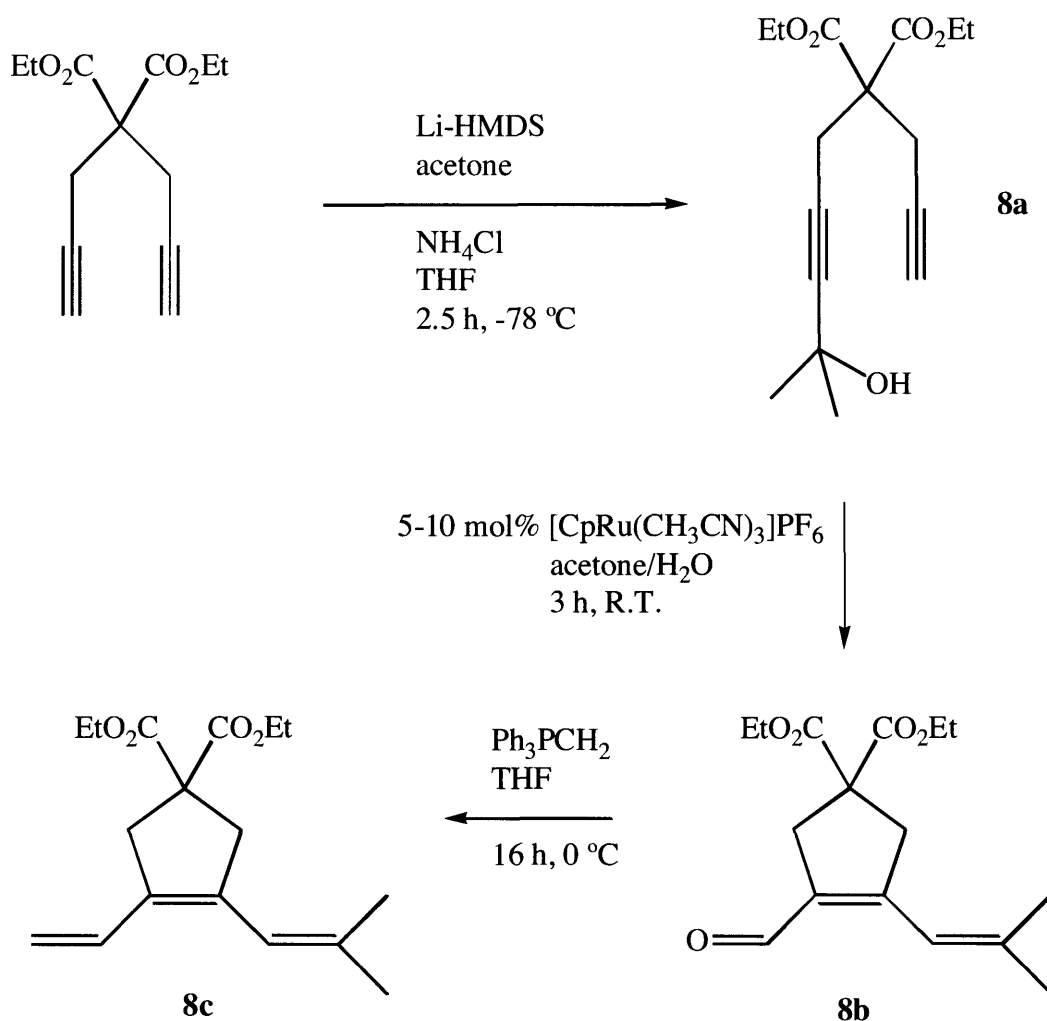
A $\text{Mo}(\text{NAr})(\text{CHR})(\text{O-}t\text{-Bu})_2$ initiator with an alkylidene ligand containing a five-membered ring positioned on C_{β} and C_{γ} was also developed. The alkylidene group is analogous to that which results when a five-membered ring is generated by the cyclopolymerization of 1 equivalent of DEDPM by $\text{Mo}(\text{NAr})(\text{trans-CHCHCHMe})(\text{O-}t\text{-Bu})_2(\text{quin})$ and may be viewed as a model of the first insertion product. A parallel may also be drawn between the structure and characteristics of the propagating species and the structure and characteristics of the five-membered ring initiator. The effect of the presence of a five-membered ring versus that of a six-membered ring (or of a simple vinyl group) adjacent to the metal center on initiation may be ascertained.

The synthesis of $\text{Mo}(\text{NAr})(\text{CH[5]})(\text{O-}t\text{-Bu})_2(\text{quin})$ (Scheme 3.7) requires the metathesis reaction of a five-membered ring triene (**8c**) with $\text{Mo}(\text{NAr})(\text{CHCMe}_3)[\text{OCMe}(\text{CF}_3)_2]_2$. A five-membered triene containing one unsubstituted and one disubstituted olefinic endgroup was selected in order to prevent the formation of bimetallic species upon reaction of the triene with the molybdenum catalyst. The first step in the synthesis of the five-membered ring triene²²⁹ (**8c**) involves deprotonation of DEDPM with Li-HMDS, followed by quenching with acetone to produce the diynol (**8a**) (Scheme 3.8). $[\text{CpRu}(\text{CH}_3\text{CN})_3]\text{PF}_6$ ²³⁰ cycloisomerizes^{231,232} the diynol (**8a**) to give an aldehyde with a five-membered ring (**8b**). The aldehyde is then subjected to a

Wittig reaction to produce the five-membered ring triene (**8c**).



Scheme 3.7. Synthesis of Mo(NAr)(CH[5])(O-*t*-Bu)₂.



Scheme 3.8. Synthesis of the five-membered ring triene substrate (Diethyl 3-(2-methylprop-1-enyl)-4-vinylcyclopent-3-ene-1,1-dicarboxylate (**8c**)).

Upon reaction of the five-membered ring triene (**8c**) with $\text{Mo}(\text{NAr})(\text{CHCMe}_3)[\text{OCMe}(\text{CF}_3)_2]_2$ in pentane, $\text{Mo}(\text{NAr})(\text{CH}[5])[\text{OCMe}(\text{CF}_3)_2]_2$ was generated in high yield in the form of a flaky, yellow solid with low solubility in pentane. Only the syn rotamer is observed in solution, with the alkylidene H_γ appearing at 5.96 ppm and the alkylidene H_α appearing at 12.79 ppm ($^1J_{\text{CH}} = 120\text{ Hz}$) in CD_2Cl_2 . Reaction of this species with 2.5 equivalents of $\text{LiO-}t\text{-Bu}$ in a minimal amount of pentane afforded $\text{Mo}(\text{NAr})(\text{CH}[5])(\text{O-}t\text{-Bu})_2$.

Recrystallization of this complex from pentane yielded crystalline material. The syn rotamer is the primary product observed in solution. The alkylidene H_δ is observed at 6.01 ppm, and the alkylidene H_α is observed at 11.87 ppm in CD_2Cl_2 and at 12.35 in C_6D_6 at 22 °C ($^1J_{CH} = 117.7$ Hz) (Figure 3.5).

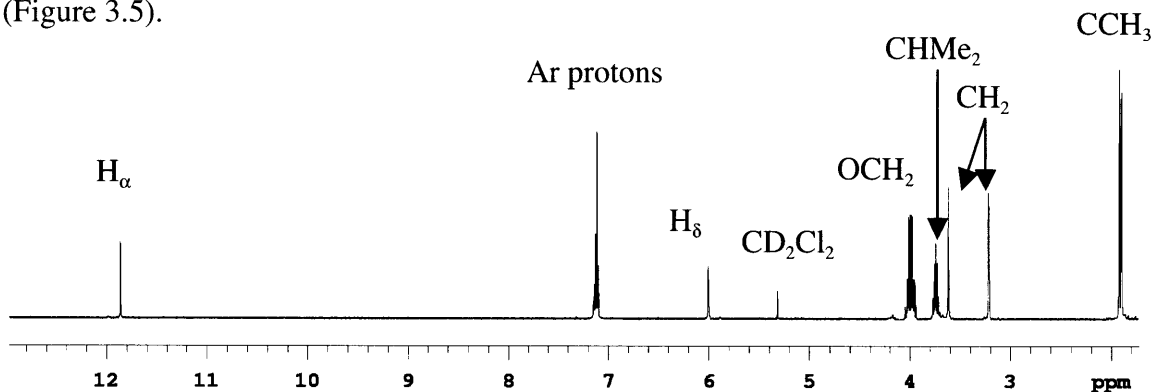


Figure 3.5. The partial (2.8 to 13 ppm) 1H NMR spectrum of $Mo(NAr)(CH[5])(O-t-Bu)_2$ (22 °C, CD_2Cl_2).

The X-ray structure of $Mo(NAr)(CH[5])(O-t-Bu)_2$ features a distorted tetrahedral molybdenum complex with the angles between the ligands ranging from $107.27(7)^\circ$ to $115.04(7)^\circ$ (Figure 3.6, Table 3.2). The alkylidene group is oriented syn to the imido group, and the $Mo(1)-N(1)-C(25)$ bond angle is $175.60(1)^\circ$. The $Mo(1)-C(1)-C(1)$ bond angle is $135.48(1)^\circ$, which is larger than the $Mo(1)-C(1)-C(1)$ bond angle of $128.99(2)^\circ$ in the X-ray structure of $Mo(NAr)(trans-CHCHCHMe)(O-t-Bu)_2(quin)$, presumably due to the greater steric bulk of the five-membered ring alkylidene group versus the butenylidene group. The $Mo(1)-N(1)$, $Mo(1)-O(1)$, $Mo(1)-O(1)$, and $Mo(1)-C(1)$ bond distances are all within the expected ranges for a structure of this type.

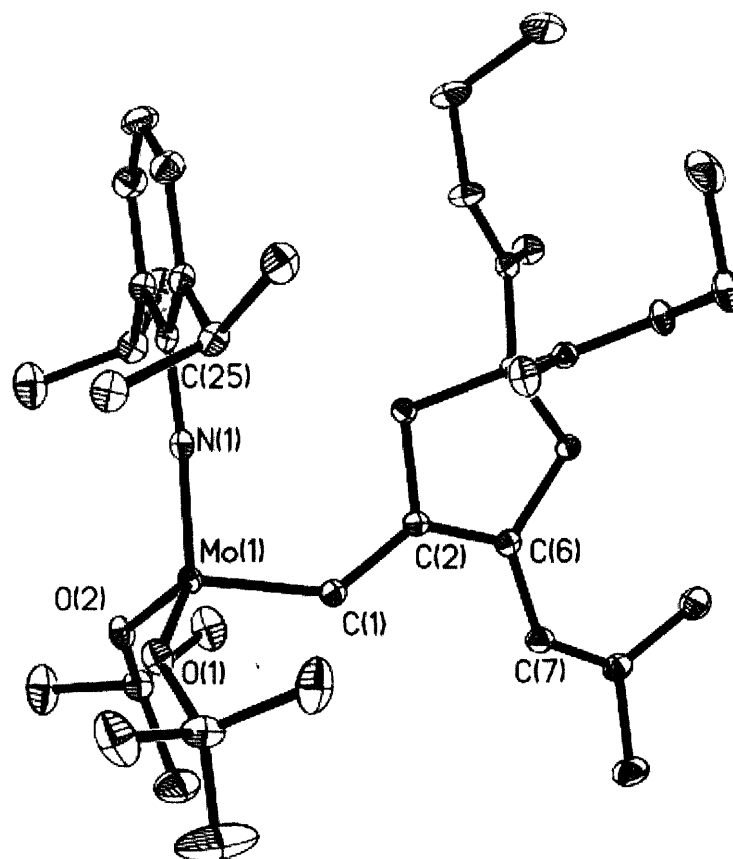


Figure 3.6. Thermal ellipsoid drawing of $\text{Mo}(\text{NAr})(\text{CH}[5])(\text{O}-t\text{-Bu})_2$ at the 50% probability level.

Table 3.2. Selected bond lengths [\AA] and angles [$^\circ$] for $\text{Mo}(\text{NAr})(\text{CH}[5])(\text{O}-t\text{-Bu})_2(\text{quin})$.

Bond Lengths [\AA]			
Mo(1)-N(1)	1.7333(2)	Mo(1)-O(1)	1.8840(1)
Mo(1)-C(1)	1.9217(2)	Mo(1)-O(2)	1.8791(1)
Bond Angles [$^\circ$]			
N(1)-Mo(1)-O(1)	115.04(7)	N(1)-Mo(1)-C(1)	99.91(8)
N(1)-Mo(1)-O(2)	113.92(7)	Mo(1)-N(1)-C(25)	175.60(1)
O(2)-Mo(1)-C(1)	108.42(7)	Mo(1)-C(1)-C(2)	135.48(1)
O(1)-Mo(1)-C(1)	107.27(7)		

The quinuclidine adduct of $\text{Mo}(\text{NAr})(\text{CH}[5])(\text{O}-t\text{-Bu})_2$ could not be crystallized. In CD_2Cl_2 at 22 °C, a 30 mM solution of $\text{Mo}(\text{NAr})(\text{CH}[5])(\text{O}-t\text{-Bu})_2$ and 1 equivalent of quinuclidine rapidly formed an equilibrium mixture comprised of 71% of the base-free, syn rotamer and 29% of the base-bound chiral, anti rotamer. Quinuclidine H_α resonances are observed at 2.80 ppm in CD_2Cl_2 and at 2.90 in C_6D_6 (Figure 3.7) for both bound and free quinuclidine. The chiral, anti alkylidene H_α proton appears as a broad singlet at 12.33 ppm in CD_2Cl_2 and 13.12 ppm in C_6D_6 ($^1J_{\text{CH}} = 143.6$ Hz). $\text{Mo}(\text{NAr})(\text{CH}[5])(\text{O}-t\text{-Bu})_2(\text{quin})$ is more stable than $\text{Mo}(\text{NAr})(\text{trans-CHCHCHMe})(\text{O}-t\text{-Bu})_2(\text{quin})$ in solution; only 30% decomposition (compared to 63%) was observed over a period of 14 hours at 22 °C in C_6D_6 .

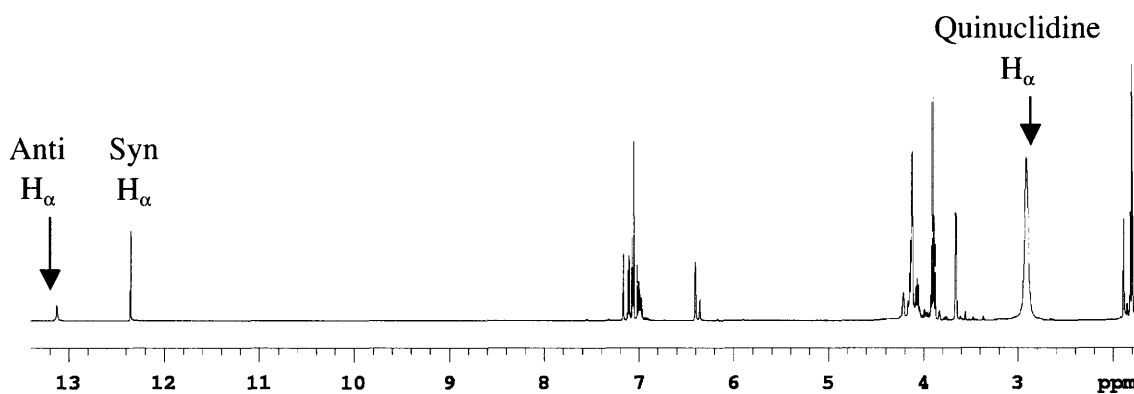
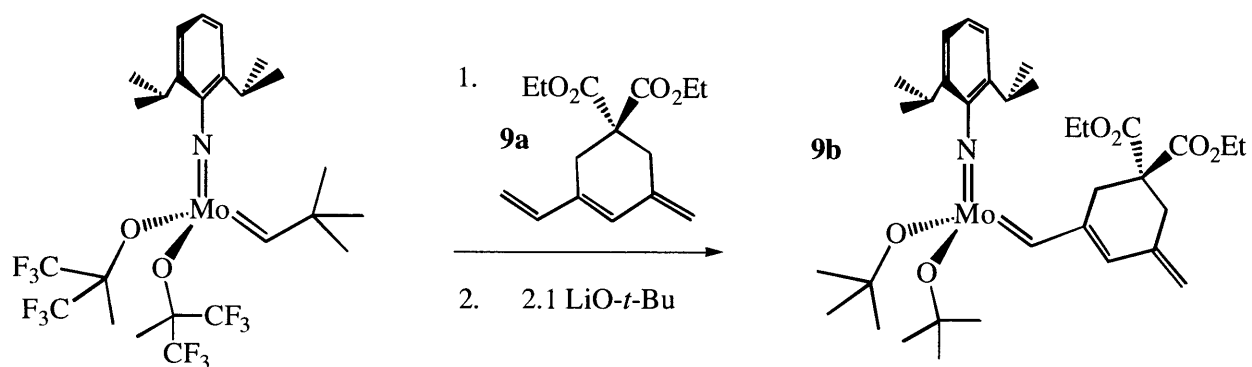


Figure 3.7. The partial (2.8 to 13.4 ppm) ^1H NMR spectrum of $\text{Mo}(\text{NAr})(\text{CH}[5])(\text{O}-t\text{-Bu})_2(\text{quin})$ (22 °C, C_6D_6).

3.2.5 The Di-*tert*-butoxide Six-Membered Ring Alkylidene Catalyst

The development of an initiator with an alkylidene ligand containing a six-membered ring that is analogous to the alkylidene that results when a six-membered ring is generated by the cyclopolymerization of 1 equivalent of DEDPM is also important. It has been shown previously that 1-vinyl-3-methylene-5,5-bis(carboxyethyl)cyclohex-1-ene (**9a**) (Scheme 3.9) is produced upon reaction of DEDPM with $\text{Mo}(\text{NAr})(\text{CHCMe}_3)[\text{OCMe}(\text{CF}_3)_2]_2$ in the presence of ethylene.²¹³ Reaction of this substrate with $\text{Mo}(\text{NAr})(\text{CHCMe}_3)[\text{OCMe}(\text{CF}_3)_2]_2$ produces $\text{Mo}[1\text{-methylidene-3-methylen-5,5-bis(carboxyethyl)cyclohex-1-ene}](\text{NAr})[\text{OCMe}(\text{CF}_3)_2]_2$ in very

low yield (< 12%).²¹³ Over a period of 1 to 24 hours in pentane, DME, or toluene, no more than 45% of the starting material is consumed. Several impurities are also present, one of which may arise from the formation of bimetallic molybdenum complexes. Mo[1-methylidene-3-methylen-5,5-bis(carboxyethyl)cyclohex-1-ene](NAr)(O-*t*-Bu)₂ (**9b**) is observed in solution upon reaction of Mo[1-methylidene-3-methylen-5,5-bis(carboxyethyl)cyclohex-1-ene](NAr)[OCMe(CF₃)₂]₂ with 2.1 equivalents of LiO-*t*-Bu (Scheme 3.9). The alkylidene H_α resonance for this species is observed at 11.59 ppm in CD₂Cl₂, and the vinyl proton H_γ resonance of the six-membered ring is observed at 5.59 ppm. The addition of 1 equivalent of quinuclidine did not affect the chemical shift of the alkylidene H_α resonance. Unfortunately, this six-membered ring initiator could not be isolated.



Scheme 3.9. Synthesis of Mo[1-methylidene-3-methylen-5,5-bis(carboxyethyl)cyclohex-1-ene](NAr)(O-*t*-Bu)₂ (**9b**).

3.3 DEDPM Polymerization

DEDPM is cyclopolymerized to produce either five- or six-membered rings along the polyene backbone. Five- and six-membered ring model compounds²³³ were used to establish the assignment of NMR resonances.²⁰⁹ In the 125 MHz CDCl₃ ¹³C NMR spectrum, five-membered ring poly(DEDPM) carbonyl carbons appear around 172.1 ppm, and six-membered ring carbonyl carbons appear at about 171.1 ppm. Six-membered ring poly(DEDPM) quaternary carbons appear between 54.0 to 55.0 ppm, and five-membered ring quaternary carbons appear

between 57.0 to 58.5 ppm. The percentages of five- and six-membered rings can be approximated by integrating the ^{13}C NMR resonances corresponding to either the quaternary or carbonyl carbon atoms, although these values may contain up to 30% error.²⁰⁹

Polymer regularity may also be estimated using ^1H NMR spectroscopy. The CDCl_3 ^1H NMR spectrum of poly(DEDPM) comprised of 95% five-membered rings contains broadened peaks at 1.3, 3.4, 4.3, and 6.7 ppm corresponding to the ester CH_3 , the five-membered ring CH_2 , the ester CH_2 , and the backbone vinyl CH protons, respectively. In contrast, the ^1H NMR spectrum of poly(DEDPM) comprised of a mixture of five- and six-membered rings contains additional broadened (overlapping) peaks at 2.9, 3.2, and 3.4 ppm corresponding to six-membered ring CH_2 protons with five- or six-membered ring neighbors. A large distribution of backbone vinyl CH protons between 5.8 and 6.8 ppm is also observed. Unfortunately, proton peak overlap renders quantification impossible.

Highly conjugated, fresh polymers containing greater than 20 rings have a deep purple metallic color and form a thick film that can be crushed up to form a powder. Polymers of this type are soluble in chloroform, dichloromethane, and DME and are dark purple in solution. Polymers containing greater than 40% six-membered rings are soluble in tetrahydrofuran, benzene, and toluene, whereas polymers containing more than 40% five-membered rings are not. While these polymers are relatively stable to air, decomposition is observed after exposure to air over an extended period of time. After 48 hours at room temperature, polymers that are not stored under nitrogen in solid form decompose to give high molecular weight polymer. Loss of conjugation also occurs, presumably due to oxidation, which is evidenced by the red color observed in solution and blue-shifted λ_{max} values.²¹³ Very small (< 1% of total injection weight) peaks with molecular weights 25 to 60 times that of the primary peak are always observed in the GPC traces of polymers produced by $\text{Mo}(\text{NAr})(\text{CHR})(\text{O}-t\text{-Bu})_2(\text{quin})$ catalysts and may result from post-polymerization decomposition.²⁰⁹

3.3.1 The Neopentylidene, Neophylidene, and Ferrocenylmethylidene Catalysts

Several polymerizations employing $\text{Mo}(\text{NAr})(\text{CHR})(\text{O}-t\text{-Bu})_2$ ($\text{R} = \text{CMe}_2\text{Ph}$, CMe_3 , Fc) as the initiator were performed, and the results are listed in Table 3.3. Quinuclidine adducts in these experiments were generated by adding 1 equivalent (or more if specified) of quinuclidine to the initiator solution, which was stirred for 15 minutes prior to the addition of DEDPM. As expected, polymer produced by $\text{Mo}(\text{NAr})(\text{CHR})(\text{O}-t\text{-Bu})_2$ catalysts contained greater than 90% five-membered rings, and these highly regular polymers were insoluble in THF. Although polymer exclusively consisting of five-membered rings has reportedly been produced by $\text{Mo}(\text{NAr})(\text{CHCMe}_2\text{Ph})(\text{O}-t\text{-Bu})_2(\text{quin})$,^{209,210} trace amounts of six-membered rings were always observed in these reactions. A ^{13}C NMR spectrum of poly(DEDPM) formed by the reaction of 30 equivalents of DEDPM with $\text{Mo}(\text{NAr})(\text{CHCMe}_3)(\text{O}-t\text{-Bu})_2(\text{quin})$ in CH_2Cl_2 , starting at $-30\text{ }^\circ\text{C}$, is shown in Figure 3.8. Higher percentages of six-membered rings were observed in the absence of quinuclidine and when the reactions were started above $0\text{ }^\circ\text{C}$. Greater than 95% five-membered rings was not observed when 30 equivalents of excess quinuclidine were added.

Table 3.3. Reaction conditions for the synthesis of poly(DEDPM) and the percentages of five-membered rings produced during the cyclopolymerization.

Catalyst	Conc (mM)	Solvent	Equiv DEDPM	T ($^\circ\text{C}$)	% 5-Mem Rings
$\text{Mo}(\text{NAr})(\text{CHCMe}_3)(\text{O}-t\text{-Bu})_2$	16.0	DME	20	-30	> 95
$\text{Mo}(\text{NAr})(\text{CHCMe}_3)(\text{O}-t\text{-Bu})_2$	3.3	CH_2Cl_2	70	22	> 90
$\text{Mo}(\text{NAr})(\text{CHCMe}_3)(\text{O}-t\text{-Bu})_2 + 1.1$ quin	2.7	CH_2Cl_2	70	22	> 95
$\text{Mo}(\text{NAr})(\text{CHFc})(\text{O}-t\text{-Bu})_2$	8.1	DME	30	-30	> 95
$\text{Mo}(\text{NAr})(\text{CHFc})(\text{O}-t\text{-Bu})_2 + 1.1$ quin	6.6	DME	30	22	93
$\text{Mo}(\text{NAr})(\text{CHFc})(\text{O}-t\text{-Bu})_2 + 30$ quin	6.1	CH_2Cl_2	30	22	92

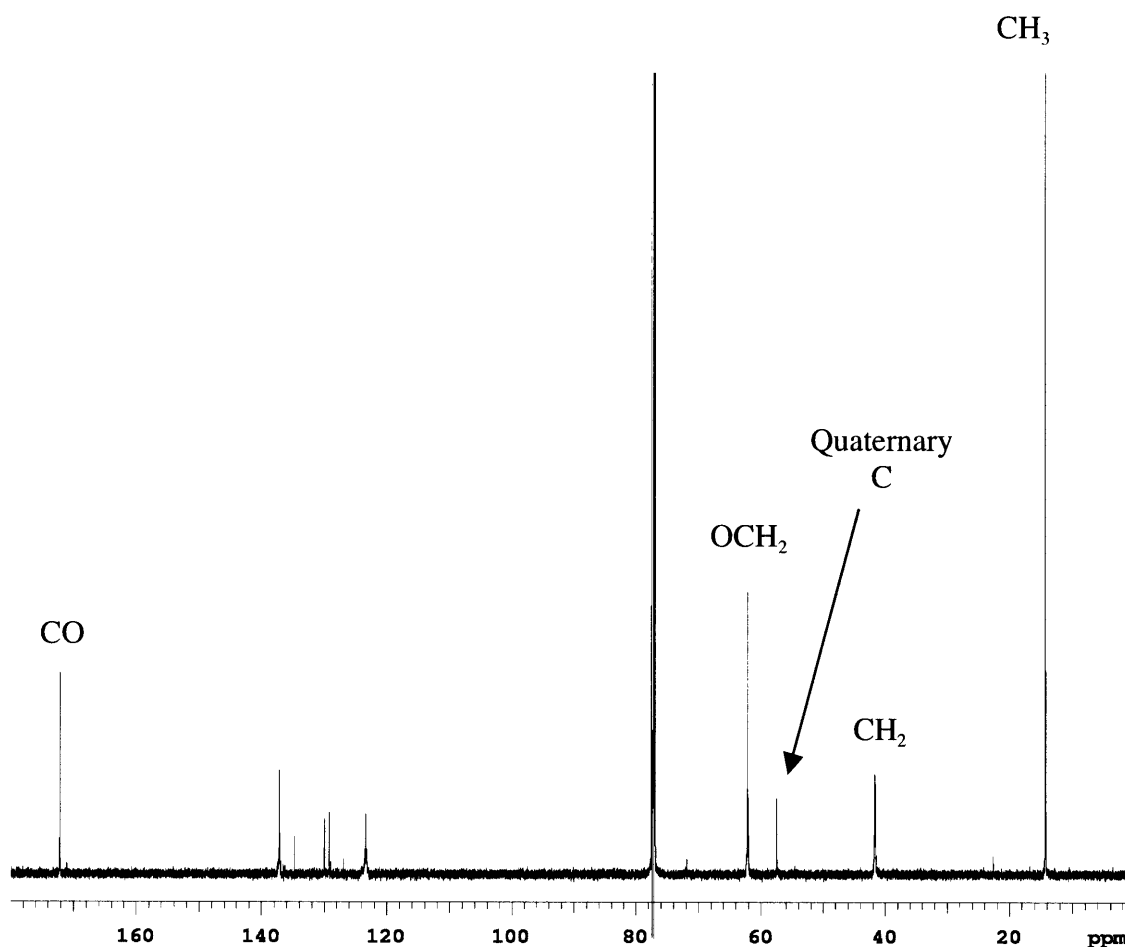


Figure 3.8. Poly(DEDPM) containing approximately 95% five-membered rings.

Bulk polymerizations of DEDPM were performed using $\text{Mo}(\text{NAr})(\text{CHCMe}_3)(\text{O}-t\text{-Bu})_2$ as the initiator, starting at $-30\text{ }^\circ\text{C}$. In agreement with reported values when $\text{Mo}(\text{NAr})(\text{CHCMe}_2\text{Ph})(\text{O}-t\text{-Bu})_2$ was employed as a catalyst,²⁰⁹ polymers produced in these reactions were characterized by polydispersities between 1.13 and 1.30 (Table 3.4). Experimental molecular weights increase linearly with increasing amounts of monomer (Figure 3.9). Also in accordance with reported values, $M_n(\text{found})/M_n(\text{calculated})$ ratios were calculated to be between 1.4 and 1.9 employing a dn/dc value of 0.63, the selection of which will be discussed later. Starting the polymerization reaction of 38 equivalents of DEDPM at room

temperature resulted in an $M_n(\text{found})/M_n(\text{calculated})$ ratio that was 10% greater than that for the polymer produced when the polymerization was started at $-30\text{ }^\circ\text{C}$. Higher than expected polydispersities and $M_n(\text{found})/M_n(\text{calculated})$ ratios may have resulted from catalytic decomposition or greater rates of propagation relative to initiation. In order to probe the latter possibility, the development of more efficient initiators was explored.

Table 3.4. Molecular weights and polydispersities for polyenes formed by the cyclopolymerization of DEDPM by $\text{Mo}(\text{NAr})(\text{CHR})(\text{O}-t\text{-Bu})_2(\text{quin})$ ($\text{R} = \text{trans-CHCHMe}$, CMe_3 , [5]) in CD_2Cl_2 .

R	Temperature of Initiation ($^\circ\text{C}$)	Equiv DEDPM	M_n Calculated (g/mol)	M_n Found (g/mol)	PDI
CHCHMe	22	38	9100	9909	1.02
CHCHMe	22	55	14000	15240	1.05
CHCHMe	22	75	19100	24960	1.05
CHCHMe	-30	20	4900	5043	1.07
CHCHMe	-30	38	9100	9087	1.07
CHCHMe	-30	55	13100	13990	1.05
CHCHMe	-30	75	17900	19100	1.09
CHCHMe	-30	95	22600	25020	1.08
CMe_3	22	38	9100	17380	1.13
CMe_3	-30	20	4900	9277	1.50
CMe_3	-30	38	9100	15830	1.18
CMe_3	-30	55	13200	21060	1.14
CMe_3	-30	75	17900	28000	1.24
CMe_3	-30	95	22600	33450	1.16
[5]	-30	5	1700	2056	1.04
[5]	-30	9	2600	3113	1.02
[5]	-30	55	13500	16160	1.12

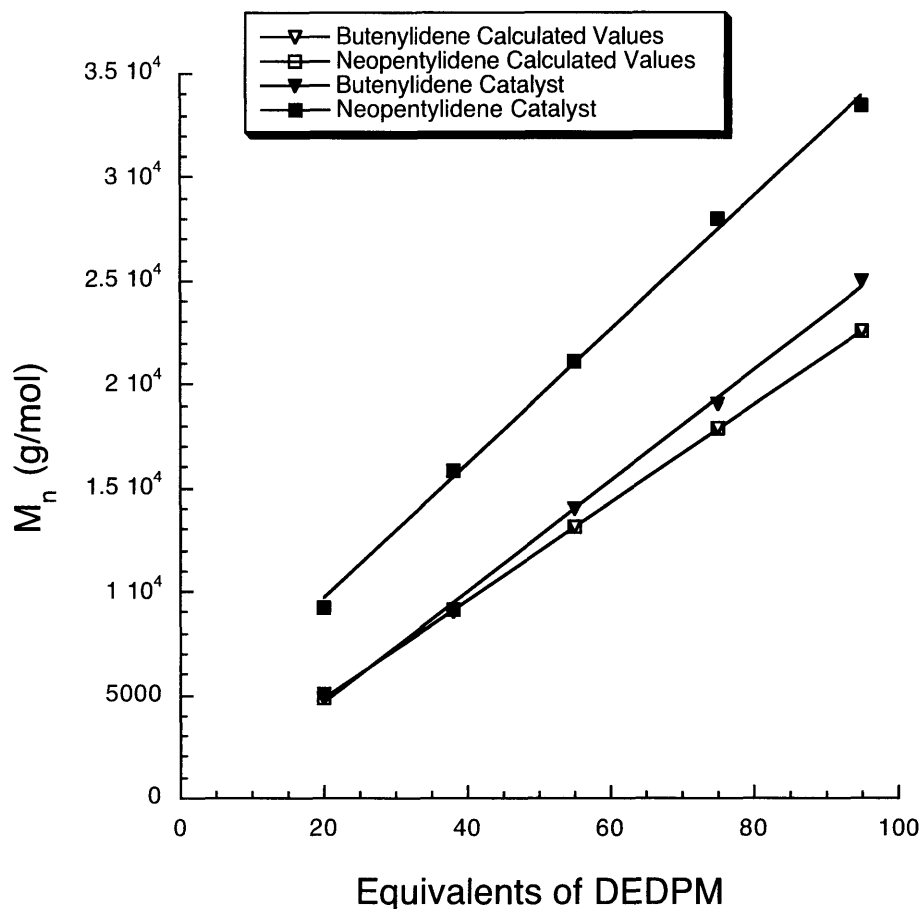


Figure 3.9. Number average molecular weight (M_n) of poly(DEDPM) (g/mol) produced by $\text{Mo}(\text{NAr})(\text{CHR})(\text{O}-t\text{-Bu})_2(\text{quin})$ ($\text{R} = \text{CMe}_3$; Neopentylidene Catalyst, *trans*-CHCHMe; Butenyliene Catalyst) versus equivalents of monomer (See Table 3.4 for data).

3.3.2 The Di-*tert*-butoxide and Hexafluoro-*tert*-Butoxide Butenyliene Catalysts

A polymerization reaction employing $\text{Mo}(\text{NAr})(\text{trans-CHCHCHMe})[\text{OCMe}(\text{CF}_3)_2]_2(\text{quin})$ demonstrated the potential of the butenyliene catalyst for fast initiation. The reaction of 30 equivalents of DEDPM with this species at room temperature in CD_2Cl_2 produced polymer that contained 51% five-membered rings and was characterized by a unimodal GPC trace and a PDI of 1.10. This should be compared to an average PDI of 1.23

reported for poly(DEDPM) produced by $\text{Mo}(\text{NAr})(\text{CHCMePh}_2)[\text{OCMe}(\text{CF}_3)_2]_2$ at 22 °C in DME.²¹³

Poly(DEDPM) containing approximately 95% five-membered rings was produced by $\text{Mo}(\text{NAr})(\text{trans-CHCHCHMe})(\text{O-}t\text{-Bu})_2(\text{quin})$ when the reaction mixture was started at -30 °C. The polymerization reactions were performed in methylene chloride to ensure that long polyenes remained soluble. DEDPM is cyclopolymerized in a first-order manner; plots of $\ln([\text{DEDPM}]/[\text{standard}])$ (standard = hexamethylbenzene) versus time are virtually linear for over 4 half lives (Figure 3.10). Since quinuclidine coordinates only weakly to the initiator, the dissociation of the base from the catalyst is rapid compared to the insertion of monomer into the $\text{M}=\text{C}$ double bond. First-order rate constants (k_p) were calculated for reactions at -10, 0, and 10 °C and are listed in Table 3.5. While the reaction of $\text{Mo}(\text{NAr})(\text{CHR})(\text{O-}t\text{-Bu})_2(\text{quin})$ (R = propagating alkylidene) with DEDPM at temperatures greater than 10 °C is too fast to be accurately monitored by NMR, the reaction of $\text{Mo}(\text{NAr})(\text{CHR})(\text{O-}t\text{-Bu})_2(\text{quin})$ (R = propagating alkylidene) with DEDPM at temperatures below -10 °C is impractically slow. At 0 °C, the average k_p value was measured to be $0.24 \text{ M}^{-1}\text{s}^{-1}$. The activation parameters ΔH^\ddagger and ΔS^\ddagger were calculated to be 10 kcal/mol and -24 cal/mol•K, respectively (Figure 3.11).

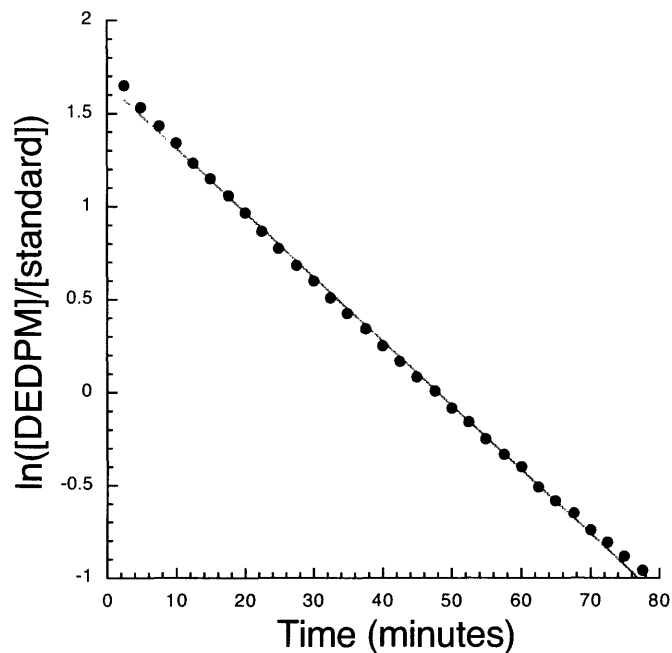


Figure 3.10. Consumption of 40 equivalents of DEDPM by $\text{Mo}(\text{NAr})(\text{trans-CHCHCHMe})(\text{O-}t\text{-Bu})_2(\text{quin})$ in CD_2Cl_2 at 0°C ($k_p = 0.24 \text{ M}^{-1}\text{s}^{-1}$).

Table 3.5. Rates constants of polymerization (k_p) of 40 equivalents of DEDPM by $\text{Mo}(\text{NAr})(\text{trans-CHCHCHMe})(\text{O-}t\text{-Bu})_2(\text{quin})$ in CD_2Cl_2 from -10 to 10°C .

Concentration (mM)	Temperature ($^\circ\text{C}$)	k_p ($\text{M}^{-1}\text{s}^{-1}$)
5	10	0.49
1.9	10	0.50
3.9	0	0.24
2.1	0	0.23
3.9	-10	0.12

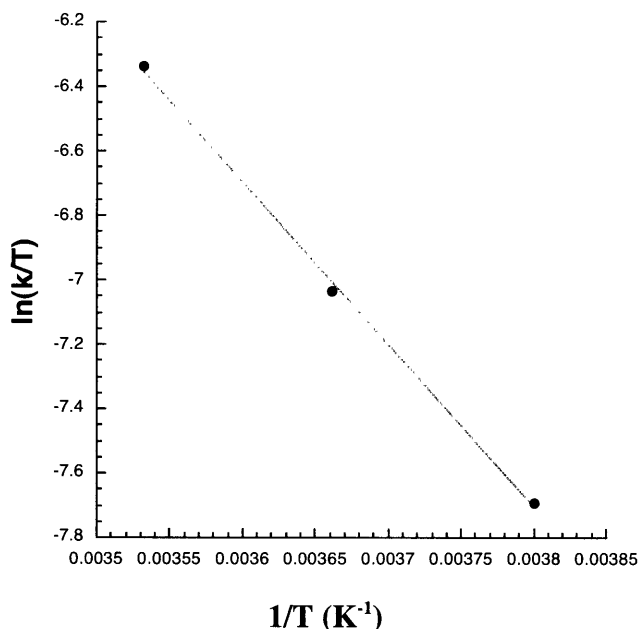


Figure 3.11. Plot of $\ln(k/T)$ versus $1/T$ (K^{-1}) for $\text{Mo}(\text{NAr})(\text{trans-CHCHCHMe})(\text{O-}t\text{-Bu})_2(\text{quin})$: $\Delta H^\ddagger = 10$ kcal/mol and $\Delta S^\ddagger = -24$ cal/mol \cdot K.

A bulk polymerization of 38 equivalents of DEDPM by $\text{Mo}(\text{NAr})(\text{trans-CHCHCHMe})(\text{O-}t\text{-Bu})_2(\text{quin})$ was conducted at room temperature in CH_2Cl_2 . The reaction was quenched with ferrocenecarboxaldehyde, yielding ferrocene-capped polymer. According to MALDI-TOF analysis, the resulting polymer was characterized by a PDI of 1.02 and an $M_n(\text{found})/M_n(\text{calculated})$ ratio of 1.08 ($M_n(\text{found}) = 9886$ g/mol; $M_n(\text{calculated}) = 9122$ g/mol) (Figure 3.12). GPC analysis of this polymer confirmed a PDI of 1.02 and an $M_n(\text{found})/M_n(\text{calculated})$ ratio of 1.08 when a dn/dc value of 0.63 was used. Polymerizations of 20 to 95 equivalents of DEDPM, by $\text{Mo}(\text{NAr})(\text{trans-CHCHCHMe})(\text{O-}t\text{-Bu})_2(\text{quin})$, starting at -30 °C, were performed, and the resulting polymers were analyzed by GPC using a dn/dc value of 0.63. The dn/dc value was selected based on MALDI-TOF analysis and the agreement between the molecular weights of polymer produced by $\text{Mo}(\text{NAr})(\text{CHCMe}_3)(\text{O-}t\text{-Bu})_2(\text{quin})$ and published molecular weights (determined by light scattering) of polymer produced by

$\text{Mo}(\text{NAr})(\text{CHCMe}_2\text{Ph})(\text{O}-t\text{-Bu})_2(\text{quin})$.²⁰⁹ $\text{Mo}(\text{NAr})(\text{CHCMe}_3)(\text{O}-t\text{-Bu})_2(\text{quin})$ is expected to behave similarly to $\text{Mo}(\text{NAr})(\text{CHCMe}_2\text{Ph})(\text{O}-t\text{-Bu})_2(\text{quin})$ as an initiator. The adjustment of dn/dc is required because poly(DEDPM) is significantly more rigid than polystyrene. Compared to the polydispersities associated with polymers produced by the neopentylidene initiator, polydispersities for polymer produced by the butenylidene initiator were significantly lower, ranging from 1.02 to 1.09 (Table 3.4). Polymer molecular weight increased linearly with increasing amounts of monomer and $M_n(\text{found})/M_n(\text{calculated})$ ratios were significantly closer to 1 when $\text{Mo}(\text{NAr})(\text{trans-CHCHCHMe})(\text{O}-t\text{-Bu})_2(\text{quin})$ was employed as the initiator than when $\text{Mo}(\text{NAr})(\text{CHCMe}_3)(\text{O}-t\text{-Bu})_2(\text{quin})$ was employed as the initiator (Figure 3.9, Table 3.4).

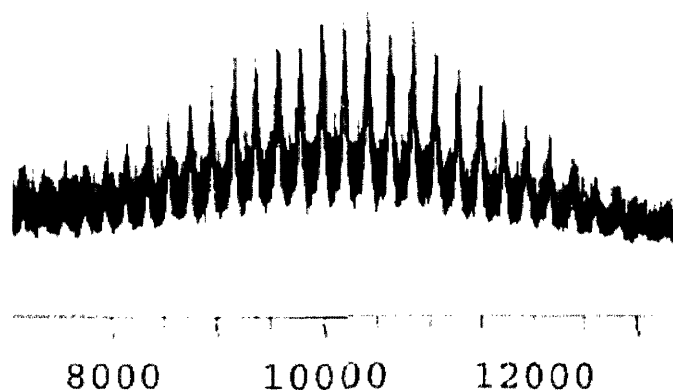


Figure 3.12. MALDI-TOF spectrum of ferrocene-capped polymer formed by the polymerization of 38 equivalents of DEDPM by $\text{Mo}(\text{NAr})(\text{trans-CHCHCHMe})(\text{O}-t\text{-Bu})_2(\text{quin})$ in CH_2Cl_2 at 22 °C (PDI = 1.02, $M_n(\text{f/c}) = 1.08$).

3.3.3 The Diadamantoxide Butenylidene Catalyst

$\text{Mo}(\text{NAr})(\text{trans-CHCHCHMe})(\text{OAd})_2(\text{quin})$ also cyclopolymerizes DEDPM in a first-order manner (Figure 3.13). First-order rate constants (k_p) for polymerization reactions at -10, 0, and 10 °C are listed in Table 3.7. At 0 °C, k_p was measured to be $0.13 \text{ M}^{-1}\text{s}^{-1}$, which is about half the rate constant of $0.24 \text{ M}^{-1}\text{s}^{-1}$ measured for $\text{Mo}(\text{NAr})(\text{trans-CHCHCHMe})(\text{O}-t\text{-Bu})_2(\text{quin})$. The activation parameters ΔH^\ddagger and ΔS^\ddagger were calculated to be 10 kcal/mol and $-26 \text{ cal/mol}\cdot\text{K}$, respectively (Figure 3.14). Unfortunately, polymer produced by $\text{Mo}(\text{NAr})(\text{trans-}$

$\text{CHCHCHMe}(\text{OAd})_2(\text{quin})$ at $0\text{ }^\circ\text{C}$ in CH_2Cl_2 contained only 87% five-membered rings. Since five- and six-membered rings may be produced at different rates, the higher percentage of six-membered rings produced by $\text{Mo}(\text{NAr})(\text{trans-CHCHCHMe})(\text{OAd})_2(\text{quin})$ may contribute to the lower k_p values that are measured for catalysts containing adamantoxide versus *tert*-butoxide ligands.

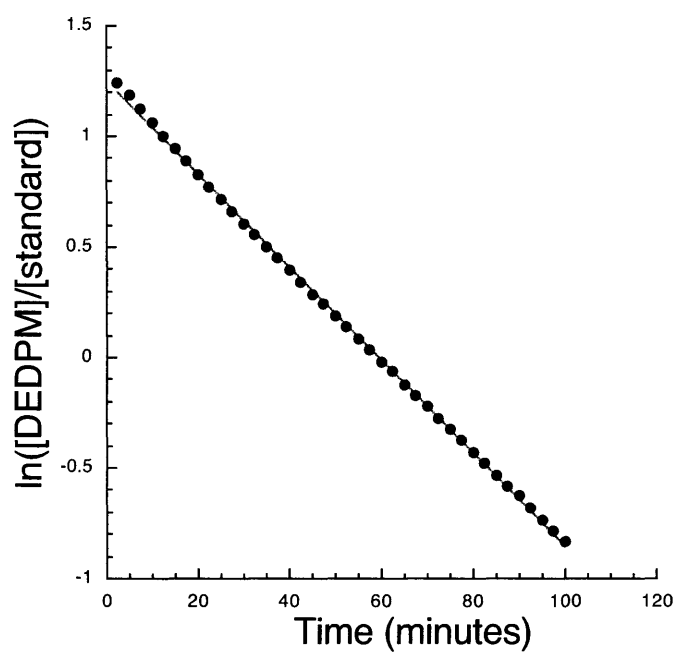


Figure 3.13. Consumption of 40 equivalents of DEDPM by $\text{Mo}(\text{NAr})(\text{trans-CHCHCHMe})(\text{OAd})_2(\text{quin})$ in CD_2Cl_2 at $0\text{ }^\circ\text{C}$ ($k_p = 0.13\text{ M}^{-1}\text{s}^{-1}$).

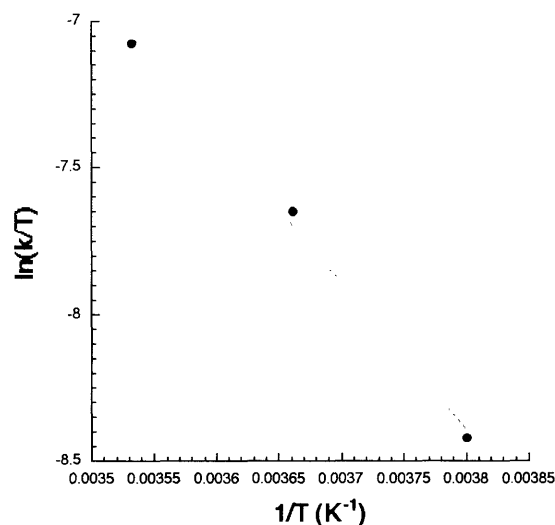


Figure 3.14. Plot of $\ln(k/T)$ versus $1/T$ (K^{-1}) for $\text{Mo}(\text{NAr})(\text{trans-CHCHCHMe})(\text{OAd})_2(\text{quin})$: $\Delta H^\ddagger = 10$ kcal/mol and $\Delta S^\ddagger = -26$ cal/mol \cdot K.

Table 3.6. Rate constants of polymerization (k_p) of 40 equivalents of DEDPM by $\text{Mo}(\text{NAr})(\text{trans-CHCHCHMe})(\text{OAd})_2(\text{quin})$.

Concentration (mM)	Temperature ($^{\circ}\text{C}$)	k_p ($\text{M}^{-1}\text{s}^{-1}$)
2.4	10	0.27
2.7	0	0.13
2.7	-10	0.058

3.3.4 The Five-Membered Ring Alkylidene Catalyst

Poly(DEDPM) generated by $\text{Mo}(\text{NAr})(\text{CH}[5])(\text{O-}t\text{-Bu})_2(\text{quin})$ was similar in quality to that produced by $\text{Mo}(\text{NAr})(\text{trans-CHCHCHMe})(\text{O-}t\text{-Bu})_2(\text{quin})$. The polymerization reactions were quenched with 1.5 equivalents of the five-membered ring aldehyde (**8b**), affording symmetric polymers containing roughly 95% five-membered rings. Since the synthesis of **8b** is time-consuming, a smaller excess of aldehyde was used in these reactions. Polydispersities ranged between 1.02 and 1.12 for polymerization reactions started at -30 $^{\circ}\text{C}$, and $M_n(\text{found})/M_n(\text{calculated})$ ratios ranged from 1.18 to 1.21 (Table 3.7). Slightly higher molecular weights for polymer produced by $\text{Mo}(\text{NAr})(\text{CH}[5])(\text{O-}t\text{-Bu})_2(\text{quin})$ than for polymer produced

by Mo(NAr)(*trans*-CHCHCHMe)(O-*t*-Bu)₂(quin) can be attributed to error introduced when 1.5 equivalents of the capping reagent (**8b**) were used instead of the usual 10-fold excess. It is possible that catalyst decomposition may have occurred before the Wittig-like polymer-capping reaction was complete.

Table 3.7. Molecular weight ratios ($M_n(f/c) = M_n(\text{found})/M_n(\text{calculated})$) and polydispersities for polyenes formed by the cyclopolymerization of DEDPM by Mo(NAr)(CH[5])(O-*t*-Bu)₂(quin) in dichloromethane, starting at -30 °C.

Equiv DEDPM	Concentration (mM)	PDI	$M_n(f/c)$
5	12.8	1.02	1.18
9	29.1	1.04	1.21
55	2.3	1.12	1.20

3.3.5 The Mo(NAr)(CHR')(O-*t*-Bu)₂(quin) Propagating Catalyst

(R' = polymer chain)

After the consumption of DEDPM by the catalyst is complete, the propagating species remains active for further polymerization. However, in the absence of DEDPM, the alkylidene H_α resonances corresponding to the propagating species decomposed by 83% after a period of 2 hours in CD₂Cl₂ at room temperature. Multiple unidentifiable products were formed during this process. While catalyst decomposition during the polymerization process cannot be monitored directly, catalyst decomposition may contribute to the observed higher than expected experimental molecular weights.

3.4 Initiation Studies

Gaining a better understanding of the initiation process is essential for catalyst design and development. Catalytic behavior can be investigated by studying the products of the first few cycles in the polymerization of DEDPM. Initiation experiments can be used to calculate the rate of propagation relative to initiation (k_p/k_i) for a catalyst using ¹H NMR.²³⁴ These k_p/k_i values

should be viewed as rough estimates due to unavoidable integration error. In a truly living system, values for k_p/k_i should be less than or equal to 1.

The identification of insertion products enables the progress of the living polymerization reaction to be monitored as increasing amounts of monomer react with the catalyst. The presence of first- and second-insertion products in ^1H NMR spectra indicates that trimers, tetramers, and other short oligomers can potentially be synthesized in high yield. Identifying which alkylidene H_α resonances correspond to insertion products in which a five-membered ring is adjacent to the metal and which alkylidene H_α resonances correspond to insertion products in which a six-membered ring is adjacent to the metal is also important. However, these data will only reflect catalyst behavior in extremely low monomer concentrations.

3.4.1 The Neopentylidene, Neophylidene, and Ferrocenylmethylidene Initiators

Significantly higher rates of propagation relative to initiation are observed by ^1H NMR for polymerizations employing quinuclidine adducts of $\text{Mo}(\text{NAr})(\text{CHFc})(\text{O}-t\text{-Bu})_2$, $\text{Mo}(\text{NAr})(\text{CHCMe}_3)(\text{O}-t\text{-Bu})_2$ and $\text{Mo}(\text{NAr})(\text{CHCMe}_2\text{Ph})(\text{O}-t\text{-Bu})_2$ ^{209,210} as catalysts. When 3 equivalents of DEDPM were added to a quinuclidine adduct of $\text{Mo}(\text{NAr})(\text{CHCMe}_3)(\text{O}-t\text{-Bu})_2$ formed *in situ* in CD_2Cl_2 at room temperature, only 69% of the initiator was consumed, resulting in a k_p/k_i of 5.81. Six alkylidene H_α peaks are evident in the ^1H NMR spectrum: 11.20 ppm (starting material), 11.54 ppm (very small, Mo-6-5-P), 11.57 ppm (very small, Mo-6-6-P), 12.02 ppm (large, Mo-5-5-P), 12.04 ppm (very small, Mo-5-6-P), and 12.7 ppm (small, anti rotamers) (P = polymer chain). These peaks were identified using initiation studies of $\text{Mo}(\text{NAr})(\text{trans-CHCHCHMe})(\text{O}-t\text{-Bu})_2(\text{quin})$ and will be discussed later. It is important to note here the absence of first and second insertion product alkylidene H_α resonances despite incomplete monomer consumption and the presence of propagating species alkylidene H_α resonances.

As reported previously, rates of propagation relative to rates of initiation (k_p/k_i) were even greater when an equivalent of quinuclidine was not added.^{209,210} The rate of propagation relative to the rate of initiation (k_p/k_i) for $\text{Mo}(\text{NAr})(\text{CHCMe}_3)(\text{O}-t\text{-Bu})_2$ was measured to be 34 in CD_2Cl_2

(k_p/k_i was reported²⁰⁹ to be 114 for $\text{Mo}(\text{NAr})(\text{CHCMe}_2\text{Ph})(\text{O}-t\text{-Bu})_2$, but this seems unreasonably high for a reasonably living polymerization catalyst). In fact, only 81% of the initiator was consumed when 30 equivalents of DEDPM were reacted with $\text{Mo}(\text{NAr})(\text{CHCMe}_3)(\text{O}-t\text{-Bu})_2$ in CD_2Cl_2 , starting at $-30\text{ }^\circ\text{C}$.

3.4.2 The Di-*tert*-butoxide and Hexafluoro-*tert*-Butoxide Butenylidene Initiators

3.4.2.1 Calculation of k_p/k_i for $\text{Mo}(\text{NAr})(\text{trans-CHCHCHMe})(\text{O}-t\text{-Bu})_2(\text{quin})$ and $\text{Mo}(\text{NAr})(\text{trans-CHCHCHMe})[\text{OCMe}(\text{CF}_3)_2]_2(\text{quin})$

The behavior of $\text{Mo}(\text{NAr})(\text{trans-CHCHCHMe})(\text{O}-t\text{-Bu})_2(\text{quin})$ as an initiator was analyzed by reacting 0.2 to 30 equivalents of DEDPM with the catalyst and observing the products by ^1H NMR. When 1.1 equivalents of DEDPM were added to $\text{Mo}(\text{NAr})(\text{trans-CHCHCHMe})(\text{O}-t\text{-Bu})_2(\text{quin})$ in CD_2Cl_2 at $22\text{ }^\circ\text{C}$, peaks corresponding to the first and second insertion products were observed, demonstrating that the butenylidene catalyst does indeed initiate faster than the neopentylidene catalyst (Figure 3.15). Ratios for the rate of propagation versus initiation (k_p/k_i) are listed in Table 3.8. Average k_p/k_i values for initiations performed at $22\text{ }^\circ\text{C}$ were 0.39 in CD_2Cl_2 and 0.55 in C_6D_6 , and these values were not significantly different at lower temperatures ($k_p/k_i = 0.41$ in CD_2Cl_2 , starting at $-30\text{ }^\circ\text{C}$). Upon addition of up to 2.53 equivalents of DEDPM to a solution of $\text{Mo}(\text{NAr})(\text{trans-CHCHCHMe})(\text{O}-t\text{-Bu})_2(\text{quin})$ in either C_6D_6 or CD_2Cl_2 , the pale red solution developed a deep red color over a period of 10 seconds. The initiator was completely consumed when greater than 3 equivalents of DEDPM were added.

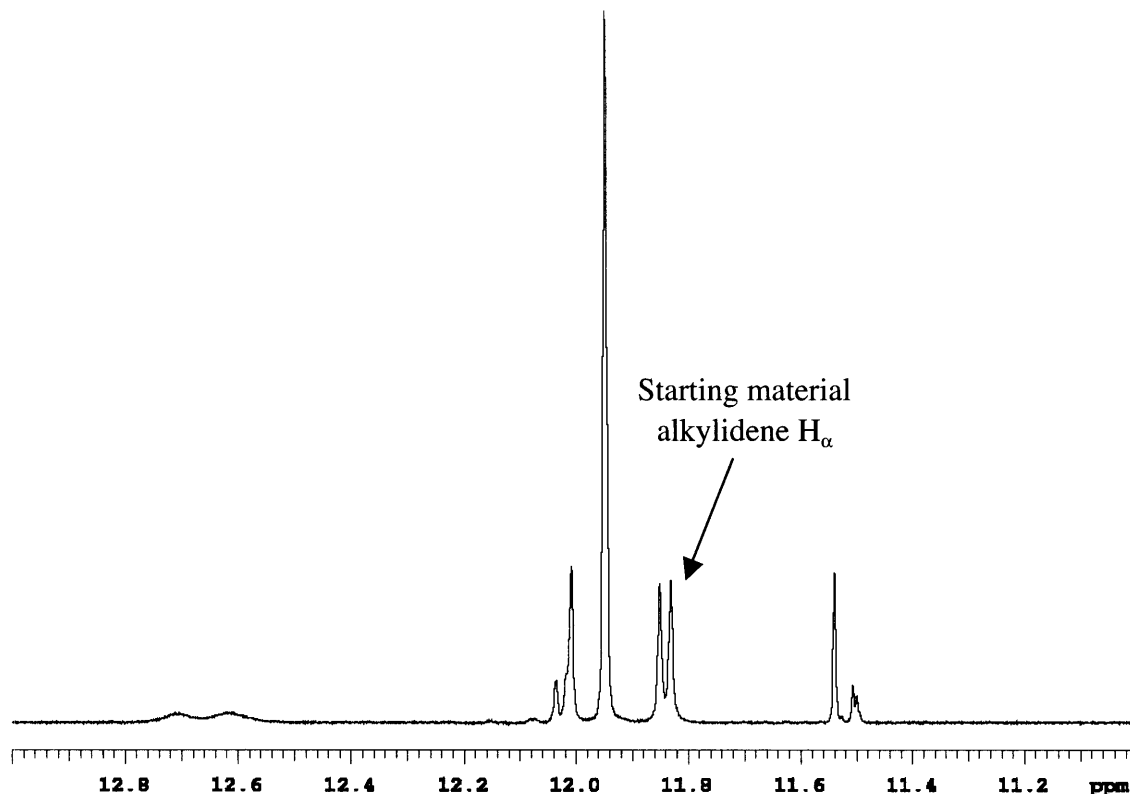


Figure 3.15. ^1H NMR spectrum (CD_2Cl_2 , 22°C) of the alkylidene region for reaction of 1.10 equivalents of DEDPM with $\text{Mo}(\text{NAr})(\text{trans-CHCHCHMe})(\text{O-}t\text{-Bu})_2(\text{quin})$.

Table 3.8. Rates of propagation versus rates of initiation for reactions of $\text{Mo}(\text{NAr})(\text{trans-CHCHCHMe})(\text{O-}t\text{-Bu})_2(\text{quin})$ with 1.06 to 2.53 equivalents of DEDPM at 22°C (for comparison, $k_p/k_i = 5.8$ for $\text{Mo}(\text{NAr})(\text{CHCMe}_3)(\text{O-}t\text{-Bu})_2(\text{quin})$).

Solvent	Concentration (mM)	Equiv of DEDPM	k_p/k_i
C_6D_6	12.9	2.53	0.53
C_6D_6	27.7	1.06	0.53
C_6D_6	14.2	2.05	0.54
C_6D_6	11.8	1.28	0.61
CD_2Cl_2	16.1	1.28	0.44
CD_2Cl_2	10.5	2.07	0.37
CD_2Cl_2	23.2	1.20	0.36
CD_2Cl_2	15.0	1.10	0.37
CD_2Cl_2	14.4	1.30	0.43

The alkylidene H_α chemical shifts of the insertion products produced in the reaction of 0.20 to 30 equivalents of DEDPM with $\text{Mo}(\text{NAr})(\text{trans-CHCHCHMe})[\text{OCMe}(\text{CF}_3)_2]_2(\text{quin})$

were directly compared to the alkylidene H_α chemical shifts of the insertion products produced in the reaction of DEDPM with $\text{Mo}(\text{NAr})(\text{trans-CHCHCHMe})(\text{O-}t\text{-Bu})_2(\text{quin})$ by replacing the $\text{OCMe}(\text{CF}_3)_2$ ligands of these insertion products with $\text{O-}t\text{-Bu}$ ligands. In these reactions, between 0.7 and 30 equivalents of DEDPM were added to $\text{Mo}(\text{NAr})(\text{trans-CHCHCHMe})[\text{OCMe}(\text{CF}_3)_2]_2(\text{quin})$ in CD_2Cl_2 at 22 °C. The reaction mixture was stirred for 30 minutes before 8 equivalents of excess $\text{LiO-}t\text{-Bu}$ were added. Figure 3.16 shows the ^1H NMR spectrum of the alkylidene H_α region for the products of the reaction of 1.10 equivalents of DEDPM with $\text{Mo}(\text{NAr})(\text{trans-CHCHCHMe})[\text{OCMe}(\text{CF}_3)_2]_2(\text{quin})$ at 22 °C in CD_2Cl_2 , followed by the addition of excess $\text{Li-O-}t\text{-Bu}$. The rates of initiation versus the rates of propagation (k_p/k_i) for $\text{Mo}(\text{NAr})(\text{trans-CHCHCHMe})[\text{OCMe}(\text{CF}_3)_2]_2(\text{quin})$ were calculated to be slightly greater than 1 and are listed in Table 3.9. Slower rates of initiation may be attributed to tighter binding of quinuclidine to the metal when the catalyst contains $\text{OCMe}(\text{CF}_3)_2$ ligands rather than the more electron-donating $\text{O-}t\text{-Bu}$ substituents.

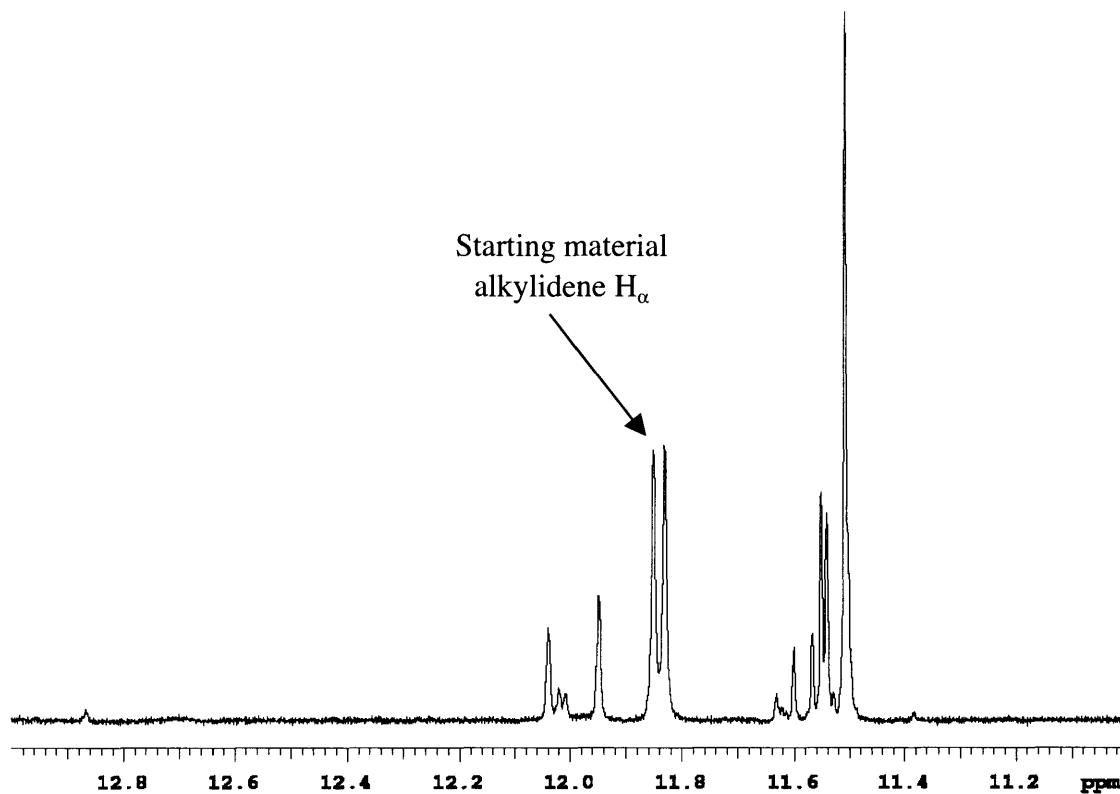


Figure 3.16. ^1H NMR spectrum (CD_2Cl_2 , 22 °C) of the alkylidene region for the reaction of 1.10 equivalents of DEDPM with $\text{Mo}(\text{NAr})(\text{trans-CHCHCHMe})[\text{OCMe}(\text{CF}_3)_2]_2(\text{quin})$, followed by the addition of excess $\text{LiO-}t\text{-Bu}$ to the reaction.

Table 3.9. Rates of propagation versus rates of initiation for reactions of $\text{Mo}(\text{NAr})(\text{trans-CHCHCHMe})[\text{OCMe}(\text{CF}_3)_2]_2(\text{quin})$ with 0.78 to 2.40 equivalents of DEDPM at 22 °C.

Solvent	Conc. (mM)	Equiv of DEDPM	k_p/k_i
C_6D_6	10.3	0.78	1.23
C_6D_6	8.3	1.08	1.31
C_6D_6	10.5	2.29	1.14
C_6D_6	10.5	1.14	1.23
C_6D_6	10.5	1.14	1.28
CD_2Cl_2	9.1	2.40	1.10
CD_2Cl_2	9.7	0.95	1.19
CD_2Cl_2	12.5	1.12	1.10
CD_2Cl_2	14.2	1.00	1.18
CD_2Cl_2	9.2	1.88	1.33
CD_2Cl_2	12.5	1.39	1.38
CD_2Cl_2	11.4	1.30	1.46

3.4.2.2 Identification of Alkylidene H_α Resonances (General)

In order to facilitate peak identification, charts have been generated containing data from initiation reactions of 0.2 to 30 equivalents of DEDPM with Mo(NAr)(*trans*-CHCHCHMe)(O-*t*-Bu)₂(quin) in C₆D₆ (Figures 3.17) and CD₂Cl₂ (Figure 3.18) at 22 °C. Results of the reactions of 0.2 to 30 equivalents of DEDPM with Mo(NAr)(*trans*-CHCHCHMe)[OCMe(CF₃)₂]₂(quin), followed by the addition of LiO-*t*-Bu are displayed in Figure 3.19. Type A charts show the chemical shift and integration percentage of each alkylidene H_α resonance, including that of the remaining initiator. The percentages are calculated based on the total integration value of all alkylidene H_α resonances. This type of chart shows the growth and/or decay of each alkylidene H_α resonance as increasing numbers of equivalents of DEDPM are added. Type B charts show the chemical shift and integration percentage of each alkylidene H_α resonance corresponding only to the products of initiation. The percentages are calculated based on the total integration value of all initiation product alkylidene H_α resonances, not including the initiator alkylidene H_α resonance. This second type of chart is useful for distinguishing first insertion products from second insertion products because the integration values are weighted according to the amount of unconsumed initiator. This adjustment compensates for the low percentages of all initiation products formed when very small amounts of DEDPM are reacted.

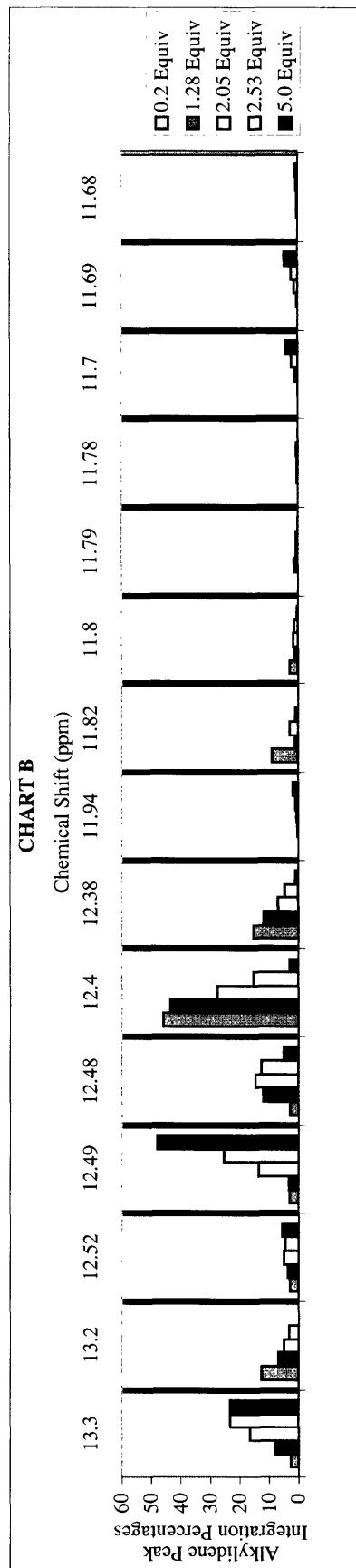
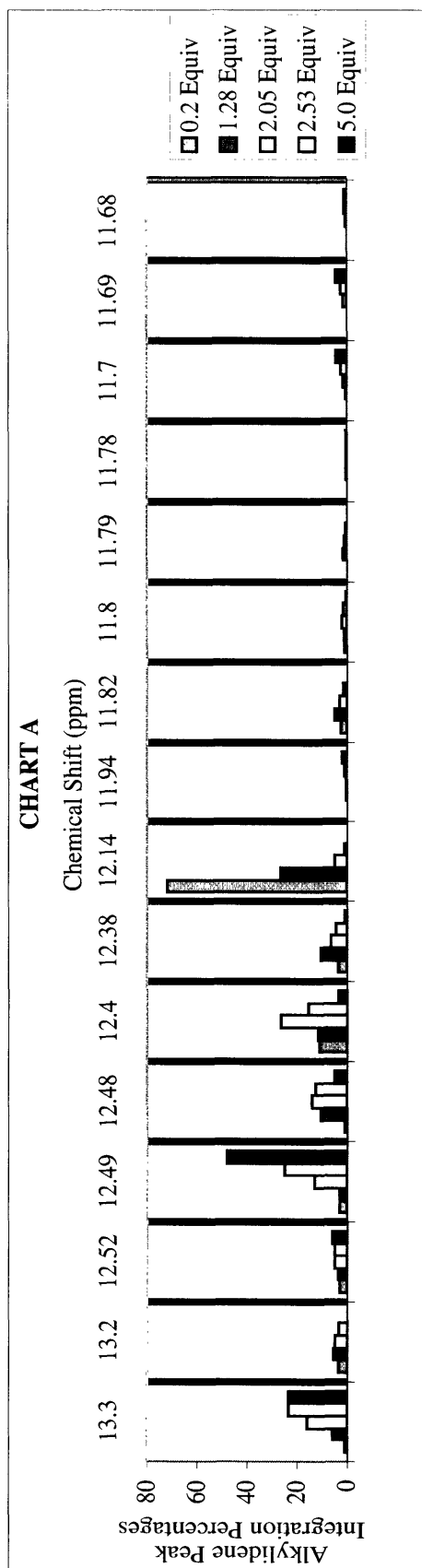


Figure 3.17. Chart A: the percentage of each alkyldiene H_{α} peak, including that of the remaining starting material (12.14 ppm), that is present after the reactions of 0.2 to 10.0 equivalents of DEDPM with $\text{Mo}(\text{NAr})(\text{trans-CHCHMe})(\text{O-}t\text{-Bu})_2(\text{quin})$ in C_6D_6 at 22 °C. Chart B: the percentage of each insertion product alkyldiene H_{α} peak compared to the total integration of all insertion product alkyldiene H_{α} peaks generated under the same conditions as in Chart A.

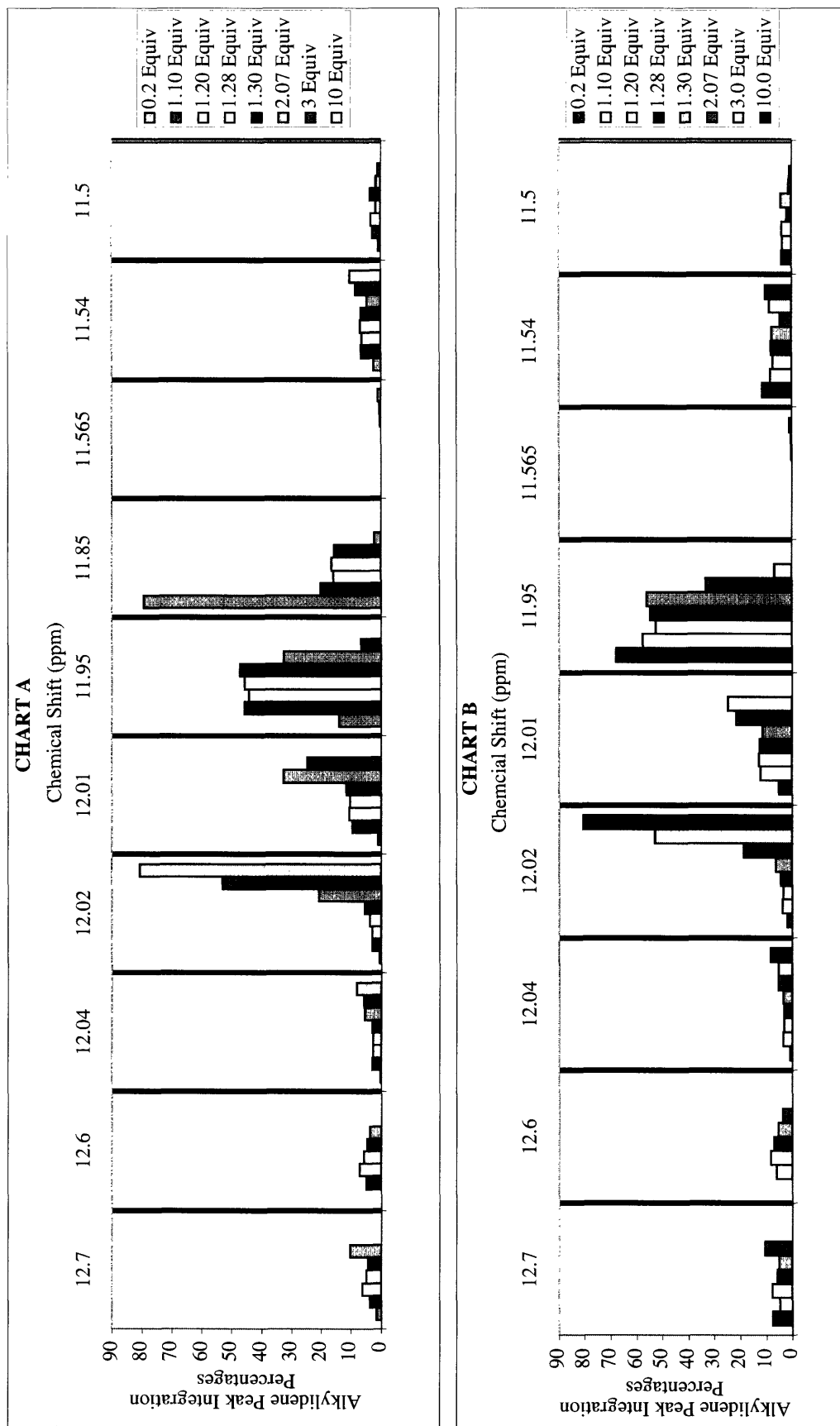


Figure 3.18. Chart A: the percentage of each alkylidene H_α peak, including that of the remaining starting material (11.85 ppm), that is present after the reactions of 0.2 to 10.0 equivalents of DEDPM with Mo(NAr)(*trans*-CHCHMe)(*O*-*t*-Bu)₂(quin) in CD₂Cl₂ at 22 °C. Chart B: the percentage of each insertion product alkylidene H_α peak compared to the total integration of all insertion product alkylidene H_α peaks generated under the same conditions as in Chart A.

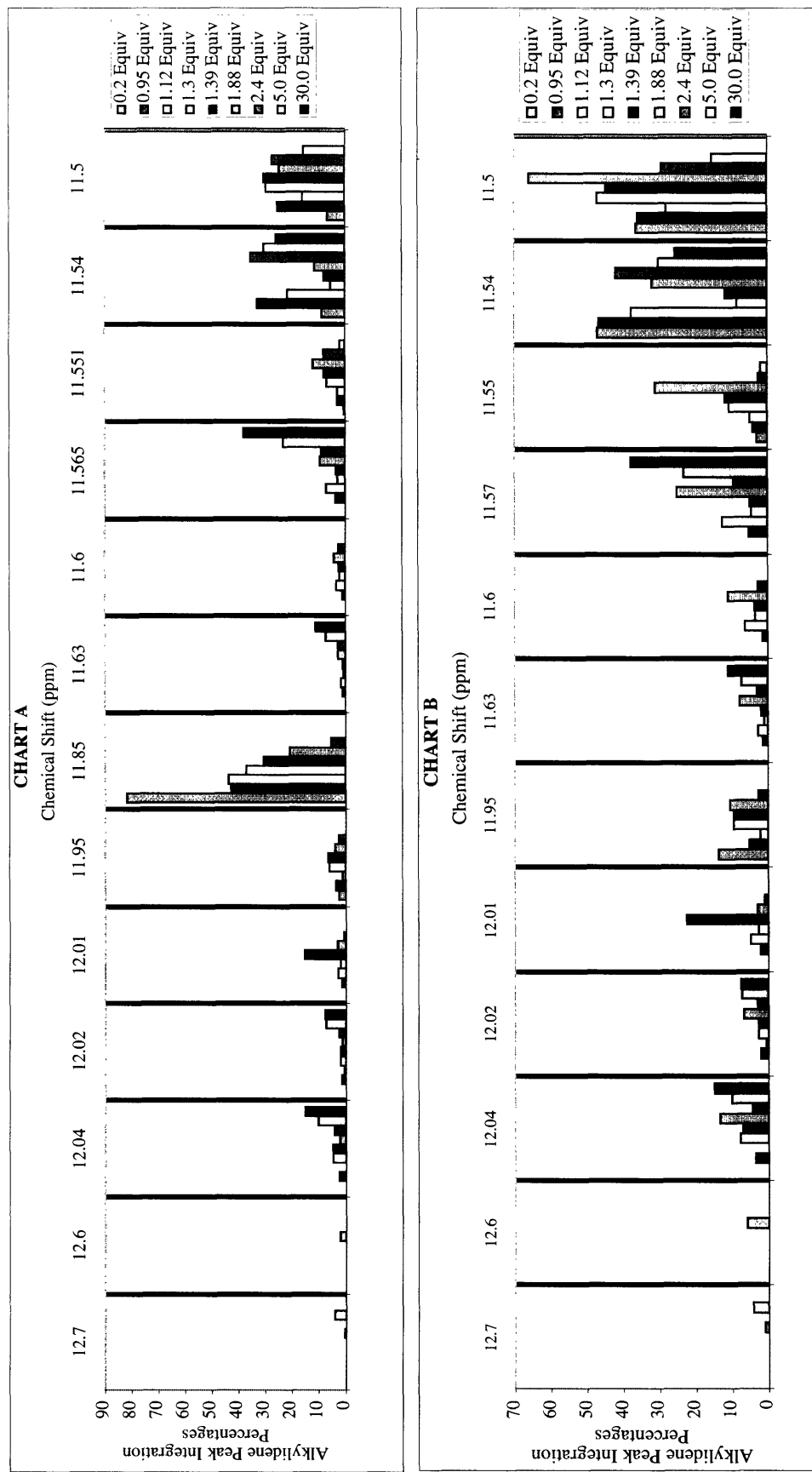


Figure 3.19. Chart A: the percentage of each alkylidene H_{α} peak, including that of the remaining starting material (11.85 ppm), that is present after the reactions of 0.2 to 10.0 equivalents of DEDPM with $\text{Mo}(\text{NAr})(\text{trans-CHCHMe})[\text{OCMe}(\text{CF}_3)_2(\text{quin})]$ in CD_2Cl_2 at 22 °C, followed by the addition of excess LiO-*t*-Bu. Chart B: the percentage of each insertion product alkylidene H_{α} peak compared to the total integration of all insertion product alkylidene H_{α} peaks generated under the same conditions as in Chart A.

The assignments of insertion product alkylidene H_α resonances in the 1H NMR spectra are based on several factors. When the rate of propagation is slower than the rate of initiation, the first insertion product alkylidene H_α resonances should predominate in the spectra of initiation reactions in which very small amounts of DEDPM have been added. Second insertion product alkylidene H_α resonances should grow at the expense of the starting material and first insertion products as increasing numbers of equivalents of DEDPM are added. The chemical shifts of the alkylidene H_α resonances corresponding to initiation products containing 3 or more rings in the alkylidene chain are not expected to be sensitive to variations more than two rings away from the metal. Therefore, the propagating species should be represented by single alkylidene H_α resonances that grow at the expense of the second insertion products and any remaining first insertion products or unconsumed initiator.

The products in which a five- or six-membered ring is situated adjacent to the molybdenum center can be distinguished using two pieces of evidence. The dominance (in terms of integration value) of alkylidene H_α resonances in the regions of 12.40 to 12.52 ppm in C_6D_6 spectra and 11.95 to 12.04 in CD_2Cl_2 spectra of initiation reactions involving $Mo(NAr)(trans-CHCHCHMe)(O-t-Bu)_2(quin)$, which has been shown to afford predominantly five-membered rings, supports the identification of peaks in this region as products in which a five-membered ring is situated adjacent to the molybdenum center in the alkylidene chain (Figures 3.17, 3.18). Greater integration percentages for the alkylidene H_α peaks in the region of 11.49 to 11.62 ppm in the CD_2Cl_2 spectra of initiation products produced by $Mo(NAr)(trans-CHCHCHMe)[OCMe(CF_3)_2]_2(quin)$ (which tends to produce a mixture of five- and six-membered rings) and converted to $Mo(NAr)(CHCR')(O-t-Bu)_2(quin)$ species (Figure 3.19) support the assignment of these peaks as the alkylidene H_α protons of products in which a six-membered ring in the alkylidene chain is adjacent to the metal. The second piece of evidence is the chemical shifts of the model initiators. The achiral, syn alkylidene H_α resonance of $Mo[1-methylidene-3-methylen-5,5-bis(carboxyethyl)cyclohex-1-ene](NAr)(O-t-Bu)_2$ (**9b**) appears at 11.59 ppm in CD_2Cl_2 , while that of $Mo(CH[5])(NAr)(O-t-Bu)_2$ appears at 11.87 ppm in CD_2Cl_2 .

and at 12.35 in C_6D_6 . The chemical shifts of the alkyldiene H_α resonances of these model complexes should be nearly identical to those of the five- and six-membered ring first insertion products.

3.4.2.3 Identification of Alkyldiene H_α Resonances Corresponding to Products in Which a Five-Membered Ring in the Alkyldiene Chain is Adjacent to the Metal Center

Two isomers of the five-membered ring first insertion product are possible because the double bond between between C_8 and C_e may have either a *cis* or *trans* configuration (Figure 3.20). Using the charts in Figures 3.17 and 3.18 as guides, it is clear that the first insertion product alkyldiene H_α protons are observed as two overlapping singlets at 11.95 ppm in the CD_2Cl_2 spectrum and as two separate singlets at 12.40 and 12.38 ppm in the C_6D_6 spectrum. These peaks grow into the spectrum when very small amounts of DEDPM are added and decrease in intensity as the second insertion products and the propagating species are formed. The larger peak at 12.40 ppm in the C_6D_6 spectrum most likely corresponds to the product in which the double bond between the five-membered ring and the *trans*-butene end group has a *trans* configuration.

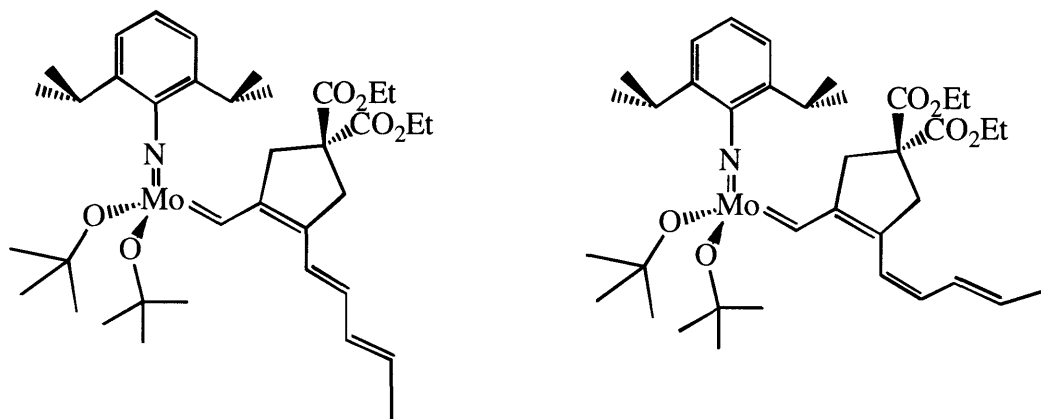


Figure 3.20. Two possible first insertion products formed during the cyclopolymerization of DEDPM by $Mo(NAr)(trans-CHCHCHMe)(O-t-Bu)_2(quin)$.

The chemical shifts of the first insertion product alkylidene vinyl protons between 5.0 and 6.5 ppm were examined by reacting 0.2 equivalents of DEDPM with Mo(NAr)(*trans*-CHCHCHMe)(O-*t*-Bu)₂(quin). In the C₆D₆ ¹H NMR spectrum, two vinyl doublets of doublets are observed for the primary first insertion product at 6.00 and 6.15 ppm, both of which show *trans* coupling with $J_{\text{CH}} = 14$ Hz. A doublet corresponding to the vinyl H₈ is observed at 6.56 ppm, which also shows *trans* coupling with $J_{\text{CH}} = 14$ Hz. The final vinyl proton is observed as a multiplet at 5.42 ppm. In CD₂Cl₂, the vinyl H₈ proton is observed as a doublet at 6.47 ppm with $J_{\text{CH}} = 15$ Hz, two vinyl doublets of doublets are observed at 6.22 and 5.95 ppm, and a vinyl multiplet is observed at 5.68 ppm (Figure 3.21). A small *cis* coupled doublet of doublets at 6.14 ppm with $J_{\text{CH}} = 11$ Hz may correspond to a first insertion product in which the double bond between the *trans*-butene group and the five-membered ring has a *cis* configuration.

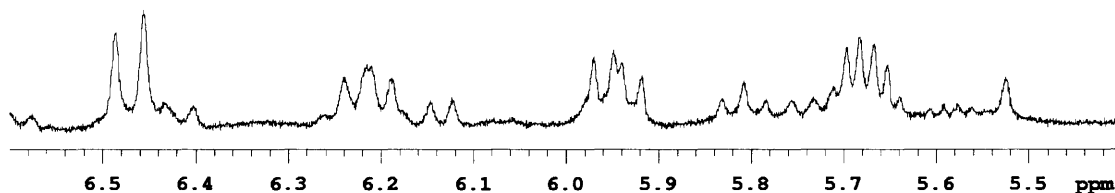


Figure 3.21. The partial (5.4 to 6.6 ppm) ¹H NMR spectrum of the reaction of 0.2 equivalents of DEDPM with Mo(NAr)(*trans*-CHCHCHMe)(O-*t*-Bu)₂(quin) at 22 °C in CD₂Cl₂.

Single alkylidene H_α peaks at 12.01 ppm in the CD₂Cl₂ spectrum and at 12.48 ppm in the C₆D₆ spectrum corresponding to second insertion products in which five-membered rings are adjacent to the metal (Mo-5-5 or Mo-5-6; Figure 3.22) grow in at the expense of the first insertion product alkylidene H_α peaks as greater amounts of DEDPM are added. When greater amounts of DEDPM are added, these peaks decrease in intensity as the propagating species are generated. Two propagating species alkylidene H_α peaks are observed in a ratio of about 10 to 1 at 12.02 and 12.04 ppm in CD₂Cl₂, respectively, and at 12.49 and 12.52 ppm in C₆D₆, respectively. The larger peaks represent the Mo-5-5-P (P = polymer chain) propagating species,

and the smaller peaks correspond to the Mo-5-6-P propagating species. When Mo(NAr)(*trans*-CHCHCHMe)[OCMe(CF₃)₂]₂(quin) is employed as the initiator and the OCMe(CF₃)₂ ligands replaced with O-*t*-Bu, the peaks at 12.02 ppm in CD₂Cl₂ and 12.49 ppm in C₆D₆ are smaller than the peaks at 12.04 in CD₂Cl₂ and 12.52 ppm in C₆D₆, supporting the identification of these alkylidene H_α peaks as the Mo-5-5-P and Mo-5-6-P propagating species, respectively.

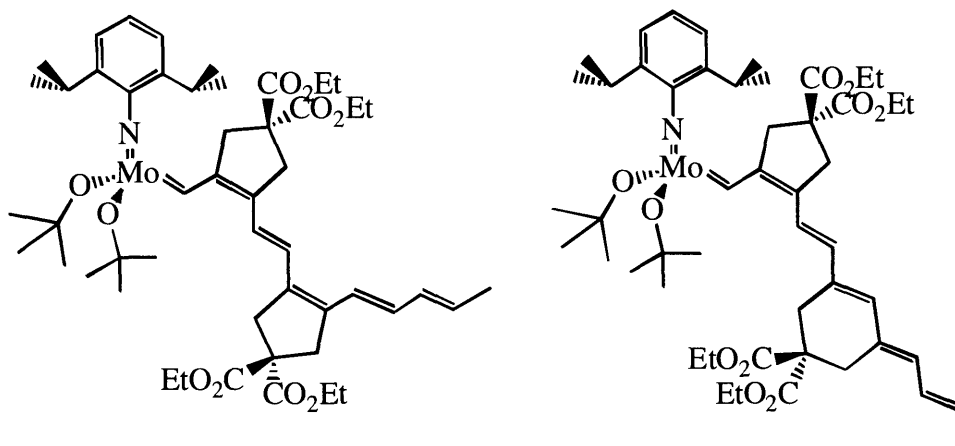


Figure 3.22. Two possible second insertion products (Mo-5-5 and Mo-5-6) in which a five-membered ring in the alkylidene chain is adjacent to the metal.

Broadened alkylidene H_α peaks corresponding to the quinuclidine-bound chiral, anti rotamers of insertion products in which a five-membered ring is adjacent to the metal in the alkylidene chain are observed at 12.6 and 12.7 ppm in CD₂Cl₂ and at 13.2 and 13.3 ppm in C₆D₆ in the spectra of initiation reactions of Mo(NAr)(*trans*-CHCHCHMe)(O-*t*-Bu)₂(quin). When Mo(NAr)(*trans*-CHCHCHMe)[OCMe(CF₃)₂]₂(quin) is employed as the initiator and the OCMe(CF₃)₂ ligands of the initiation products are replaced with O-*t*-Bu ligands, these resonances are much smaller. These downfield peaks are also less significant when enough equivalents of DEDPM have reacted such that only the propagating species alkylidene H_α peaks are observed. The greater steric bulk of a large alkylidene group may favor dissociation of quinuclidine. Peak broadness may be attributed to an exchange of bound and unbound quinuclidine. While the addition of excess quinuclidine does not affect the integral values of these broadened resonances, it does make them appear sharper.

Attempts to purify the molybdenum insertion products generated by the reaction of 1.4 equivalents of DEDPM with $\text{Mo}(\text{NAr})(\text{trans-CHCHCHMe})(\text{O-}t\text{-Bu})_2(\text{quin})$ were unsuccessful. The propagating species are less soluble than the first and second insertion products and may be separated by precipitation from pentane at $-30\text{ }^\circ\text{C}$. Unfortunately, the first and second insertion products could not be isolated by solubility differences or crystallization techniques.

3.4.2.4 Identification of Alkylidene H_α Resonances Corresponding to Products in Which a Six-Membered Ring in the Alkylidene Chain is Adjacent to the Metal Center

The identification of insertion products in which a six-membered ring in the alkylidene chain is adjacent to the metal center is more complicated than the identification of insertion products in which a five-membered ring in the alkylidene chain is adjacent to the metal center (Figure 3.19). As a result, many H_α alkylidene peaks observed in the ^1H NMR spectra of these reactions cannot be specifically identified. The reaction of 0.2 equivalents of DEDPM with $\text{Mo}(\text{NAr})(\text{trans-CHCHCHMe})[\text{OCMe}(\text{CF}_3)_2]_2(\text{quin})$, followed by the addition of excess $\text{LiO-}t\text{-Bu}$, produced insertion products with alkylidene H_α resonances at 11.95 (Mo-5), 11.54 (Mo-6), and 11.50 (Mo-6) ppm in the CD_2Cl_2 spectrum. The end-group vinyl protons of the primary Mo-6 first insertion product appear at 6.45 ppm (doublet of doublets; $J_{\text{CH}} = 13\text{ Hz}$), 5.70 ppm (doublet; $J_{\text{CH}} = 12\text{ Hz}$), and at 5.59 ppm (multiplet) (Figure 3.23). From these J_{CH} values, it is not clear whether the $\text{C}=\text{C}$ double bond between the *trans*-butene end group and the six-membered ring has a *cis* or *trans* configuration. The allylic CH proton is observed at 5.53 ppm.

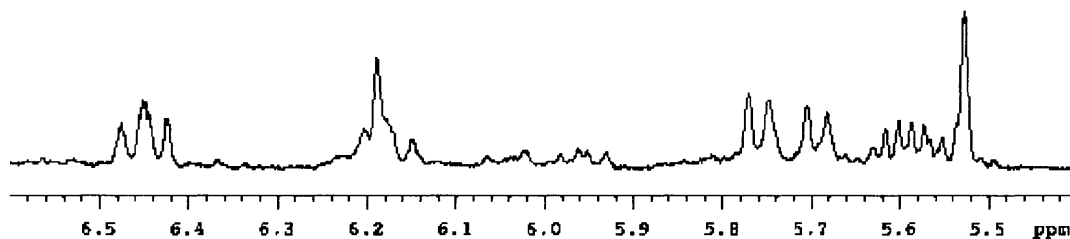


Figure 3.23. The partial (5.4 to 6.6 ppm) ^1H NMR spectrum of the reaction of 0.2 equivalents of DEDPM with $\text{Mo}(\text{NAr})(\text{trans-CHCHCHMe})[\text{OCMe}(\text{CF}_3)_2]_2(\text{quin})$ at 22 °C in CD_2Cl_2 , followed by the addition of excess $\text{LiO-}t\text{-Bu}$.

The Mo-6 first insertion product alkylidene H_α peaks at 11.50 ppm and 11.54 ppm overlap with peaks that grow in intensity as increasing amounts of DEDPM are added. The original Mo-6 first insertion product peaks at 11.50 ppm and 11.54 ppm are not observed in the spectra of reactions in which more than 1.3 equivalents of DEDPM were added. The new peak at 11.54 ppm corresponds to a propagating species that grows indefinitely with increasing equivalents of DEDPM. The new peak at 11.50 corresponds to a second insertion product (Figure 3.24) because it disappears when more than 5 equivalents of DEDPM have been added. Peaks at 11.55 ppm and 11.60 ppm also correspond to second insertion products that grow at the expense of the initiator and first insertion products and begin to decrease in intensity when more than 2 equivalents of DEDPM have been added (Figure 3.24).

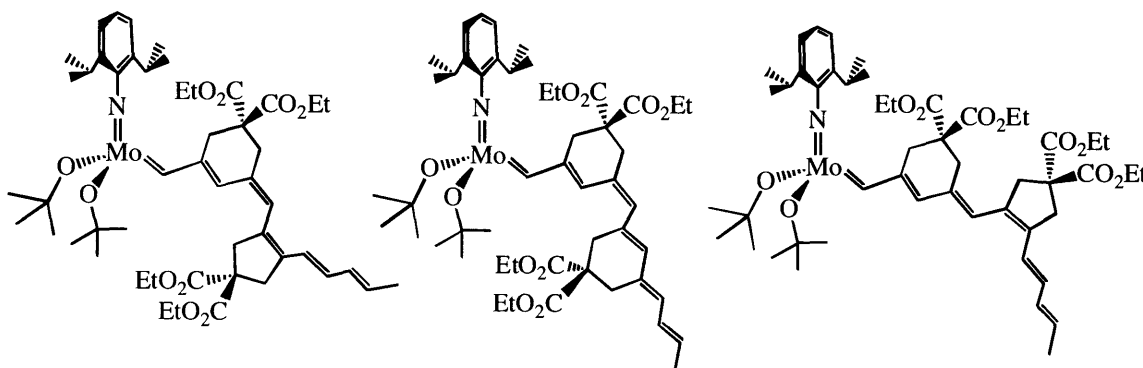


Figure 3.24. Three possible insertion products (Mo-6-5, Mo-6-6, and Mo-6-5) in which a six-membered ring in the alkylidene chain is adjacent to the metal.

When more equivalents of DEDPM are reacted with Mo(NAr)(*trans*-CHCHCHMe)[OCMe(CF₃)₂]₂(quin), followed by the addition of excess LiO-*t*-Bu, alkyldiene H_α resonances for the propagating species in which five-membered rings in the alkyldiene chains are adjacent to the metal grow in at 12.02 ppm (Mo-5-5-P) and 12.04 ppm (Mo-5-6-P) in a ratio of 1:2. Alkyldiene H_α resonances for complexes in which six-membered rings are adjacent to the metal grow in at 11.54 (Mo-6-5-P), 11.57 (Mo-6-6-P), and 11.63 ppm. Identification of the Mo-6-5-P and Mo-6-6-P propagating species is based on the greater integration value of the Mo-6-5-P peak at 11.54 ppm versus the Mo-6-6-P peak at 11.57 ppm when Mo(NAr)(*trans*-CHCHCHMe)(O-*t*-Bu)₂(quin) is employed as the initiator than when Mo(NAr)(*trans*-CHCHCHMe)[OCMe(CF₃)₂]₂(quin) is employed as the initiator. The peak at 11.63 ppm may correspond to a different isomer (i.e. *syn* versus *anti* or *cis* versus *trans*) of the Mo-6-6-P propagating species.

Further identification of alkyldiene H_α peaks for insertion products in which a six-membered ring is adjacent to the metal is not possible. Although adjacent five-membered rings are likely to reside on opposite sides of the polyene backbone to relieve steric congestion, it is not clear whether six-membered rings are connected by a double bond with a *cis* or *trans* orientation. The possibility of different isomers existing for the first and second insertion products, as well as the propagating species, leads to complicated NMR spectra. NMR spectra for the “translated” insertion products of the reaction of DEDPM with Mo(NAr)(*trans*-CHCHCHMe)[OCMe(CF₃)₂]₂(quin) are even more complicated in C₆D₆, and for this reason the H_α alkyldiene resonance integration versus chemical shift charts are not discussed.

When Mo(NAr)(*trans*-CHCHCHMe)(O-*t*-Bu)₂(quin) was employed as the initiator in reactions with less than 3 equivalents of DEDPM at -30 and 0 °C, between 8 and 12 percent of the initiation products contained a six-membered adjacent to the metal in the alkyldiene chain. Although warmer temperatures lead to greater percentages of six-membered rings,²⁰⁹ the percentages of six-membered rings adjacent to the metal in the alkyldiene chain did not differ significantly when initiations were performed at -30 °C. Since longer polymer chains produced

under these conditions contained 95% five-membered rings, the formation of six-membered rings may be slightly more favorable in low concentrations of DEDPM. Interestingly, when $\text{Mo}(\text{NAr})(\text{trans-CHCHCHMe})[\text{OCMe}(\text{CF}_3)_2]_2(\text{quin})$ was employed as the initiator under the same conditions, between 75 and 85% of the initiation products contained a six-membered ring adjacent to the metal in the alkylidene chain. Polyenes produced by this catalyst contained approximately 50:50 mixtures of five- and six-membered rings.^{213,214}

3.4.3 The Diadamantoxide Butenylidene Initiator

$\text{Mo}(\text{NAr})(\text{trans-CHCHCHMe})(\text{OAd})_2(\text{quin})$ behaves similarly to $\text{Mo}(\text{NAr})(\text{trans-CHCHCHMe})(\text{O-}t\text{-Bu})_2(\text{quin})$ as an initiator. An analogous pattern of insertion product alkylidene H_α resonances is observed in the CD_2Cl_2 ^1H NMR spectrum. The first and second insertion product alkylidene H_α resonances appear at 11.93 and 11.99 ppm, respectively, and the propagating species Mo-5-5-P and Mo-5-6-P alkylidene H_α resonances appear at 12.00 and 12.01 ppm, respectively. Based on the integration of the alkylidene H_α resonances, only 80% of the insertion product alkylidene chains contained a five-membered ring adjacent to the metal center (compared to approximately 90% when $\text{OR} = \text{O-}t\text{-Bu}$). The Mo-5-6-P alkylidene H_α resonance was also larger relative to the Mo-5-5-P alkylidene H_α resonance by approximately 50% when $\text{OR} = \text{OAd}$ than when $\text{OR} = \text{O-}t\text{-Bu}$. The average rate of propagation relative to initiation (k_p/k_i) was 0.23 in CD_2Cl_2 at 22 °C, which is slightly lower than the average k_p/k_i of 0.39 for $\text{Mo}(\text{NAr})(\text{trans-CHCHCHMe})(\text{O-}t\text{-Bu})_2(\text{quin})$ (Table 3.10).

Table 3.10. Rates of propagation versus rates of initiation for reactions of $\text{Mo}(\text{NAr})(\text{trans-CHCHCHMe})(\text{OAd})_2(\text{quin})$ with DEDPM at 22 °C.

Solvent	Concentration (mM)	Equiv of DEDPM	k_p/k_i
CD_2Cl_2	13.4	1.0	0.24
CD_2Cl_2	15.9	1.0	0.23
$\text{CD}_2\text{Cl}_2 + 20$ quin	8.7	1.0	0.23

3.4.4 The Di-*tert*-butoxide Five-Membered Ring Alkylidene Initiator

Mo(NAr)(CH[5])(O-*t*-Bu)₂(quin) behaves similarly to Mo(NAr)(*trans*-CHCHCHMe)(O-*t*-Bu)₂(quin) as an initiator. Since an alternating *cis/trans* arrangement of five-membered rings along the polyene backbone is preferred,^{172,209} the cyclopolymerization of 1 equivalent of DEDPM by Mo(NAr)(CH[5])(O-*t*-Bu)₂ to form a five-membered ring only produces one isomer of the first insertion product. The average rate of propagation relative to initiation (k_p/k_i) was calculated to be 0.36 (Table 3.11) in CD₂Cl₂ at 22 °C. A k_p/k_i value less than 1 may be attributed to the absence of a second ring in the alkylidene chain. Unfortunately, the presence of a five-membered ring adjacent to the metal in the alkylidene ligand did not enhance α -selectivity during initiation reactions. When Mo(NAr)(CH[5])(O-*t*-Bu)₂(quin) was employed as the initiator in reactions with 0.2 to 1 equivalents of DEDPM in CD₂Cl₂ at 22 or -30 °C, approximately 10% of the initiation products contained a six-membered ring adjacent to the metal in the alkylidene chain.

Table 3.11. Rates of propagation versus rates of initiation for reactions of Mo(NAr)(CH[5])(O-*t*-Bu)₂(quin) with 1.05 to 1.37 equivalents of DEDPM in CD₂Cl₂ at 22 °C.

Concentration (mM)	Equiv DEDPM	k_p/k_i
10.8	1.05	0.35
12.9	1.15	0.34
15.8	1.25	0.38
17.2	1.37	0.35

3.5 Synthesis and Isolation of Oligomers

3.5.1 Synthesis of Oligomers by Mo(NAr)(*trans*-CHCHCHMe)(O-*t*-Bu)₂(quin)

Having a faster rate of initiation relative to the rate of propagation, Mo(NAr)(*trans*-CHCHCHMe)(O-*t*-Bu)₂(quin) should be capable of producing narrow distributions of short oligomers. Large amounts of catalyst are required in order to synthesize small oligomers since so few equivalents of monomer are used. Mo(NAr)(*trans*-CHCHCHMe)(O-*t*-Bu)₂(quin) can be easily synthesized and was therefore used in initial oligomer purification studies. 2.8

Equivalents of DEDPM were reacted with 0.95 g of Mo(NAr)(*trans*-CHCHCHMe)(O-*t*-Bu)₂(quin). The oligomers were capped with ferrocenecarboxaldehyde in order to facilitate crystallization. Unfortunately, oligomers containing six-membered rings and dimeric and trimeric five-membered ring oligomers have limited solubility in pentane, which is used to remove ferrocenecarboxaldehyde and molybdenum oxo byproducts. Significant quantities of pentane are required to remove ferrocenecarboxaldehyde compared to the volume required to remove molybdenum oxo byproducts. Consequently, more five-membered ring dimers and trimers are lost during workup.

Solubility differences were employed to separate the pentane insoluble oligomers into two portions. Decomposed or erroneous poly-DEDPM chains of unknown identity and chains containing 3 and 4 five-membered rings (0.5 g total weight) were extracted into ether. The remaining insoluble material was comprised of a mixture of chains containing between 4 and 7 five-membered rings. Chain length was estimated by comparing the integration values of the ester CH₂ resonances between 4.2 and 4.3 ppm and the five-membered ring CH₂ resonances between 3.3 and 3.5 ppm with the vinyl CH (the one furthest from the metal) resonance(s) at 5.82 ppm.

Column chromatography (SiO₂, 33% THF/66% pentane) was used to separate oligomer mixtures in the ether insoluble portion containing approximately 5 rings (0.1 g) from those containing approximately 7 rings (0.040 g). In the CDCl₃ ¹H NMR spectrum of the mixture containing approximately 5 rings, the two vinyl protons adjacent to ferrocene are observed as sharp doublets at 6.36 and 6.82 ppm. Resonances at 5.82, 6.21, and 6.42 ppm are also observed for the butadiene end group. Several overlapping CH sextets corresponding to different chain isomers are observed around 5.82 ppm. All other vinyl CH resonances overlap between 6.5 and 6.7 ppm. The allylic CH₃ resonance at 1.82 ppm is also broadened in the ¹H NMR spectra of both mixtures.

Peak broadening and overlap may result from either the presence of oligomers with different chain lengths, or different isomers of the same chain length. Longer chains of the same

length are characterized by complicated NMR spectra if an alternating *cis/trans* configuration of double bonds is not observed along the polyene backbone. Unfortunately, all attempts to obtain crystalline material were unsuccessful.

A second reaction of 2.6 equivalents of DEDPM with 1.034 g of Mo(NAr)(*trans*-CHCHCHMe)(O-*t*-Bu)₂(quin) was performed. The reaction was quenched with 10 equivalents of benzaldehyde, which is volatile and can therefore be removed easily without the loss of short oligomers. However, the product must still be washed with about 400 mL of pentane to remove the molybdenum oxo byproducts. Another 600 mL of pentane was then added to a saturated 10 mL CH₂Cl₂ solution of the oligomer mixture, crashing out a red powder (0.7 g) that was collected via filtration. The filtrate was concentrated to 200 mL, generating a second batch of red powder (0.25 g) that was also collected via filtration. The final filtrate contained a mixture of the five-membered ring dimer, oligomers containing at least one six-membered ring, and unidentifiable material.

Column chromatography (SiO₂, 33% hexane/67% ether) was used to separate the second batch of red powder into 5 portions of oligomers consisting solely of five-membered rings. Although the first portion contained a mixture of material, the second portion (0.02 g) contained the five-membered ring dimer (Figure 3.25), which was characterized by ¹H and ¹³C NMR (Figure 3.26). Based on ¹J_{CH} coupling constants of 15 Hz, the double bonds between the phenyl and *trans*-butene groups and the five-membered rings have *trans* configurations. Four ring CH₂ resonances representing 2 protons each are observed at 3.31, 3.38, 3.39, and 3.42 ppm in the CDCl₃ ¹H NMR spectrum. Two quaternary carbons of equal intensity appear at 57.30 and 57.36 ppm in the ¹³C NMR spectrum, along with two carbonyl carbons at 172.07 and 172.11 ppm.

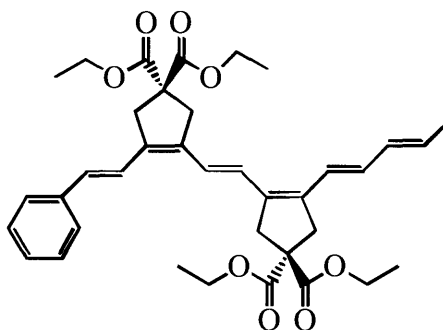


Figure 3.25. Dimeric product containing two five-membered rings formed by the reaction of $\text{Mo}(\text{NAr})(\text{trans-CHCHCHMe})(\text{O-}t\text{-Bu})_2(\text{quin})$ with DEDPM and isolated via column chromatography.

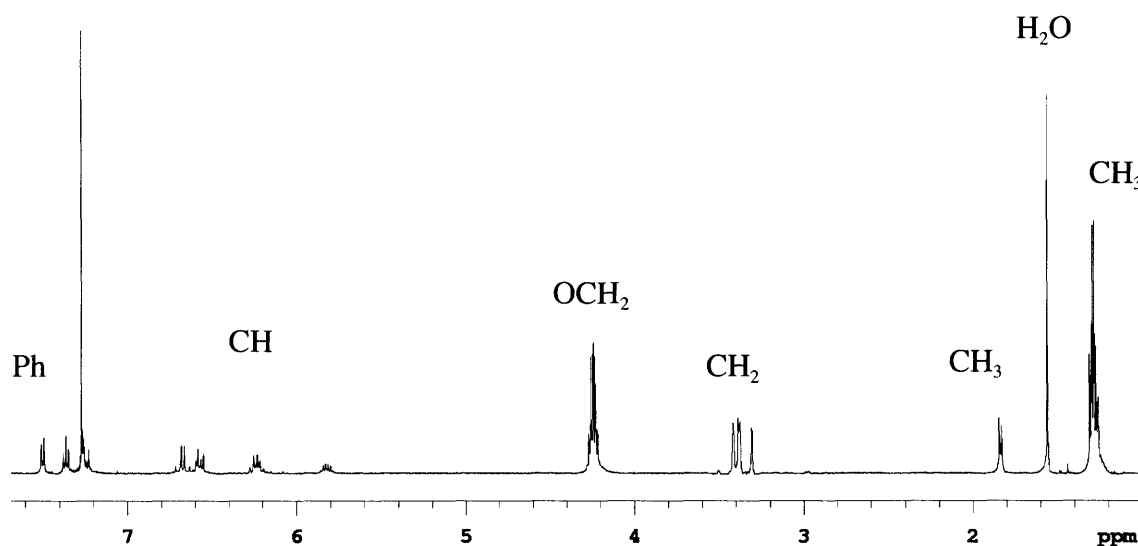


Figure 3.26. CDCl_3 ^1H NMR of the dimeric product containing two five-membered rings formed by the reaction of $\text{Mo}(\text{NAr})(\text{trans-CHCHCHMe})(\text{O-}t\text{-Bu})_2(\text{quin})$ with DEDPM.

The third portion was shown by ^1H NMR and HPLC separation to consist of two primary trimeric five-membered ring isomers (Figure 3.27). Although four different isomers are possible (Figure 3.28), the double bond between the phenyl group and the five-membered ring component most likely has a *trans* configuration. Several other minor isomers were also evident. The fourth portion contained oligomers with 4 to 6 rings, and the fifth portion contained unidentifiable material. Several different isomers for longer oligomers are also observed in the HPLC spectrum.

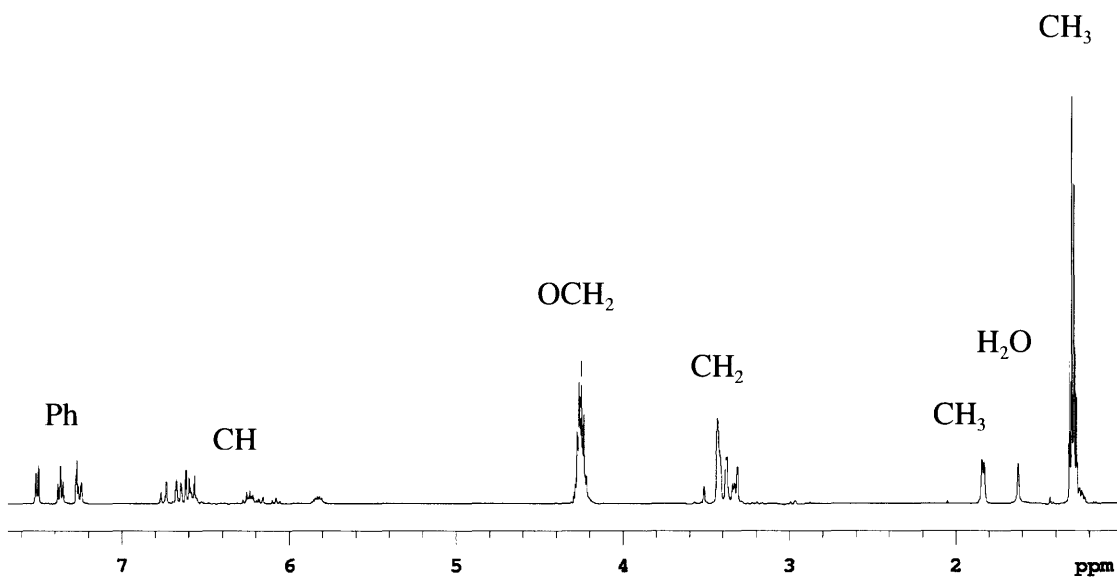


Figure 3.27. CDCl_3 ^1H NMR of the trimeric products containing three five-membered rings formed by the reaction of $\text{Mo}(\text{NAr})(\text{trans-CHCHCHMe})(\text{O-}t\text{-Bu})_2(\text{quin})$ with DEDPM.

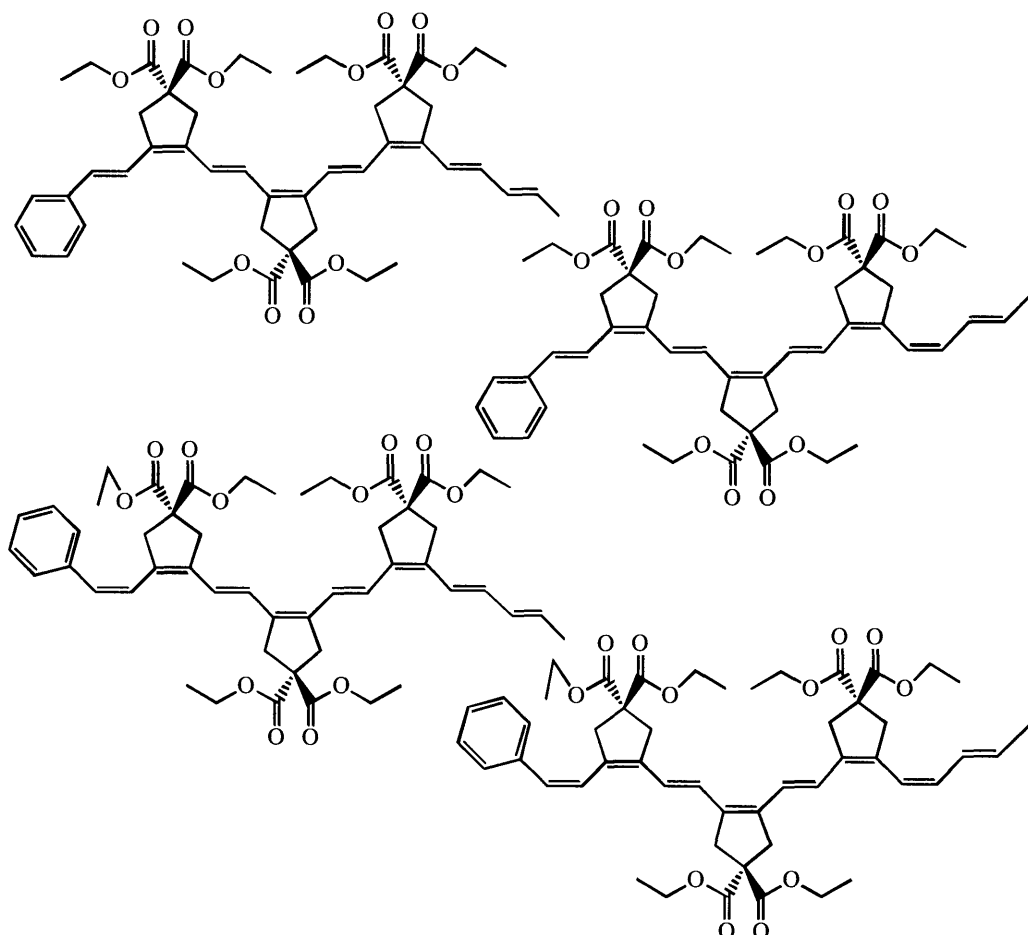


Figure 3.28. Different possible five-membered ring trimeric isomers formed by reacting DEDPM with $\text{Mo}(\text{NAr})(\text{trans-CHCHCHMe})(\text{O-}t\text{-Bu})_2(\text{quin})$ and quenching with benzaldehyde.

3.5.2 Synthesis of Oligomers by Mo(NAr)(CH[5])(O-*t*-Bu)₂(quin)

Symmetric oligomers were synthesized by reacting 1 equivalent (15.6 mg) of DEDPM with 65 mg of Mo(NAr)(CH[5])(O-*t*-Bu)₂(quin) in CD₂Cl₂ at -30 °C and quenching the reaction with the five-membered ring aldehyde (**8b**). The solvent was removed, and the mixture of molybdenum oxo byproducts and oligomeric products was washed with pentane. A silica gel column with a 1:2 Et₂O/pentane solvent mixture as the eluent was used to separate the pentane soluble components. This yellow-colored mixture contained the five-membered ring dimer and trimer (Figure 3.29), as well as molybdenum oxo byproducts and oligomers containing at least one six-membered ring. Very little of the dimer, which forms when Mo(NAr)(CH[5])(O-*t*-Bu)₂(quin) reacts directly with the five-membered ring aldehyde (**8b**), was recovered. Approximately 12 mg (19% yield by weight) of the yellow trimer containing three five-membered rings was recovered and analyzed by ¹H NMR (Figure 3.30). Three ring CH₂ singlet resonances representing four protons each are observed at 3.28, 3.31, and 3.36 ppm in the CD₂Cl₂ ¹H NMR spectrum.

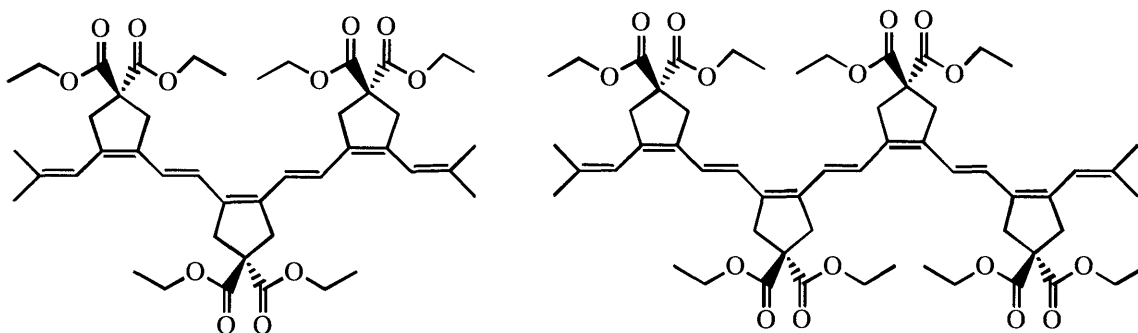


Figure 3.29. Symmetric trimeric and dimeric products produced by the reaction of DEDPM with Mo(NAr)(CH[5])(O-*t*-Bu)₂(quin) and isolated by column chromatography.

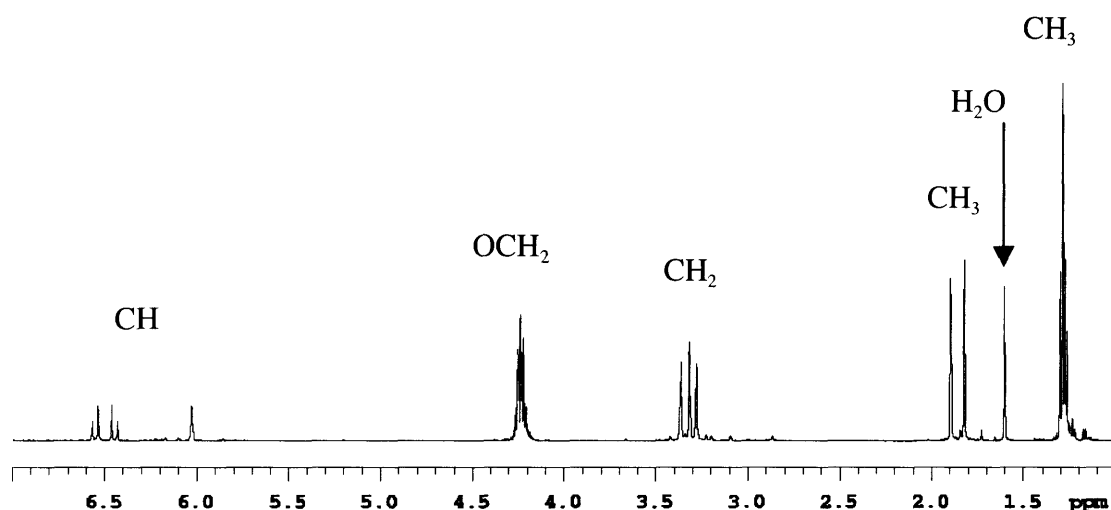


Figure 3.30. CDCl_3 ^1H NMR of the symmetric trimeric product containing three five-membered rings (See Figure 3.29) formed by the reaction of $\text{Mo}(\text{NAr})(\text{CH}[5])(\text{O}-t\text{-Bu})_2(\text{quin})$ with DEDPM.

Approximately 4 mg (6% yield by weight) of high molecular weight red-colored oligomers was removed from the pentane insoluble portion by extracting the shorter oligomers with ether. The ether soluble orange oligomers were separated by silica gel column chromatography using a 3:2 Et_2O /pentane solvent mixture. Clean separation of the five-, six-, and seven-mers (9 mg, 14% total yield by weight) could not be achieved. However, 36 mg of the tetramer (Figure 3.29) was isolated cleanly in 56% yield by weight. Four singlet resonances representing 4 ring CH_2 protons each are observed at 3.29, 3.35, 3.37, and 3.39 ppm in the CD_2Cl_2 ^1H NMR spectrum (Figure 3.31). Four ring CH_2 carbons representing two carbons each are also observed in the ^{13}C NMR CDCl_3 spectrum at 40.19, 41.50, 41.61, and 44.80 ppm, demonstrating the symmetry of the oligomer.

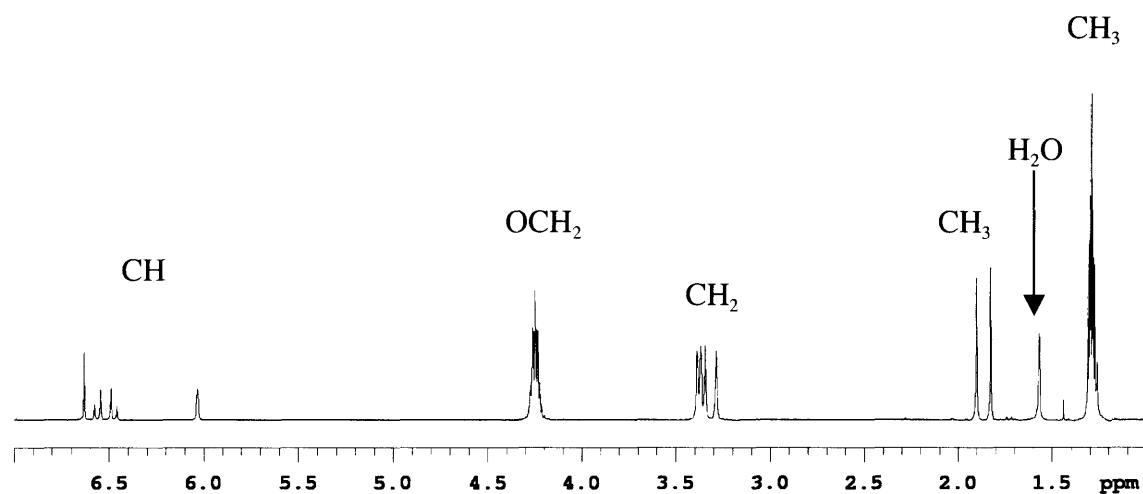


Figure 3.31. CDCl_3 ^1H NMR of the symmetric tetramer containing four five-membered rings (See Figure 3.29) formed by the reaction of $\text{Mo}(\text{NAr})(\text{CH}[5])(\text{O}-t\text{-Bu})_2(\text{quin})$ with DEDPM.

The symmetric oligomers were analyzed by HPLC. The symmetric five-membered ring trimer and tetramer gave rise to single peaks, confirming that the purified compounds consisted of a single isomer. Mixtures of oligomers containing 2 to 10 five-membered rings with 7 to 21 double bonds were also analyzed by HPLC and shown to consist primarily of single isomers (Figure 3.32). The $\text{E}(0-0)$ and $\text{E}(0-1)$ (λ_{max}) values for each chain length are listed in Table 3.12. The absorbance spectra are shown in Figure 3.33. Very small secondary peaks corresponding to oligomers containing at least one six-membered ring were also observed. Unfortunately, an increasing number of secondary peaks were observed in the HPLC spectrum for oligomers containing more than 10 monomers.

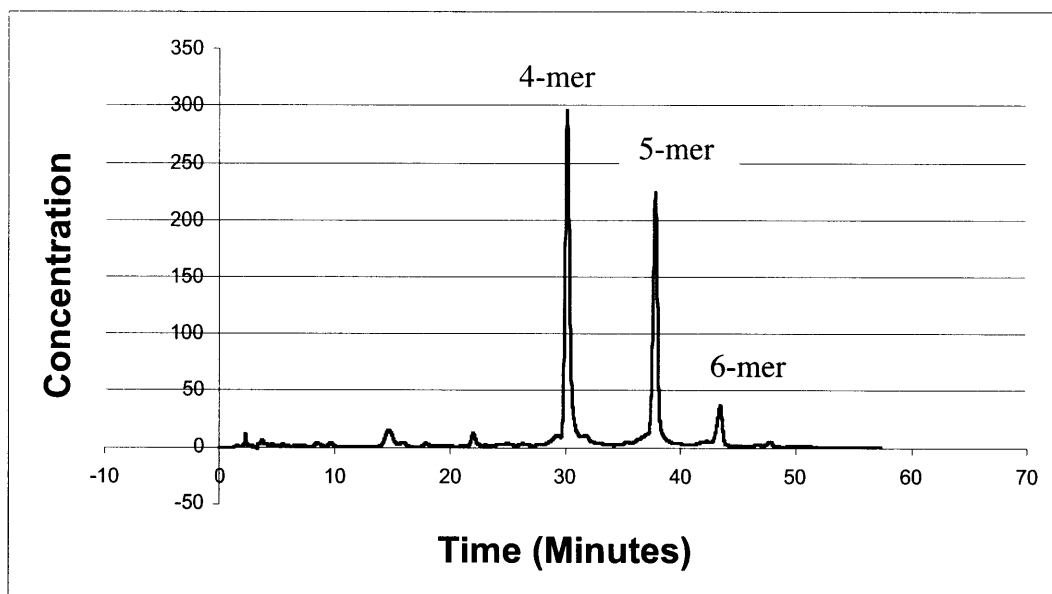


Figure 3.32. HPLC separation of oligomers comprised of 4 to 6 five-membered rings.

Table 3.12. $E(0-1)$ (λ_{\max}) and $E(0-0)$ values for oligomers comprised of 2 to 10 five-membered rings.

Number of Five-Membered Rings	Number of Double Bonds	$E(0-1)$ (λ_{\max})	$E(0-0)$
2	5	338	352
3	7	384	400
4	9	426	444
5	11	452	478
6	13	472	502
7	15	486	518
8	17	500	534
9	19	510	548
10	21	518	554

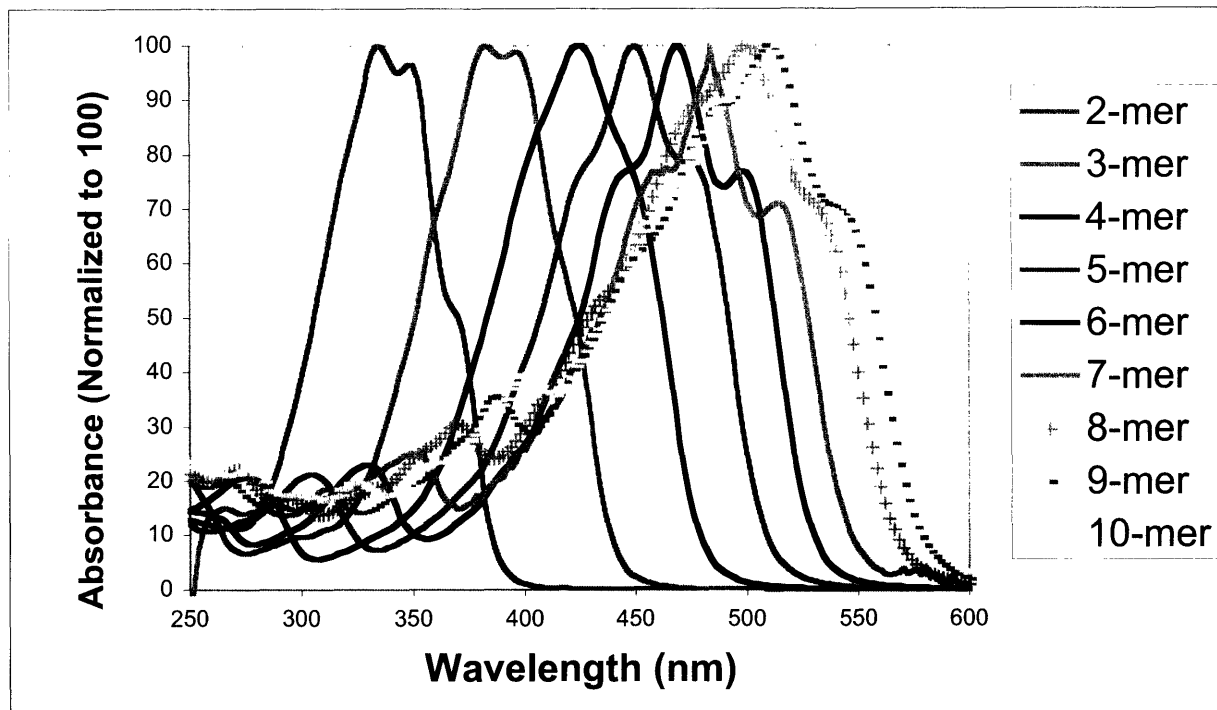


Figure 3.33. 300 K absorption spectra of oligomers comprised of 2 to 10 five-membered rings.

3.6 DEDPM Polymerization Employing Various Schrock-Group Catalysts

The results for the polymerization of DEDPM by several recently developed Schrock-group molybdenum catalysts are listed in Table 3.13. These reactions produced polymer containing 43 to 90% five-membered rings. Greater solubility in THF appeared to be correlated with less regularity in polymer structure; polyenes containing lower percentages of five-membered rings dissolved readily. While the polymer produced by $\text{Mo}(\text{NCPH}_3)(\text{CHCMe}_3)(\text{OAd})(\text{Np})$ was comprised of 90% five-membered rings, it formed a deep red solution in THF, indicating a lower level of conjugation in the backbone.

Table 3.13. Polymerization of 30 equivalents of DEDPM by recently developed Schrock-group catalysts. ^aCatalysts synthesized by Amritanshu Sinha.
^bCatalysts prepared by Tatiana Pilyugina.

Catalyst	Conc (mM)	Conditions	% Five-Membered Rings	Description of GPC Trace in THF
^a Mo(NAr)(CHCMe ₃)(OAd)(Np)	8.0	22 °C, DME	78	
^a Mo(NAr)(CHCMe ₃)(O- <i>t</i> -Bu)(Np)	12.2	-30 °C, DME	78	
^a Mo(NAr)(CHCMe ₃)(Np) ₂	10.4	-30 °C, DME	68	Multimodal with extremely high molecular weight
^a Mo(NAr)(CHCMe ₃)(Np) ₂ + 1.1 quinuclidine	6.9	-30 °C, DME	69	Multimodal with extremely high molecular weight
^b Mo(NCPh ₃)(CHCMe ₃)(OAr)(Np)	6.8	-30 °C, DME	90	
^b Mo(NCPh ₃)(CHCMe ₃)(OAr)(Np) + 1.1 quinuclidine	2.7	22 °C, CH ₂ Cl ₂	43	Multimodal with extremely high molecular weight
^b Mo(NCPhCyhex)(CHCMe ₃)(OAr)(Np)	2.1	22 °C, DME	90	

The polyenes produced by these catalysts were characterized by multimodal GPC traces (measured in THF versus a polystyrene standard). Two primary peaks with molecular weights of about 10² and 10³ times the expected molecular weights were observed. The addition of 1 equivalent of quinuclidine prior to the addition of DEDPM decreased the concentration of polymer having a molecular weight 10³ times the value calculated for a perfectly living system. Living behavior and the amount of five-membered rings did not change significantly when CH₂Cl₂ was employed as a solvent rather than DME.

Extremely high molecular weight measurements result because only a small amount of catalyst participates in the polymerization. The catalysts listed in Table 3.13 do not decompose readily. The high molecular weights result from a significantly higher rate of propagation

relative to initiation. The initiation problem is apparent in an NMR scale room temperature reaction of 9 equivalents of DEDPM with the quinuclidine adduct of $\text{Mo}(\text{NAr})(\text{CHCMe}_3)(\text{Np})_2$ (7.0 mM in CD_2Cl_2). Although all of the DEDPM was cyclopolymerized, less than 10% of the propagating species was consumed, according to integration values of the alkylidene H_α resonances.

None of the catalysts listed in Table 3.13 showed potential for success as a living catalyst for the cyclopolymerization of 1,6-heptadiynes to form all five- or six-membered rings. However, many other possibilities have yet to be explored.

3.7 Conclusions

The $\text{Mo}(\text{NAr})(\text{trans-CHCHCHMe})(\text{O-}t\text{-Bu})_2(\text{quin})$ and $\text{Mo}(\text{NAr})(\text{CH[5]})(\text{O-}t\text{-Bu})_2(\text{quin})$ catalysts both appear to be better initiators than the $\text{Mo}(\text{NAr})(\text{CHCRMe}_2)(\text{O-}t\text{-Bu})_2(\text{quin})$ ($\text{R} = \text{Me, Ph}$) catalysts. Poly(DEDPM) produced by these catalysts was characterized by polydispersities below 1.1 and $M_n(\text{found})$ values very close to the M_n values calculated for a perfectly living system. The process of initiation was studied, and the first and second insertion products and the propagating species were identified in solution. $\text{Mo}(\text{NAr})(\text{CH[5]})(\text{O-}t\text{-Bu})_2(\text{quin})$ enabled the synthesis and isolation of very short, symmetric oligomers. In general, these catalysts are excellent tools for the custom-designed synthesis of conjugated oligomers and polymers.

3.8 Experimental Section

General Details. All reactions were conducted under an atmosphere of dinitrogen in a Vacuum Atmospheres drybox or using standard Schlenk techniques. Non-deuterated solvents were sparged with nitrogen for 45 minutes, followed by passage through a 1 gallon column of activated alumina as described in the literature.⁵⁷ Deuterated solvents were stirred over CaH_2 for 48 hours, vacuum-transferred and stored over 4 Å molecular sieves. Commercial reagents were used without further purification. Diethyl dipropargylmalonate²³⁵ was synthesized according to a

reported procedure. A DEDPM ^{13}C labeled quaternary carbon was introduced using diethyl malonate with a ^{13}C labeled central carbon. $\text{Mo}(\text{NAr})(\text{CHCMe}_2\text{Ph})[\text{OCMe}(\text{CF}_3)_2]_2$, $\text{Mo}(\text{NAr})(\text{CHCMe}_3)[\text{OCMe}(\text{CF}_3)_2]_2$, $\text{Mo}(\text{NAr})(\text{CHCMe}_2\text{Ph})(\text{O}-t\text{-Bu})_2$, $\text{Mo}(\text{NAr})(\text{CHCMe}_3)(\text{O}-t\text{-Bu})_2$, and $\text{Mo}(\text{NAr})(\text{CHFc})(\text{O}-t\text{-Bu})_2$ (Ar = 2,6-diisopropylphenyl) were synthesized according to reported procedures.^{224,225} NMR data were recorded using a Varian Inova-500 spectrometer. Chemical shifts are reported in parts per million (ppm), and coupling constants are reported in Hertz. The residual protons or ^{13}C atoms of the deuterated solvents were used as internal references. ^{19}F NMR chemical shifts were referenced to the external standard $\text{C}_6\text{H}_5\text{F}$. Elemental analyses (C, H, N, Cl) were performed by Kolbe Mikroanalytisches Laboratorium, Mülheim an der Ruhr, Germany.

GPC analyses were conducted using a system equipped with two Waters 7.8 X 300 nm columns (Ultrastyrigel 10^4 Å and Styragel HR5E) in series and a Wyatt Technology mini Dawn light scattering detector coupled with a Knauer differential refractometer. A Knauer 64 HPLC pump was used to supply HPLC grade dichloromethane (or THF if noted) at a flow rate of 1.0 mL/min. The auxiliary constant of the apparatus (5.9×10^{-4}) was calibrated using a polystyrene standard. Data analysis was carried out using ASTRette 1.2 software (Wyatt Technology).

The polymer MALDI-TOF mass spectrum was recorded on a Bruker Omni-Flex MALDI-TOF, and data were analyzed using Xtof Software Version 5.1.5 by Bruker Daltonics, Inc. The sample was prepared by Andrea Gabert as a 0.1 mg/mL solution in THF with a matrix solution of 10 mg/mL in THF. In collaboration with Professor Ron Christensen, Professor Elizabeth Stemmler, and Lucas Amundson at Bowdoin college, the oligomer samples were prepared in MeOH and run through a Waters C_{18} reverse-phase column with a mobile phase of 37% CH_3CN , 48% MeOH, with 15% H_2O . The molecular mass of the oligomers was measured using IonSpec High-Resolution MALDI-ICR-FTMS. Samples were deposited on the sample probe and a 337-nm N_2 Laser was used for desorption. A saturated solution of 2,5-dihydrobenzoic acid in acetone (10 μL) and a 0.1 M solution of Na^+ salt (1 μL) was used as the

matrix. Cationized oligomers were prepared by adding the sample (in dichloromethane) to the probe tip containing the dried matrix.

X-ray structures were done by Peter Mueller. Crystals were coated in Paratone-N oil and frozen in an inert gas stream during analysis. Data were collected on a Siemens Platform three-circle diffractometer equipped with a Bruker Apex-CCD detector at low temperature, and integration was performed using SAINT. The initial solution was obtained and refined using SHELXTL.

General Procedure for Initiation and Polymerization Reactions. If required, quinuclidine adducts were formed by reacting the specified catalyst with 1.1 equivalents of quinuclidine in the specified reaction solvent for 15 minutes at room temperature. Separate solutions containing the initiator (2 to 30 mM) and DEDPM in equal volumes of solvent (DME or dichloromethane) were prepared and cooled to $-30\text{ }^{\circ}\text{C}$ if specified (total volume = 2 to 5 mL for bulk experiments, 0.8 mL for NMR scale experiments). The solutions were combined and stirred vigorously. Products of initiation reactions employing fewer than 5 equivalents of DEDPM were observed by NMR after 10 minutes. Ratios of k_p/k_i were calculated according to a procedure reported in the literature.²³⁴ When enough DEDPM was added such that between 20% and 80% of the initiator was consumed, the ratio between the integral values of the alkylidene H_{α} resonances corresponding to unconsumed initiator and the total integral value of all alkylidene H_{α} resonances was calculated. This ratio (r) was used to calculate k_p/k_i from the following equation in which M = equivalents of DEDPM: $M + (k_p/k_i)\ln(r) + (1-(k_p/k_i))(r-1) = 0$.²³⁴

Polymerization reactions were stirred for 1.5 hours (or longer for lower temperature reactions). The reactions were quenched with 10 equivalents of benzaldehyde or ferrocenecarboxaldehyde. These aldehydes react with the propagating catalyst in Wittig-like reactions, affording molybdenum oxo byproducts and polymer chains capped with benzyl or ferrocenyl groups. Ferrocenecarboxaldehyde was used in order to include a redox-active component in the polymer that could aid in MALDI-TOF studies and facilitate oligomer crystallization. The five-membered ring aldehyde (**8b**) was also employed as a capping reagent

in order to generate symmetric oligomers. The reactions were then stirred for another hour at room temperature. Pentane (50 mL) was added to precipitate the polymer as a metallic purple powder, which was collected via vacuum filtration and dried. Unless otherwise noted, polymer yields are essentially quantitative. Polydispersities and molecular weights are determined by GPC online viscometry using refractive index and light scattering detectors ($\lambda = 690$ nm) that were calibrated versus polystyrene standards.

Mo(NAr)(*trans*-CHCHCHMe)(O-*t*-Bu)₂(quin). Solid LiO-*t*-Bu (1.064 g, 13.29 mmol) was added to a solution of Mo(NAr)(CHR)[OCMe(CF₃)₂]₂(quin) (2.654 g, 3.320 mmol) in pentane (25 mL), and the reaction mixture was stirred for 1 hour at room temperature. The reaction mixture was concentrated in vacuo, redissolved in 20 mL of pentane, and filtered. The product was concentrated to 5 mL and stored at -30 °C for 12 hours. Clear crystals of LiO-*t*-Bu and LiOCMe(CF₃)₂ formed first and were filtered off. The solution was concentrated to saturation and stored at -30 °C for another 12 hours. A batch of large dark purple crystals formed and were collected and dried. Three additional recrystallizations yielded mixtures of both purple and clear crystals that were separated mechanically. Yield: 1.565 g, 81%. ¹H NMR (20 °C, C₆D₅CD₃) (achiral, syn rotamer) δ (ppm) 1.26 (m, 6H, quin H _{β}), 1.26 (m, 1H, quin H _{γ}), 1.33 (d, 12 H, *i*-Pr CH₃), 1.38 (s, 18H, O-*t*-Bu), 1.84 (d, 3H, allylic CH₃), 2.94 (m, 6H, quin H _{α}), 4.15 (br sept, 2H, *i*-Pr CH), 4.71 (dq, 1H, vinyl H _{γ}), 7.08 (m, 3H, H_m + H_p), 7.95 (br t, 1H, vinyl H _{β}), 12.11 (d, 1H, vinyl H _{α} ; $J_{\text{HH}} = 11$ Hz); (chiral, anti rotamer) δ (ppm) 2.15 (d, 3H, allylic CH₃), 8.09 (br t, 1H, vinyl H _{β}), 12.58 (d, 1H, vinyl H _{α} ; $J_{\text{HH}} = 13$ Hz). ¹H NMR (22 °C, C₆D₆) (achiral, syn rotamer) δ (ppm) 1.26 (m, 6H, quin H _{β}), 1.27 (m, 1H, quin H _{γ}), 1.34 (d, 12 H, *i*-Pr CH₃), 1.39 (s, 18H, O-*t*-Bu), 1.78 (d, 3H, allylic CH₃), 2.88 (m, 6H, quin H _{α}), 4.17 (sept, 2H, *i*-Pr CH), 4.77 (dq, 1H, vinyl H _{γ}), 7.1 (m, 3H, H_m + H_p), 8.00 (br t, 1H, vinyl H _{β}), 12.11 (d, 1H, vinyl H _{α} ; $J_{\text{CH}} = 121.5$ Hz); (chiral, anti rotamer) δ (ppm) 2.04 (d, 3H, allylic CH₃) 8.14 (br t, 1H, vinyl H _{β}), 12.49 (d, 1H, vinyl H _{α} , $^1J_{\text{CH}} = 141.7$ Hz). ¹³C NMR (RT, C₆D₆) (syn rotamer) δ (ppm) 16.9 (1C, ester CH₂), 21.7 (1C, quin C _{γ}), 24.5 (2C, C(CH₃)₂), 27.1 (1C, quin C _{β}), 28.6 (2C, C(CH₃)₂), 32.5 (6C, OC(CH₃)₃), 35.6 (1C, allylic CH₃), 48.4 (3C, quin C _{α}), 77.2 (2C, OC(CH₃)₃), 117.2,

123.7, 128.3, 144.0, 146.6 152.5 (2 vinyl and 6 aryl CHs), 272.3 (1C, vinyl CH_α). Anal. Calcd. for C₃₁H₅₄MoN₂O₂: C, 63.9; H, 9.34; N, 4.81. Found: C, 63.67; H, 9.52; N, 4.77.

Mo(NAr)(*trans*-CHCHCHMe)(OAd)₂(quin). Solid LiOAd (0.400 g, 2.55 mmol) was added to a solution Mo(NAr)(*trans*-CHCHCHMe)[OCMe(CF₃)₂]₂(quin) (0.581 g, 0.728 mmol), and the reaction mixture was stirred for 20 minutes at room temperature. The reaction mixture was concentrated in vacuo, and the product abstracted into pentane (10 mL). The solution was concentrated to 5 mL and stored at -30 °C for 12 hours. A precipitated formed and was filtered off. The remaining solution was stored at -30 °C for another 12 hours, resulting in the formation of dark purple crystals that were collected and dried. Two additional batches of crystals were collected in the same manner. Yield: 0.331 mg, 62%. ¹H NMR (22 °C, C₆D₅CD₃) (achiral, syn rotamer) δ (ppm) 1.26 (m, 1H, quin H_γ), 1.38 (d, 12 H, *i*-Pr CH₃), 1.52 (m, 6H, quin H_β), 1.79 (d, 3H, allylic CH₃), 1.8-2.2 (br ms, 6H + 3H + 6H, adamantyl CH₂ + CH + CH₂), 2.96 (br s, 6H, quin H_α), 4.22 (sept, 2H, *i*-Pr CH), 4.75 (dq, 1H, vinyl H_γ), 7.09 (m, 3H, H_m + H_p), 7.97 (br t, 1H, vinyl H_β), 12.19 (d, 1H, vinyl H_α; ¹J_{CH} = 128.2 Hz; J_{HH} = 10 Hz); (achiral, anti rotamer) δ (ppm) 12.49 ppm (d, 1H, vinyl H_α; J_{HH} = 12 Hz). Anal. Calcd. for C₄₃H₆₆MoN₂O₂: C, 69.89; H, 9.00; N, 3.79. Found: C, 69.77; H, 8.93; N, 3.67.

2-(4-Hydroxy-4-methyl-pent-2-ynyl)-2-prop-2-ynyl-malonic acid diethyl ester (8a).²²⁹ DEDPM (4.022g, 17.02 mmol) was dissolved in 250 mL of dry THF. Under the flow of nitrogen, the reaction mixture was cooled to -78 °C, and a 1M solution of Li-HMDS (17.02 mL, 17.02 mmol) was added via syringe. The reaction mixture was stirred for 15 minutes before acetone (1.2 mL) was added dropwise to the solution. After 2 hours, the reaction was quenched with a saturated solution of NH₄Cl, warmed to room temperature, and extracted into ether. The organic layer was dried over MgSO₄ and concentrated in vacuo. The resulting oil was purified by column chromatography (silica gel: 40% ether/60% hexane). Yield: 2.43 g, 48%. ¹H NMR (22 °C, CDCl₃) δ (ppm) 1.28 (t, 6H, ester CH₃), 1.47 (s, 6H, CH₃), 1.7 (br s, 1H, OH), 2.03 (br s, 1H, CH), 2.96 (br s, 2H, CH₂), 2.98 (s, 2H, CH₂), 4.24 (q, 4H, ester CH₂).

3-Formyl-4-(2-methyl-propenyl)-cyclopent-3-ene-1,1-dicarboxylic acid diethyl ester

(8b).²²⁹ H₂O (0.2 mL) was added to a solution of **8a** (2.1 g, 7.1 mmol) in degassed acetone (80 mL). The reaction mixture was stirred at room temperature for 1 hour under nitrogen. [CpRu(CH₃CN)₃]PF₆²³⁰⁻²³² (0.040 g, 0.092 mmol) was added, and the reaction mixture was stirred for another 3 hours. The reaction mixture was then filtered through a pad of silica gel with ether as the eluent, and the solvent was removed in vacuo. The product was purified by column chromatography (silica gel: 60% ether/40% hexane). Yield: 0.781 g, 37%. ¹H NMR (22 °C, CDCl₃) δ (ppm) 1.25 (t, 6H, CH₃), 1.87 (s, 3H, CH₃), 1.93 (s, 3H, CH₃), 3.22 (s, 2H, CH₂), 3.41 (s, 2H, CH₂), 4.21 (q, 4H, CH₂), 6.29 (s, 1H, CH), 9.88 (s, 1H, CH).

Diethyl 3-(2-methylprop-1-enyl)-4-vinylcyclopent-3-ene-1,1-dicarboxylate (8c).²²⁹

NaH (0.117g of 60% NaH, 2.92 mmol) was added to a suspension of Ph₃PMeI (1.287g, 3.18 mmol) in dry, degassed THF (300 mL) under nitrogen. After 1 hour at room temperature, the reaction became a bright yellow color and was stirred for an additional 2 hours. The reaction mixture was cooled to 0 °C, and **8b** (0.781 g, 2.65 mmol) was added dropwise as a solution in THF. The solution became colorless as the aldehyde was added. The reaction mixture was stirred at room temperature overnight, producing a light brown suspension containing a tan solid. The reaction mixture was concentrated in vacuo, producing a brown oil. Addition of ether (300 mL) to the product resulted in the formation of a brown precipitate. The ether solution was decanted off and washed 3 times with water (40 mL each), dried over MgSO₄, filtered, and concentrated in vacuo to give a yellow oil, which was purified by column chromatography (silica gel: 20% ether/80% hexane). Yield: 0.359 g, 46%. ¹H NMR (22 °C, CDCl₃) δ (ppm) 1.24 (t, 6H, CH₃), 1.77 (s, 3H, CH₃), 1.85 (s, 3H, CH₃), 3.18 (s, 2H, CH₂), 3.30 (s, 2H, CH₂), 4.22 (q, 4H, CH₂), 5.09 (s, 1H, CH₂), 5.12 (d, 1H, CH₂), 5.92 (s, 1H, CH), 9.88 (dd, 1H, CH).

Mo(NAr)(CH[5])[OCMe(CF₃)₂]₂. A solution of **8c** (0.359 g, 1.23 mmol) in pentane (2 mL) was added to a stirring suspension of orange Mo(NAr)(CHCMe₃)[OCMe(CF₃)₂]₂ (0.683 g, 1.17 mmol) in pentane (10 mL) at room temperature. The orange solid in the suspension rapidly dissolved, and a yellow precipitate began to crash out of the solution. After 30 minutes, the

reaction mixture was filtered, and a flaky yellow solid was collected. The solution was concentrated and a second batch of yellow solid was collected via filtration. Yield: 0.847 g, 84%. ^1H NMR (22 °C, C_6D_6) δ (ppm) 0.85 ppm (t, 6H, ester CH_3), 1.25 (d, 12H, *i*-Pr CH_3), 1.40 (s, 6H, CH_3), 1.59 (s, 3H, CH_3), 1.70 (s, 3H, CH_3), 3.62 (s, 2H, CH_2), 3.70 (sept, 2H, *i*-Pr CH), 3.85 (q, 4H, CH_2), 4.00 (s, 2H, CH_2), 6.17 (s, 1H, CH_γ), 7.0-7.3 (m, 3H, aryl Hs), 13.08 (s, 1H, CH_ω). ^1H NMR (22 °C, CD_2Cl_2) δ (ppm) 1.07 ppm (t, 6H, ester CH_3), 1.19 (d, 12H, *i*-Pr CH_3), 1.42 (s, 6H, CH_3), 1.91 (s, 3H, CH_3), 1.96 (s, 3H, CH_3), 3.21 (s, 2H, CH_2), 3.51 (sept, 2H, *i*-Pr CH), 3.71 (s, 2H, CH_2), 4.00 (q, 4H, CH_2), 5.96 (s, 1H, CH), 7.19 (d, 2H, aryl Hs), 7.19 (t, 1H, aryl H), 12.79 (s, 1H, CH; $^1J_{\text{CH}} = 120$ Hz). ^{19}F NMR (22 °C, CD_2Cl_2) δ (ppm) -78.50 (d, 12F, CF_3). Anal. Calcd. for $\text{C}_{36}\text{H}_{45}\text{F}_{12}\text{NO}_6$: C, 47.43; H, 4.98; N, 1.54. Found C, 47.55; H, 4.87; N, 1.48.

Mo(NAr)(CH[5])(O-*t*-Bu) $_2$. Suspensions of Mo(NAr)(CH[5])[OCMe(CF_3) $_2$] $_2$ (0.421 g, 0.468 mmol) and LiO-*t*-Bu (0.094 g, 1.171 mmol) in 5 mL and 3 mL of pentane, respectively, were mixed at room temperature and stirred for 15 minutes. The solid material rapidly dissolved, and the solution acquired a deep red color. The solution was concentrated to 2 mL and stored at -30 °C for 12 hours. A dark red solid precipitated and was collected via filtration. Yield: 0.104 g, 33%. ^1H NMR (22 °C, C_6D_6) (syn rotamer) δ (ppm) 0.8-1.6 (36H total) (t, 6H, ester CH_3), (d, 12 H, *i*-Pr CH_3), (s, 18H, O-*t*-Bu CH_3), 1.75 (s, 3H, allylic CH_3), 1.80 (s, 3H, allylic CH_3), 3.65 (s, 2H, CH_2), 3.89 (q, 4H, ester CH_2), 4.11 (s, 2H, CH_2), 4.13 (sept, 2H, *i*-Pr CH), 6.40 (s, 1H, CH), 7.0 (t, 1H, CH_ρ), 7.1 (d, 2H, CH_m), 12.35 (s, 1H, CH_α ; $^1J_{\text{CH}} = 123.1$ Hz). ^1H NMR (22 °C, CD_2Cl_2) δ (ppm) 1.06 (t, 6H, ester CH_3), 1.18 (d, 12H, *i*-Pr CH_3), 1.29 (s, 18H, O-*t*-Bu CH_3), 1.90 (s, 3H, allylic CH_3), 1.92 (s, 3H, allylic CH_3), 3.21 (s, 2H, CH_2), 3.61 (s, 2H, CH_2), 3.74 (sept, 2H, *i*-Pr CH), 3.97 (dq, 4H, ester CH_2), 6.01 (s, 1H, CH), 7.09-7.14 (m, 3H, aryl CHs), 11.87 (s, 1H, CH_α ; $^1J_{\text{CH}} = 117.7$ Hz). ^{13}C NMR (22 °C, CD_2Cl_2) δ (ppm) 14.2 (2C, ester CH_3), 20.1 (1C, allylic CH_3), 20.3 (1C, allylic CH_3), 23.9 (2C, $\text{C}(\text{CH}_3)_2$), 28.4 (2C, $\text{C}(\text{CH}_3)_2$), 28.5 (2C, $\text{C}(\text{CH}_3)_2$), 32.0 (6C, $\text{OC}(\text{CH}_3)_3$), 43.7 (1C, CH_2), 46.0 (1C, CH_2), 58.1 (1C quat C), 61.8 (2C, ester CH_3), 78.3 (2C, $\text{OC}(\text{CH}_3)_3$), 119.9, 123.2, 123.3, 127.4, 136.2, 143.5, 146.5, 150.9 (4

vinyl and 6 aryl CHs), 172.5 (1C, carbonyl C), 273.1 (1C, CH_α). Anal. Calc. For C₃₆H₅₇MoNO₆: C, 62.14; H, 8.26; N, 2.01. Found: C, 61.97; H, 8.16; N, 1.94.

Mo(NAr)(CH[5])(O-*t*-Bu)₂(quin). A solution of Mo(NAr)(CH[5])(O-*t*-Bu)₂ (0.300 g, 0.334 mmol) and quinuclidine (0.044 g, 0.367 mmol) in 3 mL of pentane was stirred for 10 minutes at room temperature. A solution of LiO-*t*-Bu (0.107 g, 1.335 mmol) in pentane (3 mL) was added to the quinuclidine adduct at room temperature. The reaction mixture was concentrated in vacuo to yield a red-brown oil from which a solid could not be precipitated or crystallized. Yield: 0.193 g, 73%. ¹H NMR (22 °C, CD₂Cl₂) (syn rotamer) δ (ppm) (chemical shifts are the same as for Mo(NAr)(CH[5])(O-*t*-Bu)₂) 2.80 (Quin H_α); (chiral, anti rotamer) δ (ppm) 12.33 ppm (s, 1H, CH_α). ¹H NMR (22 °C, C₆D₆) (chiral, anti rotamer) δ (ppm) 1.82 (s, 3H, allylic CH₃), 1.88 (s, 3H, allylic CH₃), 2.90 (quin H_α), 6.35 (s, 1H, CH), 13.12 (s, 1H, CH_α; ¹J_{CH} = 143.6 Hz). Anal. Calcd. for C₄₃H₇₀MoN₂O₆: % C, 64.00; H, 8.74; N, 3.47. Found: C, 63.87; H, 8.68; N, 3.41.

Benzyl Capped Five-Membered Ring Dimer. ¹H NMR (22 °C, CDCl₃) δ (ppm) 1.29 (m, 12H, ester CH₃), 1.84 (d, 3H, allylic CH₃), 3.31 (s, 2H, CH₂), 3.38 (s, 2H, CH₂), 3.39 (s, 2H, CH₂), 3.42 (s, 2H, CH₂), 4.24 (m, 8H, CH₂), 5.83 (sext, 1H, CH), 6.22 (m, 1H, CH), 6.23 (m, 1H, CH), 6.55-6.72 (m, 4H, CHs), 7.26 (t, 1H, *p*-Ph CH), 7.36 (t, 2H, *m*-Ph CH), 7.50 (d, 2H, *o*-Ph CH). ¹³C NMR (22 °C, CDCl₃) δ (ppm) 14.31 (4C, ester CH₃), 18.76 (1C, CH₃), 41.28 (1C, 5-member ring CH₂), 41.46 (1C, 5-member ring CH₂), 41.46 (1C, 5-member ring CH₂), 41.57 (1C, 5-member ring CH₂), 57.30 (1C, quat C), 57.36 (1C, quaternary C), 62.03 (2C ester CH₂), 62.05 (2C ester CH₂), 121.44, 122.47, 122.82, 123.47, 126.83, 126.83, 127.93, 128.90, 128.90, 130.83, 131.51, 131.95, 132.40, 134.77, 136.08, 136.35, 136.97, 137.61 (18H, vinyl and aromatic CHs), 172.07 (1H, carbonyl C), 172.11 (1H, carbonyl C). MALDI-ICR-FTMS Calcd. for C₃₇H₄₄O₈ [M+Na] 639.73. Found [M+Na] 639.32.

Benzyl Capped Five-Membered Ring Trimer. ¹H NMR (22 °C, CDCl₃) δ (ppm) 1.29 (m, 18H, ester CH₃), 1.82 (d, 3H, allylic CH₃), 3.2-3.6 (ss, 2H each, 6 CH₂), 4.23 (m, 12H, CH₂), 5.82 (sext, 1H, CH), 6.05-6.79 (ms, 1H each, 9 CH), 7.27 (t, 1H, *p*-Ph CH), 7.38 (t, 2H, *m*-Ph

CH), 7.51 (d, 2H, *o*-Ph CH). MALDI-ICR-FTMS Calcd. for C₅₀H₆₀O₁₂ [M+Na] 875.99. Found [M+Na] 875.42.

Symmetric Five-Membered Ring Trimer. ¹H NMR (22 °C, CDCl₃) δ (ppm) 1.28 (m, 18H, ester CH₃), 1.82 (s, 6H, allylic CH₃), 1.90 (s, 6H, allylic CH₃), 3.28 (s, 4H, CH₂), 3.31 (s, 4H, CH₂), 3.36 (s, 4H, CH₂), 4.23 (m, 12H, CH₂), 6.03 (s, 2H, CH), 6.44 (d, 2H, CH), 6.55 (d, 2H, CH). MALDI-ICR-FTMS Calcd. for C₄₅H₆₀O₁₂ [M+Na] 815.94. Found [M+Na] 815.42.

Symmetric Five-Membered Ring Tetramer. ¹H NMR (22 °C, CDCl₃) δ (ppm) 1.28 (m, 24H, ester CH₃), 1.83 (s, 6H, allylic CH₃), 1.90 (s, 6H, allylic CH₃), 3.29 (s, 4H, CH₂), 3.35 (s, 4H, CH₂), 3.37 (s, 4H, CH₂), 3.39 (s, 4H, CH₂), 4.29 (m, 16H, CH₂), 6.03 (s, 2H, CH), 6.47 (d, 2H, CH), 6.56 (d, 2H, CH), 6.63 (s, 2H, CH). ¹³C NMR (22 °C, CDCl₃) δ (ppm) 14.29 (8C, ester CH₃), 20.73 (2C, allylic CH₃), 27.87 (2C, allylic CH₃), 40.19 (2C, 5-mem ring CH₂), 41.50 (2C, 5-mem ring CH₂), 41.61 (2C, 5-mem ring CH₂), 44.80 (2C, 5-mem ring CH₂), 58.14 (1C, quaternary C), 57.34 (1C, quaternary C), 61.95 (2C ester CH₂), 62.07 (2C ester CH₂), 119.38, 121.68, 122.99, 125.07, 133.74, 135.76, 136.90, 137.30, 137.70 (9H, vinyl CHs), 172.19 (1H, carbonyl C), 172.27 (1H, carbonyl C). MALDI-ICR-FTMS Calcd. for C₅₈H₇₆O₁₆ [M+Na] 1052.2. Found [M+Na] 1052.54.

3.9 Acknowledgements

I'd like to thank Zachary Tonzetich for his contribution to the synthesis of Mo(NAr)(CH[5])(O-*t*-Bu)₂(quin) and for many helpful discussions. I'd also like to thank Prof. Ronald L. Christensen, Prof. Elizabeth A. Stemmler, and Lucas Amundson for performing HPLC purification, UV/VIS and MALDI analysis of oligomers. I'm grateful to Andrea Gabert for performing polymer MALDI analysis, to Dr. Peter Mueller for performing the X-ray crystallography studies, and to Amritanshu Sinha and Tatiana Pilyugina for donating new Schrock-group catalysts for analysis. Funding by DOE and ARMY ISN is sincerely appreciated.

Appendix 1

Synthesis and Reactions of [MesNpy]Hf(R)₂ (R = Np, Bn)

A.1 Introduction

Catalysts containing the $[(\text{MesNCH}_2)_2\text{C}(\text{CH}_3)(2\text{-C}_5\text{H}_4\text{N})]^{2-}$ ($[\text{MesNpy}]^{2-}$) ligand have been shown to polymerize 1-hexene in a highly living manner.⁴⁶⁻⁴⁹ Modification of the alkyl ligands in $[\text{MesNpy}]\text{HfR}_2$ is one approach to fine-tuning catalytic behavior. Neopentyl and benzyl alkyl groups are interesting because they do not contain any β -hydrogens. Use of $\text{B}(\text{C}_6\text{F}_5)_3$ as an activator instead of $\{\text{Ph}_3\text{C}\}\{\text{B}(\text{C}_6\text{F}_5)_4\}$ may also affect polymerization behavior.

A.2 Complexes and reactions of hafnium complexes containing the

$[(\text{MesNCH}_2)_2\text{C}(\text{CH}_3)(2\text{-C}_5\text{H}_4\text{N})]^{2-}$ ($[\text{MesNpy}]^{2-}$) ligand

The reaction of 2 equivalents of neopentyllithium with $[\text{MesNpy}]\text{HfCl}_2$ cleanly produced $[\text{MesNpy}]\text{Hf}(\text{Np})_2$. Although $[\text{MesNpy}]\text{Zr}(\text{Np})_2$ can be activated with $\{\text{Ph}_3\text{C}\}\{\text{B}(\text{C}_6\text{F}_5)_4\}$ to produce $\{[\text{MesNpy}]\text{Zr}(\text{Np})\}\{\text{B}(\text{C}_6\text{F}_5)_4\}$,⁴⁷ $[\text{MesNpy}]\text{Hf}(\text{Np})_2$ did not react readily with $\{\text{Ph}_3\text{C}\}\{\text{B}(\text{C}_6\text{F}_5)_4\}$ or $\text{B}(\text{C}_6\text{F}_5)_3$.

The reaction of 2.5 equivalents of PhCH_2MgCl with $[\text{MesNpy}]\text{HfCl}_2$ afforded $[\text{MesNpy}]\text{Hf}(\text{Bn})_2$ in high yield. This species can be activated with $\{\text{Ph}_3\text{C}\}\{\text{B}(\text{C}_6\text{F}_5)_4\}$ to produce the benzyl cation $\{[\text{MesNpy}]\text{Hf}(\text{Bn})\}\{\text{B}(\text{C}_6\text{F}_5)_4\}$ and $\text{Ph}_3\text{CCH}_2\text{Ph}$. Based on the upfield chemical shift of the pyridine *ortho*-hydrogen at 7.37 ppm, the pyridyl ligand does not coordinate to hafnium. An upfield shift of 6.07 ppm for the peak corresponding to the benzyl *ortho*-protons is observed. The cation is most likely stabilized by coordination of the benzyl group to hafnium in a mono or bimolecular manner, which was proposed to be the case for the analogous zirconium benzyl cation (Figure A.1).⁵⁰

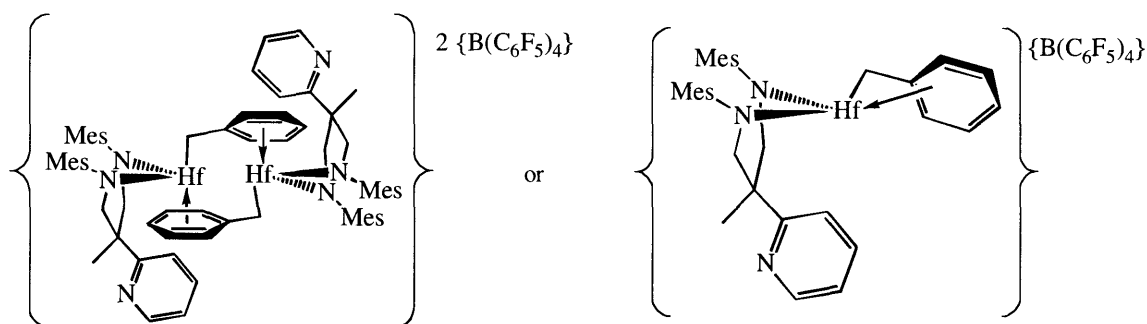
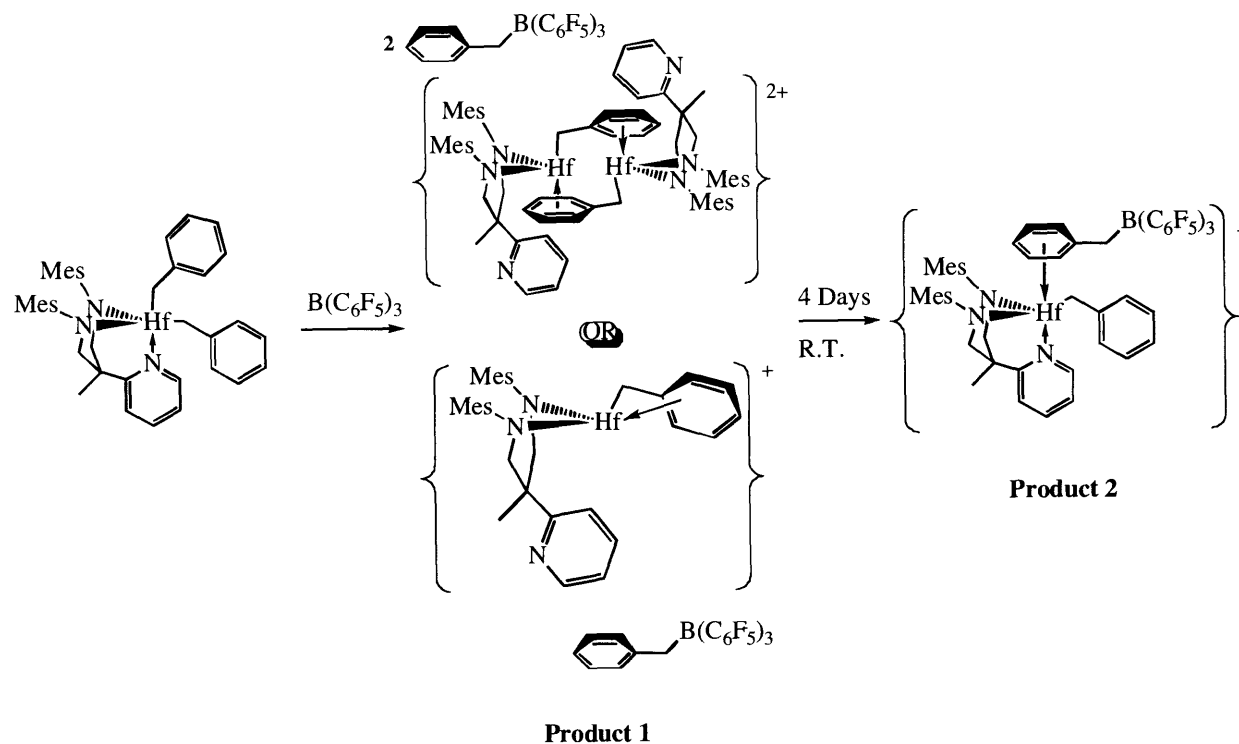


Figure A.1. Possible configurations of the benzyl cation $\{\text{MesNpy}\}\text{Hf}(\text{Bn})\}\{\text{B}(\text{C}_6\text{F}_5)_4\}$ produced by the activation of $[\text{MesNpy}]\text{Hf}(\text{Bn})_2$ with $\{\text{Ph}_3\text{C}\}\{\text{B}(\text{C}_6\text{F}_5)_4\}$.

Abstraction of a benzyl group from $[\text{MesNpy}]\text{Hf}(\text{Bn})_2$ by $\text{B}(\text{C}_6\text{F}_5)_3$ is rapid, and the initial product is also believed to be either the dimer containing two bridging benzyl groups or a single complex in which the benzyl ring is coordinating to the hafnium center in an μ -2 manner (Scheme A.1). In contrast to when $\{\text{Ph}_3\text{C}\}\{\text{B}(\text{C}_6\text{F}_5)_4\}$ is employed as an activator, the geometry of the cation transforms over a period of 4 days at room temperature when $\text{B}(\text{C}_6\text{F}_5)_3$ is used. The pyridyl group was observed to coordinate to hafnium, displacing the coordinating aryl ring of the benzyl ligand to form Product 2 (Scheme A.2). In the C_6D_6 ^1H NMR spectrum of product 2, the pyridine *ortho*-hydrogen resonance is shifted downfield from 7.33 ppm to 8.81 ppm, and the Hf-benzyl *ortho*-hydrogen peak is shifted downfield from 6.06 ppm to below 6.8 ppm. The $\{\text{PhCH}_2\text{B}(\text{C}_6\text{F}_5)_3\}^-$ anion coordinates to hafnium, giving rise to a singlet at 2.69 ppm having through-space interactions with other hafnium-bound ligands in the ^1H NOESY spectrum. Products 1 and 2 are both stable up to 70 °C, but show signs of decomposition after 10 minutes at 80 °C. Product 2 is stable for weeks at room temperature.



Scheme A.1. Activation of $[\text{MesNpy}]\text{Hf}(\text{Bn})_2$ with $\text{B}(\text{C}_6\text{F}_5)_3$.

Neither Product 1, nor Product 2 polymerized 1-hexene at a detectable rate. When 100 equivalents of 1-hexene were added to Product 2 at room temperature, two weeks were required for consumption of 50% of the 1-hexene. It is unclear whether or not Product 1 or 2 is the active species. The possibility that a very small amount of Product 1 present in solution was responsible for the polymerization of 1-hexene cannot be discounted.

A.3 Experimental Section

General Procedures. $[\text{MesNpy}]\text{HfCl}_2$ was synthesized according to a reported procedure.⁴⁷ General conditions were the same as those reported in Chapters 1 and 2.

[MesNpy]Hf(Np)₂. A suspension of [MesNpy]HfCl₂ (0.200 g, 0.308 mmol) in ether (15 mL) was cooled to -30 °C. To the cold solution was added neopentylolithium (0.048 g, 0.615 mmol), and the resulting mixture was stirred at room temperature for 40 minutes until the cloudy suspension became an orange-yellow solution. The solvent was removed in vacuo to yield an orange powder, which was redissolved in ether (5 mL) and recrystallized twice at -30 °C to yield a white powder. Yield: 0.106 g, 48%. ¹H NMR (C₆D₅Br) δ 0.94 (3H, s, CH₃), 1.03 (2H, s, CH₂), 1.14 (2H, s, CH₂), 1.091 (9H, s, CH₃), 1.347 (9H, s, CH₃), 0.5-1.3 (6H, broad s, *o*-CH₃), 0.5-1.3 (6H, broad s, *o*-CH₃), 2.15 (6H, s, *p*-CH₃), 2.87 (2H, d, bb CH₂), 4.13 (2H, d, bb CH₂), 6.7-7.0 (7H, ms, 3 py H, 4 mes-H), 9.28 (1H, d, py *o*-H).

[MesNpy]Hf(Bn)₂. A suspension of [MesNpy]HfCl₂ (0.500 g, 0.770 mmol) in ether (25 mL) was cooled to -30 °C. To the cold solution was added PhCH₂MgCl (1.926 g, 1.926 mmol) and the resulting mixture was stirred at room temperature for 45 minutes until the cloudy suspension became a yellow solution. Dioxane (0.210 g, 2.38 mmol) was added to the solution, and the resulting white powder was filtered off through packed celite. The solvent was removed in vacuo to yield a pale yellow powder, which was washed with pentane and recrystallized at -30 °C. ¹H NMR (C₆D₅Br): δ 0.88 (3H, s, CH₃), 1.8 (4H, broad m, Bn CH₂), 2.1 (6H, broad s, *o*-CH₃), 2.28 (6H, s, *p*-CH₃), 2.5 (6H, broad s, *o*-CH₃), 2.80 (2H, d, bb CH₂), 4.16 (2H, d, bb CH₂), 6.5-7.1 (17H, ms, 3 py H, 4 Mes CH, 10 Bn CH), 8.83 (1H, d, py *o*-H).

Activation of [MesNpy]Hf(Np)₂ with B(C₆F₅)₃. Suspensions of [MesNpy]Hf(Np)₂ (0.015g, 0.021 mmol) and B(C₆F₅)₃ (0.011 g, 0.021 mmol) in C₆D₅Br (0.4 mL) were cooled to -30 °C and mixed. When the resulting suspension became a solution, the reaction mixture was transferred to an NMR tube. The ¹H NMR spectrum was nearly identical to that of [MesNpy]Hf(Np)₂, indicating that no reaction had occurred with the exception of the formation of an unknown product integrating to approximately 4%. A ¹H NMR taken 2 days later showed extensive catalyst decomposition.

Activation of [MesNpy]Hf(Bn)₂ with B(C₆F₅)₃. Suspensions of [MesNpy]Hf(Bn)₂ (0.015g, 0.020 mmol) and B(C₆F₅)₃ (0.010 g, 0.020 mmol) in C₆D₅Br (0.4 mL) were cooled to

–30 °C and mixed. When the resulting suspension became a yellow solution, the reaction mixture was transferred to an NMR tube. **Product 1:** ^1H NMR (after 10 minutes) ($\text{C}_6\text{D}_5\text{Br}$) δ 1.25 (3H, s, CH_3), 1.5 (6H, broad s, *o*- CH_3), 2.12 (6H, s, *p*- CH_3), 2.2 (6H, broad s, *o*- CH_3), 2.21 (2H, broad s, Bn *o*- CH_2), 2.90 (2H, d, bb CH_2), 3.33 (2H, s, B- CH_2), 4.11 (2H, d, bb CH_2), 6.06 (2H, d, coord. Bn CH), 6.6-7.2 (16H, ms, 2 py H, 4 Mes CH, 10 Bn CH), 7.33 (1H, d, py *o*-H), 7.65 (1H, m, py H). **Product 2:** ^1H NMR (after 4 days at room temperature) ($\text{C}_6\text{D}_5\text{Br}$) δ 1.38 (3H, s, CH_3), 1.81 (6H, broad s, *o*- CH_3), 2.21 (6H, s, *p*- CH_3), 2.44 (6H, s, *o*- CH_3), 2.69 (2H, s, B- CH_2), 3.10 (2H, s, Bn *o*- CH_2), 3.21 (2H, d, bb CH_2), 4.39 (2H, d, bb CH_2), 6.8-7.2 (15H, ms, 1 py H, 4 Mes CH, 10 Bn CH), 7.42 (1H, d, py H), 7.63 (1H, t, py H), 8.81 (1H, d, py *o*-H).

Activation of $[\text{MesNpy}]\text{Hf}(\text{Bn})_2$ with $\{\text{Ph}_3\text{C}\}\{\text{B}(\text{C}_6\text{F}_5)_4\}$. Suspensions of $[\text{MesNpy}]\text{Hf}(\text{Bn})_2$ (0.015g, 0.020 mmol) and $\{\text{Ph}_3\text{C}\}\{\text{B}(\text{C}_6\text{F}_5)_4\}$ (0.018 g, 0.020 mmol) in $\text{C}_6\text{D}_5\text{Br}$ (0.4 mL) were cooled to –30 °C and mixed. When the resulting suspension became a yellow solution, the reaction mixture was transferred to an NMR tube. ^1H NMR (after 10 minutes = after 2 weeks) ($\text{C}_6\text{D}_5\text{Br}$): δ 1.24 (3H, s, CH_3), 1.4 (6H, broad s, *o*- CH_3), 2.12 (6H, s, *p*- CH_3), 2.2 (6H, broad s, *o*- CH_3), 2.20 (2H, broad s, Bn CH_2), 2.90 (2H, d, bb CH_2), 3.83 (2H $\text{PhCH}_2\text{CPh}_3$) 4.12 (2H, d, bb CH_2), 6.07 (2H, d, coord. Bn *o*-CH), 6.6-7.2 (16H, ms, 2 py H, 4 Mes CH, 10 Bn CH), 7.37 (1H, d, py *o*-H), 7.69 (1H, m, py H).

Reactions of a $\text{B}(\text{C}_6\text{F}_5)_3$ activated solution of $[\text{MesNpy}]\text{Hf}(\text{Np})_2$ with 1-hexene. Suspensions of $[\text{MesNpy}]\text{Hf}(\text{Bn})_2$ (0.015g, 0.020 mmol), $\text{B}(\text{C}_6\text{F}_5)_3$ (0.010 g, 0.020 mmol), and the internal standard Ph_2CH_2 (0.005 g, 0.020 mmol) in $\text{C}_6\text{D}_5\text{Br}$ (0.4, 0.4, 0.2 mL, respectively) were cooled to –30 °C and mixed. When the resulting suspension became a yellow solution, the reaction mixture was transferred to an NMR tube, and 100 equivalents of 1-hexene were added. Polymerization was not significant enough at room temperature for measurement of a rate constant, and only 50% polymerization of 1-hexene was evident after 2 weeks.

Reactions of a $\{\text{Ph}_3\text{C}\}\{\text{B}(\text{C}_6\text{F}_5)_4\}$ activated solution of $[\text{MesNpy}]\text{Hf}(\text{Bn})_2$ with 1-hexene. Suspensions of $[\text{MesNpy}]\text{Hf}(\text{Bn})_2$ (0.015g, 0.020 mmol), $\{\text{Ph}_3\text{C}\}\{\text{B}(\text{C}_6\text{F}_5)_4\}$ (0.018 g,

0.020 mmol), and the internal standard Ph₂CH₂ (0.005 g, 0.020 mmol) in C₆D₅Br (0.4, 0.4, 0.2 mL, respectively) were cooled to -30 °C and mixed. When the resulting suspension became a yellow solution, the reaction mixture was transferred to an NMR tube, and 100 equivalents of 1-hexene were added. No polymerization was observed initially or after 2 weeks.

Appendix 2
Crystallographic Parameters and Tables

Table A.1. Atomic coordinates ($\times 10^4$) and equivalent isotropic displacement parameters ($\text{\AA}^2 \times 10^3$) for $[\text{Ar}_{\text{Cl}}\text{N}_2\text{NMe}]\text{Hf}(i\text{-Bu})_2$.

$U(\text{eq})$ is defined as one third of the trace of the orthogonalized U_{ij} tensor.

	x	y	z	U(eq)
Hf(1)	7874(1)	7487(1)	1150(1)	25(1)
Cl(3)	7592(1)	8958(1)	2884(1)	49(1)
Cl(1)	6999(1)	5353(1)	2471(1)	55(1)
Cl(4)	8396(1)	10500(1)	433(1)	55(1)
Cl(2)	7613(1)	4952(1)	-191(1)	61(1)
N(2)	8614(2)	8881(2)	1528(1)	33(1)
N(1)	8158(2)	5894(2)	1197(1)	35(1)
C(14)	7202(3)	5172(2)	1124(2)	35(1)
C(19)	6822(3)	4702(3)	511(2)	44(1)
C(25)	7735(3)	10570(3)	1195(2)	43(1)
C(5)	7653(3)	7796(3)	55(2)	39(1)
C(24)	7044(4)	11425(3)	1317(2)	57(1)
C(23)	6499(4)	11493(3)	1917(2)	63(1)
C(15)	6552(3)	4872(3)	1671(2)	41(1)
C(16)	5576(3)	4208(3)	1610(2)	50(1)
C(18)	5833(4)	4037(3)	435(2)	57(1)
C(17)	5210(4)	3801(3)	988(2)	57(1)
C(20)	7920(3)	9760(2)	1655(2)	34(1)
C(22)	6663(3)	10731(3)	2391(2)	50(1)
C(21)	7372(3)	9885(3)	2262(2)	40(1)
N(3)	9858(2)	7165(2)	1670(1)	33(1)
C(1)	5965(3)	7576(2)	1419(2)	39(1)
C(9)	9352(3)	5406(3)	1345(2)	47(1)
C(11)	9906(3)	9024(3)	1747(2)	46(1)
C(10)	10319(3)	6244(3)	1346(2)	46(1)
C(6)	8656(3)	8092(3)	-392(2)	44(1)
C(13)	9839(4)	6986(3)	2407(2)	52(1)
C(12)	10586(3)	8083(3)	1547(2)	52(1)
C(2)	4949(4)	8075(4)	981(3)	83(2)
C(8)	9438(4)	7171(4)	-573(2)	58(1)
C(7)	8133(5)	8623(3)	-1040(2)	67(1)
C(4)	4974(4)	9149(4)	824(3)	81(2)
C(3)	3673(4)	7767(6)	1171(4)	109(3)

Table A.2. Atomic coordinates ($\times 10^4$) and equivalent isotropic displacement Parameters ($\text{\AA}^2 \times 10^3$) for $[\text{Ar}_{(\text{FNM}_{\text{e}2})_2}\text{Npy}]\text{Hf}(\text{F})\text{Cl}$.

$U(\text{eq})$ is defined as one third of the trace of the orthogonalized U^{ij} tensor.

	x	y	z	U(eq)
C(1)	8400(20)	2500	3800(20)	47(5)
C(2)	10020(20)	2500	4710(30)	56(6)
C(3)	10470(20)	2500	6290(20)	36(5)
C(4)	9170(20)	2500	6860(20)	31(4)
C(5)	7460(20)	2500	5887(19)	30(4)
C(6)	6000(20)	2500	6443(17)	32(4)
C(7)	4885(14)	1762(8)	5931(13)	37(3)
C(8)	3234(16)	967(8)	3770(14)	38(3)
C(9)	2393(18)	504(8)	4515(17)	50(4)
C(10)	1490(20)	-165(10)	3880(20)	76(5)
C(16)	6690(20)	2500	8210(20)	55(6)
Cl(1)	1156(6)	2500	1187(5)	44(1)
F(1)	5385(15)	2500	1109(12)	64(3)
F(3)	2438(11)	715(5)	5953(10)	64(2)
Hf(1)	4221(1)	2500	2625(1)	32(1)
N(2)	4107(12)	1653(6)	4273(10)	35(3)
N(1)	7086(18)	2500	4319(16)	45(4)
C(13)	3001(19)	710(9)	2263(15)	50(4)
C(12)	2110(20)	65(10)	1610(19)	75(5)
C(11)	1320(20)	-372(10)	2390(20)	87(6)
N(3)	3947(16)	1175(7)	1534(12)	55(3)
C(15)	5720(20)	848(11)	2008(16)	80(6)
C(14)	3190(20)	1178(10)	-162(16)	75(5)

Table A.3. Atomic coordinates ($\times 10^4$) and equivalent isotropic displacement Parameters ($\text{\AA}^2 \times 10^3$) for $[\text{Ar}_{\text{F}_2}\text{Npy}]\text{Hf}(i\text{-Bu})_2$.

$U(\text{eq})$ is defined as one third of the trace of the orthogonalized U_{ij} tensor.

	x	y	z	U(eq)
Hf(1)	1738(1)	382(1)	1342(1)	23(1)
N(1)	2193(2)	1715(3)	968(1)	26(1)
N(2)	1317(2)	1334(3)	1874(1)	27(1)
N(3)	382(2)	1196(3)	967(1)	26(1)
F(1)	2412(2)	-188(2)	575(1)	38(1)
F(2)	3399(2)	3485(2)	719(1)	53(1)
F(3)	1308(3)	-753(3)	1965(1)	54(1)
F(4)	1132(2)	2607(3)	2727(1)	52(1)
C(1)	3108(3)	-185(4)	1616(2)	34(1)
C(2)	3814(4)	413(4)	1931(2)	43(1)
C(3)	4149(4)	1449(5)	1705(2)	49(1)
C(4)	3526(4)	671(6)	2389(2)	66(2)
C(5)	1190(3)	-1241(3)	1047(2)	29(1)
C(6)	1768(3)	-2305(3)	1090(2)	28(1)
C(7)	1502(4)	-3109(4)	696(2)	44(1)
C(8)	1751(4)	-2904(4)	1542(2)	39(1)
C(9)	1905(3)	2827(4)	1070(2)	29(1)
C(10)	1022(3)	2896(3)	1295(2)	30(1)
C(11)	1131(3)	2519(4)	1802(2)	32(1)
C(12)	839(4)	4153(4)	1323(2)	40(1)
C(13)	-273(3)	636(4)	724(2)	33(1)
C(14)	-1041(3)	1102(5)	526(2)	38(1)
C(15)	-1142(3)	2233(5)	579(2)	41(1)
C(16)	-482(3)	2819(4)	826(2)	33(1)
C(17)	284(3)	2307(4)	1016(2)	28(1)
C(18)	2835(3)	1644(4)	668(1)	25(1)
C(19)	2975(3)	640(4)	461(2)	29(1)
C(20)	3581(4)	396(4)	172(2)	36(1)
C(21)	4137(3)	1216(5)	58(2)	41(1)
C(22)	4044(3)	2265(5)	243(2)	42(1)
C(23)	3416(3)	2452(4)	537(2)	33(1)
C(24)	1220(3)	941(4)	2309(1)	28(1)
C(25)	1219(4)	-182(5)	2364(2)	40(1)
C(26)	1154(4)	-771(5)	2756(2)	52(2)
C(27)	1075(4)	-182(5)	3148(2)	49(2)
C(28)	1058(3)	962(5)	3125(2)	41(1)
C(29)	1128(3)	1491(4)	2717(2)	35(1)

Table A.4. Crystal data and structure refinement for
 Mo(NAr)(*trans*-CHCHCHMe)(O-*t*-Bu)₂(quin).

Identification code	Mo(NAr)(<i>trans</i> -CHCHCHMe)(O- <i>t</i> -Bu) ₂ (quin)	
Empirical formula	C ₃₁ H ₅₄ MoN ₂ O ₂	
Formula weight	582.70	
Temperature	100(2) K	
Wavelength	0.71073 Å	
Crystal system	Monoclinic	
Space group	Pn	
Unit cell dimensions	a = 9.3667(3) Å	α = 90°
	b = 10.5520(4) Å	β = 91.0640(10)°
	c = 16.3250(4) Å	γ = 90°
Volume	1613.24(9) Å ³	
Z	2	
Density (calculated)	1.200 Mg/m ³	
Absorption coefficient	0.433 mm ⁻¹	
F(000)	624	
Crystal size	0.10 x 0.08 x 0.08 mm ³	
Theta range for data collection	1.93 to 30.03°.	
Index ranges	-13 ≤ h ≤ 13, -14 ≤ k ≤ 14, -22 ≤ l ≤ 22	
Reflections collected	36482	
Independent reflections	9391 [R(int) = 0.0383]	
Completeness to theta = 30.03°	100.0 %	
Absorption correction	Semi-empirical from equivalents	
Max. and min. transmission	0.9662 and 0.9580	
Refinement method	Full-matrix least-squares on F ²	
Data / restraints / parameters	9391 / 2 / 336	
Goodness-of-fit on F ²	1.041	
Final R indices [I > 2σ(I)]	R1 = 0.0313, wR2 = 0.0679	
R indices (all data)	R1 = 0.0361, wR2 = 0.0699	
Absolute structure parameter	0.000(19)	
Largest diff. peak and hole	0.947 and -0.226 e.Å ⁻³	

Table A.5. Atomic coordinates ($\times 10^4$) and equivalent isotropic displacement parameters ($\text{\AA}^2 \times 10^3$) for $\text{Mo}(\text{NAr})(\text{CHCHCHMe})(\text{O}-t\text{-Bu})_2(\text{quin})$.

$U(\text{eq})$ is defined as one third of the trace of the orthogonalized U^{ij} tensor.

	x	y	z	U(eq)
Mo(1)	11283(1)	7241(1)	1344(1)	14(1)
C(1)	10170(2)	6957(2)	338(1)	19(1)
C(2)	10598(3)	7109(2)	-504(2)	21(1)
C(3)	9868(2)	6795(3)	-1182(1)	26(1)
C(4)	10402(3)	6971(3)	-2029(2)	38(1)
N(1)	12716(2)	7550(2)	2633(1)	17(1)
C(11)	11861(4)	7260(3)	3356(2)	24(1)
C(12)	12766(3)	7347(3)	4162(2)	27(1)
C(13)	14252(2)	7847(2)	3953(1)	24(1)
C(14)	14956(2)	6888(2)	3389(1)	25(1)
C(15)	13980(2)	6700(2)	2622(1)	25(1)
C(16)	13228(2)	8871(2)	2697(1)	25(1)
C(17)	14092(3)	9106(2)	3498(1)	30(1)
N(2)	12804(2)	7689(2)	816(1)	17(1)
C(21)	14024(2)	7878(2)	368(1)	16(1)
C(22)	14410(2)	9127(2)	142(1)	18(1)
C(23)	15579(2)	9288(2)	-365(1)	24(1)
C(24)	16357(2)	8261(2)	-637(1)	27(1)
C(25)	15987(2)	7051(2)	-396(2)	24(1)
C(26)	14827(2)	6827(2)	103(1)	19(1)
C(220)	13572(3)	10259(2)	432(2)	20(1)
C(221)	14518(3)	11213(2)	893(2)	30(1)
C(222)	12784(3)	10914(3)	-280(2)	34(1)
C(260)	14457(2)	5482(2)	349(1)	24(1)
C(261)	15705(3)	4850(2)	807(2)	30(1)
C(262)	13976(3)	4697(2)	-400(2)	32(1)
O(1)	11145(2)	5599(1)	1835(1)	22(1)
C(31)	10592(2)	4343(2)	1734(1)	22(1)
C(32)	11611(4)	3479(3)	2204(2)	62(1)
C(33)	9132(3)	4296(4)	2092(3)	66(1)

C(34)	10550(4)	3934(3)	848(2)	50(1)
O(2)	10222(2)	8571(1)	1860(1)	19(1)
C(41)	8958(2)	9300(2)	1689(1)	21(1)
C(42)	9130(3)	10028(2)	892(1)	31(1)
C(43)	7667(2)	8427(2)	1650(2)	29(1)
C(44)	8831(3)	10221(3)	2406(2)	34(1)

Table A.6. Crystal data and structure refinement for Mo(NAr)(CH[5])(O-*t*-Bu)₂.

Identification code	Mo(NAr)(CH[5])(O- <i>t</i> -Bu) ₂	
Empirical formula	C ₃₆ H ₅₇ MoNO ₆	
Formula weight	695.77	
Temperature	100(2) K	
Wavelength	0.71073 Å	
Crystal system	Triclinic	
Space group	P-1	
Unit cell dimensions	a = 9.5227(13) Å	α = 95.113(4)°
	b = 11.7582(16) Å	β = 102.926(4)°
	c = 19.324(2) Å	γ = 113.726(4)°
Volume	1891.3(4) Å ³	
Z	2	
Density (calculated)	1.222 Mg/m ³	
Absorption coefficient	0.387 mm ⁻¹	
F(000)	740	
Crystal size	0.10 x 0.10 x 0.03 mm ³	
Theta range for data collection	1.93 to 28.28°.	
Index ranges	-12 ≤ h ≤ 12, -15 ≤ k ≤ 15, -25 ≤ l ≤ 25	
Reflections collected	38735	
Independent reflections	9388 [R(int) = 0.0446]	
Completeness to theta = 28.28°	99.9 %	
Absorption correction	Semi-empirical from equivalents	
Max. and min. transmission	0.9885 and 0.9623	
Refinement method	Full-matrix least-squares on F ²	
Data / restraints / parameters	9388 / 0 / 411	
Goodness-of-fit on F ²	1.043	
Final R indices [I > 2σ(I)]	R1 = 0.0355, wR2 = 0.0809	
R indices (all data)	R1 = 0.0448, wR2 = 0.0847	
Largest diff. peak and hole	0.742 and -0.421 e.Å ⁻³	

Table A.7. Atomic coordinates ($\times 10^4$) and equivalent isotropic displacement parameters ($\text{\AA}^2 \times 10^3$) for $\text{Mo}(\text{NAr})(\text{CH}[5])(\text{O}-t\text{-Bu})_2$.

$U(\text{eq})$ is defined as one third of the trace of the orthogonalized U_{ij} tensor.

	x	y	z	U(eq)
Mo(1)	-851(1)	-303(1)	-1735(1)	15(1)
N(2)	-993(2)	-1773(2)	-1588(1)	17(1)
O(1)	774(2)	1092(1)	-1031(1)	22(1)
O(2)	-2809(2)	-191(1)	-1922(1)	24(1)
O(3)	-454(2)	-4965(1)	-3205(1)	24(1)
O(4)	1953(2)	-3833(1)	-3367(1)	24(1)
O(5)	-1644(2)	-4466(1)	-4745(1)	20(1)
O(6)	-3013(2)	-3963(1)	-4060(1)	24(1)
C(1)	-216(2)	-263(2)	-2612(1)	17(1)
C(2)	96(2)	-1105(2)	-3074(1)	16(1)
C(3)	-242(2)	-2417(2)	-2939(1)	17(1)
C(4)	-118(2)	-3102(2)	-3622(1)	15(1)
C(5)	921(2)	-2033(2)	-3948(1)	16(1)
C(6)	762(2)	-879(2)	-3634(1)	16(1)
C(7)	1290(2)	316(2)	-3876(1)	20(1)
C(8)	2091(2)	730(2)	-4362(1)	22(1)
C(9)	2446(3)	2031(2)	-4512(1)	34(1)
C(10)	2718(3)	33(2)	-4800(1)	31(1)
C(11)	611(2)	-3993(2)	-3404(1)	17(1)
C(12)	73(3)	-5878(2)	-2939(1)	32(1)
C(13)	-284(5)	-6906(3)	-3553(2)	59(1)
C(14)	-1778(2)	-3884(2)	-4154(1)	17(1)
C(15)	-3143(2)	-5323(2)	-5285(1)	26(1)
C(16)	-3719(3)	-6619(2)	-5110(1)	37(1)
C(17)	2216(2)	2225(2)	-938(1)	23(1)
C(18)	2845(3)	2798(2)	-138(1)	43(1)
C(19)	1781(3)	3094(2)	-1382(2)	45(1)
C(20)	3405(3)	1870(2)	-1192(1)	38(1)
C(21)	-3987(2)	-35(2)	-2466(1)	28(1)
C(22)	-5460(3)	-406(3)	-2201(1)	44(1)

C(23)	-3291(4)	1340(3)	-2528(2)	80(1)
C(24)	-4349(3)	-893(3)	-3179(1)	40(1)
C(25)	-1112(2)	-2926(2)	-1417(1)	17(1)
C(26)	239(2)	-2978(2)	-965(1)	20(1)
C(27)	101(3)	-4134(2)	-808(1)	27(1)
C(28)	-1330(3)	-5226(2)	-1090(1)	30(1)
C(29)	-2640(3)	-5167(2)	-1548(1)	26(1)
C(30)	-2569(2)	-4034(2)	-1723(1)	19(1)
C(31)	1795(2)	-1780(2)	-664(1)	23(1)
C(32)	1793(3)	-1072(2)	31(1)	39(1)
C(33)	3276(3)	-2031(3)	-552(2)	42(1)
C(34)	-3990(2)	-3960(2)	-2221(1)	21(1)
C(35)	-5128(3)	-5200(2)	-2759(1)	31(1)
C(36)	-4901(2)	-3518(2)	-1785(1)	27(1)

REFERENCES

- (1) Coates, G. W.; Hustad, P. D.; Reinartz, S. *Angew. Chem., Int. Ed.* **2002**, *41*, 2236.
- (2) Britovsek, G. J. P.; Gibson, V. C.; Wass, D. F. *Angew. Chem., Int. Ed.* **1999**, *38*, 428.
- (3) Coates, G. W. *J. Chem. Soc., Dalton Trans.* **2002**, 467.
- (4) Gibson, V. C.; Spitzmesser, S. K. *Chem. Rev.* **2003**, *103*, 283.
- (5) Kempe, R. *Angew. Chem., Int. Ed.* **2000**, *39*, 468.
- (6) Guérin, F.; McConville, D. H.; Vittal, J. J. *Organometallics* **1996**, *15*, 5586.
- (7) Guérin, F.; McConville, D. H.; Payne, N. C. *Organometallics* **1996**, *15*, 5085.
- (8) Guérin, F.; McConville, D. H.; Vittal, J. J. *Organometallics* **1997**, *16*, 1491.
- (9) Scollard, J. D.; McConville, D. H. *J. Am. Chem. Soc.* **1996**, *118*, 10008.
- (10) Jayaratne, K. C.; Sita, L. R. *J. Am. Chem. Soc.* **2000**, *122*, 958.
- (11) Zhang, Y.; Keaton, R. J.; Sita, L. R. *J. Am. Chem. Soc.* **2003**, *125*, 9062.
- (12) Keaton, R. J.; Jayaratne, K. C.; Henningsen, D. A.; Koterwas, L. A.; Sita, L. R. *J. Am. Chem. Soc.* **2001**, *123*, 6197.
- (13) Keaton, R. J.; Jayaratne, K. C.; Fettinger, J. C.; Sita, L. R. *J. Am. Chem. Soc.* **2000**, *122*, 12909.
- (14) Tshuva, E. Y.; Goldberg, I.; Kol, M. *J. Am. Chem. Soc.* **2000**, *122*, 10706.
- (15) Tshuva, E. Y.; Goldberg, I.; Kol, M.; Goldschmidt, Z. *Chem. Commun.* **2001**, 2120.
- (16) Tshuva, E. Y.; Groysman, S.; Goldberg, I.; Kol, M.; Goldschmidt, Z. *Organometallics* **2002**, *2002*, 662.
- (17) Groysman, S.; Tshuva, E. Y.; Goldberg, I.; Kol, M.; Goldschmidt, Z.; Shuster, M. *Organometallics* **2004**, *23*, 5291.
- (18) Segal, S.; Goldberg, I.; Kol, M. *Organometallics* **2005**, *24*, 200.
- (19) Tian, J.; Hustad, P. D.; Coates, G. W. *J. Am. Chem. Soc.* **2001**, *123*, 5134.
- (20) Mason, A. F.; Coates, G. W. *J. Am. Chem. Soc.* **2004**, *126*, 16326.
- (21) Jeon, Y.-M.; Park, S. J.; Heo, J.; Kim, K. *Organometallics* **1998**, *17*, 3161.
- (22) Killian, C. M.; Tempel, D. J.; Johnson, L. K.; Brookhart, M. *J. Am. Chem. Soc.* **1996**, *118*, 11664.
- (23) Brookhart, M.; Desimone, J. M.; Grant, B. E.; Tanner, M. J. *Macromolecules* **1995**, *28*, 5378.
- (24) Mashima, K.; Fujikawa, S.; Tanaka, Y.; Urata, H.; Oshiki, T.; Tanaka, E.; Nakamura, A. *Organometallics* **1995**, *14*, 2633.
- (25) Mitani, M.; Mohri, J.; Yoshida, Y.; Saito, J.; Ishii, S.; Tsuru, K.; Matsui, S.; Furuyama, R.; Nakano, T.; Tanaka, H.; Kojoh, S.; Matsugi, T.; Kashiwa, N.; Fujita, T. *J. Am. Chem. Soc.* **2002**, *124*, 3327.
- (26) Mitani, M.; Nakano, T.; Fujita, T. *Chem. Eur. J.* **2003**, *9*, 2396.
- (27) Yoshida, Y.; Matsui, S.; Fujita, T. *J. Organomet. Chem.* **2005**, *690*, 4382.
- (28) Furuyama, R.; Mitani, M.; Mohri, J.-i.; Mori, R.; Tanaka, H.; Fujita, T. *Macromolecules* **2005**, *38*, 1546.
- (29) Furuyama, R.; Saito, J.; Ishii, S.; Makio, H.; Mitani, M.; Tanaka, H.; Fujita, T. *J. Organomet. Chem.* **2005**, *690*, 4398.
- (30) Schrodi, Y.; Schrock, R. R.; Bonitatebus, P. J. *J. Organometallics* **2001**, *20*, 3560.
- (31) Schrock, R. R.; Schattenmann, F.; Aizenberg, M.; Davis, W. M. *Chem. Commun.* **1998**, 199.

- (32) Schrock, R. R.; Liang, L.-C.; Baumann, R.; Davis, W. M. *J. Organomet. Chem.* **2000**, *591*, 163.
- (33) Schrock, R. R.; Casado, A. L.; Goodman, J. T.; Liang, L.-C.; Bonitatebus, P. J., Jr.; Davis, W. M. *Organometallics* **2000**, *19*, 5325.
- (34) Schrock, R. R.; Bonitatebus, P. J., Jr.; Schrodi, Y. *Organometallics* **2001**, *20*, 1056.
- (35) Schrock, R. R.; Baumann, R.; Reid, S. M.; Goodman, J. T.; Stumpf, R.; Davis, W. M. *Organometallics* **1999**, *18*, 3649.
- (36) Baumann, R.; Davis, W. M.; Schrock, R. R. *J. Am. Chem. Soc.* **1997**, *119*, 3830.
- (37) Baumann, R.; Schrock, R. R. *J. Organomet. Chem.* **1998**, *557*, 69.
- (38) Baumann, R.; Stumpf, R.; Davis, W. M.; Liang, L.-C.; Schrock, R. *J. Am. Chem. Soc.* **1999**, *121*, 7822.
- (39) Warren, T. H.; Schrock, R. R.; Davis, W. M. *Organometallics* **1996**, *15*, 562.
- (40) Aizenberg, M.; Turculet, L.; Davis, W. M.; Schattenmann, F.; Schrock, R. R. *Organometallics* **1998**, *17*, 4795.
- (41) Flores, M. A.; Manzoni, M.; Baumann, R.; Davis, W. M.; Schrock, R. R. *Organometallics* **1999**, *18*, 3220.
- (42) Goodman, J. T.; Schrock, R. R. *Organometallics* **2001**, *20*, 5205.
- (43) Liang, L.-C.; Schrock, R. R.; Davis, W. M. *J. Am. Chem. Soc.* **1999**, *120*, 5797.
- (44) Schrock, R. R.; Seidel, S. W.; Schrodi, Y.; Davis, W. M. *Organometallics* **1999**, *118*, 428.
- (45) Warren, T. H.; Schrock, R. R.; Davis, W. M. *Organometallics* **1998**, *17*, 308.
- (46) Mehrkhodavandi, P.; Pryor, L. L.; Schrock, R. R. *Organometallics* **2003**, *22*, 4569.
- (47) Mehrkhodavandi, P.; Schrock, R. R.; Bonitatebus, P. J. *J. Organometallics* **2002**, *21*, 5785.
- (48) Mehrkhodavandi, P.; Bonitatebus, P. J., Jr.; Schrock, R. R. *J. Am. Chem. Soc.* **2000**, *122*, 7841.
- (49) Mehrkhodavandi, P.; Schrock, R. R. *J. Am. Chem. Soc.* **2001**, *123*, 10746.
- (50) Mehrkhodavandi, P. *Ph.D. Thesis*. Massachusetts Institute of Technology **2002**.
- (51) Gold, L. *J. Chem. Phys.* **1958**, *28*, 91.
- (52) Schrock, R. R.; Adamchuk, J.; Ruhland, K.; Lopez, L. P. H. *Organometallics* **2003**, *22*, 5079.
- (53) Schrock, R. R.; Adamchuk, J.; Ruhland, K.; Lopez, L. P. H. *Organometallics* **2005**, *24*, 857.
- (54) Ruhland, K. *Results Reported in Postdoctoral Research Summary, Schrock Group*. Massachusetts Institute of Technology **2001**.
- (55) Bonitatebus, P. J., Jr. *Unpublished Results*.
- (56) Liu, Z.; Somsook, E.; White, C. B.; Rosaaen, K. A.; Landis, C. R. *J. Am. Chem. Soc.* **2001**, *123*, 11193.
- (57) Pangborn, A. B.; Giardello, M. A.; Grubbs, R. H.; Rosen, R. K.; Timmers, F. J. *Organometallics* **1996**, *15*, 1518.
- (58) Diamond, G. M.; Jordan, R. F.; Petersen, J. L. *Organometallics* **1996**, *15*, 4030.
- (59) Gade, L. H.; Mountford, P. *Coord. Chem. Rev.* **2001**, *216*, 65.
- (60) Wolfe, J. P.; Wagaw, S.; Marcoux, J.-F.; Buchwald, S. L. *Acc. Chem. Res.* **1998**, *31*, 805.
- (61) Hartwig, J. F. *Angew. Chem., Int. Ed. Engl.* **1998**, *37*, 2046.
- (62) Brookhart, M.; Green, M. L. H.; Wong, L. *Prog. Inorg. Chem.* **1988**, *36*, 1.
- (63) Cochran, F. V.; Bonitatebus, P. J., Jr.; Schrock, R. R. *Organometallics* **2000**, *19*, 2414.

- (64) Deck, P. A.; Konate, M. M.; Kelly, B. V.; Slebodnick, C. *Organometallics* **2004**, *23*, 1089.
- (65) Shah, S. A. A.; Dorn, H.; Voigt, A.; Roesky, H. W.; Parisini, E.; Schmidt, H.-G.; Noltemeyer, M. *Organometallics* **1996**, *15*, 3176.
- (66) Turculet, L.; Tilley, T. D. *Organometallics* **2002**, *19*, 2414.
- (67) Edelbach, B. L.; Rahman, A. K. F.; Lachicotte, R. J.; Jones, W. D. *Organometallics* **1999**, *18*, 3170.
- (68) Kraft, B. M.; Lachicotte, R. J.; Jones, W. D. *J. Am. Chem. Soc.* **2000**, *122*, 8559.
- (69) Murphy, E. F.; Murugavel, M. R.; Roesky, H. W. *Chem. Rev.* **1997**, *97*, 3425.
- (70) Plenio, H. *Chem. Rev.* **1997**, *97*, 3363.
- (71) Schrock, R. R.; Lee, J.; Liang, L.-C.; Davis, W. M. *Inorg. Chim. Acta* **1998**, *270*, 353.
- (72) Kui, S. C. F.; Zhu, N.; Chan, M. C. W. *Angew. Chem., Int. Ed.* **2003**, *42*, 1628.
- (73) Mitani, M.; Fujita, T. *ACS Symposium Series* **2003**, *857*, 26.
- (74) Friedrich, S.; Schubart, M.; Gade, L. H.; Scowen, I. J.; Edwards, A. J.; McPartlin, M. *Chem. Ber.* **1997**, *130*, 1751.
- (75) Blake, A. J.; Collier, P. E.; Gade, L. H.; McPartlin, M.; Mountford, P.; Schubart, M.; Scowen, I. J. *Chem. Commun.* **1997**, 1555.
- (76) Shirakawa, H. *Synth. Metals* **2001**, *125*, 3.
- (77) Skotheim, T. A.; Elsenbaumer, R. L.; Reynolds, J. R.; Eds. *Handbook of Conducting Polymers, 2nd Ed.* Marcel Dekker: New York, **1997**.
- (78) Heeger, A. J. *Angew. Chem., Int. Ed.* **2001**, *40*, 2591.
- (79) Naarmann, H. *Synth. Metals* **1987**, *17*, 223.
- (80) MacDiarmid, A. G. *Angew. Chem., Int. Ed.* **2001**, *40*, 2581.
- (81) Roncali, J. *Chem. Rev.* **1997**, *97*, 173.
- (82) Ledoux, I.; Samuel, I. D. W.; Zyss, J.; Yaliraki, S. N.; Schattenmann, F. J.; Schrock, R. R.; Silbey, R. J. *Chem. Phys.* **1999**, *245*, 1.
- (83) Marder, S. R.; Perry, J. W.; Klavetter, F. L.; Grubbs, R. H. *Chem. Mater.* **1989**, *1*, 171.
- (84) Kajzar, F.; Etemad, S.; Baker, G. L.; Messier, J. *Solid State Commun.* **1987**, *63*, 1113.
- (85) Drury, M. R. *Solid State Commun.* **1988**, *68*, 417.
- (86) Matyjaszewski, K. *J. Polym. Sci., Part A* **1993**, *31*, 995.
- (87) Matyjaszewski, K. *Macromolecules* **1993**, *26*, 1787.
- (88) Darling, T. R.; Davis, T. P.; Fryd, M.; Gridnev, A. A.; Haddleton, D. M.; Ittel, S. D.; Matheson, R. R., Jr.; Moad, G.; Rizzardo, E. *J. Polym. Sci., Part A* **2000**, *38*, 1706.
- (89) Thorn-Csanyi, E.; Herzog, O. *J. Mol. Catal: A Chem.* **2004**, *213*, 123.
- (90) Thorn-Csanyi, E.; Kraxner, P. *Macromol. Chem. Phys.* **1997**, *198*, 3827.
- (91) Schlick, H.; Stelzer, F.; Tasch, S.; Leising, G. *J. Mol. Catal: A Chem.* **2000**, *160*, 71.
- (92) Buchmeiser, M. R. *Chem. Rev.* **2000**, *100*, 1565.
- (93) Mullner, R.; Winkler, B.; Stelzer, F.; Tasch, S.; Hochfilzer, C.; Leising, G. *Synth. Metals* **1999**, *105*, 129.
- (94) Thorn-Csanyi, E.; Kraxner, P. *J. Mol. Catal: A Chem.* **1997**, *115*, 21.
- (95) Klavetter, F. L.; Grubbs, R. H. *J. Am. Chem. Soc.* **1988**, *110*, 7807.
- (96) Klavetter, F. L.; Grubbs, R. H. *Synth. Metals* **1989**, *28*, D105.
- (97) Klavetter, F. L.; Grubbs, R. H. *Synth. Metals* **1989**, *28*, D99.
- (98) Gorman, C. B.; Ginsburg, E. J.; Sailor, M. J.; Moore, J. S.; Jozefiak, T. H.; Lewis, N. S.; Grubbs, R. H.; Marder, S. R.; Perry, J. W. *Synth. Metals* **1991**, *41*, 1033.

- (99) Jozefiak, T. H.; Ginsburg, E. J.; Gorman, C. B.; Grubbs, R. H.; Lewis, N. S. *J. Am. Chem. Soc.* **1993**, *115*, 4705.
- (100) Schimetta, M.; Leising, G.; Stelzer, F. *Synth. Metals* **1995**, *74*, 99.
- (101) Schimetta, M.; Stelzer, F. *Macromolecules* **1994**, *27*, 3769.
- (102) Cacialli, F.; Daik, R.; Dounis, P.; Feast, W. J.; Friend, R. H.; Haylett, N. D.; Jarrett, C. P.; Schoenenberger, C.; Stephens, J. A.; Widawski, G. *Phil. Trans. Royal Soc. London, Series A: Math., Phys., Engin. Sci.* **1997**, *355*, 707.
- (103) Feast, W. J.; Gibson, V. C.; Johnson, A. F.; Khosravi, E.; Mohsin, M. A. *Polymer* **1994**, *35*, 3542.
- (104) Okada, M.; Grubbs, R.; Penelle, J.; Boutevin, B.; Amedouri, B.; Rivas, B. L.; Lazar, M., Eds. *Polymer Synthesis Oxidation Processes*. In *Adv. Polym. Sci.* **1992**, *102*.
- (105) Masuda, T.; Abdul Karim, S. M.; Nomura, R. *J. Mol. Catal: A Chem.* **2000**, *160*, 125.
- (106) Masuda, T.; Hayano, S.; Iwawaki, E.; Nomura, R. *J. Mol. Catal: A Chem.* **1998**, *133*, 213.
- (107) Masuda, T.; Higashimura, T. *Acc. Chem. Res.* **1984**, *17*, 51.
- (108) Masuda, T.; Higashimura, T. *Adv. Polym. Sci.* **1986**, *81*, 121.
- (109) Masuda, T.; Izumikawa, H.; Misumi, Y.; Higashimura, T. *Macromolecules* **1996**, *29*, 1167.
- (110) Masuda, T.; Matsumoto, T.; Yoshimura, T.; Higashimura, T. *Macromolecules* **1990**, *23*, 4902.
- (111) Masuda, T.; Mishima, K.; Fujimori, J.; Nishida, M.; Muramatsu, H.; Higashimura, T. *Macromolecules* **1992**, *25*, 1401.
- (112) Masuda, T.; Takahashi, T.; Niki, A.; Higashimura, T. *J. Polym. Sci., Part A* **1986**, *24*, 809.
- (113) Masuda, T.; Tsuchihara, K.; Ohmameuda, K.; Higashimura, T. *Macromolecules* **1989**, *22*, 1036.
- (114) Masuda, T.; Yoshimura, T.; Higashimura, T. *Macromolecules* **1989**, *22*, 3804.
- (115) Mizumoto, T.; Masuda, T.; Higashimura, T. *J. Polym. Sci., Part A* **1993**, *31*, 2555.
- (116) Mizumoto, T.; Masuda, T.; Higashimura, T. *Macromol. Chem. Phys.* **1995**, *196*, 1769.
- (117) Yoshino, K.; Yoshimoto, K.; Morita, S.; Kawai, T.; Kim, S. H.; Kang, K. L.; Choi, S. K. *Synth. Metals* **1995**, *69*, 81.
- (118) Yoshimura, T.; Masuda, T.; Higashimura, T. *Macromolecules* **1988**, *21*, 1899.
- (119) Yoshimura, T.; Masuda, T.; Higashimura, T.; Ishihara, T. *J. Polym. Sci., Part A* **1986**, *24*, 3569.
- (120) Yoshimura, T.; Masuda, T.; Higashimura, T.; Okuhara, K.; Ueda, T. *Macromolecules* **1991**, *24*, 6053.
- (121) Misumi, Y.; Masuda, T. *Macromolecules* **1998**, *31*, 7572.
- (122) Minaki, N.; Hayano, S.; Masuda, T. *Polymer* **2002**, *43*, 3579.
- (123) Hayano, S.; Masuda, T. *Macromol. Chem. Phys.* **1997**, *198*, 3041.
- (124) Hayano, S.; Masuda, T. *Macromolecules* **1998**, *31*, 3170.
- (125) Hayano, S.; Masuda, T. *Macromolecules* **1999**, *32*, 7344.
- (126) Kaneshiro, H.; Hayano, S.; Masuda, T. *Macromol. Chem. Phys.* **1999**, *200*, 113.
- (127) Yoshida, T.; Abe, Y.; Masuda, T.; Higashimura, T. *J. Polym. Sci., Part A* **1996**, *34*, 2229.
- (128) Isobe, E.; Masuda, T.; Higashimura, T.; Yamamoto, A. *J. Polym. Sci., Part A* **1986**, *24*, 1839.
- (129) Gal, Y. S.; Choi, S. K.; Kim, C. Y. *J. Polym. Sci., Part A* **1989**, *27*, 31.

- (130) Tsuchihara, K.; Masuda, T.; Higashimura, T.; Nishida, M.; Muramatsu, H. *Polym. Bull.* **1990**, *23*, 505.
- (131) Okano, Y.; Masuda, T.; Higashimura, T. *J. Polym. Sci., Part A* **1987**, *25*, 1181.
- (132) Sone, T.; Asako, R.; Masuda, T.; Tabata, M.; Wada, T.; Sasabe, H. *Macromolecules* **2001**, *34*, 1586.
- (133) Tamura, K.; Masuda, T.; Higashimura, T. *Polym. Bull.* **1993**, *30*, 537.
- (134) Nakano, M.; Masuda, T.; Higashimura, T. *Macromolecules* **1994**, *27*, 1344.
- (135) Izumikawa, H.; Masuda, T.; Higashimura, T. *Polym. Bull.* **1991**, *27*, 193.
- (136) Matsumoto, T.; Masuda, T.; Higashimura, T. *J. Polym. Sci., Part A* **1991**, *29*, 295.
- (137) Karim, S. M. A.; Nomura, R.; Kajii, H.; Hidayat, R.; Yoshino, K.; Masuda, T. *J. Polym. Sci., Part A* **2000**, *38*, 4717.
- (138) Seki, H.; Masuda, T.; Higashimura, T. *J. Polym. Sci., Part A* **1995**, *33*, 117.
- (139) Sanda, F.; Kawaguchi, T.; Masuda, T.; Kobayashi, N. *Macromolecules* **2003**, *36*, 2224.
- (140) Iwawaki, E.; Hayano, S.; Masuda, T. *Polymer* **2001**, *42*, 4055.
- (141) Fujimori, J.; Masuda, T.; Higashimura, T. *Polym. Bull.* **1988**, *20*, 1.
- (142) Fujita, Y.; Misumi, Y.; Tabata, M.; Masuda, T. *J. Polym. Sci., Part A* **1998**, *36*, 3157.
- (143) Masuda, T.; Takahashi, T.; Higashimura, T. *Macromolecules* **1985**, *18*, 311.
- (144) Masuda, T.; Isobe, E.; Higashimura, T. *Macromolecules* **1985**, *18*, 841.
- (145) Masuda, T.; Okano, Y.; Tamura, K.; Higashimura, T. *Polymer* **1985**, *26*, 793.
- (146) Colthup, E. C.; Meriwether, L. S. *J. Org. Chem.* **1961**, *26*, 5169.
- (147) Yamada, K.; Nomura, R.; Masuda, T. *Macromolecules* **2000**, *33*, 9179.
- (148) Oh, S. Y.; Ezaki, R.; Akagi, K.; Shirakawa, H. *J. Polym. Sci., Part A* **1993**, *31*, 2977.
- (149) Shen, Z.; Faron, M. F. *J. Polym. Sci., Part A* **1984**, *22*, 1009.
- (150) Wallace, K. C.; Liu, A. H.; Davis, W. M.; Schrock, R. R. *Organometallics* **1989**, *8*, 644.
- (151) Schlund, R.; Schrock, R. R.; Crowe, W. E. *J. Am. Chem. Soc.* **1989**, *111*, 8004.
- (152) Knoll, K.; Schrock, R. R. *J. Am. Chem. Soc.* **1989**, *111*, 7989.
- (153) Schrock, R. R. In *Metathesis Polymerization of Olefins and Polymerization of Alkynes*; Imamoglu, Y., Ed.; Kluwer, **1998**, 357.
- (154) Schottenberger, H.; Buchmeiser, M. R.; Herber, R. H. *J. Organomet. Chem.* **2000**, *612*, 1.
- (155) Buchmeiser, M. R.; Hallbrucker, A.; Kohl, I.; Schuler, N.; Schottenberger, H. *Des. Monomers Polym.* **2000**, *3*, 421.
- (156) Buchmeiser, M. R.; Schuler, N.; Kaltenhauser, G.; Ongania, K.-H.; Lagoja, I.; Wurst, K.; Schottenberger, H. *Macromolecules* **1998**, *31*, 3175.
- (157) Buchmeiser, M. R. *Adv. Polym. Sci.* **2005**, *176*, 89.
- (158) Buchmeiser, M. R. *Polym. Mater. Org. Synth. Cat.* **2003**, 345.
- (159) Buchmeiser, M. R. *Late Transition Metal Polymerization Catalysis* **2003**, 155.
- (160) Buchmeiser, M. R. *Macromolecules* **1997**, *30*, 2274.
- (161) Buchmeiser, M.; Schrock, R. R. *Macromolecules* **1995**, *28*, 6642.
- (162) Schrock, R. R.; Luo, S.; Lee, J. C. J.; Zanetti, N. C.; Davis, W. M. *J. Am. Chem. Soc.* **1996**, *118*, 3883.
- (163) Schrock, R. R.; Luo, S.; Zanetti, N.; Fox, H. H. *Organometallics* **1994**, *13*, 3396.
- (164) Stille, J. K.; Frey, D. A. *J. Am. Chem. Soc.* **1961**, *83*, 1697.
- (165) Gibson, H. W.; Bailey, F. C.; Epstein, A. J.; Rommelmann, H.; Kaplan, S.; Harbour, J.; Yang, X. Q.; Tanner, D. B.; Pochan, J. M. *J. Am. Chem. Soc.* **1983**, *105*, 4417.
- (166) Gal, Y. S.; Jung, B.; Lee, W. C.; Choi, S. K. *Synth. Metals* **1995**, *69*, 549.
- (167) Gal, Y. S.; Choi, S. K. *J. Polym. Sci., Part A* **1993**, *31*, 345.

- (168) Halbach, T. S.; Mix, S.; Fischer, D.; Maechling, S.; Krause, J. O.; Sievers, C.; Blechert, S.; Nuyken, O.; Buchmeiser, M. R. *J. Org. Chem.* **2005**, *70*, 4687.
- (169) Halbach, T. S.; Krause, J. O.; Nuyken, O.; Buchmeiser, M. R. *Macromol. Chem. Rapid Commun.* **2005**, *26*, 784.
- (170) Krause, J. O.; Nuyken, O.; Buchmeiser, M. R. *Chem. Eur. J.* **2004**, *10*, 2029.
- (171) Hamilton, J. G.; Frenzel, U.; Kohl, F. J.; Weskamp, T.; Rooney, J. J.; Herrmann, W. A.; Nuyken, O. *J. Organomet. Chem.* **2000**, *606*, 8.
- (172) Buchmeiser, M.; Ed. *Metathesis Polymerization*. In *Adv. Polym. Sci.* **2005**, *176*.
- (173) Krause, J. O.; Zarka, M. T.; Anders, U.; Weberskirch, R.; Nuyken, O.; Buchmeiser, M. R. *Angew. Chem., Int. Ed.* **2003**, *42*, 5965.
- (174) Krause, J. O.; Wang, D.; Anders, U.; Weberskirch, R.; Zarka, M. T.; Nuyken, O.; Jaeger, C.; Haarer, D.; Buchmeiser, M. R. *Macromol. Symp.* **2004**, *217*, 179.
- (175) Gal, Y.-S.; Jin, S.-H.; Park, J.-W.; Lee, W.-C.; Lee, H.-S.; Kim, S.-Y. *J. Polym. Sci., Part A* **2001**, *39*, 4101.
- (176) Ahn, H. K.; Kim, Y. H.; Jin, S. H.; Choi, S. K. *Polym. Bull.* **1992**, *29*, 625.
- (177) Kim, Y. H.; Kwon, S. K.; Choi, S. K. *Bull. Kor. Chem. Soc.* **1992**, *13*, 459.
- (178) Han, S. H.; Kim, U. Y.; Kang, Y. S.; Choi, S. K. *Macromolecules* **1991**, *24*, 973.
- (179) Ryoo, M. S.; Lee, W. C.; Choi, S. K. *Macromolecules* **1990**, *23*, 3029.
- (180) Jang, M. S.; Kwon, S. K.; Choi, S. K. *Macromolecules* **1990**, *23*, 4135.
- (181) Jin, S.-H.; Choi, S.-J.; Ahn, W.; Cho, H.-N.; Choi, S.-K. *Macromolecules* **1993**, *26*, 1487.
- (182) Jin, S. H.; Cho, H. N.; Choi, S. K. *J. Polym. Sci., Part A* **1993**, *31*, 69.
- (183) Jin, S. H.; Kim, S. H.; Cho, H. N.; Choi, S. K. *Macromolecules* **1991**, *24*, 6050.
- (184) Park, J. W.; Lee, J. H.; Cho, H. N.; Choi, S. K. *Macromolecules* **1993**, *26*, 1191.
- (185) Kim, Y. H.; Gal, Y. S.; Kim, U. Y.; Choi, S. K. *Macromolecules* **1988**, *21*, 1991.
- (186) Cho, O. K.; Kim, Y. H.; Choi, K. Y.; Choi, S. K. *Macromolecules* **1990**, *23*, 12.
- (187) Koo, K. M.; Han, S. H.; Kang, Y. S.; Kim, U. Y.; Choi, S. K. *Macromolecules* **1993**, *26*, 2485.
- (188) Jeon, S.-J.; Cho, D.-J.; Shim, S.-C.; Kim, T.-J.; Gal, Y.-S. *J. Polym. Sci., Part A* **1999**, *37*, 877.
- (189) Jeon, S.-J.; Shim, S. C.; Cho, C. S.; Kim, T.-J.; Gal, Y.-S. *Bull. Kor. Chem. Soc.* **2000**, *21*, 980.
- (190) Jeon, S.-J.; Shim, S. C.; Cho, C. S.; Kim, T.-J.; Gal, Y.-S. *J. Polym. Sci., Part A* **2000**, *38*, 2663.
- (191) Kubo, H.; Hayano, S.; Misumi, Y.; Masuda, T. *Macromol. Chem. Phys.* **2002**, *203*, 279.
- (192) Kang, K. L.; Kim, S. H.; Cho, H. N.; Choi, K. Y.; Choi, S. K. *Macromolecules* **1993**, *26*, 4539.
- (193) Kim, S.-H.; Choi, S.-J.; Park, J.-W.; Cho, H.-N.; Choi, S.-K. *J. Am. Chem. Soc.* **1994**, *116*, 2339.
- (194) Choi, D.-C.; Kim, S.-H.; Lee, J.-H.; Cho, H.-N.; Choi, S.-K. *Macromolecules* **1997**, *30*, 176.
- (195) Lee, H. J.; Oh, J. M.; Choi, S. J.; Kim, H. K.; Choi, S. K. *Polym. Bull.* **1994**, *32*, 433.
- (196) Gal, Y. S.; Jin, S. H.; Choi, S. K. *J. Mol. Catal: A Chem.* **2004**, *213*, 115.
- (197) Anders, U.; Wagner, M.; Nuyken, O.; Buchmeiser, M. R. *Macromolecules* **2003**, *36*, 2668.
- (198) Choi, S.-K.; Gal, Y.-S.; Jin, S.-H.; Kim, H. K. *Chem. Rev.* **2000**, *100*, 1645.
- (199) Anders, U.; Nuyken, O.; Buchmeiser, M. R. *J. Mol. Catal: A Chem.* **2004**, *213*, 89.

- (200) Anders, U.; Krause, J. O.; Wang, D.; Nuyken, O.; Buchmeiser, M. R. *Des. Monomers Polym.* **2004**, *7*, 151.
- (201) Lee, H.-J.; Kang, S.-J.; Kim, H. K.; Cho, H.-N.; Park, J. T.; Choi, S.-K. *Macromolecules* **1995**, *28*, 4638.
- (202) Lee, H.-J.; Gal, Y.-S.; Lee, W.-C.; Oh, J.-M.; Jin, S.-H.; Choi, S.-K. *Macromolecules* **1995**, *28*, 1208.
- (203) Kwon, S.-K.; Kim, Y.-H.; Choi, S.-K. *J. Polym. Sci., Part A* **1995**, *33*, 2135.
- (204) Kim, Y. H.; Kwon, S.-K.; Choi, S.-K. *Macromolecules* **1997**, *30*, 6677.
- (205) Choi, S.-J.; Kin, S.-H.; Ahn, W.; Cho, H.-N.; Choi, S.-K. *Macromolecules* **1994**, *27*, 4871.
- (206) Kim, S.-H.; Kim, Y.-H.; Cho, H.-N.; Kwon, S.-K.; Kim, H.-K.; Choi, S.-K. *Macromolecules* **1996**, *29*, 5422.
- (207) Choi, S. K. *Macromol. Symp.* **1990**, *33*, 145.
- (208) Gal, Y.-S.; Jin, S.-H.; Lee, H.-J.; Kim, S.-H.; Lee, W.-C.; Choi, S.-K. *Macromol. Res.* **2003**, *11*, 80.
- (209) Anders, U.; Nuyken, O.; Buchmeiser, M. R.; Wurst, K. *Macromolecules* **2002**, *35*, 9029.
- (210) Anders, U.; Nuyken, O.; Buchmeiser, M. R.; Wurst, K. *Angew. Chem., Int. Ed.* **2002**, *41*, 4044.
- (211) Anders, U.; Nuyken, O.; Buchmeiser, M. R. *Des. Monomers Polym.* **2003**, *6*, 135.
- (212) Schattenmann, F. J.; Schrock, R. R. *Macromolecules* **1996**, *29*, 8990.
- (213) Fox, H. H.; Wolf, M. O.; O'Dell, R.; Lin, B. L.; Schrock, R. R.; Wrighton, M. S. *J. Am. Chem. Soc.* **1994**, *116*, 2827.
- (214) Fox, H. H.; Schrock, R. S. *Organometallics* **1992**, *11*, 2763.
- (215) Schattenmann, F. J.; Schrock, R. R.; Davis, W. M. *J. Am. Chem. Soc.* **1996**, *118*, 3295.
- (216) Zhang, N.; Wu, R.; Li, Q.; Pakbaz, K.; Yoon, C. O.; Wudl, F. *Chem. Mater.* **1993**, *5*, 1598.
- (217) Christensen, R. L.; Faksh, A.; Meyers, J. A.; Samuel, I. D. W.; Wood, P.; Schrock, R. R.; Hultsch, K. C. *J. Phys. Chem. A* **2004**, *108*, 8229.
- (218) Schrock, R. R.; Lee, J.-K.; O'Dell, R.; Oskam, J. H. *Macromolecules* **1995**, *28*, 5933.
- (219) Oskam, J. H.; Schrock, R. R. *J. Am. Chem. Soc.* **1992**, *114*, 7588.
- (220) Oskam, J. H.; Schrock, R. R. *J. Am. Chem. Soc.* **1993**, *115*, 11831.
- (221) Schrock, R. R. *Polyhedron* **1995**, *14*, 3177.
- (222) Christensen, R. L.; Barney, E. A.; Broene, R. D.; Galinato, M. G. I.; Frank, H. A. *Arch. Biochem. Biophys.* **2004**, *430*, 30.
- (223) Wood, P.; Samuel, I. D. W.; Schrock, R.; Christensen, R. L. *J. Chem. Phys.* **2001**, *115*, 10955.
- (224) Fox, H. H.; Yap, K. B.; Robbins, J.; Cai, S.; Schrock, R. R. *Inorg. Chem.* **1992**, *31*, 2287.
- (225) Schrock, R. R.; Murdzek, J. S.; Bazan, G. C.; Robbins, J.; DiMare, M.; O'Regan, M. J. *Am. Chem. Soc.* **1990**, *112*, 3875.
- (226) Albagli, D.; Bazan, G. C.; Wrighton, M. S.; Schrock, R. R. *J. Am. Chem. Soc.* **1992**, *114*, 4150.
- (227) Schrock, R. R.; Crowe, W. E.; Bazan, G. C.; DiMare, M.; O'Regan, M. B.; Schofield, M. H. *Organometallics* **1991**, *10*, 1832.
- (228) Fox, H. H.; Lee, J.-K.; Park, L. Y.; Schrock, R. R. *Organometallics* **1993**, *12*, 759.
- (229) Tonzetich, Z. *Unpublished Results*.
- (230) Trost, B. M.; Older, C. M. *Organometallics* **2002**, *21*, 2544.

- (231) Trost, B. M.; Rudd, M. T. *J. Am. Chem. Soc.* **2005**, *127*, 4763.
- (232) Trost, B. M.; Rudd, M. T. *J. Am. Chem. Soc.* **2002**, *124*, 4178.
- (233) Fu, G. C.; Nguyen, S. T.; Grubbs, R. H. *J. Am. Chem. Soc.* **1993**, *115*, 9856.
- (234) Bazan, G.; Khosravi, E.; Schrock, R. R.; Feast, W. J.; Gibson, V. C.; O'Regan, M. B.; Thomas, J. K.; Davis, W. M. *J. Am. Chem. Soc.* **1990**, *112*, 8378.
- (235) Tsang, P. *Unpublished Results*.

CURRICULUM VITAE

EDUCATION:

- 2001-present **Massachusetts Institute of Technology**, Cambridge, MA
- Ph.D. in Inorganic Chemistry, February 2006
 - Cumulative GPA 4.75/5.00
- 1997-2001 **Cornell University**, Ithaca, NY
- B.A. in Chemistry, Cum Laude with Honors in Chemistry
 - Dean's List Scholar 7/8 semesters, GPA 3.65/4.00

EXPERIENCE:

- 2002-present **Graduate research with Prof. Richard R. Schrock, M.I.T.**
- Studied early transition metal catalysts for the living polymerization of olefins and alkynes
- 1998-2001 **Undergraduate research with Prof. Francis J. DiSalvo, Cornell**
- Member of Cornell Center for Materials Research, REU Program
 - Explored the use of metal clusters as building blocks for extended networks and composite materials
- 1997-1999 **Cephalon, Inc.**, West Chester, PA
(summers)
- Synthesized tyrosine kinase inhibitors for use in cancer studies

AWARDS AND HONORS:

- 2005 Cambridge Science Foundation Travel Grant for presentation of research at San Diego ACS National Meeting
- 2002 Excellence in Teaching by a Graduate Student at M.I.T.
- 2001 Merck Index Award; presented at graduation by the Cornell Chemistry Department
- 2000 Regional Technology Fellow; awarded by the Eastern Technology Council and the Technology Council Foundation for Future Employees in recognition of research work at Cephalon, Inc.
- 1997 High School Valedictorian (West Chester East High School)

ACTIVITIES:

- Women's Ice Hockey Club (Captain/Treasurer)
- Intramural softball, ice hockey, basketball
- Softball umpire

PUBLICATIONS AND PRESENTATIONS:

- Schrock, R. R.*; **Adamchuk, J.**; Ruhland, K.; Lopez, L. P. H. *Organometallics* **2005**, 24, 857.
- Schrock, R. R.*; **Adamchuk, J.**; Ruhland, K.; Lopez, L. P. H. *Organometallics* **2003**, 22, 5079.
- Jin, S.; **Adamchuk, J.**; Xiang, B.; DiSalvo, F. J.* *J. Am. Chem. Soc.* **2002**, 124, 9229.
- Jin, S.; Zhou, R.; Scheuer, E. M.; **Adamchuk, J.**; Rayburn, L. L.; DiSalvo, F. J.* *Inorg. Chem.* **2001**, 40, 2666.
- Cyclopolymerization of 1,6-Heptadiynes by Well-defined Molybdenum Imido Alkylidene Initiators.* **Adamchuk, J.** 229th ACS National Meeting, San Diego, CA, March 13-17, **2005**.

GENERAL ACKNOWLEDGEMENTS

I'd like to thank Professor Dick Schrock for being a great advisor; I've learned so much under his guidance. And it has truly been an honor to work for a Nobel laureate. I'm incredibly grateful for Dick's support and patience as I searched for my path to a future in Chemistry. In addition, I'm grateful to have had the opportunity to participate in extracurricular activities at MIT and to take a class in Marketing Management, both of which have also helped prepare me for a rewarding career.

I'm grateful to Professors Joseph Sadighi and Kit Cummins, my thesis committee members, and the entire Inorganic faculty. Professor Joseph Sadighi, my thesis chair, has been very helpful during my time at MIT, and I am grateful for his support. The intelligence and enthusiasm of the faculty and students has made MIT a very exciting place to be, and has made me challenge myself to the best of my capabilities.

Earning my Ph.D. in the Schrock lab has been a very rewarding experience, and I've enjoyed working with members of the Schrock group. I'm particularly grateful to Parisa Mehrkhodavandi, who trained me in my research techniques and demonstrated the value of attention to detail. And I'm also particularly grateful to Zachary Tonzetich, who I'm certain will always be one of the most successful people I know. It has been a pleasure bonding with my box roommate Andrea Gabert, who has taught me several ways to avoid injury in the lab, and with Tanya Pilyugina, who has taught me to always wear glasses when I check my email. Lara Pryor has also been a good friend, and I have enjoyed getting to know the newbies, Jai Min Chin and Jillian Hafer. I'm grateful to everyone for fun times and helpful discussions. I'm very fortunate to have worked with such a great group of people.

Of course I would also like to thank Chris Hoffman and my parents for their love and support. I'm glad to have made it to the end... which really is just the beginning.

Please see pages 53, 87, and 158 for additional acknowledgements.